DSE Defend Our Territory: Draft Final Report

Group S01

Faculty Aerospace Engineering

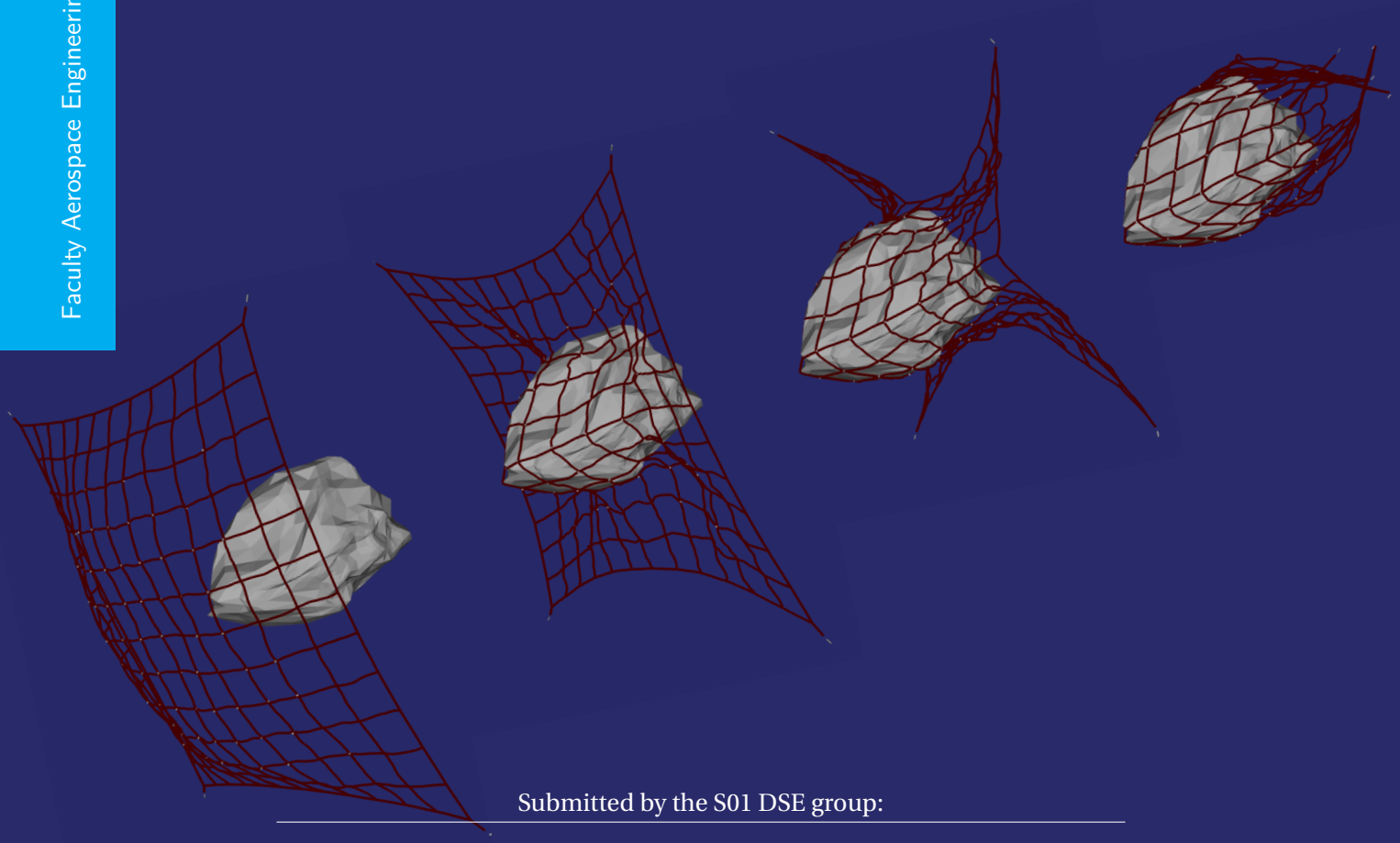

Submitted by the S01 DSE group:

Emilie Bessette	4534921	Sebastian Oliver Scholts	4547330
Benjamin Dutruel	4552229	Antoni Plonczak	4598253
Nicolas Fosséprez	4558073	Paul Schedler	4589823
Modjtaba Haydarie	1528955	Kimberly van den Bogaard	4559169
Ilse (Agnes) Molenberg	4494776		

Under the guidance of:
Angelo Cervone (Principal Tutor)
Silvana Radu (Customer)
Teresa Steinke and Mark Schelbergen (Coaches)

TU Delft Delft University of Technology

Challenge the future

PREFACE

Before you lies the Final Report of the Defend Our Territory (DOT) Design Synthesis Exercise. It has been written by a team of nine students during the spring of 2019, to fulfil the graduation requirements of the Aerospace Engineering Bachelor's degree at Delft University of Technology.
The aim of the DOT mission is to design an asteroid sensing network of PocketQubes to characterise a very small near Earth asteroid. The purpose of this report is to present the preliminary detailed design of the ANTREA (Advanced Net To Rescue Earth from Asteroids) design that the team elaborated to fulfil the mission's aim.

This project would not have been possible without the helpful guidance and support from the team's tutor and coaches. We would therefore like to personally thank Dr. Angelo Cervone, Silvana Radu, Teresa Steinke, and ir. Mark Schelbergen for their precious counsel and assistance. Furthermore, we would like to thank the Aerospace Engineering staff from TU Delft, especially Dr. Stefano Speretta, Dr. Sergio Turteltaub, Dr. ir. Julien van Campen, Dr. Alessandra Menicucci and ir. Jasper Bouwmeester for their valuable advice, highly appreciated knowledge, and time. Finally we would like to thank the Geoscience Centre staff, especially Prof. dr. ir. Evert Slob for his advice, highly appreciated knowledge, and time.

Finally we would like to express our gratitude to Rafał Michalczyk and Wojciech Gołębiowski, from SKA Polska for their imperative help, and kindness to let us use their ADRiNET software: the Toolchain for Dynamic Simulation of Elastic and Deformable Net-like Structure. We would also like to thank them for discretising our net design, providing us with an asteroid model, teaching us how to use their software, and providing key advice during the simulations.

Executive Overview

Asteroids are of great value for scientific purposes, for they can be considered as the building blocks of life on our planets and can therefore provide valuable insight on the origin of our solar system and on its evolution. They are also, on the other hand, a threat to us, through their risk of potentially hazardous collision with Earth. To assess characteristics such as their size, orbital period, and semi-major axis, the light they emit is observed by remote instruments such as telescopes. However, the data found only gets more accurate as their distance to Earth decreases. Today's asteroid databases are thus found to be quite inaccurate, especially for small asteroids, reducing our ability to predict in detail a potential forthcoming crash before the asteroid's actual close approach to Earth. Hence, improving today's asteroid characterisation methods is of utmost importance for being able to predict such a catastrophic event.

A cheap and new mean of access to space is simultaneously making its way to the top of the space sector. Measuring no more than a 5 cm cube, PocketQubes (PQ) represent today's lightest, cheapest and possibly smartest way to get equally small scientific instruments in orbit. Combining the two aspects of filling in the present knowledge gap on Very Small Near Earth Objects, and of demonstrating the promising technology of PocketQubes led to the Defend Our Territory mission, and more specifically to the ANTREA design.

This Executive Overview will present the steps taken towards the choice of this design, as well as a summary of the design and its subsystems, and other useful information about it.

Mission Overview

Leaving Earth in May of 2033 for a planned arrival to asteroid 2017FU102 in April of 2036, ANTREA consists of a 15×15 m net, which was found to be the most fitting way of landing on the asteroid, mainly considering its fast rotational rate and non-existent gravity pull. The net will wrap itself around the asteroid, with 69 PocketQubes weighing between 116 and 180 g attached to its nodes. These will then measure crucial properties such as the asteroid's shape and size, its surface composition, hardness, temperature distribution, dynamics and internal materials, with aim to characterise it in a distributed way. The team designed different elements of the mission systems: the net itself, its Deployer, which should fit in a 27 L available volume in the Mothership, as well as the PQs' subsystems such as their structure, electrical power system, communications, thermal control, command and data handling, and payload instruments. The Lander will be taken to the target asteroid with a Mothership.

User Requirements and Constraints

The assigned project objective that was attributed to the team at the beginning of this project reads as follows: "The objective of your project is to identify, trade-off and preliminarily design possible mission profiles and technology solutions for in-situ characterisation of the main properties (surface and internal) of very small Near Earth Objects with size of a few meters. The mission shall be based on the Delfi-PQ platform developed by TU Delft, but must include other elements and design trades in order to make its ambitious objectives feasible." Top-level requirements were then derived from this project objective, dealing with several matters such as general mission, schedule and cost requirements, system and performance requirements, as well as requirements on safety, reliability, and sustainability of the design. Based on these user requirements, the team developed system and subsystem requirements relevant to the chosen design. The user requirements and constraints can be found at the beginning of this report, while the more detailed requirements, specific to every subsystem, are present in their relevant subsystem chapters.

Trade-Off and Design Presentation

For the reader to have a better understanding on how the team ended up with the ANTREA design, the last trade-off conducted by the team is presented in this report. Three concepts were compared: the SINGLE, FLEX and NET concepts. SINGLE was about deploying 125 individual PQs towards the target asteroid, with every PQ possessing a separate deployment, landing, attachment, but also power generation and communication system. The second concept, namely the FLEX one, consisted of a 75 m long flexible solar tape on which 40 PQs would be attached. Communication and power cables would also be connecting the PQs in a line. This concept also came with a harpoon system that would have been shot at the asteroid's surface, and a deployer, which would have needed an ADCS and propulsion unit to wrap the system around the asteroid. The last NET

concept was about 72 PQs attached at the nodes of a 12.1 m square net, with flexible solar panels placed in between the PQs. The three concepts are shown in the following three figures:

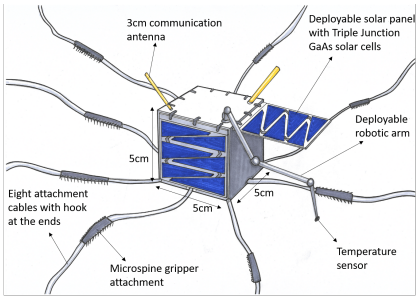

Figure 1: SINGLE: PQ with individual attachment, power, and communication shown.

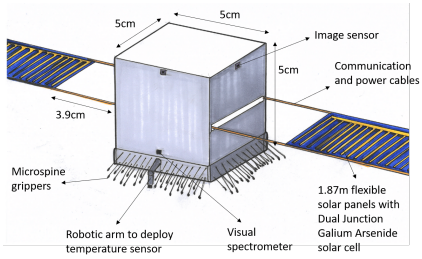

Figure 2: FLEX: PQ with attachments, payloads and solar tape shown.

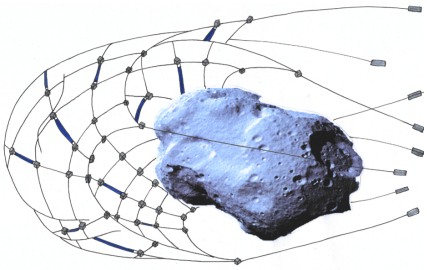

Figure 3: NET: Net wrapping around asteroid after deployment.

The trade-off criteria used were the following: performance, feasibility, risk, innovation, and sustainability. Most of them also had sub-criteria, to assess every possible relevant aspect of every design. Moreover, an Analytic Hierarchy Process (AHP) was conducted with the project's tutor, the customer, the two team's coaches, and the team members, to yield criteria weights that would reflect the member's point of view on the criteria's importance with respect to other criteria. A sensitivity analysis was conducted on the trade-off's results, but the final result did not change, showing the robustness of the trade-off. The winner was the NET concept, which was renamed to ANTREA and which entered the detailed design phase. ANTREA is the abbreviation of Advanced Net To Rescue Earth from Asteroids, as well as one of the oldest fishing nets found in the village of Antrea, which was then part of Finland [1]. This winning concept was adapted and optimised, to yield a system of 69 PQs, attached on the nodes of a 15 m square net, with 4 weights attached at each corner for deployment purposes. The solar tape idea was discarded and individual solar panels were preferred. All user requirements were deemed to be met with this design.

Market Analysis

A market analysis was performed on the ANTREA design, by analysing multiple elements relating to the impact it would have if it were put on the market nowadays. It was found that aspects of the project in which potential customers might be interested in were: the PQ technology, particular subsystems such as the net, deployer, landing principle or structure, properties of the target asteroid, and the autonomous nature of the design. Potential applications of the system were studied, which included for instance using the net to remove space debris, using the deployment for a solar sail, asteroid mining, asteroid deflection, professional and amateur astronomy applications, landing on the Moon or on another celestial body, etc. Some existing companies and entities such as government agencies, scientists, institutes were identified as potential customers of the team's product or services that it could provide, and what is expected to yield of these applications or collaborations was also assessed. Finally the barriers that might present themselves for these applications, and mitigation strategies applicable to these barriers were defined. After doing this analysis, a market value for the system's main individual parts was computed, the product's competitors were identified and a SWOT analysis on the design was performed to present how the product would prosper on the market.

ANTREA: Technical Overview

The Systems Engineering approach that was followed during this design concerns the approach to the technical budgets and performance, and contingency management. The ANTREA system was broken down into segments, which were themselves broken down into subsystems for mass and volume budgets. A target value was constructed by taking the total available mass and volume from the user requirements (50 kg and 27 L respectively) and subtracting 10% contingency on the system level. This was allocated per segments based on preliminary subsystem sizing done by every department. As the project progressed, actual values of every subsystem were collected and combined into the actual values for segments; they were translated into current values in order to monitor the progress of the design and for evaluating whether volume and mass requirements were complied with. This resulted in the final allocation made after the final iteration.

The power budget is broken down into all subsystems which actively contribute to the power consumption. This was iterated together with the energy capacity of the system so that the required power could be provided

through all phases of the mission.

The system has seven operational modes (transfer, activation, data acquisition, communication, safe, End of Life and recharge), all specified by the subsystems active in that mode and conditions for mode transition.

An N^2 chart was constructed, which shows the interfaces between the segments and subsystems of the system. That technical overview was then translated into a physical external and internal layout of the PQs, and the definition of three types of PQS: the Communication PocketQubes (CPQ), the Payload PocketQubes 1 (PPQ-1), and the Payload PocketQubes 2 (PPQ-2), which contain different instruments, display differences in their structure and functions.

Functional Analysis

The technical functions of the ANTREA design were analysed, through the format of a Functional Flow Diagram (FFD) and a Functional Breakdown Structure (FBS), with aim to show how the design would technically fulfil its mission objective. Defining the design's functions was done hand in hand with refining the requirements, to assess them in more detail. These diagrams also include the different modes through which the system's subsystem will go through to perform their individual roles. It was deemed necessary to include a function breakdown to the following subsystems: Thermal Control, Electrical Power System, and Command and Data handling, due to their complexity and various links with other subsystems and modes.

Astrodynamic Analysis

To assess which target asteroid would be best to travel to, a Monte Carlo simulation was conducted. Asteroid 2017FU102 was chosen due to its size, close-approach distance and date with Earth, communication window and small uncertainties in its orbit values. Knowing on which asteroid the Lander will be deployed, a launcher selection was done, in terms of the amount of mass that would need to be taken to space, the launcher's launch and mission loads, launch sites and margins of accuracy. The Vega launcher was chosen, which will nominally be launched on April 15, 2033 from Kourou, French Guiana. It will bring its payload, which will consist of the Mothership with the Deployer and ANTREA system inside of it to a Highly Elliptical Orbit (HEO), minimising the ΔV required. The Mothership will then be released and will travel through an interplanetary transfer to rendezvous with the asteroid. It was decided to consider the situation where the Mothership would arrive at the asteroid a bit in advance, to have time to look for the asteroid. This was done because all retrieved data about the target asteroid are estimations based on the light it emits, as measured from Earth, and might not reflect reality. More information about the asteroid could be retrieved as it approaches Earth during its close-approach of 2036. The Rendezvous has been simplified to 4 manoeuvres, to yield optimum conditions for the deployment of the ANTREA system on the asteroid. In order to perform this trajectory the Mothership will have to provide a ΔV 2697 m/s

Design of the Net

Mainly employed for landing advantages, several aspects of the mission were key to designing the net on which the PQs will be attached. The net is deployed by ejecting bullets at a velocity of 2 m/s which entangle on the backside of the asteroid. The net provides a structural connection as well as the distribution of power and data cables that connect the PQs. The final design displays a 15×15 m square net, with a mesh of 1.25 m. It is partly made out of Technora fiber, partly of Technora hull with two power and four data cables in it. By ejecting the net at 2 m/s, the net velocity would be 0.79 m/s and after landing and entanglement, the four bullets will reel in the cable to secure the net around the asteroid. This net is the first of its kind with masses, the PocketQubes, attached at the nodes.

The deployment simulations were performed with the ADRiNET software: The Toolchain for Dynamic Simulation of Elastic and Deformable Net-like Structure provided by SKA-Polska. Their asteroid model was used. After performing simulations where different deployment and asteroid position and rotation were tested for, it was concluded that the current net design would not be deploying. The conclusions drawn can be used to improve the design of the net and create a more feasible, reliable and efficient design.

Deployer

The Deployer, which is the element that would deploy the Lander from the inside of the Mothership was designed as a cube of $30 \times 30 \times 30$ cm and 1 mm thick plates. It was proved that it could survive loads up to 10.5 g

without bending and all launch vibrations, as its natural frequencies are at least 20 times bigger. This was calculated with a 2 Degrees-of-Freedom simplified model. The roof of the box will open as a door fixed on one side by a hinge and pushed by springs on the other. The ejection tubes consist of 4 cylinders put at an angle of 10 deg with respect to the vertical axis, in each corner of the box. The structure and the cylinders are made out of aluminium Al-7075 T6. Inside the tubes, springs that will eject the bullets, with the help of a push plate, at an ejection speed of 2 m/s. The springs will be compressed and released with the help of pin-pullers, the model P10 from Tini Aeropsace[1].

Structure of PQ

The structure of the PQs was designed to be able to sustain main load events such as launching and landing ones. The internal structure was designed as four aluminium rods that would sustain the other subsystems' instruments by the method of stacks, which consists in superimposing PCB plates, on which the instruments can be connected. For the external structure, it was decided to make it out of FR-4, where the thickness would be of 2 mm all around, except on the -Z side, where it would measure 4 mm, to have enough space to screw the four previously mentioned rods into place. Moreover, a layer of damping Sorbothane material was added on that same side, to increase the chances of success of sustaining the landing loads.

Payload

As the main aim of this mission is filling in the knowledge gap about on Very Small Near Earth Objects, and as most subsystem's designs were directly influenced by it, the payload subsystem was evaluated with a high level of detail. To measure the desired asteroid characteristics as mentioned by the user requirements, several kinds of scientific payload will be taken on-board. These include three temperature sensors that will measure the asteroid's surface temperature, four image sensors, with two being monochrome image sensors, one being a colour one and the last one a near infrared one. One of the monochrome image sensors will be placed on the -Z face of the PQs to determine the asteroid's shape and size during landing. The other image sensors will be used to analyse the surface composition and roughness of the asteroid. An Inertial Measurement Unit (IMU) will also be present in the PQs, to measure the asteroid's hardness, in combination with the data retrieved from the other monochrome image sensor. Other needed instruments were a mass spectrometer to determine the surface composition, a transceiver and an antenna to perform radio science, with aim to provide tomography of the asteroid. Finally, specific mechanisms were designed, for some of the scientific instruments to work.
For the radio experiment, the antenna is made out of tape measure and will be stowed with a wire which is cut by a wire cutter to deploy it. The image sensors and mass spectrometer will be attached to the outside and held within their operating temperature range with the use of heating wires. The mechanism for the temperature sensors consists of two hinge points with torsional springs and two arms of which the second one contains a kink to put the temperature sensor inside the PQ when in stowed position. It is stowed by a wire which will be cut by a wire cutter. The torsional springs will then deploy the mechanism. The total science data amounts to (uncompressed) 54.490 Gb.

Communication

For communication purposes, some of the PQs were designed to be able to communicate with Earth (CPQ), whilst others were only designed to communicate between themselves. A maximum of 3 CPQs were designed to be active at the same time. They will possess a microstrip antenna attached on their +Z surface. The previously mentioned data volume of 54.490 Gb was rounded to 55 Gb and a compression rate of 10 without losses was applied to it, yielding an amount of transmitted data of 5.5 Gb.
To communicate this data to Earth with a reliability of 2σ (97.5%), the system had to be designed for a 17.85 h communication time window, which would start at a distance of 1.458 million km.

In terms of the ground station, the NASA DSN with the 34 m Beam Wave Guided (BWG) antennas will be used, with a frequency of operation of 2200 Mhz. The modulation method will make use of Gaussian Minimum Shift Keying (GMSK) with similar performance as the Binary Phase Shift Keying (BPSK).

[1] https://tiniaerospace.com/products/space-pinpuller/ [accessed on 19/06/2019]

Electrical Power System

Triangular Advanced Solar Cells (TASC) were chosen as they offer the most desirable characteristics for its cell area and mass. Solar cells are placed on the +Z side of every PPQ and none of the CPQ. Six solar cells are fitted on the 5×5 cm area on the +Z side consisting of the solar panel. The solar panel consists of two solar cells connected in series and three pairs connected in parallel. They generate a power of 0.11946 W per PPQ with a mass of 1.4094 g per PPQ.
Each PQ has two 0.33 Ah prismatic Li-Ion batteries each 23 g stacked on top of one another and are connected in parallel to supply power for the entire mission. In the bullets, there are three Sony/Murata US18650VTC5A batteries of 2600 mAh each that supply the power required for the communication phase.
Maximum Power Point Trackers (MPPT) were used on each pair of solar cell to maximise the power generated by the solar cells and regulating the charging voltage for the batteries; these are bq25505 from Texas Instruments. The bus is unregulated due to size constraints and therefore, there is a voltage regulator for the payload. The voltage regulator that was chosen was LT8335 which is a DC-DC boost converter that converts the voltage from 3.7 V to 3.6-5.7 V. Finally, the power cable is sized to be 0.41 mm in diameter and the current capacity is 0.45 A. The bus voltage is boosted by a DC-DC boost converter LT8335 by Linear Technology to reduce the power losses in the cable.

Thermal Control

A thermal control subsystem was essential to implement. It makes sure that the heat experienced by the PQ due to direct solar flux, the asteroid's solar reflection due to albedo, infrared radiation of the asteroid and heat flux input from spacecraft components, was neutralised and controlled. The most restricting temperature range amongst the PQs' instruments was of the batteries, which have a storage temperature between -20 and 60 degrees. It was assumed that the Mothership would provide thermal control for the system before deployment. Consequently, only the landing, performance of the measurements, and communication phases were looked at for the PQs' thermal control. PQs carrying payload instruments, two layers of insulation made out of Kapton were added. For the communications PQs, only one insulation layer was implemented, made out of Kapton and a black layer. Concerning the bullets, it was determined that the added passive thermal control was enough for them to stay within their temperature ranges. It was found that the PQs and bullets stay within their given temperature ranges, and that during specific moments (for example recharging of the batteries) the thermal control is in the proper temperature range to make this happen.

Command and Data Handling

The Command and Data Handling subsystem acts as the brain and nervous system of the Lander. Main functions of this subsystem include: sending commands, processing external commands, sending and processing data, performing telemetry, fault detection, mode selection and transition, time keeping and data storage. Preliminary data handling architecture, software and hardware functional analyses have been constructed, detailing some crucial specifications. For data handling, Serial Peripheral Interface (SPI) data bus was chosen, for which internal communications (between subsystems on the PQ) will have independent slave configuration, with the Microcontroller Unit (MCU) acting as the master, and external communications (between the PQs) will have a daisy chain configuration, with MCU units on selected PQs acting as a master, and the MCUs in their proximity acting as slaves. The hardware consists of four elements: a Texas Instruments radiation-hardened MCU (microcontroller unit), with a maximum clock frequency of 16 MHz, Intelligent Digital Peripherals with 32-Bit Hardware Multiplier (MPY), up to 64 kB of Nonvolatile Memory (FRAM) and very low power usage (0.005 mW), a 3D Plus radiation hardened NAND FLASH of 8 Gb radiation hardened memory module, a cable harness and a PCB.

Spacecraft Operations

The ANTREA system will be operated by the ESA European Space Operations Centre (ESOC). In general, the system was designed to be autonomous, however a health downlink and command uplink once a day is a possibility. It was decided that the project would be managed by the project manager, and that the spacecraft operations manager would be in charge of operations. Scientific instruments will have Principal Investigators (PIs) who will be in charge of instrument design, calibration, operation, and verification. PIs and engineers will

determine a science plan and alter it in case any anomalies occur. The contract will be established with NASA's Deep Space Network (DSN) to get the previously mentioned 28.5 h main science downlink window. After data has been sorted in useful formats, it will be made accessible to the scientific community via the ESA Planetary Science public.

Sensitivity Analysis

A sensitivity analysis was performed on the ANTREA system to assess the robustness of the design. All the unknown parameters and assumptions were investigated, and their effects on the design's subsystems and general functioning was assessed. The conclusion of this sensitivity analysis is that most subsystems were deemed to be insensitive to changes in system parameters. The thermal control subsystem present in the CPQs however, was found to be sensitive even to small changes. In contrast, the thermal control of the PPQs is insensitive to changes.

Performance Analysis

A performance analysis was also conducted, to assess the qualities and defects of the ANTREA design. In terms of the deployment performances, simulations showed that the chosen deployment speed and angle were insufficient for successful deployment of the net. It was proved however, that the Deployer's structure can effectively sustain all launch loads and natural frequencies, as specified by the Vega User's Manual [2].

Concerning the performance of the scientific payload, it was proven that the operation of the ANTREA system would yield in successful scientific measurements of the asteroid's characteristics, on the condition that all other subsystem and mission elements work correctly. These conditions concern the successful deployment of the net, the survival of the PQs to landing loads and to environmental conditions present in space, as well as the correct switching into operational modes.

The communication subsystem was designed to be operational for communication between the PQs themselves through radio communication, and from the master CPQs to Earth for the transfer of scientific data.

In terms of the command and data handling subsystem, the defined operational modes proved that the system can work autonomously for the duration of the system's operation on the asteroid's surface, by the design of a highly redundant subsystem.

Finally, concerning the assessment of the ANTREA design as a lander, it was proven that the design of a net was the best option for optimal attachment and wrapping of the system around the asteroid, as well as for the spreading of the PQs on the asteroid's surface i na distributed way. However, more research should be done on the subject of the survival of the PQs to launch loads, as many uncertainties are present in terms of the asteroid's surface composition, and thus the nature of the shock that would be present between the PQs and the surface, and the possibility of a surface spike to pierce through the PQs' walls. The damage that could be done to the internal elements of the PQs was not assessed, which can also have a direct influence on the thickness of the structure's walls that would be required to protect it. In terms of thermal control, the passive system that was designed was proven to yield successful survival of the PQs, by keeping their elements within their required temperature range, however the CPQs' thermal control was found to be quite sensitive to changes in other subsystems, which might directly reduce their performance.

Risk Analysis

All risks linked to the design were assessed, relating them in particular to the mission phases (rendezvous, deployment, approach, landing and attachment) and to the subsystems. A risk map was constructed, assessing the probability and severity of every risk, with the most catastrophic ones being for instance entanglement of the net, or failure in the deployment of the net, after which the scientific measurements could not even be done as the net would not land on the asteroid. A risk mitigation plan was set up, to find mitigation strategies for the most probable and most severe risks that were found. From this, it was concluded that all risks except one (L3) were put into the lower left diagonal of the posterior risk map, thus successfully mitigating those events.

RAMS

The Reliability, Availability, Maintainability, and Safety of the design were assessed and the following conclusions were drawn: in order to meet the reliability requirement, extensive testing and iterating the design was found to be the best strategy to adopt, especially considering the unfamiliar and demanding environmental

conditions that the system will operate in during these mission phases. In terms of redundancy, a redundancy philosophy was applied to the design, at system and subsystem levels, compensating for the risk of some PQs being destroyed during landing, as well as for single points of failures in the PQs' subsystems. Safety and reliability are achieved through: fault avoidance, fault removal, fault tolerances, fault detection and diagnosis and automatic supervision. A FMFEA or FMECA has to performed to achieve this.

Sustainability

Sustainability was defined in the context of this project as the philosophy of designing a product whose environmental impact would be minimised. Being a leading criterion for customers on the aerospace market, it was all the more necessary to define a sustainability approach, as well as a sustainable development strategy of the team's product and its contribution to sustainability. This sustainability strategy was detailed for every phase of the space mission, taking for instance into account the use of remains of solar cells instead of producing new ones, or the use of sustainable machining and fabrication techniques, prioritising Commercially Off The Shelf (COTS) components in the the system's design, and analysing the risks that the system possesses in terms of sustainability, as well as mitigating those risks and taking them into account during the design phase.

Production Plan

A production plan was made to assess in more detail what actions and which methods would have to be used to produce the team's design. The production constraints present are the Lithium-ion batteries and the solar panels. They need to be handled with care and stored in facilities that can cope with these materials. Furthermore, it consist of manufacturing the components, then the elements, after which multiple elements are connect to each other into subsystems. All subsystems assembled together into one system: ANTREA. Between every step, verification is done to make sure the component is as desired (within the error limits).

Cost Analysis

The cost is split over two parts, building the ANTREA (hardware and software) and testing of all parts. As it is still early in the design phase of ANTREA, the cost is still a rough estimated. The cost of labour is the most consuming, as it takes up around 3.5 million USD. The aim of miniaturising is to achieve scientific goals for a cheaper price. The average price of a PQ is 3575 USD, so this is quite cheap. As it is still a new technology, high cost are related to testing. The overall cost of the ANTREA will be around 5.5 Million.

Validation of Design

A traceability matrix of all user requirements was elaborated, and the compliance of the design to these requirements was assessed. Explanations for meeting the requirements or failing to comply were provided. The validation analysis concludes that ANTREA cannot be deemed a valid design as two user requirements are not met. Nonetheless, the design does possess a number of advantages that could not be foreseen by the customer, such as a mass of more than 50 % below the limit.

Project Design and Development Logic

Placing the team's project in the context of a real mission, the phases that would follow the preliminary design presented in this report were assessed. The logical orders of activities performed during the DSE working hours were summarised and the next phases of the design's life cycle from iterating the design in more detail, testing it, qualifying it, producing it, using it and disposing of it were assessed. These actions were also translated to a Gantt chart, through which a timeline was elaborated.

Conclusion

The purpose of this project and of the Defend Our Territory mission as a whole was to design an asteroid sensing network of PocketQubes to characterise a very small near Earth Asteroid. By performing trade-offs and extensive simulations and research, the team came up with the ANTREA design (Advanced Net To Rescue Earth from Asteroids). This design consists ofa 15×15 m net, which possesses PocketQubes (PQs) attached at its nodes. The main reason for choosing a net as the team's final design is directly linked to the higher chances that the design possesses in terms of landing and attaching the system on the asteroid's surfaces, as well as to evenly distribute the 69 PQs around it. With this design, all eight asteroid characteristics that were required to

be investigated by the team's customer can be investigated by ANTREA. The very small near Earth asteroid that will be investigated is the 2017FU102, and the team is confident that the scientific data retrieved from it during the DOT mission, can help in improve nowadays' asteroid models made from Earth observations, and thus better protect planet Earth from a future potential asteroid crash, hence defending our territory to a greater extent.

Recommendations

Recommendations for future work are indicated at the end of this report. They focus on both the managerial and technical aspect of this project, mainly focusing on team organisation and system engineering methods, but also on ANTREA's different elements and subsystems such as the astrodynamic analysis, the design of the net, Deployer, structure, and mechanisms of the PQ, the choice of payload instruments, communication, electrical power system, thermal control, command and data handling, and cost of the system as a whole.

Change Log

- Improved List of Abbreviations and List of Symbols.
- The Executive Overview was updated.
- chapter 4: Updated the Market Segmentation table by removing completely unfeasible applications and being more specific on its application.
- chapter 5: Updated budgets sections- updated versions of mass, volume and power budget tables, updated graphs.
- chapter 6: The FFD and FBS and the corresponding chapter were made more clear.
- chapter 8: Updated attachment subsection and simulations on net deployment and asteroid attachment.
- chapter 9: Calculations and renders were added.
- chapter 10: Updated section concerning the mechanisms.
- chapter 11: Updated payload chapter and the total data volume.
- chapter 12: Overview subsection removed, link budget table added.
- chapter 13: Updated reasoning on values such as Depth of Discharge and why there is one solar panel only on the +Z side and none on the CPQs. Added images on some of the COTS components selected.
- chapter 14: The assumption about conduction of the asteroid is explained in more detail.
- chapter 15: Updated Software Design section- updated version of the software block diagram, removed state diagram. Updated Hardware Design section: updated version of the table with components, added component depiction.
- chapter 17: The verification of the calculations was updated.
- chapter 18: Increased the amount of numerical values in the sensitivity analysis.
- chapter 19: Updated values detailing subsystems' performances in the Performance analysis.
- chapter 20: Updated explanations of the risks connected to the Deployment.
- chapter 21: The RAMS was rewritten to meet standards.
- chapter 22: Updated Sustainability according to the Market Analysis changes .
- chapter 24: The hardware cost is explained in more detail, the testing cost was updated.
- chapter 25: Updated chapter introduction, updated Feasibility Analysis section.
- chapter 26: New redefinition of the length of project phases.
- chapter 28: Recommendations were updated.

List of Abbreviations

Abbreviation	Property
1P	1 unit PocketQube
a	Risk: weight assigned to severity
ADCS	Attitude Determination and Control System
ADR	Active Debris Removal
AHP	Analytical Hierarchy Process
AIV/T	Assembly, Integration, Verification and Testing
AM0	Air Mass Coefficient
ANTREA	Advanced Net To Rescue Earth from Asteroids
AR	Acceptance Review
AU	Astronomical Unit
b	Risk: weight assigned to probability
BLDC	Brush-less Direct Current
BPSK	Binary Phase Shift Keying
BWG	Beam Wave Guided
C3	Characteristic energy
C&DH	Command and Data Handling
CDR	Critical Design Review
CFD	Communication Flow Diagram
COMMS	Communication subsystem
COSPAR	Committee On Space Research
COTS	Commercial Off The Shelf
CPQ	Communications PocketQube
CPU	Central Processing Unit
CRR	Commissioning Result Review
CSG	Guiana Space Centre
DC	Direct Current
DDS	Data Distribution System
DoD	Depth of Discharge
DOF	Degrees of Freedom
DOT	Design Option Tree
DSE	Design Synthesis Exercise
DSN	Deep Space Network
ECA	European Chemicals Agency
EIRP	Effective Isotropic Radiated Power
EM	Engineering Model
EOL	End of Life
EPS	Electrical Power System
ESA	European Space Agency
ESC	Electronic Speed Control
ESOC	European Space Operations Centre
ESTRACK	European Space Tracking
FBS	Functional Breakdown Structure
FDIR	Failure Detection, Isolation and Recovery
FEM	Finite Element Method
FFD	Functional Flow Diagram
FM	Flight Model
FMEA	Failure Mode and Effective Analysis
FMECA	Failure Mode, Effect and Critical Analysis
FRAM	Ferroelectric Random Access Memory
FRR	Flight Readiness Review
GEO	Geosynchronous Equatorial Orbit
GMAT	General Mission Analysis Tool
GMRT	Giant Metrewave Radio Telescope
GMSK	Gaussian Minimum Shift Keying
GNC	Guidance, Navigation, and Control
GTO	Geostationary Transfer Orbit
HEO	Highly Elliptical Orbit
HMPE	High Modulus-Polyethylene
HM-HT	High Modulus-Tenacity
IARC	International Agency for Research on Cancer
IMU	Inertial Measurement Unit
IR	Infrared
ISIS	Innovative Solutions In Space
ITU	International Telecommunication Union
JAXA	Japan Aerospace Exploration Agency
JPL	Jet Propulsion Laboratory
LCC	Lightbridge Communications Corporation
LCP	Left Circular Polarised
LEO	Low Earth Orbit
LIDAR	LIght Detection And Ranging
LRR	Launch Readiness Review
LRR	End of Life Readiness Review
MCU	Micro Controller Unit
MCR	Mission Close-out Review
MDR	Mission Design Review
MISO	Master In Slave Out
MOSI	Master Out Slave In
MPPT	Maximum Power Point Tracking
n.a.	not available
NASA	National Aeronautics and Space Administration
OBC	On-Board Computer
OCC	Operations Contol Centre
ORR	Operational Readiness Review
PCB	Printed Circuit Board
PHA	Potential Hazardous Asteroid
PI	Principal Investigator
PPQ	Scientific payload-carrying PocketQube
PPQ-1	PocketQube type 1
PPQ-2	PocketQube type 2
PQ	PocketQube
PST	Planetary Science Archive
PTFE	Polyetrafluoroethylene
QM	Qualification Model
QPSK	Quadrature Phase Shift Keying
QR	Qualification Review
RAMS	Reliability, Availability, Maintainability and Safety
RCP	Right Circular Polarised
RDV	Rendezvous
RF	Radio Frequency
RTC	Real Time Clock
RVB	Rendezvous Burn
S/C	Spacecraft
SCLK	Serial Clock
SMAD	Space Mission Analysis and Design
S3R	Sequential Switching Shunt Regulator
SNR	Signal-to-Nose Ratio
SOI	Sphere of Influence
SOM	Spacecraft Operations Manager
SPI	Serial Peripheral Interface
SRR	System Requirements Review
SS	Slave Select
STM	Structural and Thermal Model
SWOT	Strengths, Weaknesses, Opportunities and Threats
TASC	Triangular Advanced Solar Cells
TBD	To Be Determined
TOI	Transfer Orbit Injection
TRL	Technology Readiness Level
TT&C	Telemetry, Tracking and Command
TU	Technical University
UAV	Unmanned Aerial Vehicle
UHF	Ultra High Frequency

List of Symbols

Symbol	Unit	Property
α	$[K^{-1}]$	Resistivity temperature coefficient
α	[-]	Absorption
δ	$[mm]$	Elongation
ΔQ	$[J]$	Supplied heat
ΔT	$[°C]$	Temperature difference
ΔV	$[m/s]$	Velocity change
ϵ	[-]	Emissivity
ϵ_{ast}	$[-]$	Emissivity of asteroid
ϵ_{eff}	$[F/m]$	Effective dielectric constant
ϵ_r	$[F/m]$	Dielectric constant
η	[-]	Transmission efficiency
η_c	[-]	Efficiency of the solar cells
η_l	[-]	Line loss
η_{tot}	$[-]$	Total Efficiency

Symbol	Unit	Property
θ	$[deg]$	Ejection angle
θ_a	[°]	Incidence angle solar flux on solar cells
λ	$[m]$	Wavelength
ρ	$[g/cm^3]$	Density
ρ	$[\Omega m]$	Electrical resistivity
ρ_0	$[\Omega \times m]$	Resistivity of material at 20 °C
ρ_{cable}	$[\Omega \times m]$	Resistivity of cable
σ	$[W/m^2K^4]$	Stefan-Boltzmann constant
σ	[-]	Standard deviation
σ	$[MPa]$	Stress
σ_{al}	$[MPa]$	Yield stress aluminium
$\sigma_{critical}$	$[MPa]$	Critical buckling stress
Σ	[-]	Summation
ω	$[rad/s]$	Rotational speed
ω	$[N/m]$	Distributed load
a	$[m/s^2]$	Acceleration
a	[-]	Albedo
A	$[m^2]$	Cross-section
A'	$[m^2]$	Area
A_{ast}	$[-]$	Albedo of asteroid
a_{ast}	$[AU]$	Semi-major axis of asteroid
$A_{asteroid}$	$[m^2]$	Area exposed to indirect solar flux
A_{IR}	$[m^2]$	Area of PQ that receives IR radiation
A_out	$[m^2]$	Area of PQ that emits heat
A_{SA}	$[m^2]$	Solar panel area
A_{SC}	$[m^2]$	Area solar cell
A_{sun}	$[m^2]$	Area of PQ that receives sunlight
b	$[m]$	Wall length
C	$[Ah]$	Required rated battery capacity
C_{actual}	$[Ah]$	Actual required battery capacity
C_{req}	$[Wh]$	Total required battery capacity
C	[-]	Constant
c	$[J/K]$	Specific heat capacity
d	[m]	Distance
d	[m]	Asteroid-Sun distance
D	[%]	Degradation of solar cells per year
d_{reel}	[m]	Reel-in distance
D_w	[m]	Worst case asteroid-Sun distance
E	$[MPa]$	Young's Modulus
E	$[Wh]$	Energy
E_b/N_0	$[dB]$	Energy per bit to Noise Ratio
$E_{bullets}$	$[Wh]$	Energy stored by batteries in the bullets
E_k	$[J]$	Kinetic energy
E_s	$[J]$	Potential energy
F	$[N]$	Force
f	[-]	Packing factor
f	[-]	Maximum deployment fraction
f	$[Hz]$	Frequency
F_c	[-]	Factor of %PPQs in eclipse
F_{load}	$[N]$	Design landing load
g_0	$[m/s^2]$	Standard gravity
G/T	$[dB]$	Gain over system noise temperature
h	$[m]$	Height
I	$[mm^4]$	Moment of Inertia
I	$[Ns]$	Impulse
I_{actual}	$[A]$	Actual discharge current of battery
I_{cable}	$[A]$	Current carried by cable
I_d	[-]	Inherent degradation
I_{EOL}	$[W/m^2]$	EOL irradiance received by solar cells
I_{mp}	[A]	Maximum power point current
I_s	$[W/m^2]$	Average solar intensity received on Earth
I_{sp}	$[s]$	Specific impulse
k	$[-]$	Peukert's constant
k	$[N/m]$	Spring stiffness
L	$[m]$	Length
L	[years]	Life time Lander
l	$[m]$	Cable length
L_0	$[W]$	Solar luminosity
L_d	[-]	Time dependent degradation loss
L_{FSP}	$[dB]$	Free space loss
L_T	$[dB]$	Total propagation losses

Symbol	Unit	Property
$\dot{m}$	$[kg/s]$	Mass flow
m	$[kg]$	Mass
M	$[Nm]$	Moment
M	$[g/mol]$	Molar mass
m_{PQ}	$[kg]$	PQ mass
n	$[mol]$	Number of moles
N	[-]	Amount
N_{PPQ}	[-]	Number of PPQs being used
N_{tot}	[-]	Total amount of PQs being used
P_{diss}	[W]	Power dissipation
P_{elec}	[W]	Electrical power
P_{EOL}	[W]	End of Life power
P_{in}	$[W]$	Input power
P_{load}	$[W]$	Average power Required by the load
P_{loss}	[W]	Power loss
P_{mech}	$[W]$	Mechanical power
P_{sun}	[W]	Luminosity of the Sun
Q	$[mm^3]$	First moment of area
Q	[W]	Heat flux
Q_{env}	[W]	Absorbed environmental heat
$Q_{insulation}$	[W]	Heat-flux through insulation layer
r	$[m]$	Radius
r	[-]	Ratio
R	$[J/molK]$	Gas constant
R	$[W]$	Power loss
R	$[m]$	Distance
R	$[\Omega]$	Electrical resistance
R_{cable}	$[\Omega]$	Resistance of cable
R_{data}	$[bits/s]$	Data rate
R_{sun}	[m]	Radius of the Sun
S	$[W/m^2]$	Flux density
s	[m]	Side
$S_{asteroid}$	$[W/m^2]$	Indirect solar flux
S_{IR}	$[W/m^2]$	Flux density due to infrared radiation
T_{ast}	$[K]$	Mean temperature of asteroid
t_D	$[s]$	Nominal battery discharge time
$t_{D-actual}$	$[s]$	Actual battery discharge time
t_{op}	$[h]$	Operational time before recharging
$T_{sub-solar}$	$[K]$	Sub-solar temperature of the asteroid
T	$[N]$	Thrust
T	[°C]	Temperature
T	$[Nm]$	Torque
t	$[s]$	Time
t	[mm]	Thickness
T_t	$[s]$	Total rotational period of asteroid
T_e	$[s]$	Time spent in eclipse
t_{abs}	$[s]$	Absorption time for damping
$T_{asteroid}$	[K]	Temperature of the asteroid
T_{atm}	$[K]$	Atmospheric temperature
T_{sun}	[K]	Temperature of the Sun
U	[-]	Insulation factor
V	$[V]$	Voltage
V	$[m/s]$	Velocity
V	$[N]$	Shear force
v	$[m/s]$	Velocity
v	[mm]	Deflection
V_{bullet}	$[V]$	Voltage across battery in bullet
V_{cell}	$[V]$	Voltage across battery in PQ
V_{load}	$[V]$	Load voltage
V_{mp}	$[V]$	Maximum power point voltage
v_{PQ}	$[m/s]$	Approach speed PQs
W	$[m]$	Width
x	$[m]$	Compressed distance
y'	$[m]$	Distance from neutral line to area A'

Contents

I

PROJECT'S ORIGINS, DESCRIPTION, AND POTENTIAL

1

INTRODUCTION

Miniaturisation enables a new amazement in space, which is not led by the largest, most complex and powerful rockets nor the ambitions of superpowers determined to demonstrate their influence. This very new excitement stems from a cheaper access to space that humanity has been striving for for so long. The ideas naturally converged into smaller satellites and designs, where not big but smart matters. PocketQubes are driving this development to a new peak, empowering missions like Defend Our Territory to perform important and possibly life-saving science in combination with technology demonstration. The miniaturisation of sensors can open new worlds of applications and the DOT team is keen on presenting and manifesting its power.

The aim of the DOT mission is to design an asteroid sensing network of PocketQubes to characterise a very small near Earth asteroid. Asteroids are of great value for scientific purposes, as they can be considered as the building blocks of life on our planets and therefore provide valuable insight on the origin of our solar system and its evolution. They are observed by remote instruments such as telescopes, however, the data are found to be inaccurate, especially for small asteroids. In the Rosetta[1] and Hayabusa 2[2] missions, the characteristics turned out to be quite different than what was expected from the telescope data. It is thus of utmost importance to be able to improve today's asteroid characterisation methods, in order to reduce uncertainties that might occur during future space missions. Determining asteroids' characteristics with high accuracy is also key to the creation of deflection procedures to defend the Earth from potential asteroid impacts. A Mission Need Statement was thus drafted as follows: "The mission shall fill in the knowledge gap on Very Small Near Earth Objects in order to defend our territory". The target asteroid 2017 FU102 was chosen, and as it is very small, the PocketQube technology is an incredibly useful technology for the mission. The asteroid's close approach to Earth is expected to take place around April 3^{rd} of 2036. If for some reason the asteroid is deemed an unacceptable target in the upcoming years, asteroid 2014 HB177 with a close approach date of May 6^{th} of 2034 can serve as a backup.

The current phase of the project started with the detailed design of the chosen Lander concept: a net with PQ sensors attached at its nodes. The design was named ANTREA: Advanced Net To Rescue Earth from Asteroids. In order to do comply with this ambitious namesake aim, multiple iterations have been performed on the design's budgets. Great focus was also put on the detail of the subsystem's design.

This report is structured into four parts. In the first part "Project's Origins, Description and Potential", the user requirements are established. Also, the trade-off that led to the final ANTREA design (chapter 3), as well as the design's Market Analysis (chapter 4) are present. Part II "Detailed Technical Design" contains the technical overview (chapter 5, functional analysis of the system and astrodynamic analysis of the space mission. Additionally, the subsystem design of the Net, Deployer, Structure of the PQs, Payload, Communication, Electrical Power System (EPS), Thermal Control and Command and Data Handling (C&DH) are detailed in chapter 8 to chapter 15. Finally it contains the Spacecraft Operations and Verification of the design calculations. In part III "Design Evaluation", the sensitivity, performance and risk analyses are described. Furthermore, the Reliability, Availability, Maintainability, and Safety (RAMS) (chapter 21), the design's sustainability approach (chapter 22), the production plan (chapter 23), cost analysis chapter 24) and validation of the design (chapter 25) are elaborated on. Finally, part IV "Future of the Project" contains the Project Design Development Logic, the conclusion of this report (chapter 27) and the recommendations for future work (chapter 28).

[1] http://sci.esa.int/rosetta/ [Accessed 2 May 2019]
[2] http://www.hayabusa2.jaxa.jp/en/ [Accessed 2 May 2019]

2

User Requirements and Constraints

This chapter will summarise the User Requirements and constraints that drove the ANTREA design. Most of the User Requirements became top level requirements, however some of them like mass and volume ones were placed at a lower level. The identifier scheme that was used is based on abbreviations denoting different categories and numbering for different requirements within the same category. The meaning of the abbreviations is as follows (note: sometimes combinations of abbreviations and numbers where shortened into a new abbreviation). DOT: Defend Our Territory, AST: requirements on the asteroid type, COST: requirements on the cost of the lander, SCH: requirements on the schedule of the mission, DUR: requirements on the length of the mission, SAF: requirements on environmental safety, LAN: requirements on the lander, MS: Requirements on the Mothership, MD: requirements on the deployment system, PQ: requirements on the PocketQubes, SC: Requirements on the sensors and distributed measurements and MOD: Requirements on the adaptability of the system. The rationales for the requirements are written in italic after each requirement.

DOT-AST-1 : The minimum orbital intersection distance of the asteroid with the Earth shall be less than 0.05 AU. *This is an adapted version of the user requirement that states that we have to land on a PHA, as the minimum size of PHAs,* 140 *m, would be inconsistent with* ***DOT-AST-2****.*

DOT-AST-2 : The asteroid shall have a diameter no more than 20 m. *User requirement.*

DOT-COST-1 : Development, production, and testing costs of the Lander System shall not exceed 4 M USD. *User requirement.*

DOT-SCH-1 : The mission shall be operative on the target asteroid before 2040. *User requirement.*

DOT-DUR-1 : The instruments shall be able to provide data for no less than 1 month. *User requirement. This is the minimum time needed to allow for sufficiently valuable scientific data to be obtained.*

DOT-SAF-1 : The materials used for the production of the spacecraft shall not be hazardous to the environment. *User requirement.*

DOT-LAN : The mission shall be performed by a Lander System. *Based on the user requirement that the measurements have to be taken on the surface of the asteroid.*

DOT-LAN-MS : The Lander System shall be delivered to the asteroid by a Mothership spacecraft. *This specifies that the Lander does not have to perform the whole transfer autonomously.*

DOT-LAN-MS-3 : The Mothership shall perform a RDV manoeuvre at the asteroid. *It needs to match the asteroid's velocity and perform some manoeuvres to take pictures from multiple sides.*

DOT-LAN-MS-4 : The Mothership shall provide the Lander System <TBD> W of power during transit. *This is just to keep the Lander turned on, but in low-power mode.*

DOT-LAN-MS-5 : The Mothership shall provide the Lander System <TBD> W of power during the <TBD> hours preceding the deployment. *This is to charge the Lander's batteries before deployment start turning on its subsystems.*

DOT-LAN-MS-6 : The Mothership shall provide a communication link between the Lander System and Earth. *This is to upload information to the Lander before deployment.*

DOT-LAN-MD : The Lander System shall be composed of a Deployer and a Network of PQs called Lander. *Definition used in this requirement list.*

DOT-LAN-MD-1 : The Deployer shall sustain the loads at all mission phases. *This mostly means it has to survive launch loads.*

DOT-LAN-MD-3 : The mass of the Lander System shall not exceed 50 kg. *User requirement.*

DOT-LAN-MD-4 : The volume of the Lander System shall not exceed $30 \times 30 \times 30$ cm^3. *User requirement.*

DOT-LAN-PQ-1 : The PQs shall sustain the loads at every phase of the mission with a reliability rate of 80 % or higher. *User requirement.*

DOT-LAN-PQ-SC-1.1 : The PQ network shall measure the shape and size of the asteroid with an accuracy of <TBD>%.

DOT-LAN-PQ-SC-1.2 : The PQ network shall measure the surface composition and its roughness with an accuracy of <TBD>%.

DOT-LAN-PQ-SC-1.3 : The PQ network shall measure the material properties of the asteroid with an accuracy of <TBD>%.

DOT-LAN-PQ-SC-1.4 : The PQ network shall measure the temperature distribution of the asteroid with an accuracy of <TBD>%.

DOT-LAN-PQ-SC-1.5 : The PQ network shall measure the asteroid dynamic motion with an accuracy of <TBD>%.

DOT-LAN-PQ-SC-1.6 : The PQ network shall measure the asteroid's surface hardness with an accuracy of <TBD>%.

DOT-LAN-PQ-SC-2 : The PQs shall perform the measurements distributed around the asteroid. *The PQs need to be distributed as much as possible over the surface of the asteroid.*

DOT-MOD-1 : The Lander System shall be usable with minor modifications for other asteroids with sizes up to 1 km. *User requirement.*

More specific requirements were then drafted for the ANTREA design, based on the given User Requirements and constraints. General requirements are present below, while other more specific to every subsystem are described in following chapters.

DOT-SAF-2 : The Lander shall comply with all COSPAR requirements applicable to category I. *The applicable COSPAR category depends on the type of asteroid.*

DOT-SAF-3 : The use of COTS components shall be prioritised. *COTS components have lower development and testing cost, which also makes them better for sustainability.*

DOT-SAF-3.1 : The COTS components shall be protected from the deep space environment. *COTS components are usually not built for a space environment, so measures have to be taken to ensure they still work adequately.*

3
Trade-Off and Design Presentation

The trade-off performed during the conceptual design will be shortly explained in this chapter. This is done to gain a better understanding of how the team arrived at the design that entered the (preliminary) detailed design phase. When starting designing a Lander for this mission, many concepts were thought of. During an initial trade-off, seven concepts were explored, and graded based on five criteria: performance, feasibility, risk, sustainability and the degree of innovation. This initial trade-off resulted in three concepts to be investigated more closely. These were the concepts SINGLE, FLEX and NET. After more research was done, a second trade-off was performed between those three to establish which concept would enter the detailed design phase of this project. This trade-off will be detailed below after which a concise description of the winning design will be given.

3.1. Design Concepts

As mentioned above, the concepts considered were the SINGLE, FLEX and NET. There were made with the help of a design option tree. The concepts were still left open in some aspects according to the tree. A short description of each concept will be given below to allow for a better understanding of the trade-off. A detailed description of the designs can be found in the Baseline Report [3].

SINGLE: The Mothership deploys 125 individual PQs, with every PQ possessing an individual deployment, landing and attachment system. There is no physical connection between the PQs and as a result, they generate power themselves and communicate with each other via radio. The deployment mechanism can either consist of two treadmills, that clamp and accelerate the PQs out of the Deployer, or of a classical spring system. The attachment consists of 8 grippers mounted on the sides of each PQ, that would drop on the asteroid's surface due to their inertia once the PQ hits the surface. After that the cables would be retracted to provide

proper attachment. All User Requirements in terms of science can be met, except for the asteroid's roughness and possibly surface composition measurements. The power will be provided by deployable solar cells on 4 sides of the PQs. Depending on the frequency and ground station, the achievable data rate for this design is in the range of 12 – 52 kBit/s.

FLEX: The 40 PQs are interconnected by two cables of 75 m long, and the system is wrapped twice around the largest expected asteroid. The PQs can transfer power and data through connection cables, on which solar tape is mounted. The Deployer shoots a harpoon which provides the first point of attachment for the "winding" of the system around the asteroid. The deployer has a propulsion and ADCS unit, is ejected from the Mothership and used to control the landing of the PQs. Each PQ possesses small hooks to attach itself to the surface once it touches down. On the science side, 32 PQs are reserved for science and all User science Requirements can be met. The other 8 PQs are dedicated for communication to Earth, with a downlink data rate of 74−1018 kBit/s.

Net: 72 PQs are connected in a square net of 12.1 m in size to ensure a good distribution of the PQs on the asteroid. The PQs are connected by Dyneema fibre, and additional copper cables enabling power transfer. Flexible solar panels are included in the net. Each PQ has a maximum mass of 300 g. 64 PQs are used for science, while 8 are dedicated to communications. All User Requirements in terms of science can be met. Additionally, the downlink data rate ranks from 90 to 1218 kBit/s.

3.2. Trade-Off Criteria

To be able to evaluate all concepts in a structured and trustworthy manner, criteria were established to judge the concepts upon. The five main criteria on which the concepts were judged are: performance, feasibility, risk, innovation and sustainability. Most of these main criteria have sub-criteria as well to allow for more detailed evaluation. In the Baseline Report [3] an extensive explanation is given. Below, a short description is provided. Not all criteria were considered of equal importance. An Analytic Hierarchy Process (AHP) was performed for both the main criteria as well as for the sub-criteria, involving the project's tutor (counted double), customer (counted double), coaches (counted as 1.5) and team members (counted single). The final AHP weights can be seen in Table A.1, present in appendix A.

Performance evaluates to what extent the concept is able to accomplish the previously defined Mission Need Statement. Performance consist of six sub-criteria and is mainly based on the allocated budgets. Firstly, the payload mass relates to the mass budget available for scientific payload as a percentage of the total available mass of 50 kg. Secondly, the available power relates to the amount of power available being enough to power the payload. This is split over two stages: landing (stage 1) and active (stage 2), the latter is used while performing measurements on the asteroid. Thirdly, the payload volume corresponds to the volume budget available for scientific payload as a percentage of the total volume of 27 L. Fourthly, measurement types are based on how many of the eight asteroid characteristics can be investigated by this concept. The eight characteristics being size, shape, surface composition, materials, roughness, hardness, temperature distribution and asteroid dynamics. Moreover, the approach and facing of the PQ sub-criterion is based on the distribution of the PQs over the asteroid, the amount of PQs taken on the mission and PQs landing in the correct orientation (so with the right side up). Lastly, the amount of data evaluates the data volume that can be sent to Earth, which is indirectly the amount of power available for communication.

Regarding feasibility there are five sub-criteria. Every concept is judged on the capability to achieve deployment, approach, landing, attachment and measurements. This includes the accuracy of the approach path and the ability to control the approach, as well as the ability to determine the landing spot of the PQs, the ability of the attachments to attach and complexity of the attachment techniques.

The risk criterion consists of two sub-criteria: severity and probability, as risk is the product of those two. Risk was calculated with $Risk = Severity^a \cdot Probability^b$, where a and b are the weights of severity and probability respectively. The risk trade-off was done based on the risk map. The lowest 20% were labelled with the best score as this could directly be derived from the User Requirement on reliability (DOT-LAND-PQ-1).

Innovation is based on how creative the design is, and if it is an new application or idea. However, it did not have any sub-criteria.

Sustainability is a relevant topic in today's society, and was therefore part of the trade-off criteria. It has four sub-criteria. Firstly, the use of COTS components in the concept. Secondly, the reusability or scalability of the design, which was directly based on a User Requirement (DOT-MOD-1). Thirdly, the toxicity of the materials is evaluated, this is also based on a User Requirement (DOT-SAF-1). Lastly, the ecological footprint of the production method is judged.

3.3. Result and Sensitivity Analysis

After all concepts were judged on all criteria, the result was computed. This can be seen in Table A.1. The colours were given scores as follows: blue was given 6, green was given 4, orange was given 1 and red was given 0. This makes the gap between acceptable and not satisfactory bigger than the gap between acceptable and excellent as this was the desired strategy.

The sensitivity analysis that was performed on this trade-off showed that changing the scores of all colours did yield the same final outcome. Another sensitivity analysis was performed that changed red into orange. This did not change the outcome of the trade-off. Finally, the weights of the main criteria (performance, feasibility and risk) were switched around which did not influence the outcome. Also the weights of the sub-criteria were changed and yielded the same result. Thus, the sensitivity analysis showed that it can be stated that the trade-off is robust. The design that will enter the detailed design phase is NET.

3.4. ANTREA

As this concept entered the detailed design phase, it was given a final name: ANTREA. This has a double meaning. Firstly, ANTREA is the abbreviation of "Advanced Net To Rescue Earth from Asteroids". Secondly, an Antrea net is one of the oldest known fishing nets in the world found in the village Antrea in Finland. As the team's design is based on a net, this seemed a suitable name.

The ANTREA design consists of 69 PQs which are connected to a square shaped net of 15 × 15 m. The PQs are no longer homogeneous, but have different layouts due to volume restrictions. Furthermore, the amount of PQs used for science decreased to 59. Still, all User Requirements in terms of science can be met. Also the amount of PQs used for communication increased to 10. The power will be provided by solar cells put on the +Z side of the two types of payload PQs (the PPQs).

4

Market Analysis

Market analysis is a way of researching the market to determine its opportunities, threats and how clients will react to the product/services being produced. Market analysis is required to formulate a strategy on how to present the product/services on the market taking into account the competitors and opportunities that are presented.

In this chapter, the market segmentation will be discussed where the different customers and companies would be interested in a potential application of the system. Secondly, the cost of the product will be broken down if it entered the market right now. Furthermore, the competition will be addressed to evaluate any competitors and what will be done to ensure being a worthy competitor. Finally, a SWOT analysis is presented to show the strengths, weaknesses, opportunities and threats of the product.

4.1. Market Segmentation

It is important to differentiate the market based on what current customers need and what customers in the future will require. In this section the Market Segmentation is clearly defined by a table as can be seen in Table 4.1. The first column segments the market based on what the customer is interested in. The second column describes a potential application of the system, this could be a specific part of the system or the entire system. The third column gives an example of an existing customer such as ESA or a private company. The fourth column explains what society expects to gain out of this application. The fifth column explains the barriers that could potentially occur when implementing the application. Finally, the last column explains how the barrier could be mitigated.

Table 4.1: Market Segmentation Table

	Potential application of our system/services:	Example of a customer:	What we expect to get out of this:	Barriers present for each application:	Mitigation to the barriers
PocketQube Technologies	Using PocketQubes to perform radio experiments	Government Agencies (ESA, NASA, JAXA etc.)	Advancement in miniaturisation technology and advancement in more applications for PQs	Expensive costs for deployment compared to Cubesats	Design PQ deployer such that it is the same size of Cubesat deployer
	Using constellation of PocketQubes for certain missions instead of CubeSats	Alba Orbital, Gauss, Mini-Cubes LLC	Many satellites can be added to launcher which will reduce launch costs for a certain mission	Albeit launch costs are reduced they are still close to the launch costs of Cubesats	Design PQs with deployable solar panels that produce power comparable to that of Cubesats for example in Unicorn-2 by Alba Orbital
Particular subsystems	Using ANTREA's net without the PQs in the nodes for removing space debris	Government Agencies (ESA, NASA, JAXA etc.)	Clearing space debris making space safer for operational satellites	The ANTREA's net could miss the targetted space debris	Use antenna in the cables of the net to track it and ensure it catches the space debris
	Use deployer for deployment of solar sail	The Planetary Society	Allows a big solar sail to be deployed of 15 m x 15 m since the deployer is designed to deploy a net of this size	Not many customers interested since it is a fairly new concept	Ensure that a lot of testing is done and promote it as being sustainable as solar sails do not require fuel for its propulsion
	Using ANTREA's net to attach on a small surface on Mars used for communication between the Earth and Mars for the rovers like Curiosity	Government Agencies (ESA, NASA, JAXA etc.), Planetary Resources	Increase the data rate for rovers between Earth and Mars and hence allowing more pictures and data to be sent to Earth	ANTREA's net is unable to wrap around Mars due to the sheer size of Mars and therefore, it might bounce and not properly attach onto the small surface on Mars	Modify ANTREA's net such that there are hooks and grippers to ensure that the net adheres to the surface without any rebound
Properties of the target asteroid	Selling the data on the properties of the asteroid to companies that want to know these properties for asteroid mining	Government Agencies (ESA, NASA, JAXA etc.), Planetary Resources	Mining rare materials that can be brought back to Earth and used on Earth instead of using Earth's resources	Not many customers interested as it is not feasible at the moment with current technology	Advertise the accurate data on the properties of the asteroid to drive the research of technology to make the mission feasible
	Using the asteroid's properties to design a successful method to deflect asteroids	Government Agencies (ESA, NASA, JAXA etc.)	Ensure safety on Earth in case a PHA asteroid approaches Earth	Expensive mission costs and would require accurate information on the properties of the asteroid	Prioritise funding for this particular mission in case a PHA asteroid is expected to pass by Earth, ensure that the data collected by ANTREA is accurate enough to successfully deflect the asteroid
	Selling the data on the properties of the asteroid for scientific research of the origins of the solar system based on these properties	Scientists, Max Planck Institute for Solar System Research	A better insight on how solar systems are formed and can inspire young kids to become interested in science	Scientists would want more information other than what ANTREA is collecting and for longer periods of time	Use more PQs with a wider variety of payload sensors to detect more types of data and design the mission for a longer life-time

By analysing the mission elements of the ANTREA mission, it could be separated into 3 characteristics that could fit the needs of a certain customer. These are: PocketQube technologies, Particular subsystems, and Properties of the target asteroid.

PocketQube technologies: Customers may be interested in the PocketQube technology itself so the constant miniaturisation of satellites. This can be done by performing radio experiments. Government Agencies would be one of the leading customers and this would benefit society by the advancement of new technology. However, with every application there are certain difficulties that must be mitigated. Most difficulty involving PocketQube technologies is the fact that the technology is relatively new and therefore, costs are higher to deploy compared to CubeSats. This can be mitigated by simply designing a deployer such that it is the same size of a Cubesat deployer and hence can easily fit inside the launch vehicle.

Particular subsystems: Customers may be interested in only parts of the product, so customers would want to buy only ANTREA's net without the PQs in the nodes. This could be for instance to catch space debris, this is a topic many Government Agencies (NASA, ESA, JAXA etc.) are trying to tackle. An issue with this would be that the net could miss the space debris and would end up as space debris itself. To avoid this, the net could have antennae in the cable to allow it to be tracked and ensure that it hits the space debris.

Properties of the asteroid: Customers may be interested in knowing the different properties of the asteroid accurately. This could be for asteroid mining which has been increasingly gaining popularity over the past decade. Government Agencies would be primarily interested in such information, as well as, several private companies such as Planetary Resources. However, there are several issues, the most prominent one being The Outer Space Treaty which states: "Outer space is not subject to national appropriation by claim of sovereignty, by means of use or occupation, or by any other means[1] ". This could be mitigated by gaining the public's interest and compromising with the government agencies on making an exception for asteroid mining.

Further to what has been discussed, there is an interdependent relationship between Market Analysis and Sustainability. Nowadays, every mission that is being considered is taking sustainability into account and is a

[1] http://www.unoosa.org/oosa/en/ourwork/spacelaw/treaties/introouterspacetreaty.html [Accessed 22 June 2019]

prime factor into deciding how a mission will be conducted. Using ANTREA's net to remove space debris is a step in the direction for a sustainable environment. Furthermore, by sending constellation of PQs which each has its own mission is much more efficient and sustainable than sending individual PQs or few PQs on multiple rockets. More of this relationship including several more concepts will be discussed in chapter 22. To conclude the Market Segmentation, many of the potential applications described above are for current and future missions. However, many past space missions could have been designed and operated in a more efficient manner using the current technologies developed by ANTREA.

4.2. Market Value

The aim of miniaturising spacecraft is to make space more affordable. Therefore, the PQ will likely be put on the market for around 15,000 USD per PQ. However, it does depend on the payload so the price can go a bit up or down. Also, it has to be noted that the PQs currently only have limited power sources (solar panels), while when used autonomously, deployable solar panels will have to be added and tested. However, the price of around 15,000 USD per PQ should still be possible. The net, including weights as designed during the project, without PQs, will be put on the market for around 15,000 USD as well. Evidently, this price will change depending on the size of the net. A deployer can currently be bought for around 80,000 USD. Thus to ensure profit, the price would need to be lower, around 75,000 USD.

4.3. Competition

As of the writing of this report, there is no system or product that is able to land on a small asteroid to measure its different properties in a distributed way using the PocketQube form factor. There is however, competition on the particular subsystems, RemoveDEBRIS mission is using a net design to capture debris in space. Moreover, CubeSats present the biggest competitors when considering using PocketQube technology. Therefore, most clients will prefer using CubeSats since they have a lower overall cost when considering launching and developing costs. One of the leading companies in PocketQube technology is Alba Orbital and are selling a wide variety of PQ components, as well as PQ spacecraft. Albeit, the PQs are designed to only operate in LEO they still present competition in designing a PQ platform that lands on asteroids. Alba Orbital sells their first PocketQube, the Unicorn-1 for 159,000 euros for a 2p PQ and their second PQ, the Unicorn-2 for 199,000 euros for a 3p PQ[2]. Furthermore, GAUSS Srl is another company that could present competition since they are designing CubeSat and PocketQube deployers.[3]

4.4. SWOT Analysis

A SWOT analysis summarises the product in four categories, namely: Strengths, Weaknesses, Opportunities and Threats. The SWOT analysis is shown in Table 4.2, it is important to identify these categories as it will present how the product would prosper on the market. These characteristics are correlated with what was documented during the market segmentation.

Table 4.2: SWOT analysis

	Strengths	Weakness
External	- Uses nanotechnology, low mass and volume for launcher - Modifiable to be used for bigger target asteroids and other celestial bodies - Unmanned mission - Autonomous communication system - Modular so more units can be added together	- Limited data measured - Payload limited from low available power, mass and volume - Lack of missions involving PocketQubes - Lack of asteroid landing missions
	Opportunity	**Threat**
Internal	- Useful for scientific and research purposes - Can be useful for space debris application when modified - Can be used for constellations of satellites for communication or Earth observation - Can be used for military purposes such as surveillance or espionage - Useful information from the properties of asteroids can be used for asteroid mining companies	- Failure of mission due to the fact that it is the first of its kind because of its TLR level - Funding and schedule delays from the customer - Budget cuts - Competitors entering the market

[2] http://www.albaorbital.com/ [Accessed 22 June 2019]
[3] https://www.gaussteam.com/ [Accessed 22 June 2019]

II
Detailed Technical Design

5
ANTREA: Technical Overview

In the following chapter, outlines the most crucial technical data of ANTREA. It is intended to present the reader with a sort of overview of the system from the technical side. The chapter is opened by section 5.1, which gives a general systems engineering strategy that was used to manage the technical development of the project, which itself consists of Technical Budgets Approach (subsection 5.1.1), Contingency Management (subsection 5.1.3) and Technical Performance Management (subsection 5.1.2). What follows are the resulting Technical Budgets: Mass (section 5.2), Volume (section 5.3) and Power (section 5.4). This is followed by the explanation of system's operational modes (section 5.5), the N^2 chart of the system (section 5.6) and, finally, the presentation of the internal and external layout of the system's segments section 5.7.

5.1. Systems Engineering Approach

A correct implementation of systems engineering methods is a crucial element of system design. It is those methods that ensure a smooth integration of all the subsystems and allow for a controlled evolution of the design, that is for instance making sure that the maximum allowable values for mass and volume are not exceeded. The importance of systems engineering manifests itself especially if the system design is a concurrent engineering process: many subsystems which depend on each other are developed simultaneously hence an overview of all interfaces is essential for a successful design process.

5.1.1. Technical Budgets Approach

For both the volume and mass budgets, the allocation was broken down per segment and then per segment's subsystem. The segments and their subsystem division is presented below (Table 5.1)

Table 5.1: The breakdown of segments and subsystems

Segment	PPQs	CPQs	Net	Deployer
Subsystems	Scientific Instruments, C&DH, Batteries and EPS, Structures and mechanisms, Thermal control	Communications, C&DH, Batteries and EPS, Structures, Thermal control	Structural cables, Power and data cables, Weights, Attachments, Power generation	Ejection system, Structure

During the preliminary detailed design phase (which has resulted in the design presented in this report), there were 3 major phases of the technical budgets management:

- **Constructing allocated values.** A preliminary sizing of all subsystem was done. Based on this, the masses and volumes of all segments were compared to the total mass and volume yielding certain fractions. Those were in turn multiplied by the total available mass and volume, as specified by the customer.
- **Constructing target values.** Once the allocated values were known, the target values (subsection 5.1.2) were constructed using appropriate contingencies. The contingency levels are elaborated on in subsection 5.1.3.
- **Monitoring actual and current values.** The target values were provided to every department so that they could design for those values. Their best current estimates for subsystem volume and mass (actual values) were collected. Every change in the actual values resulted in a iteration. This method is elaborated in subsection 5.1.2.

5.1.2. Technical Performance Measurement

Previously, in subsection 5.1.1, the use of *allocated*, *target* and *actual values* was indicated. Table 5.2 gives a short explanation of the aforementioned values and also introduces the concept of *current value*. What follows

is a short description emphasising the importance of correctly using those concepts as a technical performance measurement tool.

Table 5.2: The definitions of Technical Performance Measurement terms

Name	Definition	Explanation
Allocated Specific Value	Value derived from preliminary sizing	Defined at the beginning of the project as an indication for technical resource allocation.
Target Value	$\frac{\text{Allocated Specific Value}}{100\% + \text{contingency}[\%]}$	The value that a specific department should design for.
Actual Value	Best current estimate	The most recent estimate based on design done by a specific department.
Current Value	Actual Value × (100% + contingency[%])	The indication of the what the values based on the design could become.

As already indicated in subsection 5.1.1, while the design phase progressed, the actual values of subsystems were noted after every iteration. From those, the current values were constructed. At the segment level, those values were monitored: the actual values were compared to target values and the current values were contrasted with the allocated values. An intervention from the systems engineer would be necessary in case the actual value exceeded the target value and/or the current value exceeded allocated specific value. This is an effective way of ensuring the design does not exceed the constraints set by the customer. What is more, this can also work in the other direction: if, for instance, the mass of the system is significantly lower than the target value, some more available mass can be reallocated to allow for more design freedom of the departments.

5.1.3. Contingency Management

As mentioned in subsection 5.1.1 and subsection 5.1.2, to construct the target and values in the budgets, certain contingency levels were used. The overview of the contingencies used during the system design is outlined in Table 5.3 below.

Table 5.3: The outline of contingency levels used for the systems engineering during the design.

Level	**System**	**Subsystem**		
Contingency [%]	10	5	10	20
Explanation	-	Made fully from COTS components.	Based on COTS components.	Custom design.

As can be seen in Table 5.3, there was a 10% contingency level taken on the whole system. This was done while constructing the allocated value: customer-specified maximum mass and volume were 50 kg and 27 L respectively, so the allocated values became 45 kg and 24.3 L. On the subsystem level, the contingency depended whether it included some ready-developed components or whether it needed full development. Those levels are based on ESA standards ([4]) and were agreed upon following a consultation with a space systems engineer, Dr. Angelo Cervone.

After performing the last iteration, the contingencies taken at the subsystem level were decreased to one level lower (so for instance from 20% to 10%). That is due to the fact that the system was designed in sufficient detail to increase the confidence level in matching the actual values. What is more, the evolution of the budgets with time showed a decreasing trend in the actual values (consult Figure 5.1 and Figure 5.3).

5.2. Mass Budget

This section presents the mass budgets resulting from the previously outlined systems engineering approach (section 5.1).

Budget Evolution

In Table 5.4, Table 5.5, Table 5.6 and Table 5.7, the changes in mass budgets over the 5 performed design iterations are outlined.

Table 5.4: PPQ mass evolution.

		PPQs (62; uniform)	PPQs (59; uniform)	PPQs (59; uniform)	PPQs (59; uniform)	PPQs (59; uniform)	PPQs (10; PPQ-1)	PPQs (49; PPQ-2)
Item	**Allocated [%]**	**Target Value [g]**	**Actual Value [g] (12/06)**	**Actual Value [g] (13/06)**	**Actual Value [g] (14/06)**	**Actual Value [g] (17/06)**	**Actual Value [g] (20/06)**	**Actual Value [g] (20/06)**
Instruments	59.7	221.3	227.4	27.4	27.5	27.5	8.1	17.6
C&DH	6.6	24.3	25.0	25.0	6.2	20.0	9.5	9.5
EPS	6.9	25.6	12.0	12.0	12.0	12.0	26.5	26.5
Structures & mechanisms	26.3	97.3	132.1	105.0	105.0	95.3	70.6	70.6
Thermal control	0.5	1.9	2.0	2.0	1.5	1.5	1.5	1.5
Solar panels	0.0	0.0	2.3	2.3	2.3	2.3	9.9	9.9
SUM	100.0	370.5	400.8	173.7	154.5	158.6	126.2	135.7

Table 5.5: CPQ mass evolution.

		CPQs (10; uniform)	CPQs (10; uniform)	CPQs (10; uniform)	CPQs (10; uniform)	CPQs (10; uniform)	CPQs (10; uniform)
Item	**Allocated %**	**Target Value [g]**	**Actual Value [g] (12/06)**	**Actual Value [g] (13/06)**	**Actual Value [g] (14/06)**	**Actual Value [g] (17/06)**	**Actual Value [g] (20/06)**
Instruments	59.5	194.6	200.0	204.5	204.5	75.0	75.0
C&DH	7.4	24.3	25.0	25.0	6.2	20.0	9.5
EPS	7.8	25.6	26.3	26.3	26.3	26.3	26.5
Structures	25.3	82.7	124.7	85.0	85.0	44.5	67.3
Thermal control	0.0	0.0	0.0	3.0	1.5	1.5	1.5
Solar panels	0.0	0.0	2.3	2.3	2.3	2.3	0.0
SUM	100.0	327.3	378.3	346.1	325.8	169.6	179.8

Table 5.6: Deployer mass evolution.

		Deployer					
Item	**Allocated [%]**	**Target Value [kg]**	**Actual Value [kg] (12/06)**	**Actual Value [kg] (13/06)**	**Actual Value [kg] (14/06)**	**Actual Value [kg] (17/06)**	**Actual Value [kg] (20/06)**
Ejection system	44.2	1.0	1.8	1.8	1.8	1.8	-
Structure	55.8	1.3	1.5	1.5	1.5	1.5	-
SUM	100.0	2.4	3.3	3.3	3.3	3.3	4.1

Table 5.7: Net mass evolution.

		NET					
Item	**Allocated %**	**Target Value [kg]**	**Actual Value [kg] (12/06)**	**Actual Value [kg] (13/06)**	**Actual Value [kg] (14/06)**	**Actual Value [kg] (17/06)**	**Actual Value [kg] (20/06)**
Cables structural	8.4	0.9	1.0	1.0	1.0	1.0	1.0
Cables power	8.4	0.9	1.0	1.0	1.0	1.0	0.8
Weights	67.0	6.9	8.0	8.0	8.0	8.0	8.0
Attachments	2.5	0.3	0.3	0.3	0.3	0.3	-
Solar panels	13.7	1.4	-	-	-	-	-
SUM	100.0	10.3	10.3	10.3	10.3	10.3	9.8

Figure 5.1 presents the trends in mass budget values. For definition of specific terms of different values refer to Table 5.2.

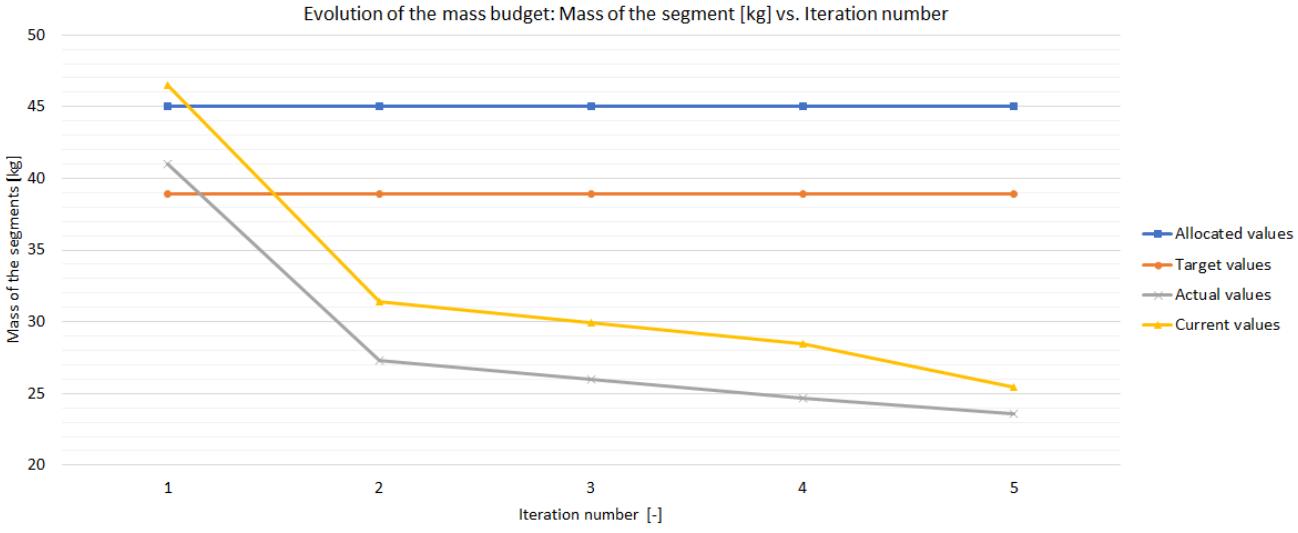

Figure 5.1: The evolution of the mass budget of the system: allocated, target, actual and current values

As can be seen from Figure 5.1, the mass of the system drastically decreased during the second iteration. The main reason for this event was the decision to exclude a seismometer from the PPQs, as it was deemed difficult to integrate and operate, and its functions were redundant (there was another instrument on board allowing for measuring the specified characteristic quantity of the asteroid).

It was considered to reallocate the remaining mass difference between the target and actual values. The most justifiable solution was an increase of PQ number in order to increase the redundancy and reliability of the system. This was however impossible due to volume constraints. It was eventually decided that the mass

difference will not be reallocated. This could change in the next phases of the project, based on customer's suggestions.

Final Allocation

Table 5.8 shows the most recent actual values that were the result of the final iteration performed by every department. Those values including contingency become the new allocated values. This is the final allocation concluding this phase of the design. In the following phases those values shall be used for the updated budgets.

Table 5.8: The final segment mass allocation resulting from the detailed design phase.

Item	Most recent actual value [kg]	New allocated value [kg]
PPQs	7.9	8.3
CPQs	1.8	1.9
Deployer	4.1	4.5
Net	9.8	10.8
SUM	23.6	25.5

5.3. Volume Budget

This section outlines the volume allocations for the system. The evolution of the budgets is presented first, which is followed by the final allocation. The budget strategy is outlined in subsection 5.1.1. An additional feature of the volume budgets is the approach to the PQ volume. In order to calculate the total volume of the system, the outer volume of the PQ times the number of the PQs had to be taken. A margin was included, as it is impossible to perfectly fit all the PQs next to each other. Initially, a 10% margin was taken around the 5×5×5 cm cube. This was based purely on a rough assumption. Finally, when the definition of the system developed, the exact envelopes around the PQs used for the system volume budget were specified (refer to Figure 5.2). They are derived from the size of elements placed on the outside of the PQ. These do not include the interfaces between the net and the PQ, as those are included in the net volume budget. Those elements are described in the PQ and CPQ layout in section 5.7.

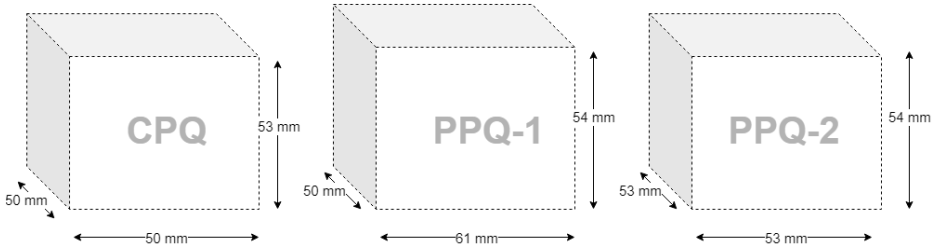

Figure 5.2: Envelopes encompassing the different PQ types, that were used for the volume budget of the whole system.

For the inner volume of the PQs, initially the exact volumes of all subsystems were used. In the more advanced phase of the project, the internal layout of the PQ was decided (section 5.7). The active subsystems (EPS, C&DH, COMMS, Scientific Payload) are placed on stacks. The stack area and total available stack height is defined by the structure and thermal protection layer volumes (see section 5.7). In order to asses whether the available volume was not exceeded, a stack height budget was made. The volume of the stacked subsystems then became: area of the stack × total available height for the stacks.

Budget Evolution

In Table 5.9, Table 5.10, Table 5.11 and Table 5.12 the changes in volume budgets over the 5 performed design iterations can be viewed. Notice that at the third iteration the volume of the active subsystems is given as one value; this is the result of previously described stack height approach.

Table 5.9: PQ volume evolution.

Item	Allocated [%]	PPQs (62; uniform) Target Value [mL]	PPQs (59; uniform) Actual Value [mL] (12/06)	PPQs (59; uniform) Actual Value [mL] (13/06)	PPQs (59; uniform) Actual Value [mL] (14/06)	PPQs (59; uniform) Actual Value [mL] (17/06)	PPQs (59; 10 PPQ-1, 49 PPQ-2) Actual Value [mL] (20/06)
Instruments	45.3	54.3	15.9	0.3			
C&DH	3.7	4.4	1.0	1.0	34.0	56.8	34.2
EPS	24.8	29.7	9.4	9.4			
Structures & mechanisms	6.8	8.1	40.8	39.7	39.7	39.7	35.2
Thermal control	8.0	9.5	0.0	2.8	2.8	3.8	0.2
Clearance	11.4	13.7	29.9	29.9	29.9	29.9	29.9
SUM	100.0	119.8	97.0	83.1	106.4	130.2	99.5

Table 5.12: Net volume evolution

		NET					
Item	**Allocated %**	**Target Value [L]**	**Actual Value (12/06)**	**Actual Value (13/06)**	**Actual Value (14/06)**	**Actual Value (17/06)**	**Actual Value (20/06)**
Cables structural	49.2	4.2	5.0	5.0	5.0	5.0	5.0
Cables power	9.8	0.8	1.0	1.0	1.0	1.0	1.0
Weights	0.0	0.0	0.0	0.0	0.0	0.0	0.0
Attachments	4.9	0.4	0.5	0.5	0.5	0.0	0.0
Antennas	0.0	0.0	0.0	0.1	-	-	-
Power generation	36.1	3.1	0.0	0.1	-	-	-
SUM	100.0	8.5	6.5	6.6	6.5	6.0	6.0

Table 5.10: CPQ volume evolution.

		CPQs (10; uniform)	CPQs (10; uniform)	CPQs (10; uniform)	CPQs (10; uniform)	CPQs (10; uniform)	CPQs (10; uniform)
Item	**Allocated %**	**Target Value [mL]**	**Actual Value [mL] (12/06)**	**Actual Value [mL] (13/06)**	**Actual Value [mL] (14/06)**	**Actual Value [mL] (17/06)**	**Actual Value [mL] (20/06)**
Instruments	61.6	72.1	27.0	27.0			
C&DH	3.0	3.5	1.0	1.0	16.6	27.8	47.9
EPS	24.8	29.1	10.9	10.9			
Structures	0.0	0.0	38.2	32.8	39.7	39.7	39.7
Thermal control	0.0	0.0	0.0	0.0	0.0	0.1	0.1
Clearance	10.6	12.5	29.3	29.3	29.3	29.3	29.3
SUM	100.0	117.1	106.4	101.0	85.6	96.8	116.9

Table 5.11: Deployer volume evolution

		Deployer					
Item	**Allocated [%]**	**Target Value [L]**	**Actual Value (12/06)**	**Actual Value (13/06)**	**Actual Value (14/06)**	**Actual Value (17/06)**	**Actual Value (20/06)**
Ejection system+structure	100.0	3.3	5.1	5.1	5.1	5.1	5.2
SUM	100.0	3.3	5.1	5.1	5.1	5.1	5.2

Figure 5.3 graphs the evolution in the volume budget values. For definition of specific terms of different values refer to Table 5.2.

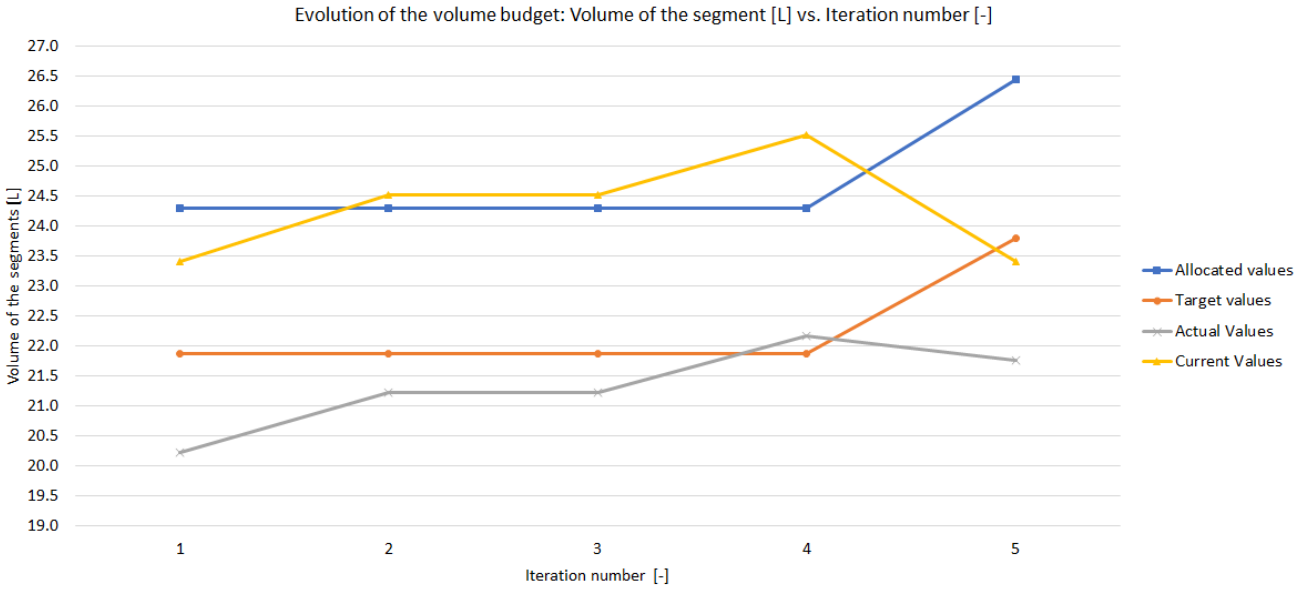

Figure 5.3: The evolution of the volume budget of the system: allocated, target, actual and current values

In section 5.2 it was mentioned that the volume became the critical constraint for the system. This is also confirmed by the trends in Figure 5.3. At the fourth iteration, action had to be taken from the systems engineering department. The cause of the increase in volume was the increase in the size of PQ envelope used for the system volume budget (see: Figure 5.2). At this stage, it was evaluated whether all PPQs could carry 4 external temperature sensors and 4 external image sensors. This concern was not raised before as the system was not so well defined and a generic margin of 10% was taken around the PQ for volume calculations. Due to the fact that the volume budget was exceeded, an iteration to the design was introduced. After consultations between the systems engineering department and payload department, it was decided to introduce PPQ-1 and PPQ-2: the '-1' would contain the temperature sensors and the '-2' would have image sensors on its sides. The optimised number was found to be 10 PPQ-1s and 49 PPQ-2s. Their layout is described in detail in section 5.7.

Final Allocation

Table 5.13 below outlines the most recent actual values of segment volumes that were the result of the final iteration performed by every department. Those values including contingency become the new allocated values. This is the final allocation concluding this phase of the design. In the following phases those values shall be used for the updated budgets.
In **??** the most recent actual values of the stack heights of all subsystems can be found. Notice the budget is given for a CPQ and a PQ. There was a 10% margin taken in this budget. Should the sizes of the components change, the use can be made of this stack margin.

Table 5.13: The final segment volume allocation resulting from the detailed design phase

Item	Most recent actual value [L]	New allocated value [L]
PPQs	9.1	9.6
CPQs	1.4	1.5
Deployer	5.2	5.7
Net	6.1	6.7
SUM	21.8	23.4

5.4. Power Budget

Table 5.15 is the most recent version of the systems power budget. It is broken down into all elements of the system that require power. The budget shows the power consumption for all modes (section 5.5). What is more, an indication of the margin between the total available energy and required energy including contingency is given, where the time of the mode is specified. The contingencies are taken from ECSS standards [4] similarly as for the mass and power budgets. All subsystems are assumed to have a 10% contingency level (based on COTS components). On top of that, a 20% margin is taken at the system level, as suggested by the European Space Agency standards mentioned above. The margins are added to the total energy required by the active elements per mode.

Table 5.14: The final PQ internal volume allocations

CPQ; number of stacks:	**3**	**PPQ; number of stacks:**	**3**
Stack	**Stack height [mm]**	**Stack**	**Stack height [mm]**
Comms stack	12.0	**Payload stack 1**	1.0
C&DH stack	4.1	**EPS stack**	12.0
EPS stack	12.0	**C&DH stack**	4.1
Margin	6.9	**Margin**	7.9
TOTAL	35.0	**TOTAL**	25.0
AVAILABLE	39.0	**AVAILABLE**	39.0

Table 5.15: The power budget of ANTREA

		MODE										
		Data acquisition										
		Transfer	Activation	Landing	Science A	Science B	Science C	Science D	COMMS	EoL	Safe	Recharge
SUBSYSTEM	Duration [s] (if specified)	-	-	96	7170	3600	3600	59	64260	-	-	-
Command and Data Handling	Peak Power [W]	0.00009	0.00038	0.00038	0.00038	0.00038	0.00038	0.00038	0.00006	0.00000	0.00038	0.00009
Subsystem	Duty Cycle [%]	100.0	100.0	100.0	100.0	100.0	100.0	100.0	100.0	0.0	100.0	100.0
	Operational Average Power [W]	**0.00009**	**0.00038**	**0.00038**	**0.00038**	**0.00038**	**0.00038**	**0.00038**	**0.00006**	**0.00000**	**0.00038**	**0.00009**
Communication	Peak Power [W]	0.00000	0.00000	0.83000	0.00000	0.00000	0.00000	0.00000	7.00000	0.00000	0.83000	0.00000
Subsystem	Duty Cycle [%]	0.0	0.0	10.4	0.0	0.0	0.0	0.0	100.0	0.0	10.0	0.0
	Operational Average Power [W]	**0.00000**	**0.00000**	**0.08646**	**0.00000**	**0.00000**	**0.00000**	**0.00000**	**7.00000**	**0.00000**	**0.08300**	**0.00000**
Scientific Payload Subsystem	Peak Power [W]	0.00000	0.00000	6.39112	3.26884	3.18600	3.12228	0.00000	0.00000	0.00000	0.00000	0.00000
IMU	Duty Cycle [%]	0.0	0.0	74.0	50.2	100.0	100.0	0.0	0.0	0.0	0.0	0.0
	Operational Average Power [W]	**0.00000**	**0.00000**	**4.72676**	**1.64126**	**3.18600**	**3.12228**	**0.00000**	**0.00000**	**0.00000**	**0.00000**	**0.00000**
Scientific Payload Subsystem	Peak Power [W]	0.00000	0.00000	2.88900	0.00000	0.00000	0.00000	0.00000	0.00000	0.00000	0.00000	0.00000
Image Sensor 1	Duty Cycle [%]	0.0	0.0	68.8	0.0	0.0	0.0	0.0	0.0	0.0	0.0	0.0
	Operational Average Power [W]	**0.00000**	**0.00000**	**1.98619**	**0.00000**	**0.00000**	**0.00000**	**0.00000**	**0.00000**	**0.00000**	**0.00000**	**0.00000**
Scientific Payload Subsystem	Peak Power [W]	0.00000	0.00000	30.38000	91.14000	0.00000	0.00000	0.00000	0.00000	0.00000	0.00000	0.00000
Image Sensors 2,3,4	Duty Cycle [%]	0.00	0.00	5.208	0.084	0.00	0.00	0.00	0.00	0.00	0.00	0.00
	Operational Average Power [W]	**0.00000**	**0.00000**	**1.58229**	**0.07627**	**0.00000**	**0.00000**	**0.00000**	**0.00000**	**0.00000**	**0.00000**	**0.00000**
Scientific Payload Subsystem	Peak Power [W]	0.00000	0.00000	0.12089	0.12089	0.00000	0.00000	0.00000	0.00000	0.00000	0.00000	0.00000
Mass Spectrometer	Duty Cycle [%]	0.0	0.0	5.2	100.3	0.0	0.0	0.0	0.0	0.0	0.0	0.0
	Operational Average Power [W]	**0.00000**	**0.00000**	**0.00630**	**0.12131**	**0.00000**	**0.00000**	**0.00000**	**0.00000**	**0.00000**	**0.00000**	**0.00000**
Scientific Payload Subsystem	Peak Power [W]	0.00000	0.00000	0.00000	0.00000	0.00000	0.00176	0.00000	0.00000	0.00000	0.00000	0.00000
External Temperature Sensor	Duty Cycle [%]	0.0	0.0	0.0	0.0	0.0	100.0	0.0	0.0	0.0	0.0	0.0
	Operational Average Power [W]	**0.00000**	**0.00000**	**0.00000**	**0.00000**	**0.00000**	**0.00176**	**0.00000**	**0.00000**	**0.00000**	**0.00000**	**0.00000**
Scientific Payload Subsystem	Peak Power [W]	0.00000	0.00000	0.00000	0.00000	0.00000	0.00000	11.46960	0.00000	0.00000	0.00000	0.00000
Radio Experiment	Duty Cycle [%]	0.0	0.0	0.0	0.0	0.0	0.0	100.0	0.0	0.0	0.0	0.0
	Operational Average Power [W]	**0.00000**	**0.00000**	**0.00000**	**0.00000**	**0.00000**	**0.00000**	**11.46960**	**0.00000**	**0.00000**	**0.00000**	**0.00000**
Image Sensor Heater	Peak Power [W]	0.00000	0.00000	0.00000	81364.50	0.00000	0.00000	0.00000	0.00000	0.00000	0.00000	0.00000
	Duty Cycle [%]	0.0	0.0	0.0	0.01	0.0	0.0	0.0	0.0	0.0	0.0	0.0
	Operational Average Power [W]	**0.00000**	**0.00000**	**0.00000**	**11.3479**	**0.00000**	**0.00000**	**0.00000**	**0.00000**	**0.00000**	**0.00000**	**0.00000**
Scientific Payload Subsystem	Peak Power [W]	0.00000	0.00260	0.00260	0.00260	0.00260	0.00260	0.00260	0.00260	0.00000	0.00260	0.00000
Internal Temperature Sensors	Duty Cycle [%]	0.0	100.0	100.0	100.0	100.0	100.0	100.0	100.0	0.0	100.0	0.0
	Operational Average Power [W]	**0.00000**	**0.00260**	**0.00260**	**0.00260**	**0.00260**	**0.00260**	**0.00260**	**0.00260**	**0.00000**	**0.00260**	**0.00000**
Reel-in mechanism	Peak Power [W]	0.00000	0.00000	0.00000	75.56000	0.00000	0.00000	0.00000	0.00000	0.00000	0.00000	0.00000
	Duty Cycle [%]	0.0	0.0	0.0	6.6	0.0	0.0	0.0	0.0	0.0	0.0	0.0
	Operational Average Power [W]	**0.00000**	**0.00000**	**0.00000**	**4.95303**	**0.00000**	**0.00000**	**0.00000**	**0.00000**	**0.00000**	**0.00000**	**0.00000**
Electric Power System	Peak Power [W]	0.00000	1.38000	1.38000	1.38000	1.38000	1.38000	1.38000	1.03500	1.38000	1.38000	1.38000
	Duty Cycle [%]	0.0	100.0	100.0	100.0	100.0	100.0	100.0	100.0	100.0	100.0	100.0
	Operational Average Power [W]	**0.00000**	**1.38000**	**1.38000**	**1.38000**	**1.38000**	**1.38000**	**1.38000**	**1.03500**	**1.38000**	**1.38000**	**1.38000**
TOTAL AVERAGE POWER [W]		0.00009	1.38298	9.77097	19.52275	4.56898	4.50702	12.85258	8.03765	1.38000	1.46598	-
TOTAL ENERGY [Wh]		-	-	0.3	38.9	4.6	4.5	0.2	143.5	-	-	-
TOTAL ENERGY INCLUDING CONTINGENCY [Wh]		-	-	0.3	51.3	6.0	5.9	0.3	189.4	-	-	-
TOTAL MAX AVAILABLE ENERGY [Wh]		192.0	192.0	192.0	191.7	152.9	148.3	143.8	192.0	63.4	192.0	-
Margin [%]		-	-	99.8	73.2	96.1	96.0	99.8	1.4	-	-	-

5.5. Operational Modes

Table 5.16 gives an overview of the operational modes of the system with short definitions and the condition to trigger them. As indicated previously in the power budget, times of certain modes are specified. They are determined by the duration of required operations in certain mode (Data Acquisition/ Communications).

Table 5.16: The definition of operational modes.

Mode		Definition	Condition
Transfer		Transfer from Earth to the target asteroid; all subsystems either in standby or deactivated.	-
Activation		Just before deployment; the OBC activates and performs a health check. System ready to perform.	Mothership command
Data acquisition	**Landing**	Landing phase; C&DH, EPS, IMU, Image sensors, Mass spectrometer and Reel-in mechanism active.	Mothership command
	Science A	System on the asteroid surface; C&DH, EPS, IMU, Image sensors, Mass spectrometer and Reel-in mechanism active.	Completion of 'Landing' + acceptable voltage levels in the batteries
	Science B	System on asteroid surface; C&DH, EPS, IMU active	Completion of 'Science A' + acceptable voltage levels in the batteries + specified time
	Science C	System on asteroid surface; C&DH, EPS, IMU, Temperature sensors active	Completion of 'Science B' + acceptable voltage levels in the batteries + specified time
	Science D	System on asteroid surface; C&DH, EPS, Radio experiment equipment active.	Completion of 'Science C' + acceptable voltage levels in the batteries + specified time
COMMS		System on asteroid surface; C&DH, EPS, Communication instruments active. The system is performing down-link and can receive uplink commands.	Data acquisition complete + acceptable voltage levels in the batteries + specified time
Safe		C&DH active, Communication instruments ready to receive uplink command. Fault Detection, Isolation, and Recovery algorithm on.	Critical failure warning/ Ground command/ Mothership command.
EoL		Non-critical functions switched off, Scientific payload switched off. Communications send low power signals used for tracking until voltage level in the batteries becomes negligible.	Uplink command.
Recharge		System on asteroid surface; C&DH, EPS active. The system switches to a low power mode and uses solar panels to charge batteries.	Low voltage levels in the batteries.

The conditions given in Table 5.16 are an indication of which signal is needed to trigger a mode:

- A command from the C&DH subsystem, which is based on the time of triggering a mode specified by the software and measured by the clock on C&DH subsystem
- A command from C&DH triggered by a failure detection during telemetry
- External command from ground/the Mothership.

What is more, some contain additional requirement in the form of completion of previous mode.

Some additional explanation of the the **Recharge** mode is provided. In this mode, all active devices are switched into a low power mode so that the amount of solar cell power used for charging the batteries can be maximised, and hence the charging time is minimised. This mode is present due to the fact that some operations require more power than the amount that can be generated by the solar cells (about 7 W; see chapter 13) and hence would be impossible to conduct should the voltage level in the batteries drop beyond the required voltage.

Below (Figure 5.4) the flow of operational modes is visualised by means of a block diagram. This is a top-level overview of how the modes are switched. The procedures carried out in modes are elaborated on in detail in the complete functional flow diagrams (see chapter 6). What is more, it can be seen that modes Science A, Science B, Science C and Science D are addressed in more general in one parts of the diagram. For more detailed definition refer to chapter 6. What is more, the switching between the different Data acquisition modes (Science A/B/C/D) would also include health checks as indicated for different modes on the diagram. This was not included to make the diagram more readable.

5.6. Systems' Interfaces

The following section outlines the general interfaces between the system's segments and subsystems. To introduce the main ones, an N^2 chart (Figure 5.5) is presented.

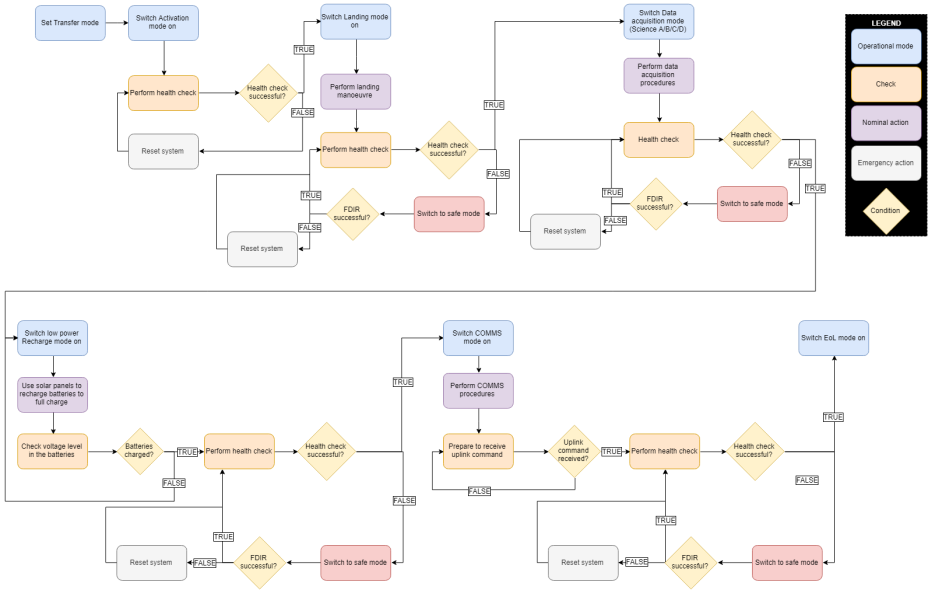

Figure 5.4: Operational modes block diagram

N^2 CHART

GROUND SEGMENT	*SEND GROUND COMMANDS*								*SEND GROUND COMMANDS*
SEND HEALTH UPDATE	**MOTHERSHIP**	*PROVIDE TRANSFER STORAGE, DEPLOY*			*INITIALISE*	*CHARGE BATTERIES*			*SEND COMMANDS*
		DEPLOYER	*PROVIDE STORAGE, DEPLOY*	*PROVIDE TRANSFER STORAGE*					
			NET	*CONTAIN*	*PROVIDE DATA DISTRIBUTION*	*PROVIDE POWER DISTRIBUTION*	*PROVIDE SURFACE CONTACT*		
				PQ STRUCTURE	*PROVIDE STORAGE AND PROTECTION*	*PROVIDE STORAGE AND PROTECTION*	*PROVIDE STORAGE AND PROTECTION*	*PROVIDE STORAGE AND PROTECTION*	*PROVIDE STORAGE AND PROTECTION*
			PROVIDE DATA TO BE DISTRIBUTED		**C&DH**	*PROVIDE POWER REQUIREMENTS, COMMAND, SELECT MODE*	*COMMAND, SELECT MODE*	*GENERATE HEAT*	*COMMAND, PROVIDE DATA, SELECT MODE*
			PROVIDE POWER TO BE DISTRIBUTED		*PROVIDE POWER, PROVIDE TELEMETRY, PROVIDE OUTPUT VOLTAGES*	**EPS**	*PROVIDE POWER*	*GENERATE HEAT*	*PROVIDE POWER*
					PROVIDE OUTPUT SCIENTIFIC DATA, PROVIDE TELEMETRY		**SCIENTIFIC PAYLOAD**		
					PROVIDE DESIRED TEMPERATURE RANGE	*PROVIDE DESIRED TEMPERATURE RANGE*	*PROVIDE DESIRED TEMPERATURE RANGE*	**THERMAL CONTROL**	*PROVIDE DESIRED TEMPERATURE RANGE*
PROVIDE HEALTH UPDATE, PROVIDE SCIENTIFIC DATA	*PROVIDE HEALTH UPDATE*				*PROVIDE TELEMETRY, PROVIDE GROUND COMMANDS*			*GENERATE HEAT*	**COMMS**

Figure 5.5: The N^2 chart of ANTREA

A clear understanding of the definition of all segments and subsystems and the interactions between them is crucial for successful integration of the product. Below, the description of the most important interfaces of the system and how they were managed together is present.

MECHANICAL INTERFACES

In order to enable a successful integration of the physical components of the design, well defined mechanical interfaces have to be established in the early project phases. This will not only impose constraints to rule out

unfeasible configurations, but also have implications on the later stages of the project, such as production, assembly and testing.

As can be seen in Figure 5.5, the main mechanical interfaces that needed to be taken into account during the definition and design of ANTREA were the interface between the Mothership and the Deployer, between the Deployer and the net, between the PQ and its subsystems and finally, on the lowest level, between the subsystems themselves.

The highest level, the interface between the Mothership and the Deployer was determined by the customer requirements (DOT-LAN-MD-4). Respecting this requirement was ensured by taking contingency on the system level before specifying the allocated value, that was then allocated per segments.

The interface between the Deployer and the net containing the rest of the system was more complex since attention had to be paid to the correct positioning of the ejection system. This limited the available volume. What is more, it was found that a larger ejection angle was beneficial for successful net deployment. However, a larger deployment angle negatively influenced the available volume inside the Deployer. This was again addressed by updating the budgets frequently, taking appropriate contingency levels, but also by ensuring that the shape of the inside of the Deployer enabled the fitting of the net.

The mechanical interface between the net and PQs was very challenging. It mainly concerned the correct attachment of the PQ to the net. This was done by means of placing brackets on the bottom of the PQ, through which the net is threaded. Attention had to be paid to ensure that no other subsystem interfered with the brackets. For details, see Figure 8.2.

Finally, on the lowest levels, it had to be ensured that the structure could fit all the subsystems. In the beginning this was implemented by means of volume budgets. Later, the active subsystems were placed in a stack configuration inside of the PQ. The stack height budget ensured that the active subsystems did not interfere with one another, while still fitting within the PQ. However, towards the end of the project, it was realised that the interface between the solar panels and the PQ structure has not been managed properly. There was a mismatch of the dimension of the panel and the +Z side of PQ. As a result, the panel did not fit and is currently extending over 3 edges of the side. This was not planned, yet due to the margin taken by the PQ envelopes, the interfaces on the higher levels were not affected. This issue shall be resolved in the next iteration of the design.

Thermal Interfaces

To allow for the intended functioning of the active subsystems on the PQ, certain temperatures ranges need to be kept. This is the primary goal of the Thermal Control subsystem (chapter 14). However, in order to ensure it can perform its task, certain recommendations on the design from the thermal interface side are stated.

Firstly, the internal components that generate high levels of heat shall not be placed in direct proximity. This could lead to overheating of components. What is more, the optimal temperature ranges of any components that need to be placed outside of the PQ structure and as a result are not protected by the thermal layer, should be analysed in detail to ensure they can operate as intended. If required, they shall be provided with active thermal control.

Electronic Interfaces

All active (power-consuming) components need to have clearly defined electronic interfaces. Up until this phase of the project, only high level electronic interfaces have been analysed, such as physical connections for power transfer in between PQs, ensuring desired voltage and current levels in power lines or designing for power supply for all active components. In the next phases of the project, when the choice of components is complete, all more detailed electronic interfaces, such as electronic connections for all devices inside the PQ shall be analysed further and optimised.

Data Interfaces

An optimised and well functioning data handling in a system can only be achieved with well defined data connections between all devices that generate or receive data. The current management of data interfaces was mainly focused on ensuring that expected data rates can be transferred between subsystems/segments, selecting data buses and creating a preliminary data flow architecture.

In the next phases of the project, it shall be ensured that all physical data connections specified in the baseline data flow architecture are feasible. What is more, a detailed analysis aimed at optimising the data flow in the system could be done.

5.7. External and Internal Layout of ANTREA

As mentioned in Table 5.1, the system consists of 4 segments: PPQs, CPQs, Deployer and the Net. The PQs are connected to the Net by brackets. Prior to the deployment, the system is stored in the Deployer.

PPQs

In total, there are 59 PPQs, of which 10 are PPQ-1s and 49 are PPQ-2s. All PPQs have a solar panel on the +Z side and an image sensor on the -Z side (Figure 5.6). PPQ-1 has 3 temperature sensors mounted on extending arms on the +X side and PPQ-2 has 3 additional image sensors: 2 on the +X side and 1 on the +Y side. All PPQs have an antenna, which is stowed initially, and extends in the +Z direction.

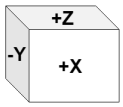

Figure 5.6: The coordinate system of PQ.

The inside of the PPQ consists of the structure, thermal protection layer and active subsystems. All the active subsystems have a dedicated stack, which is mounted on 4 poles inside the structure of the PQ. In addition to that, PPQ-1 provides storage for the 3 temperature sensors prior to their deployment.

CPQs

The CPQs have an antenna on the +Z side. The internal layout is similar to the one of PPQ: structure, thermal layer and active subsystems in a stack configuration.

NET

The NET consists of structural cables, data and power cables. The distribution of PQs on the net can be viewed in Figure 5.7. Notice the position of the four masters. In principle one master would be able to handle the data flow in the entire system. However, the number is increased to four to improve systems resistance to single point failures (redundancy) and to maximise the efficiency. If all four masters are found to have successfully passed a health check, all four will be utilised and will handle their divisions (see Figure 5.7). Should one or more of them fail, then the remaining ones will handle the new divisions of the net, computed with an algorithm.

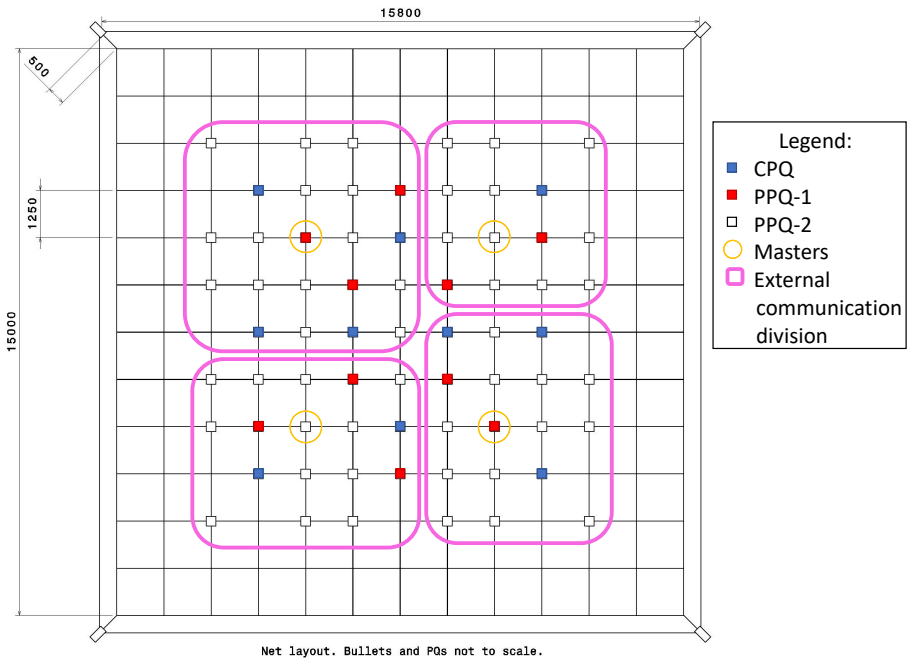

Figure 5.7: CATIA drawing of the net, with position of CPQs, PPQ-1s and PPQ-2s.

Deployer

The Deployer is a 30 × 30 × 30 cm box, with the net ejection system inside of it, which consists of 4 cylinders which channel the bullets of the net. The bullets are ejected by springs. The detailed layout is presented in chapter 9.

6
Functional Analysis

In order to properly design ANTREA, its functions had to be analysed. Defining its functions was done hand in hand with refining the requirements. This analysis resulted in a full functional architecture that shows how ANTREA will fulfil its mission objective. This chapter will explain the results of the functional analysis which are summarised by a Functional Flow Diagram (FFD) and Functional Breakdown Structure (FBS).

6.1. Functional Flow Diagram

The Functional Flow Diagram, see Figure A.1 and Figure A.2, shows the sequence of operations performed by ANTREA. Its sequence of operations is shown on multiple levels. The first level describes the global steps that ANTREA will follow. Then these steps are explained on a deeper level in the second level of the FFD. This continues until the fifth and final level which explains in detail the operations of the subsystems. The first page shows the FFD up to and including the third level. The rhombus shaped blocks represent checks that are performed by the system. Furthermore, circles containing letters A to J are included. These refer to the FFDs shown on the second page which represents the fourth and fifth level.

The DOT mission consists of multiple parts. The functions of the mission are divided into three parts: functions that the Mothership shall provide, functions that the Mothership together with the Deployer shall provide and functions that the Lander system (ANTREA) shall provide. This is visualised by the colours given to the blocks. The operational modes are highlighted with a pink header. The blocks that follow explain what happens inside this mode.

In the functions, different modes of the system are also included. Every time the system is activated due to a switch from one mode (in which it was off) to another mode (in which it is supposed to be on), the system will perform a health check. If the system has no problem it will continue performing its functions. If the system has problems it will enter the Safe mode and will try to repair itself. This happens if during the health check a value is out of its nominal range, for example a too high voltage, if there is a ground command or if the Mothership commands to enter the safe mode. This check and entering the Safe mode is not included in the Functional Flow Diagram every time a mode has to be activated, as it is considered to be part of entering a mode. How the flow of the different operational modes work is made clear in Figure 5.4. The top level of the FFD can be seen in Figure 6.1.

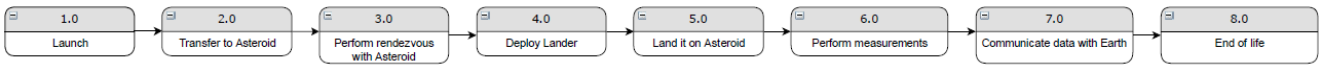

Figure 6.1: Top level Functional Flow Diagram

6.2. Functional Breakdown Structure

The Functional Breakdown Structure, see Figure A.3, displays the elements of the FFD in a categorised manner rather than a sequential one. The FBS shows all elements of the FFD except for the first level elements as this did not add any value. However, a breakdown structure is added for the Thermal control, Electrical Power System and the Command and Data Handling which thereby adds more detail to the FBS. These elements were not present in the FFD as they do not have their own flow with a beginning and end. They operate either continuously or occasionally. This difference between the subsystems in terms of functions was useful for the design integration and for defining the operational modes.

7
ASTRODYNAMIC ANALYSIS

Before the Lander can even be deployed to the asteroid, it first needs to be transported from the Earth to the asteroid. In the case of this mission, this part will be performed by the Mothership. This chapter deals with how a launcher will bring the Mothership into space, how the Mothership will travel to the asteroid and rendezvous with it such that the Lander can safely be deployed. Furthermore the final selection between the two candidate asteroids, 2017 FU102 and 201 4HB177, will be made by performing an analysis into the uncertainties of their orbit during their close approach with Earth.

7.1. REQUIREMENTS

The overview of the requirements related to Astrodynamics is presented in Table 7.1 below. A connection of some requirements to a parent requirement is indicated in the **Requirement** column. If the compliance is not yet investigated or cannot be proven at this time, the compliance box contains a "n".

Table 7.1: Requirements for astrodynamics.

Requirement ID	Requirement	Rationale	Verification Method	Compliance
DOT-SCH-2.1	The transfer orbit shall have an arrival date that is before 2040.	User Requirement	Analysis: GMAT simulation	✓
DOT-ADT-LV-1	The launch vehicle shall be Vega with the Avum upper stage. (Parent: DOT-ADT-MS-4)	This requirement is needed to know the launch loads that will be exerted on the system, from the chosen launch vehicle.	Analysis	✓
DOT-ADT-LV-2	The launch site shall be CSG (Kourou, French Guyana). (Parent: DOT-SCH-2.1, DOT-ADT-LV-1)	This is currently the only available launch site for the Vega launcher.	Inspection	✓
DOT-ADT-LV-3	The launch of the DOT mission and its Mothership to an elliptic orbit shall nominally occur in April 2033. (Parent: DOT-SCH-2.1)	This is required to ensure that the Mothership arrives to the asteroid at least 6 months before the Lander is deployed on it.	Analysis: GMAT simulation	✓
DOT-ADT-LV-4	The DOT mission's trajectory options shall be compatible with launch opportunities in May of 2033.	This is to make sure that the mission can still occur with a delayed launch, much like the Rosetta mission. Several trajectories shall be evaluated, to ensure that the Mothership will arrive to the target asteroid on the 1st of March at the earliest, even if a launch were to occur in May of 2033, instead of April of 2033.	Analysis: GMAT simulation	✓
DOT-ADT-LV-5	The launcher shall bring the Mothership to an orbit with an altitude of apogee of 60000km, +/- <TBD>km. (Parent: DOT-SCH-2.1, DOT-ADT-LV-1)	This is the highest apogee that was found to be possible with Vega-C for a 500 kg payload. Based on the Proba-3 mission.	Analysis: GMAT simulation	✓
DOT-ADT-LV-6	The launcher shall bring the Mothership to an orbit with an altitude of perigee of 250 km +/- <TBD>km. (Parent: DOT-SCH-2.1, DOT-ADT-LV-1)	A lower perigee leads to less ΔV being needed to reach the required hyperbolic velocity	Analysis: GMAT simulation	✓
DOT-ADT-LV-7	The launcher shall bring the Mothership to an orbit with an inclination of 20.07 degrees +/- <TBD>degrees in the Earth centered MJ2000 equatorial frame. (Parent: DOT-SCH-2.1)	Required for the transfer trajectory	Analysis: GMAT simulation	✓
DOT-ADT-LV-8	The launcher shall bring the Mothership to an orbit with a longitude of ascending of 90.45 degrees, +/- <TBD>degrees in the Earth centered MJ2000 equatorial frame. (Parent: DOT-SCH-2.1)	Required for the transfer trajectory	Analysis: GMAT simulation	✓
DOT-ADT-LV-9	The launcher shall bring the Mothership to an orbit with an argument of periapsis of 140.94 degrees, +/- <TBD>degrees in the Earth centered MJ2000 equatorial frame. (Parent: DOT-SCH-2.1)	Required for the transfer trajectory	Analysis: GMAT simulation	✓
DOT-LAN-MS	The Lander System shall be delivered to the asteroid by a Mothership spacecraft	This specifies that the lander doesn't have to perform the whole transfer autonomously.	Analysis	✓
DOT-LAN-MS-3.1	The Mothership shall provide pictures relevant to the landing procedures. (Parent: DOT-LAN-MS-3)	These pictures are needed to find the optimal position to deploy the Lander.	Analysis	✓
DOT-LAN-MS-3.1.1	The pictures shall provide topographical information with an accuracy of <TBD> m (Parent: DOT-LAN-MS-3.1)	Size and shape with less accuracy than what will be provided by the scientific instruments.	Analysis	n
DOT-LAN-MS-3.1.2	The pictures shall provide information about the asteroid's dynamics with an accuracy of <TBD> rad/s (Parent: DOT-LAN-MS-3.1)	Rotation speed and axis with less accuracy than what will be provided by the scientific instruments.	Analysis	n
DOT-LAN-MS-3.2	The Mothership shall decrease relative velocity to smaller than <TBD> m/s. (Parent: DOT-LAN-MS-3)	Maximum allowable speed for the landing loads to be small enough.	Analysis	✓

Table 7.2: Requirements for astrodynamics (continued).

Requirement ID	Requirement	Rationale	Verification Method	Compliance
DOT-LAN-MS-1	The Mothership shall deploy the Lander System at a distance of no more than <TBD>m from the asteroid on 1 st of March 2036. (Parent: DOT-SCH-2.1)	The Mothership needs to be at a <TBD>km distance to the asteroid to minimise the risk of missing the asteroid with the deployment system and minimise the time between deployment and landing. Landing of the 1 st of March should guarantee a measurement period of one month.	Analysis: GMAT simulation	✓
DOT-ADT-MS-1	The Mothership shall arrive as close as 1,000,000 km of the asteroids estimated position with a phase angle of no more than 30 deg on the 1st of October 2035 the latest. (Parent: DOT-SCH-2.1)	This is to ensure that the Mothership is close to the asteroid at least 6 months before its close approach with the Earth in order to have sufficient time to find the asteroid. 1σ uncertainties for the asteroids position are around 500,000 km, so a distance of 1,000,000 km should ensure that the probability that the Mothership is on the illuminated side of the asteroid is very high.	Analysis	✓
DOT-ADT-MS-2	The Mothership shall be able to have a Delta V budget no less than 2697 m/s, with a margin of <TBD>%.	This Delta V will account for nominal burns, as well as safety ones, that might be required if a new position of the asteroid is known during the close approach of 2036.	Analysis: GMAT simulation	✓
DOT-ADT-MS-3	The Mothership shall perform <TBD>number of burns around the asteroid. (Parent: DOT-ADT-MS-2)	This is to determine the asteroid's orbit. The Mothership's distance with respect to the asteroid will gradually increase with the number of burns.	Analysis: GMAT simulation	n

7.2. Close Approach

As was previously mentioned in the Midterm Report [5], there are quite large uncertainties in both asteroids' orbits. That is why a Monte-Carlo analysis was performed for both of them to find the influence of this uncertainty. Based on the result of this analysis the most suitable asteroid was selected.

7.2.1. Method

The analysis was performed by simulating 5000 potential trajectories for both of the asteroids until their periapsis for their close approach. The initial positions of 2017 FU102 and 2014 HB177 were obtained from the JPL Small Body Database and were given for the Jul 22 2017[1] and May 1 2014[2] respectively. The reason for using an initial position almost 20 years before the close approach for both of them is that the covariance matrix of the orbital elements is only given for those dates. Using the covariance matrix and the nominal initial position, a normal random vector[3] was generated for the initial position of each trajectory. These trajectories were then propagated using GMAT[4] until 1 month before the close approach of the nominal trajectory, after which they were propagated until periapsis with Earth. At the periapsis, the state is saved and the simulation is ended. Then from the state at periapsis the communication windows corresponding to different distances were calculated for each trajectory using Python.

7.2.2. Results

As was also already mentioned in the Midterm Report [5], while the asteroid 2017 FU102 has a nominal trajectory with a higher periapsis distance and shorter communication window, its uncertainties were much lower than for the asteroid 2014 HB177. The effects of these uncertainties can clearly be seen in Figure 7.1 and Figure 7.2 which is the probability distribution of the periapsis distance for both asteroids. From this, it quickly becomes clear that the large uncertainties in the orbit of 2014 HB177 make the probability of its periapsis distance being low enough for communication to be possible is much lower than for 2017 FU102. For example the probability of the periapsis of 2014 HB177 being below 1 M km is just 49%, whereas it is 87% for 2017 FU102.

[1] https://ssd.jpl.nasa.gov/sbdb.cgi?sstr=2017%20FU102;old=0;orb=0;cov=1;log=0;cad=0#elem [Accessed 22 June 2019]
[2] https://ssd.jpl.nasa.gov/sbdb.cgi?sstr=2014%20HB177;old=0;orb=0;cov=1;log=0;cad=0#elem [Accessed 22 May 2019]
[3] https://en.wikipedia.org/wiki/Multivariate_normal_distribution#Normal_random_vector [Accessed 22 June 2019]
[4] https://sourceforge.net/projects/gmat/?source=navbar [Accessed 24 June 2019]

For 1.5 M km those probabilities improve to 67.9% and 98.2% respectively. Based on these results it becomes clear that 2017 FU102 is preferable when it comes to communicating with Earth and therefore henceforth only that asteroid will be analysed for this design process.

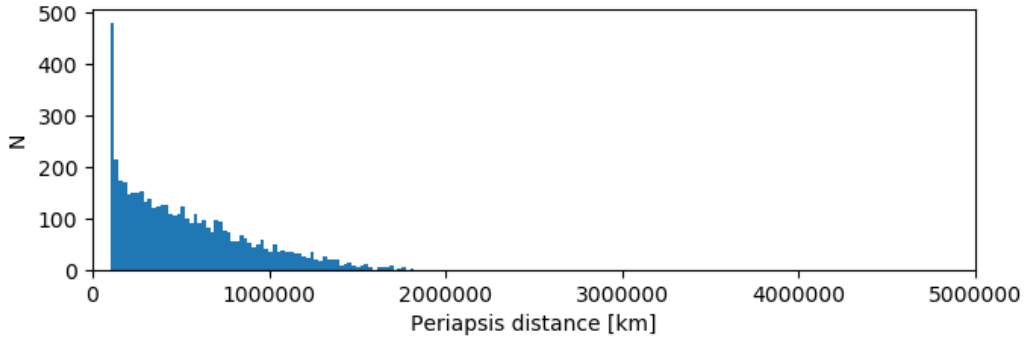

Figure 7.1: Histogram of the periapsis distances 2017 FU102, N=5000

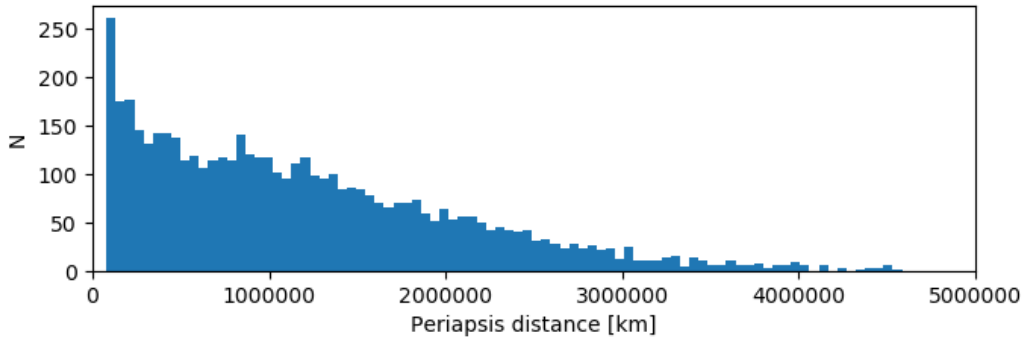

Figure 7.2: Histogram of the periapsis distances 2014 HB177, N=5000

In Figure 7.3, Figure 7.4 and Figure 7.5 the probability distributions for the communication windows associated with 0.5 M, 1 M, and 1.5 M km respectively can be found for 2017 FU102. The peaks for communication times of 0 hours are form the trajectories that have a periapsis distance that is larger than the communication distance. The probability distributions of the communication times associated with each distance will be used as a basis for sizing the communication subsystem.

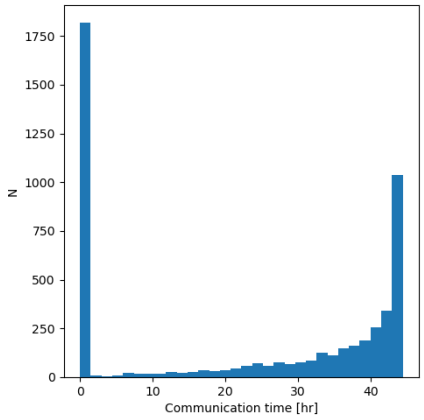

Figure 7.3: Comms time 0.5 M km, N=5000

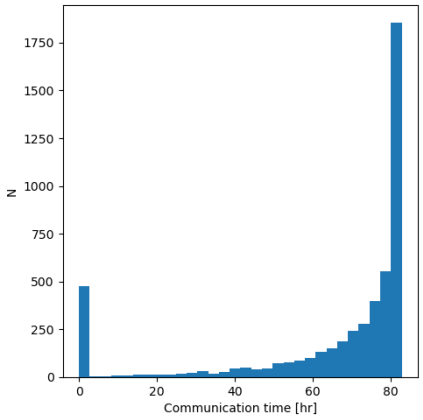

Figure 7.4: Comms time 1 M km, N=5000

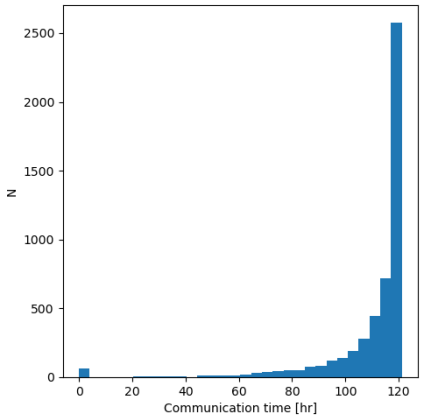

Figure 7.5: Comms time 1.5 M km, N=5000

7.3. Mothership Trajectory

The last part of this chapter concerns the Motherhip's trajectory, which will be analysed from launch until just before deployment. Firstly, the launcher that will bring the mothership into an orbit around the Earth needs to be selected, after which the transfer orbit and rendezvous manoeuvres will be designed.

7.3.1. LAUNCHER

A choice had to be made towards the launcher that will take the Mothership, itself carrying the Lander system, to elliptic orbit. A few launchers were compared, namely: the Ariane 5, the Ariane 6, the Vega, and Soyuz.

Although it is still in development as of today, the Ariane 6 launcher was still considered, as its first flight is scheduled for 2021, and would thus be ready by the time the DOT mission is launched. It was decided to consider the Mothership as being the main payload carried by said launcher, so excluding the possibility of it being launched as piggyback. Due to this, only relatively small launchers were considered, and no bigger ones were needed to be assessed. Furthermore, as it was specified to the team that all launcher costs would be fully covered by ESA, only European space transportation unions were considered. The Vega, Ariane 5 and Soyuz launch systems are all operated by Arianespace at the Guiana Space Centre.

Payload capabilities of all previously-mentioned launchers were considered and evaluated, as well as the loads that they can sustain during the most critical phases of their operation time. Additional information on their injection accuracy, their inclination, perigee and apogee altitudes, and argument of perigee for their GTO were also retrieved.

The launchers' properties were compared and it was concluded that a Vega launcher should be used, as it presents itself as an affordable launch solution for small to medium missions to an orbit that matches the mission design. It can take 1963 kg of payload including an adapter to elliptic orbit, which possesses an inclination of 5.4 degrees, and a perigee and apogee altitudes of 200 and 1500 km respectively. Moreover, it was the launcher that possessed the smallest margin of accuracy [2]. Its design limit load factors are specified to go up to -7.0g.

Furthermore, an estimated mass of 500 kg was assumed for the Mothership. By taking into account the additional maximum mass of 50 kg of the Lander system, this would result in a total payload mass of 550 kg. As this payload mass is much less than the specified maximum payload for the standard elliptical orbit in the Vega User's Manual, other missions launched by Vega were looked into to find the maximum apogee of the Highly Elliptical Orbit (HEO) it could launch the Mothership into. It would be preferable that the launch would place the Mothership into an orbit with an apogee as high as possible with the ideal case being that it would directly place it into a hyperbolic trajectory as this would minimise the ΔV that needs to be provided by the Mothership, and therefore reduces the required amount of propellant. The mission that was found to best match the required launch mass and orbit of the Mothership was the PROBA-3[5] mission, which has a launch mass of 540 kg and will be launched into a 600×60000 km orbit. This mission will however be launched by the standard Vega rocket, and the Vega-C and Vega-E variants, which should both be operational by the time of ANTREA's launch, will both provide an improvement in performance and could therefore launch the Motherhsip into an orbit with a higher apogee.

7.3.2. TRANSFER

The next step of the Mothership's journey is the interplanetary transfer from Earth to the asteroid. It will start this from a 250×60000 km orbit; A lower perigee is advantageous because this leads to a lower ΔV for the Transfer Orbit Injection (TOI) burn. In the Midterm Report [5], the optimal combination of departure and arrival dates was already investigated, however the pork-chop plots in that report ignored the Earth's gravity and just used velocity at infinity. Since this time the initial orbit is known, a new pork-chop can be made that shows more accurate ΔV values. This new pork-chop plot can be seen in Figure 7.6. The overall shape of the plot is very similar to the one in the previous report however the minimum ΔV is about twice a small. This is because as long as the velocity at infinity is substantially smaller than the escape velocity, a small increase in velocity at the periapsis of a hyperbolic orbit will result in a much larger change in velocity at infinity. As was also the case in the previous pork-chop plot, the ideal departure dates are still situated around mid 2033, and assuming the Mothership should not arrive too early near the asteroid, the group in the top left corner still contains the most optimal trajectories. An enlarged version of this group can be found in Figure 7.7, from which it can be seen that the minimum ΔV is obtained for departure dates around April 15^{th} of 2033. The optimum arrival date would be around the 1^{st} of November 2035, however it was decided to make the Mothership arrive

[5] http://www.esa.int/Our_Activities/Space_Engineering_Technology/Proba_Missions/About_Proba-3 [Accessed 22 June 2019]

one month before that to give it a bit more time to look for the asteroid, as the increase in ΔV would be only 2%.

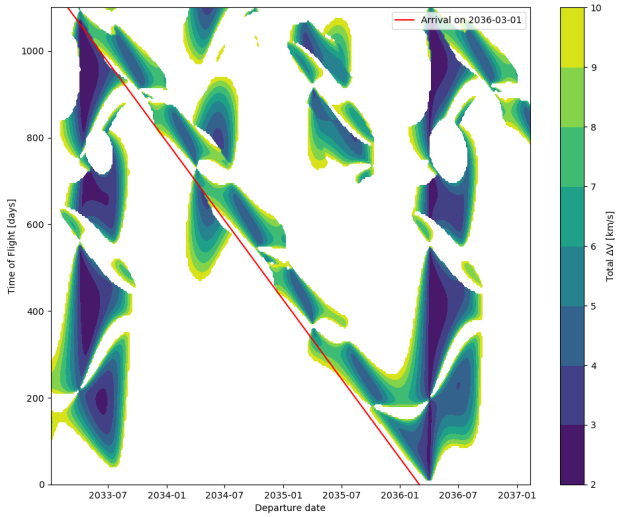

Figure 7.6: Pork-chop plot for departures from 2033 until 2036

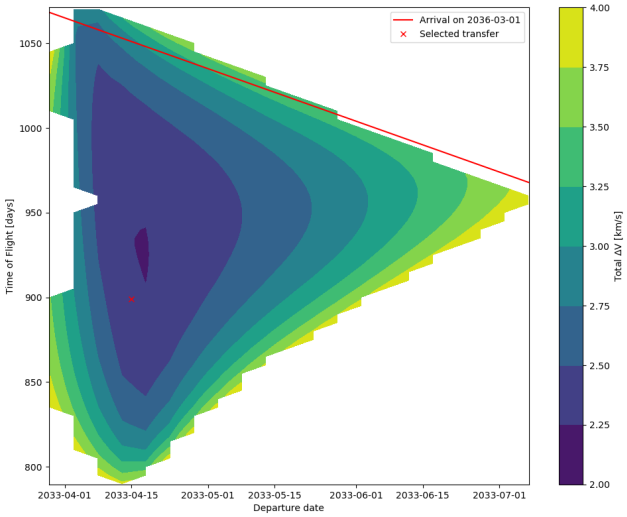

Figure 7.7: Pork-chop plot for departures for mid 2033

Using the selected departure and arrival dates, the Mothership's transfer orbit was then simulated using GMAT. Firstly a transfer with just two impulsive burns was simulated, for which the Mothership was put in a hyperbolic orbit around the Earth with the correct perigee, C3, and epoch. Then the declination and angle of ascension of the outgoing asymptote were changed by hand until the Mothership's position at the arrival date was within a few million kilometers of the asteroid. From there, the declination, angle of ascension, and C3 were further optimised using a Netwon-Raphson solver until the distance to the asteroid was reduced to less than 1000 km. Then, to find the ΔV needed to inject the Mothership into this transfer, the difference in velocity between the hyperbolic orbit and the associated elliptical orbit with an apogee at 60000 km was taken. The ΔV at arrival is found by the simple subtraction of the asteroid and Mothership velocity vectors at that point in time.

This would however only be the optimal transfer in case the asteroid's position was known exactly, which is not the case. Therefore the transfer has to be modified slightly to ensure the Mothership is able to find the asteroid. In order to maximise the amount of reflected light from the asteroid received by the Mothership, the phase angle (Sun-Asteroid-Mothership) needs to be small. The 1σ uncertainty of the asteroid's position is around 0.5 M km, therefore the transfer orbit was modified to make the Mothership pass the asteroid at a distance of 1 M km with a low phase angle for the nominal position of the asteroid, such that at least 95% of the probability region of the asteroid's position would be on the opposite side of the Mothership with respect to the Sun.

7.3.3. Rendezvous

Once the Motherhip has arrived near the asteroid, it will need to start scanning the sky to find the asteroid. Once it has found the asteroid, it will need to slowly reduce its distance with the asteroid as well as its relative velocity using a series of burns, while staying on the illuminated side. Due to the limited time available to design this trajectory and the fact that almost nothing is known about the Motherhip and its sensors, the rendezvous has been simplified to just 4 manoeuvres. The first manoeuvre (RVB1) occurs when the Mothership arrives at distance of 1 M km of the asteroid and brings it to a distance of 10000 km of the asteroid over a period of 3 months. The second burn (RVB2) brings the relative velocity between the asteroid and Mothership down to zero, which is followed by the Mothership following the asteroid for one month, after which the third burn (RVB3) sends it on an intercept course with a periapsis equal to the deployment distance occurring at the time of deployment. The final manoeuvre (RVB4) again cancels out the relative velocity such that deployment can safely take place. Finally the Mothership's trajectory is simulated until the asteroid's close approach with Earth, to see how far it would drift away if no station-keeping manoeuvres were performed. The distance and phase angle over the course of the approach as well as the time of burns can be seen in Figure 7.8. The entire transfer trajectory and the location of the manoeuvres can be seen in Figure 7.9.

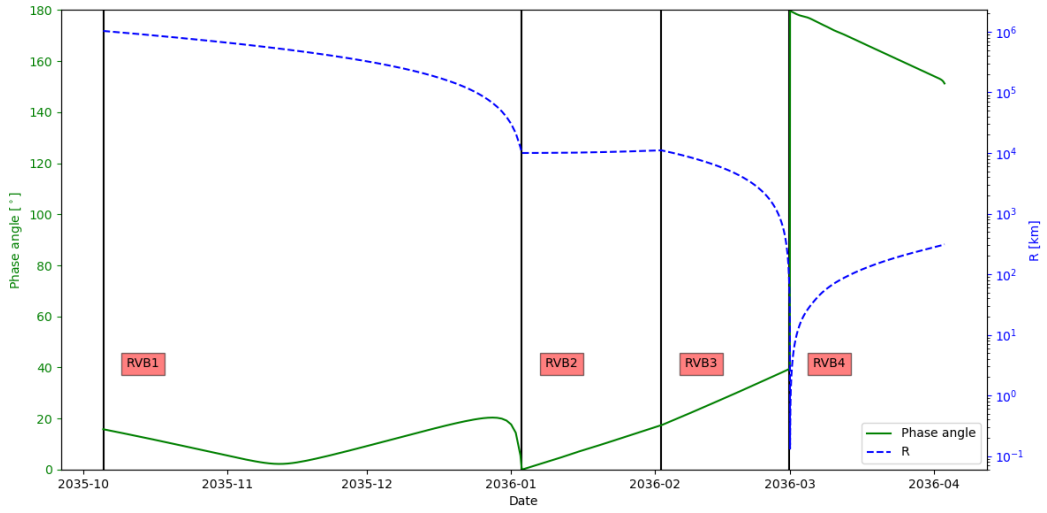

Figure 7.8: Distance of Motherhip to the asteroid and phase angle

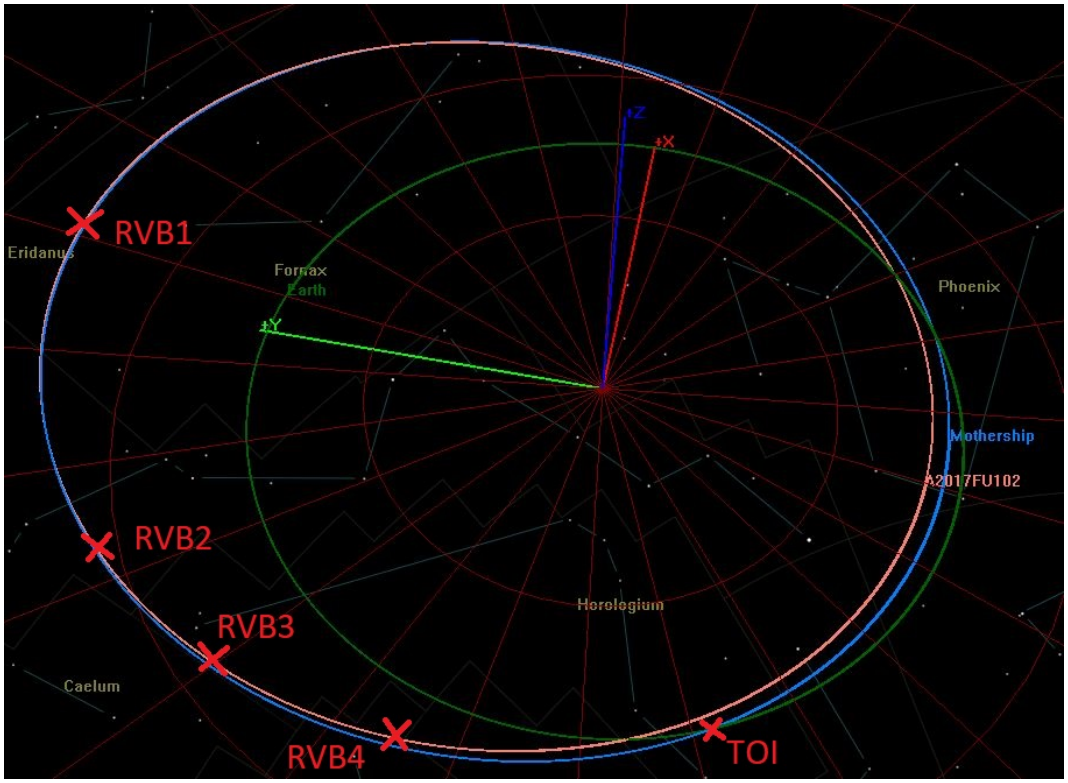

Figure 7.9: Orbits of the Earth, asteroid and Mothership around the Sun with position of burns.

7.3.4. ΔV Budget

The amount of ΔV for the three previously described trajectories is described in Table 7.3.

Table 7.3: Overview of the ΔV

Manoeuvre name	Pork-chop plot	GMAT direct transfer	GMAT multiple rendezvous burns
TOI	1915 m/s	2118 m/s	2072 m/s
RVB 1	401 m/s	399 m/s	513 m/s
RVB 2	N.A.	N.A.	106 m/s
RVB 3	N.A.	N.A.	5.7 m/s
RVB 4	N.A.	N.A.	4.6 m/s
Total	2316 m/s	2516 m/s	2697 m/s

8
Design of the Net

ANTREA relies on a net to land the PQs on the asteroid. The net will be deployed from the Deployer and will unfold and reach its full size just before hitting the asteroid, around which it will entangle and as such provide an attachment platform for the PQs. Additionally, it is an integrated part of the system, relaying data and electrical power via cables that connect the individual PQs. The net extremities, also called bullets, have to be high in mass with respect to the rest of the system, which is ideal to provide energy storage in the form of batteries.

8.1. Requirements & Constraints

The net has to meet several requirements in order to ensure mission success. These can be found Table 8.1 and range from general mass and volume requirements to constraints imposed from a net deployment dynamics point of view. A connection of some requirements to a parent requirement is indicated in the **Requirement** column. If the compliance is not yet investigated or cannot be proven at this time, the compliance box contains a "n".

Table 8.1: Requirements for the Net design.

Requirement ID	Requirement	Rationale	Verification Method	Compliance
DOT-NET-M	The mass of the NET segment shall not exceed the value specified in the mass budget including the current contingency level.	Based on the mass user requirement on the entire system and adapted such that the system functions properly.	Inspection: measurements on the assembly.	✓
DOT-NET-V	The volume of the NET segment shall not exceed the value specified in the volume budget including the current contingency level. (Parent: DOT-LAN-MD-5)	Based on the volume user requirement for the entire system and adapted such that the system functions properly.	Inspection: measurements on the assembly.	✓
DOT-LAN-PQ-SC-2.2	The network of PQs shall be able to encompass 50% of the asteroid surface area.	This is a requirement on the size of the net. A broad PQ distribution is preferred for science.	Analysis	✓
DOT-NET-1	The net shall have a deployed side length of 15 m. (Parent: DOT-LAN-PQ-SC-2.2)	Makes sure the net can entangle on the range of asteroid diameters expected.	Inspection: measurements on the assembly.	✓
DOT-NET-2	The net shall entangle and attach to the asteroid with a probability of at least 0.95 (3 sigma). (Parent: DOT-AST-2.1)	The net is crucial to mission success and shall enable landing on the asteroid.	Analysis: simulation and statistical analysis of the results.	X
DOT-NET-3	The weights shall be able to retract 10 m of rope. (Parent: DOT-AST-2.1)	Increases the probability of successful long-term attachment once entangled.	Test: physical test of the retraction mechanism.	✓
DOT-NET-4	The weights shall be able to retract the rope with a force of up to 300 N. (Parent: DOT-AST-2.1)	-	Test: physical test of the retraction mechanism.	✓
DOT-NET-5	The net shall be fully deployed <TBD>m from the asteroid. (Parent: DOT-AST-2.1)	There is an optimum distance from the asteroid where the net shall be fully deployed.	Analysis: simulation and statistical analysis of the results.	n
DOT-NET-6	The net shall be ejected at <TBD>m from the asteroid. (Parent: DOT-AST-2.1)	There is an optimum ejection distance from the asteroid.	Analysis: simulation and statistical analysis of the results.	n
DOT-NET-7	The weights shall be ejected at an angle of 10 degrees to asteroid nadir. (Parent: DOT-AST-2.1)	Deployer and system constraints. In order to keep as much volume as possible available in the deployer the ejection angle must be as small as possible.	Demonstration/test: physical test of the ejection and trajectory measurement.	✓
DOT-NET-8	The weights shall be ejected at TBD m/s. (Parent: DOT-AST-2.1)	Structural deployer constraints and structural PQ considerations (such that they do suffer damage due to impact) limit the maximum ejection velocity. Up to 10 m/s preferable for net deployment dynamics.	Demonstration/test: physical test of the ejection mechanism and performance measurement.	n
DOT-NET-9	The weights shall be able to withstand impact of <TBD> Ns.	-	Test: impact test of the weight.	n
DOT-NET-10	The weights shall be cylindrical with a diameter of 48 mm (+/- 0.01 mm) and a length of 190 mm (+/- 0.01 mm).	The bullets have to be compatible with the deployer design.	Inspection: measurement of the weights.	✓

Table 8.2: Requirements for the Net design (continued).

Requirement ID	Requirement	Rationale	Verification Method	Compliance
DOT-W-M	The mass of the weights shall not exceed the value specified in the mass budget including the current contingency level.	Functional and system performance considerations. A high bullet mass is preferable from a net deployment dynamics point of view, but is constrained by the deployer performance and user mass requirements.	Inspection: measurement of the weights.	✓
DOT-NET-11	The net shall sustain <TBD>krad.	The net is critical to mission success and has to sustain the environmental conditions encountered.	Analysis: simulation.	n
DOT-NET-12	The weights shall provide 110 Wh of energy storage.	The bullets are objects with a high density and can be exploited to provide energy storage.	Inspection: design review.	✓
DOT-NET-13	The net shall enable the distribution of power and data between the different PQs through cables	The net can be exploited to connect the PQs, which leads to a more efficient design	Test: the final cable design can be tested on ground.	✓

Requirement DOT-NET-2 was not satisfied. In the entire chapter, but mostly in section subsection 8.4.1 the reasons are presented along with possible solutions. A clear recommendation on which parameters have to be adapted can be found in section 28.2.

8.1.1. Heritage

The RemoveDEBRIS mission was the first to use a net in space [6]. It deployed a hexagonal net of 5 × 5 m on a CubeSat with an inflated balloon of 1 m in size, and was considered an active debris removal (ADR) technology demonstrator. A net has previously been an option for the cancelled ESA - ROGER mission [7] that was supposed to clean up Geostationary Earth Orbit. It was the first time (publicly) that large-scale nets were actively researched for space applications. The ESA e.deorbit mission is currently under development (planned launch 2023) and will employ two 15 × 15 m nets in order to de-orbit the 8 ton decommissioned satellite ENVISAT [8]. In general, since its inception, nets in space were connected inherently with space debris removal. The functioning and deployment principle is very similar in all missions. A net is stored in a deployer such that it does not entangle. To shoot it at a target, weights or bullets with a higher mass than the net itself are ejected towards the target with a small velocity component in the plane perpendicular to the deployer-target axis in order to open the net. In practice, this is usually done by springs or gas ejectors that are at an angle to the deployment axis. In addition to opening the net, the bullets ensure entanglement around the target.

8.2. Net Design

The missions and applications explained in subsection 8.1.1 all apply to nets designed to remove space debris, which causes the net to have a tether line connected to the Deployer. ANTREA exploits a net to reliably attach the PQ sensors to the asteroid. The focus is more on the deployment and subsequent attachment, while a tether line is non-existent. The mission is low-cost as much heritage and already gained experience in space nets was exploited for the present design. There are a few considerations that increase the complexity of the design with respect to debris removal missions:

1. The net has to provide landing and attachment for 69 PQs with an average mass of 155 g, see chapter 5. As a result, the mass of the net will be much higher than in the reference missions. This changes the deployment dynamics, as in all designs only the bullets are actively ejected which in turn accelerate the net by conservation of linear momentum (assuming no energy dissipation due to bending, torsion and tensioning of the net), $v_1 m_1 = v_2 m_2$. As the ratio $r = \frac{\text{total bullet mass}}{\text{total net mass (withouth bullets)}}$ decreases, the discrepancy between the initial bullet velocity and final net velocity increases, which in turn decreases deployment stability. Battista et al (2017) [9] recommend r to assume values in between $4-10$, which is definitely not feasible for the ANTREA net. In order to quantify the influence of this change and possible solutions, deployment simulations were carried out and are described in subsection 8.4.1.

2. The net has to provide a steady PQ position on the asteroid. Ideally on the ground, if not at least floating at a constant position and altitude above the surface to enable scientific observations.

3. The net does not just consist of a fiber for structural reasons but additionally has to house power and data cables, radically increasing the bending and torsional stiffness and altering the damping constants and non-

elastic energy dissipation during deployment.
4. The ejection speed is constrained by the structure and impact resistance of the PQs. This adds an additional difficulty as the optimum net velocity of 10 m/s as determined by Battista et al (2017) [9] is hardly attainable.

Layout

The RemoveDEBRIS net was hexagonal with 6 bullets, while the proposed ADRiNET on e.deorbit will be a square net with 4 bullets. Other shapes, such as triangular with unequal side lengths to decrease the risk of the bullets hitting each other on the backside of the target are under investigation. In order to retain simplicity and due to the complexity of net deployments, a square layout with 4 bullets was chosen. The net has a deployed size of 15 × 15 m and is able to wrap around asteroids of up to 5 m in diameter (16 m circumference assuming a sphere). The design was kicked-off with the assumption that the length of ropes connecting the bullets to the corners could be simply increased to catch larger asteroids, however this would most likely result in complicating the deployment dynamics. Consequently, it was decided to focus on the 15 × 15 m net capable of wrapping around small asteroids in the following. The cables at the corners are 0.5 m long and connect the edges of the square net to the bullets. The bullets have a 15.8 m direct cable connection in between them, which can be reeled-in to close the net. The mesh size is 1.25 m which is sufficient to catch the asteroid and reduces the total net mass. The PQs are attached at intersections of the thread as can be seen in Figure 5.7. The ratio r pointed out above is approximately 0.66 for the *ANTREA* net. The bullet ejection velocity of 2.03 m/s at an angle of $\theta = 10$ degrees to asteroid nadir results in an initial bullet velocity towards the asteroid of $2.03 * sin(10^\circ) = 2$ m/s. By conservation of linear momentum the final overall net velocity is approximately 0.79 m/s. In case r is high, the distance from ejection to full deployment can be approximated by $d = \frac{x}{\tan\theta}$, where $x = 11.1$ m is half the diagonal of the net. This results in $d = 63$ m but is not representing reality as the fraction r is way below 4 and the bullets are decelerated significantly by the net. The cooperation with SKA-Polska simulations of the net deployment were carried out and it was found that the current design does not deploy, see subsection 8.4.1. As this only occurred at a late stage of the design, it was not possible to alter the parameters significantly. Possible solutions and adaptations are presented in section 28.2.

Cable

To guarantee structural integrity of the net, high strength and low specific density fibres are desired. The elasticity of the fibre strongly influences the deployment dynamics. The best options are high modulus-polyethyleene (HMPE) synthetic fibres (Dyneema) and high modulus-high tenacity (HM-HT) synthetic fibres (Technora, Kevlar). Dyneema has been used in the RemoveDEBRIS mission [10], but for this mission the space qualified Technora has been chosen due to its high strength, impact, fatigue and heat resistance [11]. Technora[1] fibre properties are presented in Table 8.4. The net incorporates 3 different types of rope with a total length of 458.2 m.

Table 8.3: Table with the components of the net segment.

Net segment components	**Length [m]**	**Diameter (outer) [mm]**	**Mass [kg]**
Rope with power and data cables	126.25	1.9	1.012
–Technora hull	126.25	1.9	0.234
–Data cable	252.5	0.3	0.186
—-Copper wire	252.5	0.2	0.142
—-PTFE insulation	252.5	0.3	0.044
–Power cable	505	0.66	0.592
—-Copper wire	505	0.41	0.475
—-PTFE insulation	505	0.66	0.117
Technora net rope	268.75	1.3	0.498
Technora reel-in rope	63.2	0.8	0.044
PQ-net interface	[-]	[-]	0.246
Bullets	0.19	48	2.000
Total			**9.800**

The 126.25 m connection between the PQs requires two power cables, see chapter 13, and 4 data cables, see chapter 15. The respective required copper wire diameters are 0.41 mm for the power cable and 0.2 mm for the data cable. Both types have a Polytetrafluoroethylene (PTFE) insulation around them, which increases the respective diameters to 0.66 mm and 0.3 mm. The cables are twisted at a pitch of 20 mm and housed inside a Technora hull.

[1] http://www.matweb.com/search/DataSheet.aspx?MatGUID=683f3be4a8e140a380b27cf05aa93229 [Accessed on 20/06/2019]

Table 8.3 presents the cables and all components that are part of the NET segment. No detailed analysis was carried out on the required cable strength, therefore it was assumed it has to be about two times stronger than the fibres used in nets for ADR missions [7][6], resulting in an ANTREA net strength of 4000 N.As a result, the total cable diameter is 1.9 mm. Structurally problematic is the fact that the Technora fiber (E-modulus 70 GPa) is less stiff than copper (E-modulus 110 GPa)[2]. Consequently By applying the principle of superposition, it becomes apparent that the copper would carry most of the loads, which is undesired. The connection between the cable and the PQs houses a little bow to let the copper move and slide freely in the Technora hull without taking any forces. Another possible solution is presented in section 28.2. At the same time, Technora is still desired since its σ_{ult} is 14 times higher than copper's (210 MPa), which also decreases the required cross sectional area by a factor 14 and the net mass by a factor 90. The pure Technora rope in the net has a diameter of 1.3 mm, which results in a strength of 4000 N as well. The 63.2 m reel-in rope will barely take any forces during deployment and impact. It was therefore assumed a strength of 1500 N is required, resulting in a diameter of 0.8 mm.

Table 8.4: Technora material properties, from footnote 1 and [11]

Technora material properties	
Ultimate tensile strength σ_{ult} [Mpa]	3000
Failure strain [%]	4.4
Young's modulus E [GPa]	70
Density [kg/m^3]	1390
Axial damping ratio [-]	0.106
Torsional damping ratio [-]	0.079
Bending damping ratio [-]	0.014

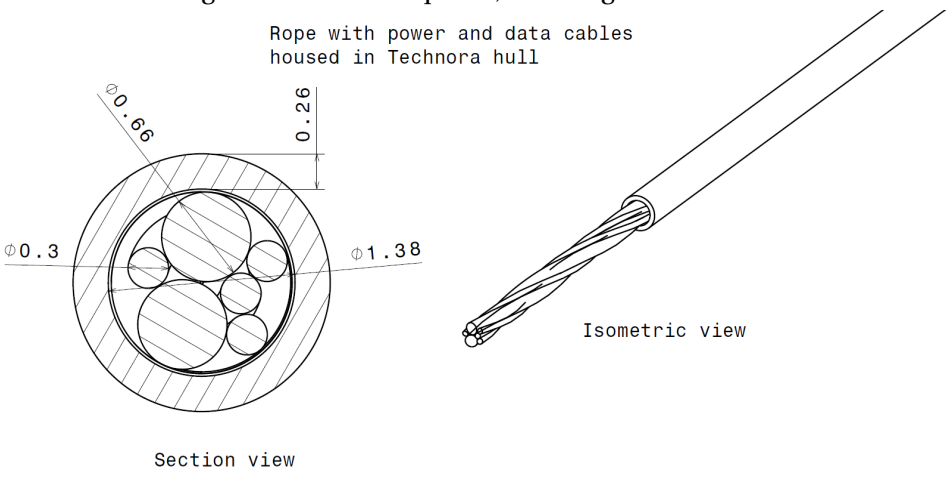

Figure 8.1: Technical drawing of the rope housing 2 power and 4 data cables inside a Technora hull.

Attachment

As calculated and pointed out in detail in the Midterm Report [5], the gravity acting due to the asteroid is negligible. On the other hand, the worst case normal acceleration away from the surface is 0.024 m/s^2, resulting in a force of up to 0.0049 N per PQ (assuming an asteroid radius of 5 m, rotation period of 90 s and PQ mass of 200 g). The net has to serve as an attachment to keep the PQs on the surface, which is done by the bullets entangling on the backside of the asteroid.

The PQs are attached on the outer side of the net when landed (i.e. facing the deployer during ejection), since they have a higher mass than the surrounding net. This ensures the PQs will always face the ground with the correct side, as the acting normal force is pulling the PQ away from the surface and it is attached to the net on the -Z side, see Figure 8.2. It is very likely that not all PQs will touch the surface but rather float a few centimetres above it. In order to increase the probability of touching and remaining on the surface, some parts that could be added to the individual PQs were taken into consideration but not implemented due to time constraints. The Jet Propulsion Laboratory developed an autonomous microspine gripping mech-

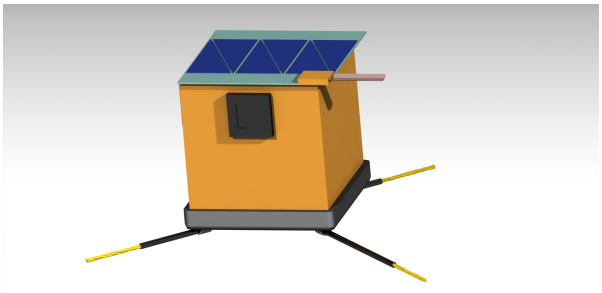

Figure 8.2: Illustration of a PQ on the net cable.

[2] http://matweb.com/search/DataSheet.aspx?MatGUID=9aebe83845c04c1db5126fada6f76f7e&ckck=1 [Accessed on 20/06/2019])

anism to attach an object to an asteroid or any not completely smooth surface [12]. The mechanism is large, bulky and relies on complex mechanisms (kinematics, gears, motors and springs) to work, which is why it is not an option for the present design. The design of a microspine itself however, which is basically a small hook that can attach to a surface and cope with lateral loads, is space-ready [13]. Since the PQs are considered too small for complex active attachment mechanisms, the possibility of using microspines passively was explored. This has previously been done on wall perching fixed wing UAVs by Lussier-Desbiens et al. (2009) [14] and was matured over time [15]. Consequently, microspines could be implemented on the PQs in a smart manner if simulations and scaled test show a sufficient amount of shearing of the PQs over the surface. It would be required to know (at least coarse, if installed on a pin that can rotate) the shearing direction in order to install the microspines. Microspines could be installed on a pin on the lower side of the PQ such that they grip the asteroid surface when the PQs slip over it. One of the leading experts in the field and author of the previously cited article on microspines, Dr. Aaron Parness from JPL, stated that "[...] there are ways [...] to use a microspine gripper that would be passive or spring-loaded instead of driven by motors and electronics." (Aaron Parness, personal communication, 14/06/2019).

Stored volume

Another challenge is the net packing inside the Deployer. The aim is to pack the net with the PQs attached as tight as possible without compromising deployment or increasing the chances of entanglement. The cancelled ROGER mission was used as a reference [7]. Its 10 × 10 m net with a mesh width of 0.2 m required a storage volume of 5 dm^3. The ROGER net (just the fibres) had a mass of 1 kg and was made out of Nylon A with a density of 1100 kg/m^3[3]. As a result, the volume of 0.91 dm^3 together with the mentioned stored volume leads to a packing factor $f = 0.181$ by applying $f = \frac{fiber_{volume}}{stored_{volume}}$. The ANTREA fibres have a volume of 0.716 dm^3 and assuming a similar packing factor, the stored volume becomes 4.13 dm^3. A margin was added to account for the thicker wires (lower minimum bend radius) and the required connection to the PQs, which reduced f to 0.149. To conclude, the required storage volume for the ANTREA net was assumed to be 5 dm^3. This number does not include the volume of the PQs themselves.

8.3. Bullet Design

The main function of the bullets is to accelerate the net out of the Deployer, span it and make sure it wraps around the asteroid. Two additional secondary functions have been identified.

1. Retracting some cable after wrapping around the asteroid in order to tighten the net.
2. Providing energy storage capacity in terms of batteries in the bullets.

The first was inspired by the RemoveDEBRIS mission [10]. A net was shot at a target satellite with the goal of de-orbiting it along a tether line. In order to increase the chances of unwrapping, the bullets had spools to retract a rope that would tighten the net. A similar approach has been followed for the DOT mission, requiring a motor and mechanism to perform the task. Net simulations on asteroid contact, see subsection 8.4.2, proved the necessity of such a system.

The second additional function followed from the fact that the system needs energy storage capacity. The bullets can be exploited for this, since they have a high density and volume in comparison to the PQs. As a result, four identical bullets that meet the requirements were placed at the four corners of the net.

Calculations for Sizing

The reel-in of ropes requires an actuator and spool. For maximum efficiency, controllability, and compatibility with the energy storage function, an electrical motor was chosen as actuator. In order to size this system, the following calculations on the motor were carried out. A Python program has been implemented to select the best combination of components, the following presents the final values.
Since ideally, mechanical power is conserved through a gearbox but there are inevitably losses, it holds that $T_1\omega_1 = \eta T_2\omega_2$ where T_1 and T_2 are the in- and output torques, ω_1 and ω_2 are the in- and output rotational

[3] http://matweb.com/search/DataSheet.aspx?MatGUID=09c6d8aaad51444f838a219bb88a6c0a [Accessed on 17/06/2019]

speeds and η is the transmission efficiency. The leading technology for the desired application are BLDC motors, the power diagram of the selected Maxon EC-max 22[4] can be seen in Figure 8.3. The motor has 3 hall sensors that measure the position of the rotor with respect to the stator. This information is fed to an electronic speed control (ESC), the Faulhaber SC 1801 P[5] that controls the motor and uses the batteries as power source. It is obvious the motor can operate continuously at high rotations per minute but not at high torques, since torque is directly related to current. Consequently, a planetary gearbox is required. The selected GPX 22 HP[6] has a reduction ratio of 590:1 and an efficiency of $\eta_r = 55$ %, which is quite low for a planetary gear due to the compact design and 4 stages. Applying $P_{mech} = T\omega$, where T equals 9 mNm and ω equals 12000 rpm = 1256.6 rad/s (the point indicated by an X in Figure 8.3).

This results in the mechanical power P_{mech} being 11.3 W. In this case, the motor and ESC efficiency are $\eta_m = 63$ % and $\eta_e = 93$ % respectively and therefore the required electrical input power amounts to 18.9 W. $T_s = r\eta T_m$, where T_s is the spindle torque, r the transmission reduction and T_m the motor torque. T_s results in 2.92 Nm with an input T_m of 0.009 Nm. The equation $F = \frac{T}{r_{spindle}}$ can be applied to calculate the force in the cable. With $T = T_s$ of before and $r_{spindle} = 0.01$ m (as the spindle plus drum, on which the cable will be, is assumed to be 1 cm), the maximum force in the cable is 292 N. The reel-in cable velocity can be computed by $v_s = \omega_s d$, where ω_s is the rotational speed of the spindle. By filling in $\omega_s = 2.13$ rad/s, the reel-in velocity becomes 0.0213 m/s.

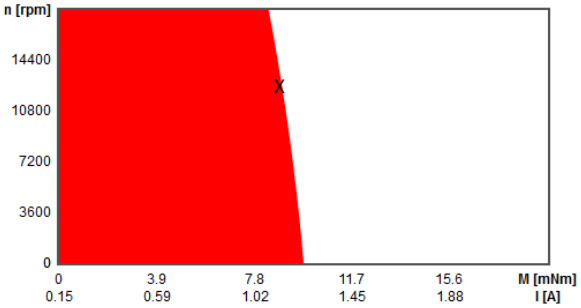

Figure 8.3: Power diagram of the Maxon EC-max 22, taken from Maxon motor, see footnote 4. Red indicates the continuous operation range, white indicates the short term operation range.

The maximum reel-in distance d_{reel} was assumed to be 10 m, which would take a time t of 470 s at 12000 motor rpm. Multiplying the time with the required input power results in the required energy, $E = P_{in}t$, where E is 2.46 Wh in the present case. Assuming 100% battery efficiency, the overall system efficiency is 33%.

For the other secondary function, one would like to fit batteries as large as possible to provide the maximum energy storage. It was found that three Sony/Murata US18650VTC5A[7] can fit inside the cylindrical shell of each bullet. They each have a capacity of 2600 mAh and a nominal voltage of 3.6 V, resulting in an energy storage capacity of 28.08 Wh per bullet and 112.32 Wh in total. This assumes a Depth of Discharge of 100%, how they will actually be used after deployment is detailed in chapter 13.

Bullet Layout

The bullet is of cylindrical shape and all previously mentioned components need to fit inside. The mass of 2 kg is governed by the deployment dynamics. The bullet shell is made of stainless steel and extra lead is added around the motor and gearbox, which can effectively act as a radiation vault and increases the mass to the required 2 kg. Between the interior components and the steel shell, a thin layer of gel is implemented to provide shock resistance and protect the mechanical and electrical assemblies. The components are listed in Table 8.5. Two IMUs are present to record the deployment for scientific reasons. The electronic speed control automatically starts a countdown during deployment (triggered by IMU voltages) and after 120 s starts to reel-in the cable. It stops if either 10 m were reeled-in or if the force in the cable exceeds the limit of 292 N, which means the applied torque is too high and decelerates the motor to a cut-off speed.

[4] https://www.maxonmotor.com/maxon/view/product/283838 [Accessed on 17/06/2019]
[5] https://www.micromo.com/media/pdfs/SC1801_DFF.PDF [Accessed on 17/06/2019]
[6] https://www.maxonmotor.com/maxon/view/product/gear/planetary/GPX/GPX22/GPX22-4-Stufig-HP/GPX22HPKLSL0590CPLW [Accessed on 17/06/2019]
[7] https://www.nkon.nl/sony-us18650vtc5a-flat-top.html?gclid=Cj0KCQjwi43oBRDBARIsAExSRQF0jprnoUkSivOfDaER-JT_crZJIOrtZEJe3XYwJzGLUUN7KCl5hZEaArRqEALw_wcB [Accessed on 17/06/2019]

Table 8.5: Table with bullet components per piece

Component	Number	Model	Mass [kg]	η_{mech}/η_{elec}	Cost [EUR]
Bullet shell	1	custom	1.002		500
Battery	3	Sony / Murata US18650VTC5A	0.045		11.85
BLDC motor	1	Maxon EC-max 22	0.083	0.63	152.73
Gearbox	1	Maxon GPX 22 HP	0.095	0.55	179.91
ESC	1	Faulhaber SC 1801 P	0.004	0.95	200
Lead	1	Custom	0.6		50
Gel	1	Custom	0.05		100
Cables, connectors, spindle	-	Custom	0.03		100
IMU	2	BMX055 [8]	0.0005		3.72
total			**2**	**0.33**	**1298.21**

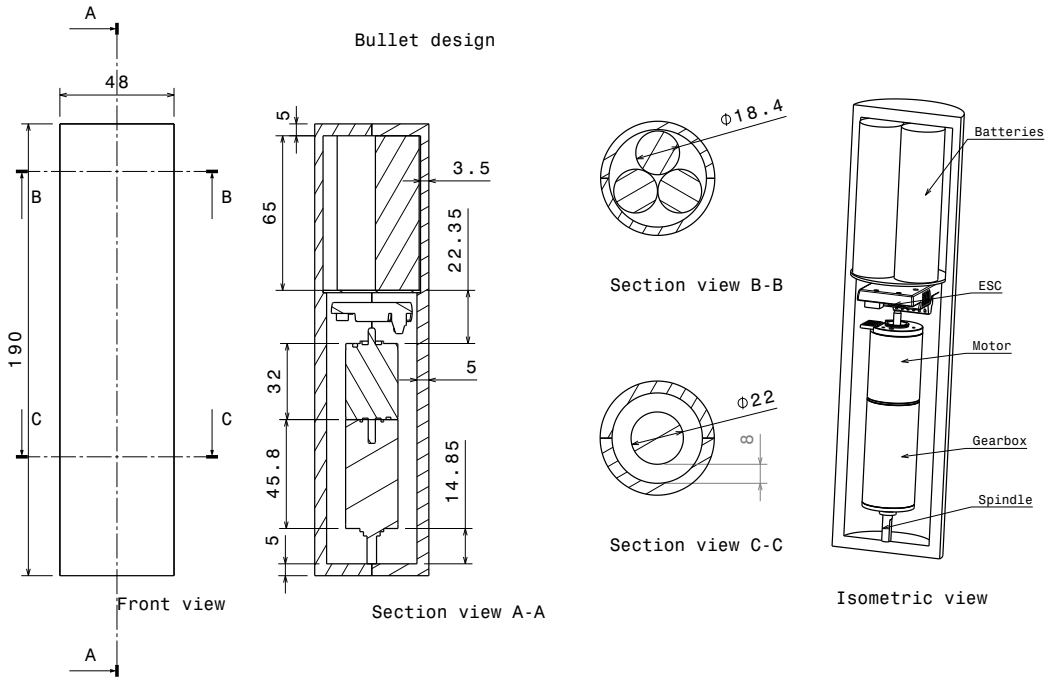

Figure 8.4: Drawing of a bullet illustrating the layout.

8.4. Simulations on Net Deployment

SKA-Polska's software ADRiNET - The Toolchain for Dynamic Simulation of Elastic and Deformable Net-like Structure, enabled net deployment and asteroid attachment dynamics simulations. The cable dynamics are based on the Cosserat rod model while tensional, torsional, and bending stiffness of the fibre are all taken into account. Additionally, a contact model has been implemented to simulate the net entangling around an object. The simulation applies a forward Euler integration scheme. A more in-depth description of the simulator can be found in [16]. The net discretised in the simulation has an identical layout as the one presented in Figure 5.7, except for the direct fibre connecting the bullets. On the other hand, the simulation assumes a Technora fibre net with a diameter of 0.5 mm, as this was the baseline SKA-Polska model. Consequently, the dynamic behaviour of the simulated net will differ slightly from the ANTREA design. However, these deviations are regarded as only relevant in further detailed design and development. The net is discretised in 173 knots (with mass and inertia) and 6003 links connecting these knots via control points. The PQs and bullets are modelled with their actual dimensions and masses. The density is assumed uniform to calculate their moment of inertia. As explained in section 8.2, there are a number of differences between the ANTREA and classical active debris removal nets, the most pronounced one being $r = \frac{\text{total bullet mass}}{\text{total net mass (without bullets)}}$.

8.4.1. Simulations Focused on Deployment

At first, deployment of the current design with the current parameters was simulated. The maximum deployment fraction $f = \frac{\text{actual net area}}{\text{fully deployed net area}}$ achieved was 0.29. This value is unacceptably low and hinders mission

success. An evolution of the deployment fraction over time can be found in Figure 8.5, along with a black line indicating time of the snapshot presented on the right. In Figure 8.6 it is visible that only the bullets are spanned outward while the rest of the net is folded. It should be noted that the deployment fraction is just one parameter indicating deployment performance. A high ultimate deployment fraction does not always result in successful deployment, as especially slow rates tend to be very chaotic, thereby increasing the chance of the net entangling itself. Oscillations during the net deployment are presented in 8.7a, 8.7b and 8.7c. Those are always present but especially strong in the depicted case. For the following deployment simulations, contact detection was deactivated to decrease computational effort, which means that entanglement could not be simulated. Unfortunately, the simulations only started at a very late stage in the design process and it was impossible to change major aspects at this point. However, the design can be altered in a number of ways.

1. The mass of the bullets can be increased to realise a higher r. The mass budget allows 50 kg, but currently only 25.5 kg are used. The bullet mass could therefore be increased to 5.75 kg each (total bullet mass increase of 15 kg), whilst still keeping 9.5 kg for eventual snowball effects on the Deployer. The added mass only manages to achieve an r of 2.1, which is still below the usual minimum of 4. In case it is required to keep the current bullet dimensions, 4 kg can be regarded as the upper limit as then the density corresponds to the density of lead.
2. The angle of ejection, θ, can be increased. On a system level, this would result in a lower volume available to store the net and PQs.
3. The centre of the net could be given an initial velocity by ejecting it, see section 28.2 for a concept on how to provide this in practise, which would reduce the momentum transfer between the net and bullet and could increase deployment stability and probability of success. This would require an additional spring (or any kind of deployment mechanism) in the centre of the Deployer.
4. The bullets can be ejected at a higher velocity to increase the deployment success rate. A more powerful ejection system would be required, possibly switching from a spring to a gas Deployer system.

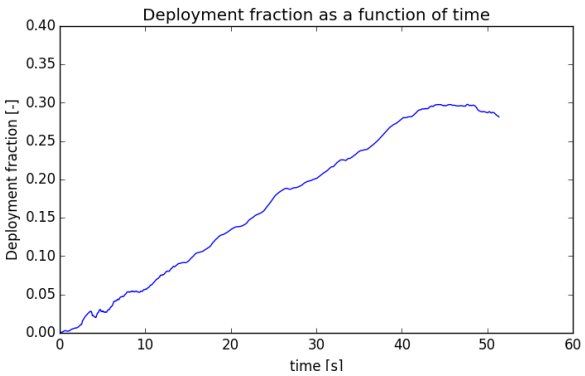

Figure 8.5: Deployment fraction vs. time after bullet ejection, current design. v_{eject} = 2 m/s, m_{bullet} = 2 kg, θ = 10 °, m_{PQ} = 0.15 kg, $V_{initial}$ = 0

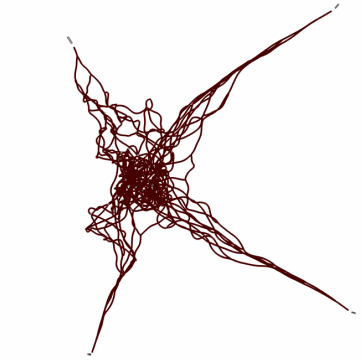

Figure 8.6: Snapshot of current design, 47.31 s after bullet ejection. v_{eject} = 2 m/s, m_{bullet} = 2 kg, θ = variable, m_{PQ} = 0.2 kg, $V_{initial}$ = 0.

(a) (b) (c)

Figure 8.7: Current net design deployment. v_{eject} = 2 m/s, m_{bullet} = 2 kg, θ = 10 °, m_{PQ} = 0.2 kg, $V_{initial}$ = 0. (a) 2.57s after bullet ejection; (b) 3.29s after bullet ejection; (c) 3.95s after bullet ejection.

Simulations were carried out, increasing the bullet mass to 5.75 kg as mentioned in item 1. At the same time, the ejection energy was kept constant at 4.12 J, which resulted in an ejection velocity of 1.18 m/s. The simulations

showed a steadier deployment than with 2 kg bullets ejected at 2 m/s. The computations were done on a range of ejection angles as described in item 2. Figure 8.8 presents a graph displaying the deployment fraction over time. The optimum was reached at an angle of 35 degrees and a deployment fraction of 0.94. It should however be kept in mind that such high ejection angles would implicate important constraints on the volume budget inside the Deployer. Looking at the deployment fraction evolution, one can notice kinks in all simulations at about 5 s and 7 s. These correspond to the bullets transferring momentum to the PQs, which are by far the most massive objects in the net. These phases are especially critical as only very lightly damped oscillations can occur on the part of the net in tension, i.e. the parts in between the PQs and the bullets.

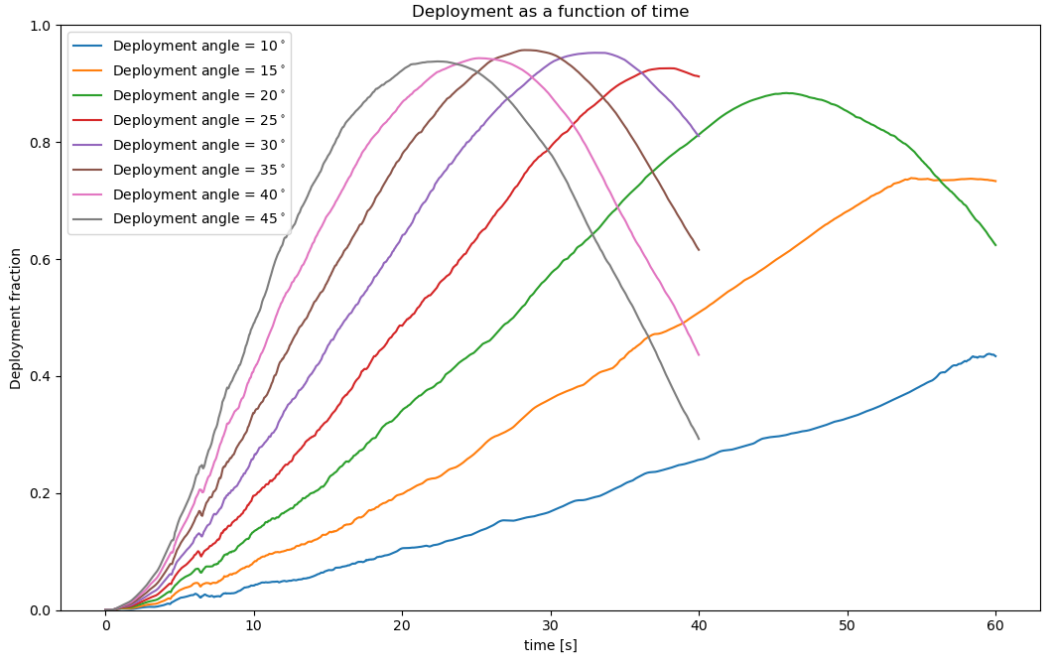

Figure 8.8: Deployment fraction vs. time after bullet ejection. v_{eject} = 1.18 m/s, m_{bullet} = 5.75 kg, θ = variable, m_{PQ} = 0.2 kg, $V_{initial}$ = 0

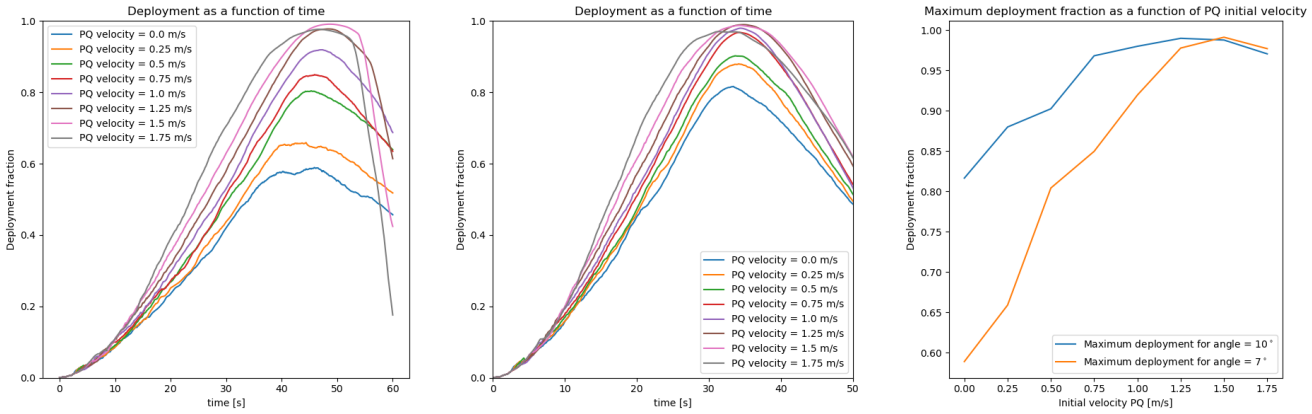

(a) (b) (c)

Figure 8.9: Influence of initial PQ velocity. v_{eject} = 2 m/s, m_{bullet} = 5.75 kg, , m_{PQ} = 0.155 kg, initial PQ velocities applied 1 s after bullet ejection. (a) θ = 10 °; (b) θ = 7 °; (c) Max deployement θ = 10 ° and θ = 7 °

Providing an initial velocity to the net (which is usually 0 m/s) and not just the bullets as described in item 3 proved to enhance the deployment fraction. The simulations were carried out using a variable initial velocity that was applied 1 s after bullet ejection. In 8.9a a graph of the deployment fraction vs. time after bullet ejection with 10 degrees ejection angle is presented for initial velocities ranging from 0 to 1.75 m/s. The deployment fraction peaked at 0.975 at an initial velocity of 1.25 m/s. 8.9b presents a similar graph for an ejection angle of 7 degrees, which peaked at 0.98 at an initial velocity of 1.5 m/s. A summary of the previous graphs is shown in 8.9c. These simulations provided insight into the optimal bullet ejection vs. net ejection velocity applied 1 s

after bullet ejection at 2 m/s. Further analysis needs to be carried out finding the optimum between the two velocity ratios and the time of net ejection, which was kept constant at this stage. In section 28.2 a functioning design applying an initial velocity is presented, but at the same time it does not in any way claim to be the most optimal in terms of ejection parameters. In the future, these ratios may be coupled with net mass parameters to enable optimal design from the beginning.

8.4.2. Simulations Focused on Asteroid Attachment

After the net deployed successfully, it has to impact, wrap around, and entangle around the asteroid. The length and number of simulations with contact detection enabled is limited, since computing a time propagation of one second at a time step of 5×10^{-6} takes about 2000 s on a decent quad-core machine. The main target parameters in the entanglement simulations are the asteroid size and distance from the Deployer as well as the asteroid rotation axis and speed. The size is fixed for this campaign while the distance was changed. In 8.10a, 8.10b and 8.10c a sequence of a net approaching, attaching and leaving the asteroid is presented. Rather obviously, the net failed to remain on the asteroid and the bullets did not entangle. The bullets had a mass of 5.75 kg were ejected at a velocity of 8.49 m/s at an angle of 19.56 degrees. The asteroid was placed 40 m from the Deployer. In this quick sequence of 8 s, the asteroid rotation (period 90 s) could hardly play a role. A successful asteroid attachment is displayed in 8.11a, 8.11b, and 8.11c. In this case all parameters remained unchanged except the distance from the Deployer to the asteroid, which decreased to 23.5 m. Not enough simulations with similar parameters were performed to draw definite conclusions, but a clue can be found by looking at the deployment fraction graphs showed in Figure 8.12 and Figure 8.13. The black vertical lines indicate the times of the previously presented figures of the failed and successful attachment. One can notice that the net in the failed attachment achieved its maximum deployment fraction at around 6 s, and start to retract before hitting the asteroid. On the contrary, the net in the successful deployment was still expanding when it hit the asteroid. To conclude, there is a possibility of correlation between the first derivative of the deployment fraction and the chance of bullet entanglement on the backside of the asteroid.

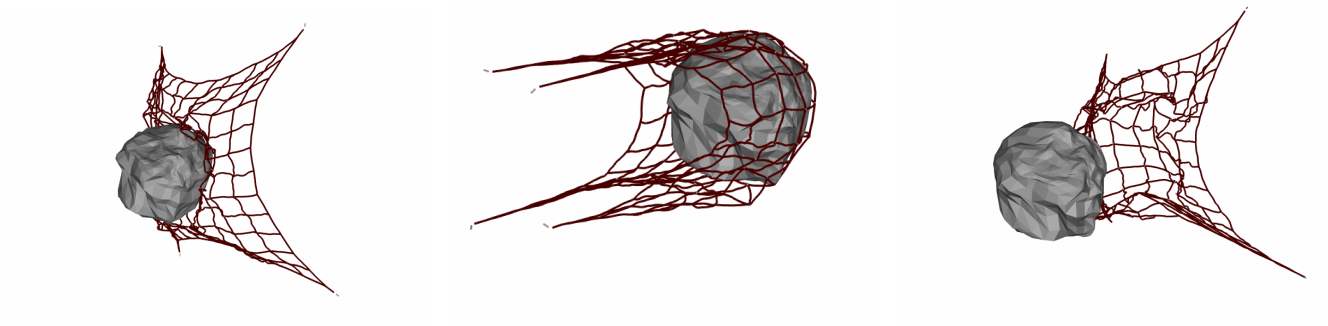

(a) (b) (c)

Figure 8.10: Failed asteroid attachment. v_{eject} = 8.49 m/s, m_{bullet} = 5.75 kg, θ = 19.56 °, m_{PQ} = 0.2 kg, $V_{initial}$ = 0, $d_{asteroid}$ = 40 m. (a) 7.43s after bullet ejection; (b) 11.76s after bullet ejection; (c) 15.19s after bullet ejection.

The orientation of the asteroid axis with respect to the Deployer plays a role in the time after initial attachment. A limited amount of simulations indicated that if the axis of rotation is coinciding with the deployment axis the bullets have a higher chance of unwrapping and detaching the net from the asteroid surface. A sequence of snapshots can be found in 8.14a, 8.14b and 8.14c. The net clearly attaches to the asteroid and is almost completely closed at 50 s after bullet ejection. The asteroid rotation (period 90 s) however leads to the bullets leaving the surface due to the centripetal accelerations they are experiencing. This is undesirable as it opens the net and could ultimately lead to it detaching from the surface. This example illustrates the absolute need for the bullets to close the net after attachment. Their effectiveness could be highly increased by adding hooks that entangle with the net when the bullet hits a part of it after attachment to the asteroid.

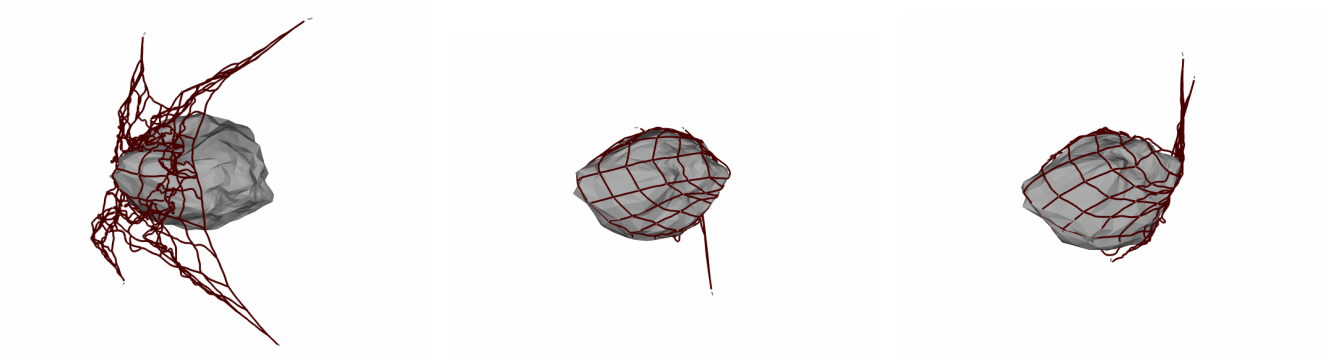

(a) (b) (c)

Figure 8.11: Successful asteroid attachment. v_{eject} = 8.49 m/s, m_{bullet} = 5.75 kg, θ = 19.56 °, m_{PQ} = 0.2 kg, $V_{initial}$ = 0, $d_{asteroid}$ = 23.5 m. (a) 4.62s after bullet ejection; (b) 14.87s after bullet ejection; (c) 21.08s after bullet ejection.

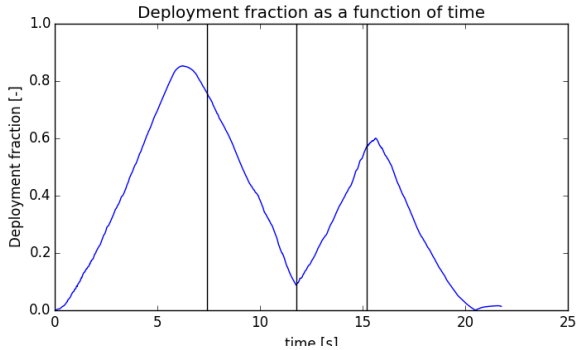

Figure 8.12: Deployment fraction vs. time after bullet ejection, failed attachment

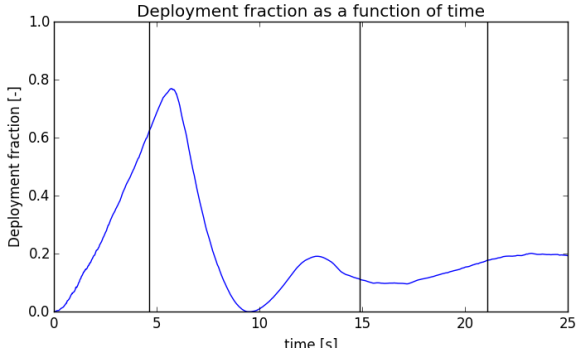

Figure 8.13: Deployment fraction vs. time after bullet ejection, successful attachment

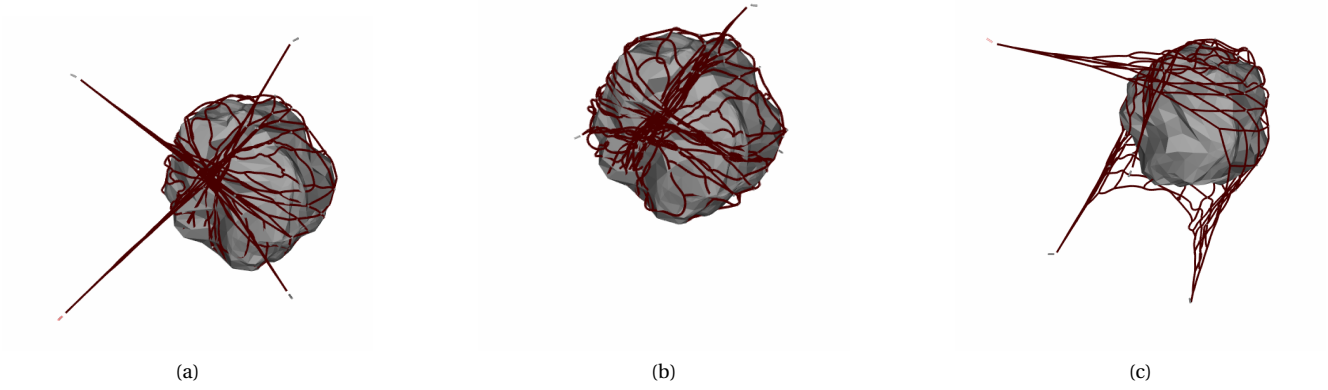

(a) (b) (c)

Figure 8.14: Successful asteroid attachment. v_{eject} = 3.16 m/s, m_{bullet} = 4 kg, θ = 18.2 °, m_{PQ} = 0.15 kg, $V_{initial}$ = 0, $d_{asteroid}$ = 37 m, $P_{asteroid}$ = 90 m, rot. axis coinciding with deployment axis. (a) 38.05s after bullet ejection; (b) 49.85s after bullet ejection; (c) 99.05s after bullet ejection.

8.4.3. Conclusion from Simulations

The performed simulations were insightful and would definitely have helped in the early stage of the design to enable a proper trade-off between parameters such as bullet mass, ejection velocity and angle. Further simulations can be performed to assess and increase the probabilities of successful deployment and entanglement. Time-constraints hindered the team from analysing oscillations and forces in the net in detail. Clear recommendations on how to achieve a final working design can be found in section 28.2. It is definitely feasible to launch a net with masses attached to it on an asteroid and let it entangle. The ANTREA team would like to thank SKA-Polska another time for their support and licence to use their software. In particular the support of Wojciech Gołębiowski and Rafał Michalczy is acknowledged. SKA-Polska set up the model asteroid, discretised the net and provided the net in packed order to simulate deployment.

9 DEPLOYER

The PQs have to be stored in the Mothership all the way to the asteroid. Once arrived, the net will have to be deployed. All of this is done by the Deployer and its design is explained in this chapter.

9.1. REQUIREMENTS

Starting from the user requirements, the Deployer requirements were first derived in the Baseline Report [3]. New requirements were added as the level of detail of the design increased. The overview of the requirements set on the Deployer is presented in Table 9.1 below. A connection of some requirements to a parent requirement is indicated in the **Requirement** column. If the compliance is not yet investigated or cannot be proven at this time, the compliance box contains a "n".

Table 9.1: Requirements for the Deployer of the Lander.

Requirement ID	Requirement	Rationale	Verification Method	Compliance
DOT-LAN-MD-1	The Deployer shall sustain the loads at all mission phases.	This is to ensure that the Deployer is strong enough against launch, mission, deployment loads in particular.	Test	✓
DOT-LAN-MD-5	The Deployer shall be able to contain the Lander.	There needs to be enough volume inside the Deployer for the Lander.	Inspection	✓
DOT-LAN-MD-8	The Deployer shall be able to operate in vacuum.	For example if it contains an explosive charge, the ignition might be more difficult to operate in vacuum.	Test	n
DOT-DEP-1	The Lander System shall sustain the vibration loads as specified in the Vega Launcher Manual. (Parent: DOT-LAN-MD-1)	The Lander System has to survive the vibrations in order to operate fully during the mission.	Test	✓
DOT-DEP-2	The Lander System shall sustain the axial and lateral loads as specified in the Vega Launcher Manual. (Parent: DOT-LAN-MD-1)	The Lander System has to survive the loads in order to operate fully during the mission.	Test	✓
DOT-DEP-M	The mass of the deployer shall not exceed the value specified in the mass budget including the current contingency level.	User requirement	Inspection: weighing the system	✓
DOT-LAN-MD-9	The risk of a premature partial deployment shall be mitigated.	-	Analysis	n
DOT-DEP-3	The Deployer shall be able to open its door autonomously before the Lander deployment.	The door closes the deployer to contain the net. It has to open in order to deploy the net.	Analysis	✓
DOT-DEP-4	The Deployer shall open upon command its single door in no more than 3s. (Parent: DOT-LAN-MD-9)	This is to ensure that the door opening time is fixed.	Analysis	✓
DOT-DEP-5	The Deployer shall open upon command its single door with a reliability rate of <TBD>%. (Parent: DOT-LAN-MD-9)	This is to minimise the risk of the door not opening.	Analysis	n
DOT-DEP-7	The release mechanism present for every one of the 4 weights (so 4 release mechanisms in total) shall trigger within a time interval of maximum <TBD>s from each other. (Parent: DOT-LAN-MD-9)	This is to reduce the risk of an asymmetric deployment.	Analysis	n
DOT-DEP-8	The release mechanism shall have a reliability rate of <TBD>%. (Parent: DOT-LAN-MD-9)	This is to reduce the risk of a failed deployment.	Analysis	n
DOT-LAN-MD-14	The Deployer shall ensure that upon separation, no parts contaminate the Mothership or the Lander.	-	Analysis	✓
DOT-DEP-6	The Deployer door shall not contaminate its surroundings during the Lander deployment. (Parent: DOT-LAN-MD-14)	Once opened, the door shall not decrease the deployment performances in any way.	Analysis	✓
DOT-DEP-V	The volume of the deployer shall not exceed the value specified in the volume budget including the current contingency level.	-	Inspection: measurements on the assembly	✓

9.2. DEPLOYER STRUCTURE

From the requirements, it is known that the Deployer structure has for main purpose to contain the net to avoid it from contaminating the Mothership. The Deployer shall sustain loads at all mission phases. It shall not exceed a certain mass and volume. It is assumed that the Mothership will protect the PQs from the space environment (radiation, temperature) until deployment.

The Deployer is designed as a cubic box of $30 \times 30 \times 30$ cm. The reason for this is that it is the maximum value allowed by the user requirement. By taking this maximum value, it allows to maximise the inner volume and increase the amount of PQs that can be carried. The Deployer is made out of 6 aluminium Al-7075 T6 plates of

1 mm thickness. This allows to reduce the weight while still being able to sustain the loads.

9.2.1. LOADS

All along the mission, the Deployer will be under the influence of loads. The most critical ones are the launch loads, and the Deployer is designed for that as a worst-case scenario. There are three types of loads the Deployer shall sustain: the vibration, axial (longitudinal) and lateral loads (as specified in the requirements).

From the Vega User's Manual [2], it was found that the axial loads varied during the launch. A load envelope can be made to show the different combinations of axial and lateral loads that the Deployer will be expected to sustain. This can be seen in Figure 9.1.

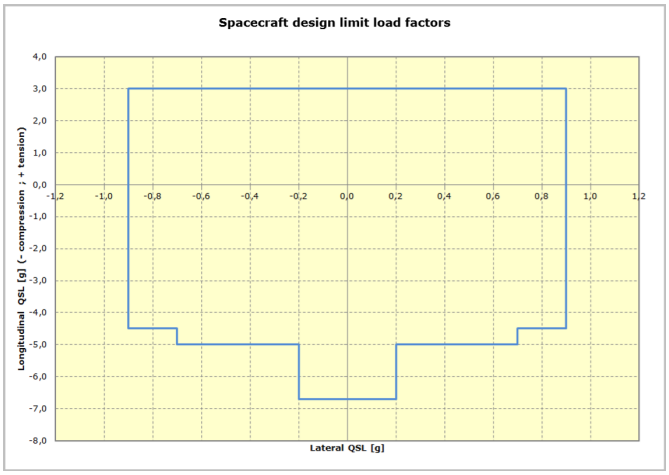

Figure 9.1: Spacecraft design limit load factors [2].

The load analysis was done analytically assuming that the weight of each plate could be represented as a distributed load. A safety factor of 1.5 is used in the calculations for the most critical load of 7g (10.5g including the safety factor) in axial direction, and 0.2g (0.3g including safety factor) in lateral direction. One should note that the safety factor of 1.5 was also used for other structural components, such as the PQ structure for example. This case is the considered the most critical as it is the one that will induce the most stress in the walls. One should note that this is for compression.

The top panel is assumed to be simply supported and will just carry its own weight. The maximum deflection v is calculated using $v = \frac{5wL^4}{384EI}$ (with w being the distributed load, L the length, E the modulus of elasticity, and I the area moment of Inertia) and is equal to 4.86 mm in the middle of the top panel. This corresponds to a stress of 18.6 MPa, and with an ultimate shear stress of 152 MPa this means that it will not fail.

For the side walls, each walls support $\frac{1}{4}$ of the weight of the top plate and their own weight. The maximum stress will be at the bottom of each wall. Using the equation $\sigma = \frac{F}{A}$ (with F being the force, and A the cross-sectional area) for a compressive stress, the maximum stress σ is computed by superposing the axial and lateral stresses. The maximum stress that the structure will undergo is equal to 0.13 MPa which is lower than the yield stress of 96.5 MPa, therefore the walls will not fail.

One last point that has to be analysed is the buckling. The critical buckling stress for a thin plate is given by $\sigma_{critical} = C \times \frac{\pi^2 E}{12(1-\nu^2)} \times (\frac{t}{b})^2$ (with ν being the Poisson ratio, t the thickness, and b the wall length). C is a constant that depends on the boundary conditions (if the wall is simply supported, constrained, etc.). The value of C was taken for a worse case scenario where the walls are simply supported and equals 4. This gives a $\sigma_{critical}$ of 2.94 MPa and as the stress in the walls is 0.13 MPa at most, the walls will not buckle.

For the vibrations, the Vega Launcher will vibrate for a certain range of frequencies and amplitudes. Those are given in Figure 9.2. In order to analyse the effect of vibrations on the Deployer, the system had to be simplified. The structure was assumed to be a beam and was analysed as a 2 degrees of freedom (DOF) system with forced base vibrations. One should take into account that this simplifies the system and does not give the most precise answer about the response of the system, although the calculated natural frequencies will be close to the real values.

The eigenvalues $\lambda_{1,2}$ of the 2DOF differential equation can be calculated and the natural frequencies

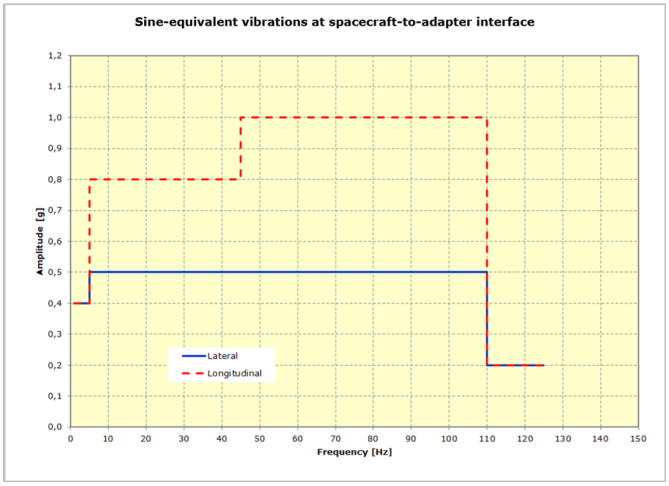

Figure 9.2: Sine-equivalent vibrations at spacecraft-to-adapter interface [2].

can be derived from it . The natural frequencies are given by $f_{1,2} = \frac{\sqrt{\lambda_{1,2}}}{2\pi}$, in Hz. In longitudinal direction, the natural frequencies are 6061.47 Hz and 2315.27 Hz. In the lateral direction, the natural frequencies are 4300.42 Hz and 1642.61 Hz. As the base vibration frequencies are between 1 and 125 Hz, one can see that the natural frequencies are at least 20 times bigger and therefore the structure is strong enough to vibrate in phase with the launcher and to not resonate, which would induce deformations and stresses that could break it.

9.2.2. Deployer Shape

As previously explained, the Deployer structure is made out of an aluminium cubic box. From the loads analysis, the Deployer is overdesigned as it can sustain higher loads than it is expected to, which can therefore also cover a higher range of unpredicted loads. Its mass respects the allocated budget. Therefore it could be improved to be lighter and still sustain the loads.

Cut-outs could have been made to improve the structure. But the main issue with the cut-outs is that the Deployer would not have met the requirement of containing the net and not letting it contaminate the Mothership. It was therefore decided to not make cut-outs in the structure.

Another optimisation of the Deployer was that the walls could be put at an angle. As the weights will be deployed at a specific angle, having the walls straight could decrease the performance of the deployment of the net. However, putting the walls at an angle would decrease the volume. As this last one was very critical and since the performance loss was actually negligible, it was decided to keep the walls straight.

9.3. Deloyment Mechanism

The second main purpose of the Deployer is to deploy the net and the PQs. Nets have recently been used in different space projects, such as the Remove Debris Mission, and those were used as inspiration of the design of the deployment mechanism. The deployment mechanism consists of three main parts: the ejection tube, the spring and its pushing plate, and the trigger mechanism.

The ejection tubes are 4 cylinders made out of aluminium Al-7075 T6. They are located at each corner of the box and tilted at angle of 10 degrees with respect to the vertical axis in the diagonal plane. This is because the weights have to be ejected at that precise angle. The tubes are 293.5 mm long, with a thickness of 1 mm. There is a 2 mm slit along the length of the tube that allows the weight to be connected to the net. At the bottom of the tubes, there is a supporting structure for the trigger mechanism.

The weights are ejected by the use of compressed springs. The main principle behind this mechanism is that the energy stored in the compressed spring is transferred to weights in the form of kinetic energy. The kinetic energy is $E_k = m \times \frac{v^2}{2}$. The potential energy of the spring is $E_s = k \times \frac{x^2}{2}$. Assuming that $E_k = E_s$, one can say that $m \times \frac{v^2}{2} = k \times \frac{x^2}{2}$ (with m being the mass of the weight, v the ejection speed, k the spring stiffness, and x the compressed distance). These make 4 unknowns for one equation.

In order to size the springs, for which many length and stiffness combinations exist, the weights had to be fixed. Each weight has a mass of 2 kg and the ejection speed is equal to 2 m/s. In addition to this, the weights are 19 cm high, which induces that the compressed length of the spring shall not be bigger than 10 cm. This led to a few combinations of stiffness and possible compression distance between 0 and 10 cm. These are shown in Figure 9.3 in blue. Each combination of stiffness and compression distance requires a compression force F given by $F = k \times x$. This is shown in red in Figure 9.3.

The last part of the deployment mechanism is the trigger mechanism. Depending on the maximal load it can support, the compression force of the spring, the spring could be fixed. For the required range of forces that would be required, it was decided to use pin-pullers as trigger mechanism. Other trigger mechanisms were considered, such as wire cutters, burn wire, etc. But in case of a re-design for a heavier mass or higher ejection speed, the required compression force of the spring would easily reach hundreds of Newtons. As pin-pullers can sustain higher loads, it was therefore decided to use them for the trigger mechanism.

The selected pin-puller comes from Tini Aerospace[1] and is the P10 model. The maximum side load it can sustain during actuation is 89 N. With a safety factor of 1.25, the spring should not apply a stress of more than 71.2 N. A specific spring was found on TheSpringStore[2], namely the model PC2540-43637-10300-SST-155702-CG-N-MM. This spring has a stiffness of 0.62 N/mm, a free length of 129.54 mm and would be compressed of 114.5 mm for a compression force of 71 N. Its diameter is 43.64 mm which will fit inside the ejection tube.

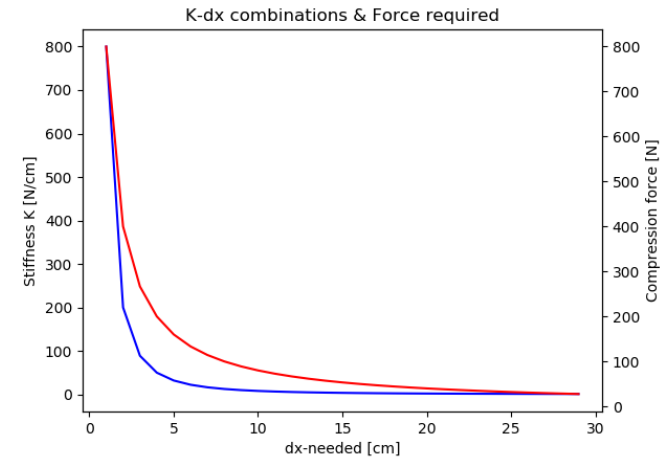

Figure 9.3: K-X Combinations & Corresponding Force

A push plate was put between the spring and the weight. This plate will transfer the compression load of the spring to the weight and ensure a proper fit inside the ejection tube. It is an aluminium Al-7075 T6 cylinder of 48 mm of diameter and 10 mm high. There is a hole on its side such that the pin of the pin-puller can fit inside and lock the mechanism.

The Deployer and its ejection system can be seen in Figure 9.4.

Figure 9.4: Deployer: Ejection mechanism.

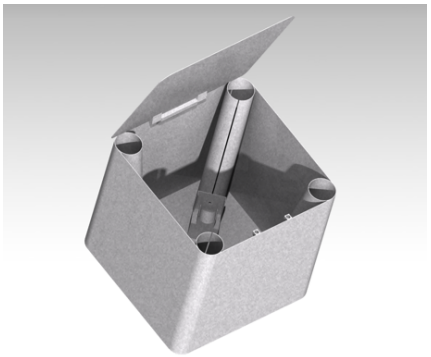

Figure 9.5: Deployer: General view.

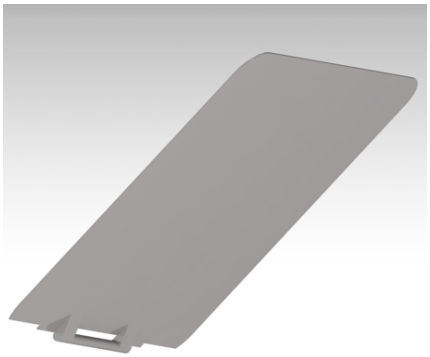

Figure 9.6: Deployer: Door.

9.4. Deployer Opening

In order to let the net be deployed, the Deployer box shall open when required. The roof panel of the Deployer was designed such that it could be opened as a door. The walls and floor panels of the box are all welded together to form one piece. The roof panel would be simply supported on the walls. On one side it has been connected with a hinge to the wall in order to open and be fully deployed at more than 90 degrees such that it does not lock on the trajectory of the weights or the net. On the other side, the door would be opened by using small compressed springs.

The springs were designed in the same approach as for the ejection springs. The potential energy of the compressed spring is transferred into the rotational kinetic energy of the door. The mass moment of inertia of the door around one of its ends is given by $I = \frac{1}{12} \times m \times b^2 + m \times (\frac{b}{2})^2$, and the kinetic energy is $E_{k_{Rot}} = I \times \frac{\omega^2}{2}$ (where ω is the rotation speed). For a chosen rotation speed of 90 degrees/s (there was no requirement on the opening speed), the springs need a force of 1.37 N. Two springs are taken for redundancy, those are the PC406-7137-6000-SST-19050-C-N-MM from TheSpringStore[3] which only need a compression distance of 7.1 mm. A locking system had to be designed on the door to avoid it from opening before deployment. As the force required is only of a few Newtons, a wire burner or wire cutter could be used.

The Deployer door can be seen in Figure 9.6.

[1] https://tiniaerospace.com/products/space-pinpuller/ [Accessed on 19/06/2019]
[2] https://www.thespringstore.com/pc100-1718-10300-sst-6130-cg-n-in.html?unit_measure=me [Accessed 22 May 2019]
[3] https://www.thespringstore.com/pc016-281-6000-sst-0750-c-n-in.html?unit_measure=me [Accessed 22 May 2019]

10
STRUCTURE OF PQ

This chapter will present the internal and external structure of the PQs, mainly looking at complying with sustaining the launch and landing loads of the mission. The design of the mechanisms needed for payload instruments, mainly for the temperature sensors present on the PPQ-1s is also present at the end of this chapter.

10.1. REQUIREMENTS

The overview of the requirements set on the PQ Structures subsystem is presented in Table 10.1 below. A connection of some requirements to a parent requirement is indicated in the **Requirement** column. If the compliance is not yet investigated or cannot be proven at this time, the compliance box contains a "n".

Table 10.1: Requirements for PQ Structures subsystem.

Requirement ID	Requirement	Rationale	Verification Method	Compliance
DOT-LAN-PQ-1	The PQs shall sustain the loads at every phase of the mission with a reliability rate of 80 % or higher.	User requirement.	Test	n
DOT-STR-1	The DOT system's structure shall support the launch environment loads. (Parent: DOT-LAN-PQ-1)	Refer to the Vega launcher manual for maximum launch loads.	Test	✓
DOT-STR-2	The structural stiffness of the PQs shall guarantee that their natural frequencies are within the requirements of the launch vehicle to avoid dynamic coupling. (Parent: DOT-LAN-PQ-1)	Refer to the Vega launcher manual for maximum frequencies.	Test	✓
DOT-STR-3	The DOT system's structure shall support the static and dynamic loads encountered during its lifetime, including production, handling, transportation, testing, launch and in-orbit operations (including landing and touchdown on the asteroid's surface). (Parent: DOT-LAN-PQ-1)	This is to ensure that the structure of the PQs will sustain all loads experienced during their lifetime.	Test	✓
DOT-STR-M	The mass of the structures shall not exceed the value specified in the mass budget including the current contingency level.	-	Inspection: measurement of the assembly	✓
DOT-STR-V	The volume of the structures shall not exceed the value specified in the volume budget including the current contingency level.	-	Inspection: measurement of the assembly	✓
DOT-PAY-TEMP-1	The temperature sensors shall touch the surface of the asteroid. (Parent: DOT-LAN-PQ-SC-1.4)	This is to ensure that the asteroid's surface temperature is measured, rather than the PQ temperature.	Analysis: simulation of the landing and statistical analysis of the sensor positions.	n
DOT-STR-6	The mechanism for the temperature sensor shall deploy the temperature sensor on the asteroid at at least 5 cm away from the PQ. (Parent: DOT-PAY-TEMP-1)	This to reduce the interference in the measurement due to the temperature of the PQ.	Analysis: a simulation of the deployment of the mechanism can be done to check to separation distance.	✓
DOT-STR-7	The mechanism for the temperature sensor shall assure the temperature sensor to be inside when in stowed position. (Parent: DOT-PAY-TEMP-1)	This way the temperature sensor is protected by the PQ when it is not yet used.	Inspection: check of system before launch	✓
DOT-STR-8	The mechanism for the temperature sensor shall have no sharp edges. (Parent: DOT-PAY-TEMP-1)	This to prevent entangling with the net.	Inspection: check of system before launch	n
DOT-STR-9	The wire to release the mechanism for the temperature sensor shall sustain a load of <TBD>N. (Parent: DOT-PAY-TEMP-1)	This to keep the mechanism stowed when the temperature sensor is not yet to be used.	Test	n
DOT-PAY-RAD-2	The signal shall be sent from the +Z plane of the PQ. (Parent: DOT-LAN-PQ-SC-1.3)	This is done to minimise disturbances in the signal due to the PQ's structure.	Inspection: design review.	✓
DOT-STR-10	The wire to release the antenna shall sustain a load of <TBD>N. (Parent: DOT-PAY-RAD-2)	This to keep the antenna stowed.	Test	n

10.2. INTERNAL AND EXTERNAL STRUCTURE

10.2.1. IMPULSE CALCULATION

In order to meet the previously mentioned requirement **DOT-LAN-PQ-1** in particular, it was necessary to assess all phases of the mission that might have major loads events on the PQ's structure, namely: launch, mission, deployment and landing loads. It was assumed that all mission and deployment loads on the PQs would be smaller than the launch and landing ones, and thus only the latter two events were studied. As the philosophy of this design was to end up with something feasible, rather than something optimised, the landing loads were first studied and a preliminary design of the PQ's structure was done. After that, the launch loads were

computed and a check was done to see if the design would sustain launch loads, which it did.

Landing Loads

In order to assess how strong the structure of the PQs would have to be to survive their collision with the asteroid's surface, a simulation of said collision was conducted. To do this simulation and to account for redundancy, it was assumed that a damping material would be added on the -Z face of the PQs, ie: the faces that will be in contact with the asteroid during landing. It was also decided to cover the -Z face edges and corners of the cube with this material. This assumption was deemed fair as its aim was to increase the chance of success of the PQs surviving the landing and has minor consequences on mass and volume of structures.

Due to the fact that not much information is available about the 2017FU102 asteroid, a damping material that was already proven to be effective for space applications was chosen, namely Sorbothane[1]. Apart from being operational in the harsh space environment that the team's net will operate (very high and low temperatures, radiation), this material has been proven to successfully sustain typical launch loads and impact forces that go up to 22.5g. As a matter of fact, Sorbothane can reduce a 22.5g force to 0g in the timespan of 5 ms[2]. This flight-proven material with exceptionally high damping and vibration capabilities was thus chosen to account for the many uncertainties linked to the target asteroid: the surface material and density that would impact the nature of the shock, as well as its mass and rotational speed that would have an influence on the dynamics and ductility of the landing of the PQs on the surface.

Assuming a maximum PQ mass of $m_{PQ} = 200$ g and maximum velocity before landing of $v_{PQ} = 2$ m/s, the impulse of the shock of 1 PQ was calculated using $m_{PQ} \cdot v_{PQ} - \int F dt = 0$, where $\int F dt$ is the impulse that was found to equal $I = 0.4$ Ns. The equation is set to zero, as it is assumed that the PQ's velocity would be zero after the impulse. Following this, it was assumed that the damping material would absorb the impulse in $t_{abs} = 5$ ms, as previously indicated by the properties of Sorbothane. The average impact force was then calculated as follows: $F = \frac{I}{t_{abs}}$, which yielded a load of $F_{load} = 80$ N. Similarly to what was done in chapter 9, this load was then multiplied by a factor of safety of 1.5 for the purpose of decreasing the chance of failure. So $F_{load} = 80 \cdot 1.5 = 120$ N thus corresponds to the maximum force exerted on the PQs for the considered situation. It is important to note that the energy that is absorbed by the Sorbothane material is then transferred into heat.

10.2.2. Internal Structure Design

It was decided to design the internal PQ structure with stacks, ie: PCB plates on which the payloads and other components could be connected. The stacks would be attached to the structure by the means of 4 rods, positioned in each corner of the cube.

A first approach to sizing this system, as well as choose its materials was to look at previous PQ missions such as the Delfi-PQ [17] as reference. By doing so, dimensions were scaled down and it was decided that the diameter of those rods would have to be 2.5 mm[3], made out of aluminium Al-7075, as specified in the PocketQube Standard [18] to be able to conduct first mechanics of material calculations. Similar to the Australian OzQube-1[4], these four rods would be connected to the -Z plate of the cube, by screwing them into place. It was thus necessary for the -Z face of the PQ to be thick enough to support these four rods. Some space was allocated in between the end of the rods and the top of the PQ, to account for the upward vertical movement that these rods might experience during landing, due to the shock of the collision between them and the asteroid's surface. Since the elongation at break of AL7075 is of 11%[5] at the temperature at which the rods will be during landing (assumed to be equal to the PQs' internal temperature inside the Mothership, which is 20 degrees Celsius), then rods of length of 35 mm with spaces of 3.85 mm above them would be required, as shown in Section view A-A of Figure A.5, present in appendix A. That figure also gives an indication on how the Sorbothane layer is placed on the PQs. To check that these dimensions would be sufficient for the four rods to have enough space to elongate during the shock on the asteroid's surface, their deflection to an axial load of $F_{load} = 120$ N was computed using $\delta = \frac{F_{load} L}{EA}$ and assuming a constant cross section and internal normal force, as well as a

[1] https://www.sorbothane.com/ [Accessed 22 May 2019]
[2] https://www.sorbothane.com/Data/Sites/31/pdfs/data-sheets/102-Sorbothane-performance-curves.pdf [Accessed 22 May 2019]
[3] http://www.albaorbital.com/hardware/2p-solid-wall-pocketqube-structure [Accessed 22 May 2019]
[4] https://twitter.com/OzQube1/media? [Accessed 22 May 2019]
[5] http://www.matweb.com/search/datasheet_print.aspx?matguid=4f19a42be94546b686bbf43f79c51b7d [Accessed 22 May 2019]

homogeneous aluminium material. Here L represents the length of the rod, E its modulus of elasticity taken as 71.7 GPa, and A is its cross-sectional area. It was found that under the found design load, one rod would elongate by 0.012 mm, which fit in the previously chosen 3.85 mm. Moreover, by referring to aluminium's yield stress of σ_{al} = 503 MPa, it was found using $\sigma = \frac{F}{A}$ that the load would be equal to F = 2469.10 N, which is well above the design load of 120 N. This system might thus seem over-designed, however, making this choice did not hinder the mass or volume budget allocations that were given to the PQ's structures, so these numbers were kept.

10.2.3. External Structure Design

For the optimisation of the external structure, it was assumed that the cubic structure and not the damping material would take in most of the landing shock, as Sorbothane was added to merely dampen the shock, not to serve as a structurally strong component that would sustain the whole structure. To choose a material, the most critical cases were considered. These include the PQ landing exactly on one of its corners and also a spike of the asteroid's surface being in contact with the PQ when landing. The compressive stress experienced during these critical load cases was computed with the previously mentioned formula $\sigma = \frac{F_{load}}{A}$, with A being the area of the surface experiencing the design load F_{load}.

If the PQ were to land on one of its -Z face corners, the surface area that would be in contact with the asteroid's surface would be the rounded corner of Sorbothane. Following indications from the PQ standard [18], either FR-4 or Aluminium Al-7075 would be acceptable for the PQ structure. As FR-4 has a lower density compared to Aluminium (1.82 g/cm against 2.81 g/cm), it was used in the structure calculations, with aim to save mass. FR-4's compressive stress at 10% deformation is equal to 413.685 Mpa. It was found that an area of 0.29 mm^2 would be needed for a force of F_{load} = 120 N. By assuming that the area of one of the PQ's corners would be equal to the cross-sectional area of a sphere, the required radius was found with $A = \pi r^2$, and the thickness was found with $t = 2 * r$, which resulted in a thickness of 0.6 mm for FR-4. By doing the same calculation with FR-4's lowest stress, namely its shear stress of 131 Mpa, a thickness of 1.08 mm was found. This corner thickness calculation was thus done by assuming a rounded corner of FR-4, although it is the Sorbothane layer which provides rounded corners to the structure. This thus has consequences on the accuracy of the result. To account for any discrepancy linked to this, and to add contingency for protection of the instruments against radiation, the value of FR-4's thickness was increased to 2 mm on five of the PQ's six faces, with the sixth face being the -Z face, where the thickness would have to be doubled to account for the screwing of the 4 previously mentioned aluminium rods.

Concerning the situation where a spike would collide with one of the PQ's faces, the Izod Impact value of FR-4 was considered, which corresponds to the material's impact resistance. Having a value of about 0.37 J/mm, FR-4 can thus breaks after absorption of 0.37 J of energy per every mm. To consider how thick FR-4 would have to be to absorb the shock's energy without breaking, the kinetic energy was computed as follows: $E_k = 0.5 * m_{PQ} \cdot v_{PQ}^2 = 0.4$ J. By making the thickness 2 mm, FR-4 could thus sustain $0.37 \cdot 2 = 0.74$ J, which would be enough for it to absorb the kinetic energy without breaking.

To conclude, the cubic hollow structure will thus be made out of FR-4 material, with 2 mm thickness all around, except on the -Z side, where it will be 4 mm thick. Some holes will be present in this structure, to let payload appendages and other mechanism stick out of the structure. However it was assumed with the help of Dr. Ir. JMJF van Campen that although stress concentrations will be present by compression of the hole, they would be minor compared to the shock of the landing, so more focus was put on that latter part during the design. The FR-4 will weigh 50.01 g. On top of the -Z face, there will be a 2 mm thick layer of damping Sorbothane material also covering the edges and 4 corners, which will result in an addition of 9.53 g. The internal structure will consist in four aluminium rods of 2.5 mm diameter, which will weigh a total of 7.72 g. In total, the structures will thus have a mass of 67.26 g, and will occupy a volume of 35.17 mL, by taking into account the respective densities. The dimensions can be seen from Figure A.5.

Launch Loads

In terms of the structure being able to sustain the launch loads and vibrations, the same method as in chapter 9 was used, but with FR-4. With a length and width of 46 mm, minimum thickness of 2 mm, modulus of elasticity of 21 GPa, and maximum PQ mass of 200 g, the following sets of 2 natural frequencies (1 frequency for every degree of freedom considered) were yielded: the lateral natural frequencies were equal to 19768.9 Hz and 7551.1 Hz, and the axial natural frequencies were equal to 14599.1 Hz and 5576.34 Hz. These are all higher than the natural frequencies experienced during launch, which are specified to lie between 1 and 125 Hz in the Vega User's Manual [2].

Concerning the launch loads, the same dimensions were used, as well as a Poisson ratio of 0.118, and a modulus of elasticity of 18.61 GPa. The results were that the walls would endure a stress of 0.0107 MPa in axial direction, a stress of 0.0130 MPa by combination of the axial and lateral direction, and a critical stress of 117.37 MPa for buckling. For the roof, a bending stress of 0.1417 MPa would be endured, anda a displacement of 0.00167 mm would occur. So the launch loads experienced in the PQs' walls and roof would thus not be a problem, as FR-4's stress properties are higher than the found values: FR-4's tensile stress is equal to 275.79 MPa, its compressive stress at 10% deformation to 413.69 MPa, and its flexural stress to 379.21 MPa.

10.3. Mechanisms

The scientific payload, which will be explained in more detail in chapter 11, imposes some requirements which need mechanisms in order to fulfil those requirements. The design of these mechanisms will be explained in this chapter. Mechanisms increase the complexity of the system, thus during the mechanisms design solutions were also found to avoid having a mechanism.

10.3.1. Heating wire

The first big challenge was to satisfy requirements of the image sensors concerning the operating temperature range (DOT-PAY-MON-1-4, DOT-PAY-MON-6, DOT-PAY-IMG-NIR-6 and DOT-PAY-IMG-COL-6) and the capability to receive light/radiation (DOT-PAY-MON-1-2, DOT-PAY-MON-3, DOT-PAY-IMG-NIR-3 and DOT-PAY-IMG-COL-3). In order to let the image sensors receive light they need to be installed on the outside of the PPQ-2s. However, the image sensors are then subjected to the space environment. The temperature ranges will be between -123 to + 120 degrees Celsius and would not comply with the operating temperature range of the image sensors. To keep the image sensors in their operating temperature range, they can be put on the inside of the PPQs, however, then a hole needs to be made in the structure and isolation layer. To keep them and the other instruments within the operating temperature range a shutter mechanism would be required for the image sensors. This would be a very complex mechanism so another solution was found. Namely, a heating wire. The image sensors will be attached on the outside of the PPQs and a wire will go through a small hole in the structure and wind around the image sensor. A current is sent through the wire which heats up the wire and thereby heats up the image sensor to a temperature which is in its operating temperature range. It can however not provide cooling during day time so the image sensor will get out of its operating range but will stay in its storage range.

In order to design the heating wire, a simple approach using the definition of specific heat capacity (c) was used: $\Delta Q = m \times c \times \Delta T$ (where ΔQ is the supplied heat, ΔT is the temperature difference and m is the mass of the heated substance). The heat capacity of the image sensor is based on the composition of the component[6]; a weighted average of the specific heat capacities of the component materials was calculated (using respective masses as weights for the average). The heater needs to raise the temperature of the sensor by 88 K (from -123 degrees Celsius to at least -35 degrees Celsius). Thus, the ΔQ could be calculated. Assuming the time of heating up is 1 s, the power needed was computed. The chosen heating wire was the Kanthal® resistance heating wire[7], with 0.15 mm. Then, using Puillet's law[8]: $R = \rho \frac{\rho \times l}{A}$ (where R is the power loss, l is the cable length and A is the cross-sectional area) and the resistivity of the heating wire, the cable could be sized (length). It was found that the wire would have 70mm. Because of its small cross-sectional area, it could fit on the back of the

[6] https://www.onsemi.com/PowerSolutions/MaterialComposition.do?searchParts=PYTHON1300 [Accessed 22 May 2019]

[7] https://www.kanthal.com/en/products/furnace-products-and-heating-systems/resistance-heating-s-and-s/resistance-heating-wire/ [Accessed 22 May 2019]

[8] https://en.wikipedia.org/wiki/Electrical_resistivity_and_conductivity [Accessed 20 June 2019]

image sensor. The mass of the cable is found to be 9×10^{-5}g. It would take up negligible volume. The power consumption is high (553 W) but due to the short duration of the operation, it can be accommodated by the energy source on the PQ. The working time of the heating wire is adjusted to the rotational period of the asteroid which will be derived from the voltage output of the solar panels. This is one of the autonomous functions that the C&DH needs to perform.

The mass spectrometer on the -Z side of the PPQs encountered the same problem as the image sensors as a hole in the structure would be required to collect surface material (requirement DOT-PAY-SPEC-1). This hole would need to be closed after landing to protect all the instruments from the extreme temperatures in space. To avoid this mechanism the same solution with the heating wire is used.

The mass spectrometer and monochrome image sensor 1 are placed on the -Z side which contains the damping layer. The instruments will be attached to the FR-4 structure of the PPQ and a hole will be made in the damping material for them. This way the requirements are about collecting surface material and receiving light are fulfilled.

10.3.2. Antenna deployment

Another instrument that requires to be deployed is the antenna on the PPQs for the radio experiment. This antenna of 17.5 mm in length cannot be deployed when ANTREA is stowed in the Deployer as it will entangle with the net. The antenna can be placed inside and pushed out by a spring. This mechanism is still quite complex and will take up quite some volume on the inside of the PPQ. Therefore, it has been decided to use tape measure as an antenna, which has been done before in space [19]. Due to its curvature it will straighten itself after it has been bend by applying a force. The antenna will thus be attached on the edge of the +Z side of the PPQs and a wire will keep it folded over the edge when ANTREA is stowed in the Deployer. After landing a wire cutter will cut the wire and thereby release the tape measure which then deploys itself. The wire cutter will be a down-scaled version of the MODE CYPRES 2[9]. The tape measure is hold by a block which will be attached to the +Z side with an adhesive, Supreme 12AOHT-LO[10]. This block will be made of FR-4 just like the structure as it is a non-conducting material which will not distort the radio signal. It was chosen to use adhesive instead of a mechanical bond to avoid introducing extra stresses into the PQ structure.

10.3.3. Temperature deployment

The final mechanism that had to be designed is the mechanism that will deploy the temperature sensor, see Figure 10.2.

Figure 10.1: Temperature sensor

This is required to fulfil requirement DOT-PAY-TEMP-1, the temperature sensor needs to touch the asteroid's surface more than 5 cm away from the PPQ. The chosen temperature sensor, see Figure 10.1, is extremely small but its operating temperature range does not comply with the minimum temperature that will be encountered on the asteroid of -123 degrees Celsius. This required the temperature sensor to be on the inside of the PPQ when it is not used. Once the temperature sensor needs to perform a measurement it will be deployed and will be lost in the night. It is desirable to repeat the measurement a few times as the asteroid is getting closer to the sun which changes its temperature. Therefore, each temperature sensor has its own mechanism.

The mechanism will be attached to the lower side of the +X side with the first hinge. This hinge consists of a rod with two closing ends which is attached to the PPQ. On this rod will be a torsional spring and the first arm of the mechanism. When the mechanism is stowed, Figure 10.2, the torsional spring will bend 184.6 degrees. When deployed the first arm needs to be under an 90 degree angle with the side of the PPQ which requires the torsional spring to still be bend 90 degrees when deployed. Therefore, a second rod is added to the lower side

[9] https://www.cypres.aero/product/changeable-mode-cypres-2/ [Accessed 22 June 2019]
[10] https://www.masterbond.com/tds/supreme-12aoht-lo [Accessed 22 June 2019]

of the attachment block to stop the first arm from rotating further.

The torsional spring is a COTS component, its the PT016-188-5875-MW-RH-0750-N-IN[11]. The dimensions of the mechanism were build around this spring. The thickness of the arms were made equal to the width of the temperature sensor which equals 1.05 mm. Both ends of the arms consist of two rings each on one side to attach to the hinge. These rings are made 1.5 mm thick to sustain the tension loads in stowed position. The position where the arm start and the rings end creates a 0.3 mm clearance between that edge and the outer part of the torsional spring. At the end of the first arm a second hing is made which joins the first and second arm. The same torsional spring is used and the second arm is also made as thick as the width of the temperature sensor. This second arm will however, has a width equal to the length of the temperature sensor, 1.35 mm, so that the temperature sensor fits perfectly on the cross-section at the end of the arm. The second arm, when stowed, will go down straight across the first hing and go over a 90 degrees angle. The last part is then going inside the PPQ through a slit in the structure underneath the first hinge. Due keep the second arm parallel to the +X side of the PPQ the closing plates of the second hinge were elongated such that it touched the +X side of the PPQ when stowed to keep the second arm straight. The length of the horizontal part is such that when deployed it sticks out just under the -Z side of the PPQ. This results in a 4 mm clearance from the wall on the inside to the temperature sensor as well. The complete mechanism is shown in Figure 10.2

The length of the slit in the structure was calculated by calculating the difference in turn radius from the second hinge to the kink of the second arm and to the end point including the temperature sensor. The latter was calculated with Pythagoras. A clearance of 0.2 mm above the arm and below the arm was chosen. The slit width is made 2 mm to also include a clearance of 0.65 mm in total. The slit is placed such that there is 1 mm between the bottom of the inside envelop and the slit, and the slit and beginning of attachment of the first hinge.

The arms and hinges will be made of Al-7075 T6. A thin wire will keep the mechanism stowed and a wire cutter (same as for the antenna deployment) will release it. The force needed to keep the mechanism stowed is the sum of the two forces required to bend the torsional spring to the stowed position. The force will be applied in the midpoint between the two hinges. The force then equals $F = \frac{2M}{d}$ where M is the required moment to bend the torsional spring and d is the distance from the hinges to the midpoint. The moment is the turn angle (184.6 degrees) times the rate of the spring which equals 0.059 Nmm. This force will create a shear force in the second arm were the wire goes around. The maximum shear force in the arm is calculated with the following formula: $\tau = \frac{VQ}{It}$ where V is the shear force, t is the width of the cross-section, I is the moment of

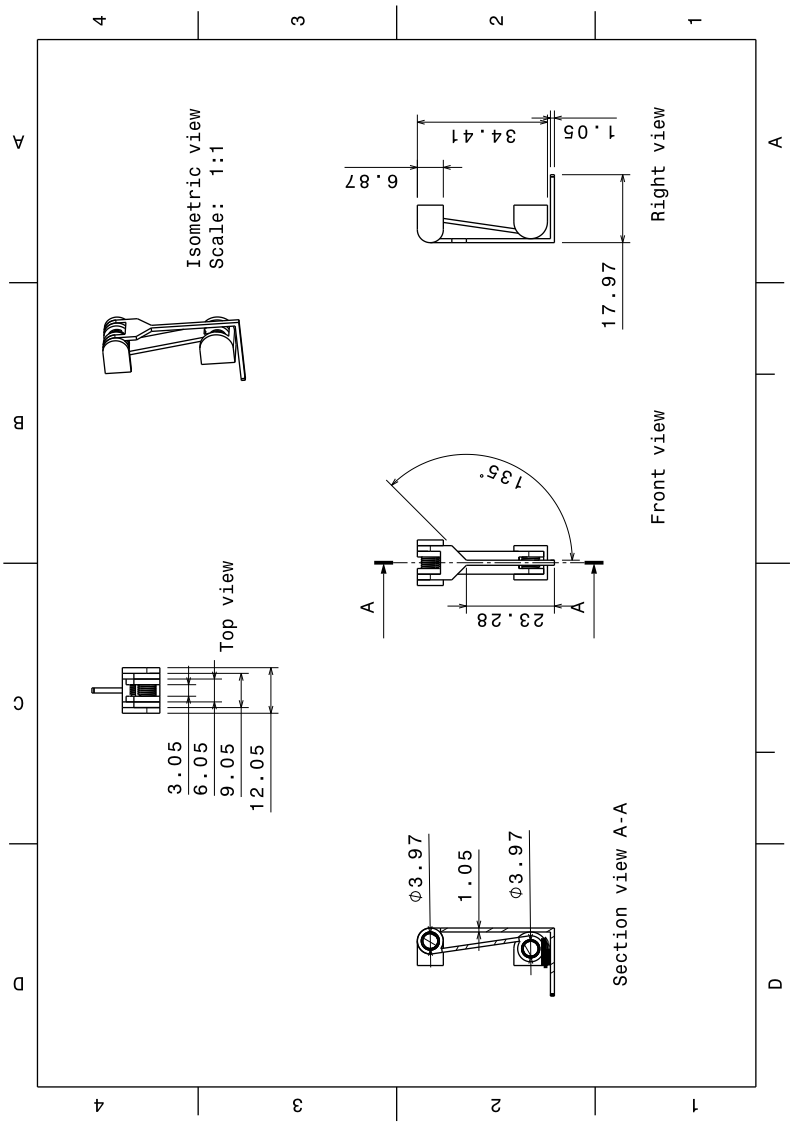

Figure 10.2: Technical drawing of temperature sensor mechanism.

[11] https://www.thespringstore.com/pt016-188-5875-mw-rh-0750-n-in.html?unit_measure=me [Accessed 22 June 2019]

inertia and Q is the first moment of area. The first moment of area equals $y' \cdot A'$ where y' is the distance from the neutral axis to where area A' starts. For a rectangular cross-section with width t and height h this can be rewritten to $-2 \cdot y' \cdot t + \frac{t \cdot h}{2}$. The maximum shear stress occurs at the location of the maximum Q. this location is calculated by setting the derivative of Q equal to zero : $y' = \frac{h}{4}$. The maximum Q equals then $Q_{max} = \frac{t \cdot h^2}{16}$. The moment of inertia for a rectangular cross-section equals $I = \frac{t \cdot h^3}{12}$. Combining this results in the formula for the maximum shear stress $\tau_{max} = \frac{3 \cdot V}{4 \cdot t \cdot h}$. Filling in the numbers results in a maximum shear stress of 0.89 MPa which is way under the maximum shear stress of aluminium Al-7075 T6 of 331 MPa[12]. The mechanism is thus strong enough.

The total mass of one mechanism is 3.3 g and its width is 12.048 mm. As the temperature sensors will be in the internal envelop of 28 mm in width, three temperature sensors with mechanism could fit on the +X side of the PPQ. These three mechanisms will be put next to each other on the +X side with 1 mm in between them. The mechanism adds 9.924 mm to the +X side of the PPQ. Therefore, the temperature sensors could only be added on 10 PPQs which do not have the image sensors on the +X and +Y side of the PPQ. This resulted in the creation of the PPQ-1 with temperature sensors and without the image sensors on the +X and +Y side, and the PPQ-2 without temperature sensors and including the image sensors on the +X and + Y side.

11
PAYLOAD

The main goal of the DOT mission is to gain more information on very small Near-Earth asteroids. Therefore, the main objective of the ANTREA design is to provide scientific data about a very Small Near-Earth asteroid. The scientific payload is thus key to providing this. This chapter will cover the design of the scientific payload of ANTREA. The payload is distributed over 10 PPQ-1s and 49 PPQ-2s. Both contain a mass spectrometer and an image sensor on the -Z side, an IMU, a transceiver and an antenna. The PPQ-1 also contains three temperature sensors, while the PPQ-2 contains three extra image sensors in monochrome, colour and the near infrared on the sides. How this configuration came to be will be detailed below.

11.1. REQUIREMENTS

The overview of the requirements set on the Scientific Payload subsystem is presented in Table 11.1 below. A connection of some requirements to a parent requirement is indicated in the **Requirement** column. If the compliance is not yet investigated or cannot be proven at this time, the compliance box contains a "n". A lot of the requirements still contain an <TBD> for accuracies and resolutions. These requirements will be marked with an "n" as it cannot yet be proven to comply with that accuracy or resolution.

Table 11.1: Requirements for the Scientific Payload subsystem.

Requirement ID	Requirement	Rationale	Verification Method	Compliance
DOT-LAN-PQ-5	The number of scientific experiments that don't meet their accuracy requirements due to an incorrect orientation of the PQs shall not exceed <TBD> % per type of experiment.	Most of the scientific experiments requires the PQs to be oriented in a certain way.	Test: perform test on multiple sized object to check that measurement is feasible.	n
DOT-LAN-PQ-SC-1.1	The PQ network shall measure the shape and size of the asteroid with an accuracy of TBD%.	User requirement	Analysis feasible.	n
DOT-PAY-MON-1-1	The monochrome image sensor 1 shall be attached on the -Z plane of the PQ to face towards the asteroid. (Parent: DOT-LAN-PQ-SC-1.1)	This is required as this image sensor will take pictures of the asteroid during the landing phase where the bottom of the PQs are facing the asteroid.	Inspection	✓
DOT-PAY-MON-1-2	The monochrome image sensor 1 shall be installed such that it receives light/radiation from the outside world in day time. (Parent: DOT-LAN-PQ-SC-1.1, DOT-ADT-MS-8)	The image sensor can only create an image if it receives light/radiation.	Analysis: simulation of the net deployment to make sure that the PQs are not obstructed by the asteroid's shadow.	✓
DOT-PAY-MON-1-3	The monochrome image sensor 1 shall take a picture every 1 meter that is travelled during landing with a resolution of <TBD>pixels. (Parent: DOT-LAN-PQ-SC-1.1)	To monitor the landing pictures shall be made at different moments in time.	Analysis: perform simulation	n

[12] http://asm.matweb.com/search/SpecificMaterial.asp?bassnum=MA7075T6 [Accessed 22 June 2019]

Table 11.2: Requirements for the Scientific Payload subsystem - continued

Requirement ID	Requirement	Rationale	Verification Method	Compliance
DOT-PAY-MON-1-3-1	The monochrome image sensor 1 shall send the taken pictures to the Mothership after every picture is taken. (Parent: DOT-ADT-MS-8)	This is to make sure that the pictures are stored in a safe place such as the Mothership. to mitigate the risk of the pictures being lost during the impact of the PQs on the asteroid's surface.	Analysis: perform simulation	n
DOT-PAY-MON-1-4	The monochrome image sensor 1 shall stay within its operating temperature of -40 to 85 degrees Celsius.	This to minimise the errors in the measurement and to prevent losing the instrument.	Test: subject system to different temperature ranges and measure the sensor's temperature.	n
DOT-LAN-PQ-SC-1.2	The PQ network shall measure the surface composition and its roughness with an accuracy of TBD%.	User requirement.	Test: perform test on objects made of different materials to check that measurement is feasible.	n
DOT-PAY-IMG-NIR-1	The NIR image sensor shall take pictures during both day and night time. (Parent: DOT-LAN-PQ-SC-1.2)	As the received NIR light will be different during day and night time due to the absence/presence of solar radiation.	Demonstration: demonstrate the capabilities of the NIR image sensor.	✓
DOT-PAY-IMG-NIR-3	The NIR image sensor shall be installed such that it receives radiation from the outside world. (Parent: DOT-LAN-PQ-SC-1.2)	The image sensor can only create an image if it receives light/radiation.	Inspection: visual inspection of the assembly.	✓
DOT-PAY-IMG-NIR-4	The NIR image sensor shall be installed such that it has the asteroid's surface in view. (Parent: DOT-LAN-PQ-SC-1.2)	Pictures should be made of the asteroid's surface to be able to analyse its composition and roughness.	Analysis: simulate landing and analyse the pointing of the NIR image sensors.	✓
DOT-PAY-IMG-NIR-4.1	The NIR image sensor shall be installed on one of the sides of the PQ. (Parent: DOT-LAN-PQ-SC-1.2, DOT-PAY-IMG-NIR-4)	When placed on the side the image sensor can "see" the asteroid's surface.	Inspection: design review.	✓
DOT-PAY-IMG-NIR-5	The NIR image sensor shall take pictures with a resolution of <TBD>pixels. (Parent: DOT-LAN-PQ-SC-1.2)	The accuracy of <TBD>pixels is required to properly analyse the asteroid's surface.	Test: component test and data analysis.	n
DOT-PAY-IMG-NIR-6	The NIR image sensor shall stay within its operating temperature of -40 to 85 degrees Celsius.	This to minimise the errors in the measurement and to prevent losing the instrument.	Test: subject system to different temperature ranges and measure the sensor's temperature.	n
DOT-PAY-MON-4	The monochrome image sensor 2 shall be installed such that it has the asteroid's surface in view. (Parent: DOT-LAN-PQ-SC-1.2)	Pictures should be made of the asteroid's surface to be able to analyse its composition and roughness.	Analysis: simulate landing and analyse the pointing of the monochrome of the image sensor.	✓
DOT-PAY-MON-4.1	The monochrome image sensor 2 shall be installed on one of the sides of the PQ. (Parent: DOT-LAN-PQ-SC-1.2, DOT-PAY-MON-4)	When placed on the side the image sensor can "see" the asteroid's surface.	Inspection: design review.	✓
DOT-PAY-MON-1	The monochrome image sensor 2 shall take pictures during day time as a minimum. (Parent: DOT-LAN-PQ-SC-1.2)	During day time visible light is present which the monochrome image sensor can detect.		✓
DOT-PAY-MON-3	The monochrome image sensor 2 shall be installed such that it receives radiation from the outside world. (Parent: DOT-LAN-PQ-SC-1.2)	The image sensor can only create an image if it receives light/radiation.	Inspection: visual inspection of the assembly.	✓
DOT-PAY-MON-5	The monochrome image sensor 2 shall take pictures with a resolution of <TBD>pixels. (Parent: DOT-LAN-PQ-SC-1.2)	The accuracy of <TBD>pixels is required to properly analyse the asteroid's surface.	Test: component test and data analysis.	n
DOT-PAY-MON-6	The monochrome image sensor 2 shall stay within its operating temperature of -40 to 85 degrees Celsius.	This to minimise the errors in the measurement and to prevent losing the instrument.	Test: subject system to different temperature ranges and measure the sensor's temperature.	n
DOT-PAY-IMG-COL-1	The colour image sensor shall take pictures during day time as a minimum. (Parent: DOT-LAN-PQ-SC-1.2)	During day time visible light is present which the monochrome image sensor can detect.		✓
DOT-PAY-IMG-COL-3	The colour image sensor shall be installed such that it receives radiation from the outside world. (Parent: DOT-LAN-PQ-SC-1.2)	The image sensor can only create an image if it receives light/radiation.	Inspection: visual inspection of the assembly.	✓
DOT-PAY-IMG-COL-4	The colour image sensor shall be installed such that it has the asteroid's surface in view. (Parent: DOT-LAN-PQ-SC-1.2)	Pictures should be made of the asteroid's surface to be able to analyse its composition and roughness.	Analysis: simulate landing and analyse the poinitng of the NIR image sensors.	✓
DOT-PAY-IMG-COL-4.1	The colour image sensor shall be installed on one of the sides of the PQ. (Parent: DOT-LAN-PQ-SC-1.2, DOT-PAY-IMG-COL-4)	When placed on the side the image sensor can "see" the asteroid's surface.	Inspection: visual inspection of the assembly.	✓

Table 11.3: Requirements for the Scientific Payload subsystem - continued

Requirement ID	Requirement	Rationale	Verification Method	Compliance
DOT-PAY-IMG-COL-5	The colour image sensor shall take pictures with a resolution of <TBD>pixels. (Parent: DOT-LAN-PQ-SC-1.2)	The accuracy of <TBD>pixels is required to properly analyse the asteroid's surface.	Test: component test and data analysis.	n
DOT-PAY-IMG-COL-6	The colour image sensor shall stay within its operating temperature of -40 to 85 degrees Celsius.	This to minimise the errors in the measurement and to prevent losing the instrument.	Test: subject system to different temperature ranges and measure the sensor's temperature.	n
DOT-PAY-SPEC-1	The mass spectrometer shall be provided with surface material from the asteroid. (Parent: DOT-LAN-PQ-SC-1.2)	The mass spectrometer can only provide useful information if it can analyse the surface material.	Analysis: simulation of the landing.	n
DOT-LAN-PQ-SC-1.3	The PQ network shall measure the material properties of the asteroid with an accu- racy of TBD%.	User requirement.	Testing: testing the instruments on different kinds of materials with different thicknesses.	n
DOT-PAY-RAD-1	The electromagnetic wave sent by the antenna shall be send omnidirectional. (Parent: DOT-LAN-PQ-SC-1.3)	In this way the signal will go through the majority of the asteroid and can therefore provide maximum scientific data.	Analysis: simulation.	✓
DOT-PAY-RAD-2	The signal shall be sent from the +Z plane of the PQ. (Parent: DOT-LAN-PQ-SC-1.3)	This is done to minimise disturbances in the signal due to the PQ's structure.	Inspection: design review.	✓
DOT-PAY-RAD-3	The electromagnetic wave shall have a frequency of <TBD>. (Parent: DOT-LAN-PQ-SC-1.3)	The frequency should be high enough to have a proper resolution but low enough such that it will go through the asteroid.	Test/demonstration: measure the wave frequency.	n
DOT-PAY-RAD-4	The transceivers that performs the radio experiment shall be placed within <TBD>mm from the antenna. (Parent: DOT-LAN-PQ-SC-1.3)	This to reduce the line loss between the transceiver and the antenna.	Inspection: design review.	n
DOT-PAY-RAD-5	The clocks on each PQ shall be synchronised up to an accuracy of <TBD> s. (Parent: DOT-LAN-PQ-SC-1.3)	-	Test: component test and data analysis; comparing the measured data with real data.	n
DOT-PAY-IMU-5	The IMU shall measure the magnetisation with an accuracy of <tbd>. (Parent: DOT-LAN-PQ-SC-1.3)	-	Test: component test and data analysis; comparing the measured data with real data.	n
DOT-LAN-PQ-SC-1.4	The PQ network shall measure the temperature distribution of the asteroid with an accuracy of TBD%.	User requirement.	Test: component test and data analysis; comparing the measured data with real data.	n
DOT-PAY-TEMP-1	The temperature sensors shall touch the surface of the asteroid. (Parent: DOT-LAN-PQ-SC-1.4)	This is to ensure that the asteroid's surface temperature is measured, rather than the PQ temperature.	Analysis: simulation of the landing and statistical analysis of the sensor positions.	n
DOT-PAY-TEMP-2	The temperature sensors shall measure the temperature with an accuracy or <TBD>degrees Celsius. (Parent: DOT-LAN-PQ-SC-1.4)	-	Test: component test and data analysis; comparing the measured data with real data.	n
DOT-LAN-PQ-SC-1.5	The PQ network shall measure the asteroid dynamic motion with an accuracy of TBD%.	User requirement.	Test: component test and data analysis; comparing the measured data with real data.	n
DOT-PAY-IMU-1	The IMU shall measure the acceleration with an accuracy of <TBD>. (Parent: DOT-LAN-PQ-SC-1.5)	-	Test: component test and data analysis; comparing the measured data with real data.	n
DOT-PAY-IMU-2	The IMU shall measure the rotational speed with an accuracy of <tbd>. (Parent: DOT-LAN-PQ-SC-1.5)	-	Test: component test and data analysis; comparing the measured data with real data.	n
DOT-PAY-IMU-4	The IMU shall stay within its operating temperature of -40 to 85 degrees Celsius.	This to minimise the errors in the measurement and to prevent losing the instrument.	Test: subject system to different temperature ranges and measure the sensor's temperature.	✓

Table 11.4: Requirements for the Scientific Payload subsystem - continued

Requirement ID	Requirement	Rationale	Verification Method	Compliance
DOT-PAY-P	The average power of payload shall not exceed the value specified in the power budget.	-	Inspection: measure power levels in all operational modes and compare to the power budget.	✓
DOT-PAY-M	The mass of the payload shall not exceed the value specified in the mass budget including the current contingency level.	-	Inspection: measurements on the assembly.	✓
DOT-PAY-V	The stack height of the payload shall not exceed the value specified in the volume budget.	The subsystem has to fit in the PQ.	Inspection: measurements on the assembly.	✓
DOT-LAN-PQ-SC-1.6	The PQ network shall measure the asteroid's surface hardness with an accuracy of TBD%.	User requirement.	Test: component test and data analysis; comparing the measured data with real data.	n

11.2. Payload Instruments

The characteristics of the asteroid that need to be measured according to the user requirements are the size, shape, surface composition, surface roughness and hardness, temperature distribution, dynamics and internal material composition of the target asteroid. First, the possible methods to determine these characteristics will be described. Some of the instruments had to be eliminated due to constraints in the design. The final chosen instruments will be elaborated on in section 11.2.

Method to Determine Asteroid's Characteristics

The shape of the asteroid can be roughly determined by using cameras while landing. The position of the PQs should however be known. Another way to determine the shape and size of the asteroid is by using a combination of accelerometers, gyroscopes and solar panels. The accelerometers and gyroscopes can measure the gravitational force and the centripetal acceleration which will allow for determining the latitude of the PQ and distance to the centre of the asteroid, while the solar panel can be used to find the longitude of the PQ. The voltage output of the solar cells will be used to determine the time of sunrise, sunset and of peak power of each PQ. The time difference between the sunrise/sunset times and peak power times per PQ divided by the period can provide the information of the longitude. For this one PQ will be used as reference point. As the Mothership will be capable of determining the position of the PQs, it can also be used to determine the shape and size from this data. The hardness of the asteroid can also be determined from the landing with the use of accelerometers and a camera to monitor how the PQs react to the surface. A hammer mechanism, which will be designed as an acoustic source for the seismometer, can also be used after the landing but will fail on a sandy surface.

The surface roughness can be determined from a camera's pictures of the surface. From these images, the surface composition can also partly be determined. An infrared camera and optical spectrometers can determine the surface composition and perform mineralogy. The surface composition in terms of present elements and molecules can be determined with the use of a mass spectrometer, for which some sample material is needed. The dust that will fly around due to the landing can be used for this if properly captured.

The temperature distribution can be determined by measuring the asteroid's temperature with temperature sensors. These sensors need to touch the surface, preferably away from the PQs, for which an arm mechanism would need to be designed.

The internal material composition can be determined by measuring the material properties. This can be done with radio science, a seismometer and magnetometers. Radio science measures the decay of the electromagnetic waves that are sent, a seismometer measures the speed of acoustic waves and magnetometers measure the degree of magnetisation of the material. With this, each instrument can determine different properties. The seismometer, however, needs to be attached to the surface as acoustic waves do not travel through vacuum, so a mechanism needs to be designed to provide this.

The asteroid's dynamics can be determined with the use of gyroscopes. The addition of solar panels, to

determine the orientation with respect to the Sun, can translate the characteristics to a global reference frame.

Finally, the asteroid's mass can be determined by the use of accelerometers or a seismometer in combination with the size data.

Chosen Payload Instruments

In order to keep the costs low and minimise the ecological footprint, COTS components will be used where possible. The COTS components in the design are shown with their specifics in Figure 11.2. For the camera, an image sensor was chosen. This is a lens-less camera and therefore takes up less volume. A computer can afterwards correct the image for the missing lens. The only disadvantage is that the image will have a lower quality compared to an image made by a camera with lens.

The optical spectrometers that can determine the surface composition was researched as well, as they provide accurate data. Two optical spectrometers were found that might be feasible. The infrared spectrometer, C11010MA [1], has a measurement head of 35 × 20 × 28 mm and the visual light spectrometer, C11009MA [2], has a measurement head of 28 × 28 × 28 mm. However, a tube is attached to the measurement heads through which the light is received. This added another 60 mm to one of its dimensions. The possibility to decrease the size of this tube was explored but its feasibility could not be assured. Therefore it was decided to not use optical spectrometers. The found image sensor, NOIL1SN1300A [3][4], allowed the optical spectrometers to be eliminated while still being able to determine the surface composition from light measurements. This image sensor comes in three different types: a monochrome, colour and near infrared type. If all three of them are used, the optical spectrometers become dispensable.

It has been decided to use four image sensors in total. Two monochrome image sensors of which will be attach on the -Z side and one on the +X side of the PPQs. The monochrome image sensor on the -Z side will be used during the approach phase of the landing to determine the shape and size of the asteroid. As it only determines the shape and size, the accuracy of this sensor is 256 × 256 pixels. The other sensors have a resolution of 1280 x 1024 pixels to study the surface. When the first part of the net first touches the asteroid, the PPQ-2s will switch to the monochrome image sensor on the +X side. They will monitor how the PPQ-2s react to the surface when landing to determine the surface hardness together with the accelerometers. The colour image sensor will be attached to the +Y side and the near infrared image sensor will be attached to the +X side to study the surface composition and roughness together with the monochrome image sensor on the +X side.

The second method to analyse the surface material in terms of its elements and molecules with a mass spectrometer was investigated. The mass spectrometer needs the surface material itself which will be collected during the landing. Therefore, the mass spectrometer will be attached on the -Z side of the PPQs. A feasible mass spectrometer was found in[5], see Figure 11.1. The data provided in the article detailed the dimension of the chip except for the thickness. It was assumed that the chip had half the thickness of a 1 Euro Cent coin which equalled 1.67 mm[6]. The mass and power consumption was not mentioned. The mass and power were extrapolated from another bigger mass spectrometer [20], the mass became negligible. This was done by dividing the mass and power by the volume and then multiplying this by the volume of the miniature mass spectrometer.

An IMU was considered as this instrument contains accelerometers, gyroscopes and magnetometers. It contains three of each to provide full three axis data. It is so small that its mass can be neglected. Each PPQ will contain one IMU. The data sheet of the chosen IMU, the BMX055[7], specified the voltage and current of all three instruments. It is assumed that this is for 1 instrument each so it was multiplied by three to calculate the maximum power required.

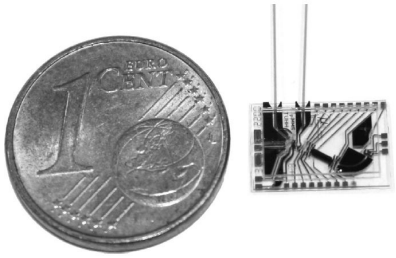

Figure 11.1: Mass spectrometer next to a 1 eurocent coin

[1] https://www.hamamatsu.com/eu/en/product/type/C11010MA/index.html [Accessed 19 May 2019]
[2] https://www.hamamatsu.com/eu/en/product/type/C11009MA/index.html [Accessed 19 May 2019]
[3] https://nl.farnell.com/on-semiconductor [Accessed 23-06-2019]
[4] https://www.onsemi.com/PowerSolutions/product.do?id=PYTHON1300 [Accessed 22 June 2019]
[5] https://www.sciencedirect.com/science/article/abs/pii/S092442470700324X [Accessed 17 May 2019]
[6] http://euro.raddos.de/pages/muenze.php?eusprache=nl [Accessed 17 May 2019]
[7] https://www.bosch-sensortec.com/bst/products/all_products/bmx055 [Accessed 9 May 2019]

Another instrument mass of which is negligible is the temperature sensor. It is the smallest temperature sensor that exists as of today. As the temperature sensor needs to touch the asteroid's surface away from the PPQ-1s it will be exposed to the space environment. The lower side of the temperature sensor's operating temperature does however not reach as low as the expected minimum temperature of -123 degrees Celsius. Therefore, a mechanism was designed to keep the sensor in the protected environment of the PPQ-1 when it is not used and deploys it when it needs to operate, see section 10.3. Once deployed the temperature sensor will do measurements until it dies when the temperature drops below -65 degrees Celsius. The asteroid will be moving closer to the Sun during the month of performing measurements. Therefore, multiple temperature sensors with each having its own mechanism will be installed so that the measurement can be done again a few days later. Due to the design of the mechanism, three temperature sensors will be installed on each PPQ-1.

The final instruments to be discussed are providing information about the internal material composition and structure. The seismometer can be used to measures the speed of acoustic waves that travel through the asteroid. A miniature seismometer found in [21] is Proto II. It is 25 × 25 × 25 mm. It could fit in the PPQ volume wise, however, due to the stack method it was not feasible to implement. Also the mass of 200 g implemented some difficulties with the deployment. Furthermore, designing an acoustic source was considered very complex. The hammer mechanism was thus not implemented either and can not be used to determine the surface hardness.

The other method to determine the internal structure is the use of a radio experiment. This experiment uses an antenna and transceiver. For this experiment one PPQ will send a signal through the asteroid and the other PPQs will receive the signal. The clock of all PPQs must be synchronised such that the starting time of the experiment is the same for all of them. The PPQ that sends the signal and its surrounding PPQs will receive a signal which is a reflection of the sent signal. In this case the experiment is actually called radar. Both radio and radar will thus be combined into one experiment. To get a complete mapping of the asteroid the experiment will be repeated such that all PPQs have sent a signal once.

To size the transceiver and antenna the frequency of the sent signal needs to be determined. The higher the frequency the better the resolution, but, the more difficult it is to detect the signal on the other side of the asteroid. The experiment can therefore be performed for multiple frequencies. For the preliminary detailed design it has been decided to use a signal of 8.5 GHz. The antenna size of half the wavelength of the signal is optimal. If the antenna is shorter than that it is also fine. The wavelength of the 8.5 GHz signal is 3.53 cm and therefore the antenna was sized to be 17.5 mm. The corresponding chosen transceiver is the QPM1002 [8] which works for frequencies of 8.5 - 10.5 GHz. When different frequencies are desired another transceiver might be chosen for the final detailed design.

Each PPQ will have one transceiver and antenna. The antenna will be attached on the +Z side near the edge to minimise distortion due to the presence of the PQ. The transceiver will be placed on the highest stack such that it is closest to the antenna to minimise signal loss before the signal is send away by the antenna.

Figure 11.2: Payload instruments in DOT mission

Instrument type	IMU	Temp. sensor	Mass spec.	Antenna	Transceiver	Image sensor 1	Image sensor 2, 3, 4
Product name	BMX055	STLM20 (grade 7)	MMS	tape measure	QPM1002	NOIL1SN1300A	NOIL1SN1300A
Dimensions [mm]	3.0 x 4.5 x 0.95	1.05 x 1.35 x 0.55	10 x 5 x 0.835	6 x 17.5 x 0.2	5 x 5 x 1	14.22 x 14.22 x 2.28	14.22 x 14.22 x 2.28
Volume [mm^3]	12.825	0.65	41.75	21	25	461	461
Mass [g]	1>>	1>>	1>>	0.09852	0.2	6.8	6.8
	A: 1.404						
	G: 54						
	M: 52,92						
Power [mW]	Total: 108.324	0.044	0.28	0	200	270	620

In Figure A.5 and Figure A.6 the layout of PPQ-1 and PPQ-2 can be seen.

[8] https://www.qorvo.com/products/p/QPM1002 [Accessed 22 June 2019]

11.3. Data Volume

All the payload measurements will generate data. This data will be send to Earth where the scientists can analyse it. To assure this the communication subsystem needs to be able to send all the data to Earth within its communication window. This will require a certain amount of power for which the EPS subsystem needs to be designed. The total data volume is thus of major importance. This section will explain how the total data volume was estimated.

The data volume generated by the IMU was split in the data volume generated by the accelerometers, gyroscopes and magnetometers. The data sheet indicated that the accelerometer uses 12 bits per readout. Furthermore, the user can choose different bandwidths depending on the application. The biggest bandwidth is chosen for the estimation and will result in the largest data volume. The sampling rate is twice the bandwidth. Multiplying the amount of bits by the sampling frequency results in the data rate. This data rate is then multiplied by the number of accelerometers in the IMU. This value is then multiplied by the duration of the measurements and the amount of IMUs that are in the mission. The accelerometers will be operated for the full duration of the landing and one full revolution. The duration of this revolution is taken as the worst case of 3600 s.

The data volume of the gyroscopes is estimated in the same way but with 16 bits per readout. The sampling time is assumed to be 1 s which is based on the fastest possible rotational period of 90 s. The operating time equals the full landing phase and two revolutions of 3600 s each.

The description of the data output of the magnetometer was more vague. Each register had a length of 8 bits so 8 bits per readout were assumed. Again the highest bandwidth was chosen. The operating time of the magnetometer is the full landing plus one revolution of 3600 s. The data volumes can be seen in Table 11.6. The total data volume of the IMU is 14.79 Gb.

The output of the solar panels will be registered during one revolution with the gyroscopes on and one revolution with the gyroscopes and accelerometer on. The total operating time will thus be 7200 s. The data that will be stored will be the logarithm of the difference between each readout including the starting value. 8 bits per readout provided sufficient accuracy. A sampling frequency of 4 Hz was assumed based on the fastest rotation of 90 s. The data is multiplied by the amount of solar cells to get the total data volume of 179.87 Mb, see Table 11.7.

The data stored from the temperature sensors, see Table 11.6, will be the logarithm of the difference between each readout including the starting value. 8 bits per readout provided sufficient accuracy. Each temperature sensor will operate for a full rotation of 3600 s. This is a bit of an over estimation as the temperature sensors might die due to the cold. However, if this is not the case they will still generate useful data and thus the full revolution is taken as operating time. Each PPQ-1 will have 3 temperature sensors and there are 10 PPQ-1s. The sampling frequency is assumed to be 100 Hz.

The data generated by the mass spectrometer, see Table 11.6, is estimated as no data sheets with this information were available. 12 bits per readout and a sampling frequency of 100 Hz is assumed. It is assumed that the mass spectrometer needs two hours to complete its analysis.

The radio experiment, see Table 11.7, will use 12 bits per readout to be sure to be able to measure even the smallest amplitudes. The sampling frequency of 18.7 Hz is taken as 2.2 times the frequency of the signal. It is assumed that the signal takes 10 ns to travel 1 m through the asteroid. The sampling time is thus taken as corresponding to the biggest diameter of 11 m plus two times 10 cm for the PPQs on each side. The experiment will be performed 59 times and for every time 60 signals are sampled as the sending PPQ will store information on both the sent signal and its received signal. The whole experiment will be repeated for 5 different frequencies in total.

The data sheet of the image sensor provided us with the information of the data rate per channel. The image

sensors generate by far the most data as the data rate is 720 Mbps per channel, see Table 11.5. Monochrome image sensor 1 uses only 1 channel and is programmed with a frame rate of 660 fps. This amount of frames is not needed for the mission. Taking 1 picture every metre travelled is sufficient which corresponds to a frame rate of 2 fps as the approach speed is 2 m/s. The data rate is reduced accordingly. Four PPQs will take pictures for the whole duration of the landing till the first touch down after 66 s. The other 55 PPQs will take pictures for the last 10 s of the approach. From the first touch down the monochrome image sensors 1 are turned off and the monochrome image sensors 2 are turned on on the 49 PPQ-2s. These will take pictures for the full duration of the wrapping around the asteroid of 10 s. The monochrome image sensor 2, the colour image sensor and the near infrared image sensor have a higher resolution and therefore the achieved frame rate at 720 Mbps is 210 fps. The frame rate of these image sensors is also reduced to 2 fps, however, the amount of data per frame is thus higher. Once on the asteroid the image sensors on the +X and +Y side of the PPQ-2s will take a video of 1 s in 6 different lighting settings, thus, at 6 different moments in one revolution.

There is a fourth temperature sensor, see "internal temp." in Table 11.5, which stays inside of the PQs to monitor the internal temperature. When the temperature goes out of the operating temperature range of an instrument while performing measurements, the obtained data will contain more errors. Every time the temperature goes out of range for an instrument the time will be stored. This way the scientists on Earth can better analyse the data. Every time stamp needs 42 bits to be properly expressed. It is assumed that the temperature will be out of range two times per revolution. The amount of revolutions in the duration of the mission, 31 days, is calculated using the fastest rotation of 90 s and dividing the mission duration by this.

All the measurements will be accompanied by time stamps. For all measurements except for the radio experiment every 10 s a time stamp is put on the data. As the sampling time for the radio experiment is so short only the starting time of each experiment is given a time stamp. This is also the most useful data for the radio experiment. The bits for the time stamps are also shown in Table 11.5, Table 11.6 and Table 11.7.

When all data volumes of all the measurements with the time stamps are added together the total data volume equals 54.490 Gb. This value turned out incorrect during the verification of the calculations which will be explained in chapter 17.

Image sensors	Landing1	Landing 2	Landing 3	Active	#PPQ-1s	10
Frames per second	660	660	210	210	#PPQ-2s	49
Mbps per channel	720	720	720	720	#Bits per time stamp	42
Mbits per frame	1.09	1.09	3.43	3.43		**Internal temp.**
Fps	2	2	2	2	Duration mission [s]	2678400
Duration [s]	66	10	10	1	Fastest rotation [s]	90
#Instruments	1	1	1	3	#Revolutions in mission	29760
#PQs recording	4	55	49	49	#Out of range per revolution	2
#Channels	1	1	4	4	#Time stamps from temp5	59520
#Experiments	1	1	1	6	Total data [Mb]	2.38
Total [Mb]	576	1200	13440	29129.14	Total [Mb]	
#Bits for time stamp	11088	23100	20580	44604	37625.23	

Table 11.5: Data volume image sensors (left), general information (top right) and data volume internal temperature sensor (bottom left).

	Temp. Sensor	**Mass spec.**	**IMU**	Accelerometer	Gyroscope	Magnetometer
Bits per read out	8	12	Bits per readout	12	16	8
Sampling frequency [Hz]	100	100	Bandwidth [Hz]	1000	-	30
Data rate [bps]	800	1200	Sampling time [s]	0.0005	1	0.033
Operating time [s]	3600	7200	Data rate [bps]	24000	16	240
#Instruments	3	1	#Instruments	3	3	3
#PQs	10	59	Operating time [s]	3676	7276	3676
Total data [Mb]	86.4	509.76	#PQs	59	59	59
#Bits for time stamp	4536000	17841600	Total [Mb]	14892.24	19.65	148.92
#Bits 1st value	36	-	#Bits for time stamp	27327384	54089784	27327384
Total data [Mb]	90.73	526.78	Total data [Mb]	14918.30	71.24	174.98

Table 11.6: Data volume temperature sensors, mass spectrometer and IMU.

	Solar panels		Radio experiment
Bits per readout	8	Bits per read out	12
Bandwidth [Hz]	-	-	-
Sampling time [s]	0.25	Sampling frequency [Hz]	18700000000
Data rate [bps]	32	Data rate [bps]	224400000000
#Measurements	1	Operating time [s]	0.000000112
Operating time [s]	7200	#PQs	59
#Solar cells	354	#Readouts per experiment	60
Total [Mb]	77.78	#Frequency experiments	5
#Bits for time stamp	107049600	Total [Mb]	424.24
#Bits 1st value	36	#Bits for time stamp	743400
Total data [Mb]	179.87	Total data [Mb]	424.95

Table 11.7: Data volume solar panels and radio experiment.

12
COMMUNICATION

In the following chapter, the design of the Communication system is outlined. Starting from the requirements, the spacecraft communication subsystem is described along with the required ground systems.

12.1. REQUIREMENTS

The overview of the requirements set on the Communication subsystem is presented in Table 12.1 below. A connection of some requirements to a parent requirement is indicated in the **Requirement** column. If the compliance is not yet investigated or cannot be proven at this time, the compliance box contains a "n".

Table 12.1: Requirements for communications.

Requirement ID	Requirement	Rationale	Verification Method	Compliance
DOT-COM-M	The mass of the Communications subsystem shall not exceed the value specified in the mass budget including the current contingency level.	-	Inspection: measurements on the assembly	✓
DOT-COM-V	The stack height of the Communication subsystem shall not exceed the value specified in the volume budget.	-	Inspection: measurements on the assembly	✓
DOT-COM-P	The average power of Communications subsystem for all the phases shall not exceed the value specified in the power budget.	-	Inspection: measure power levels in all operational modes and compare to the power budget.	✓
DOT-COM-AMP-1	The amplifier shall amplify the signal power to no less than 3.15 W. (Parent: DOT-COM-1)	This is done to meet the required E_b/N_0	Test: component test, analysis of performance.	✓
DOT-COM-AMP-1.1	The amplifier shall have an efficiency of no less than 60 %. (Parent: DOT-COM-1)	Higher efficiency increases the E_b/N_0 and lowers the generated heat	Test: component test, analysis of performance.	✓
DOT-COM-3	The communication window shall last at least <TBD> hours.	Requirement on asteroid orbit.	Analysis: perform simulation.	n
DOT-COM-3.1	The data down-link shall be maximum <TBD> hours.	This one should be a bit smaller than DOT-COM-3 to allow for margin (Parent: DOT-COM-3).	Analysis: perform simulation.	n
DOT-COM-CDH-1.1	The Communications subsystem shall be able to receive and send data to C&DH and obtain data from storage.	-	Analysis: perform simulation.	✓
DOT-COM-MOD-1	The modulator shall use GMSK method for modulation with BER no more than 10^-4. (Parent: DOT-COM-1)	-	Inspection: design review.	✓
DOT-COM-AN-1	The antenna shall transmit an isotropic signal with a gain of no less than 3 dB in the direction of Earth. (Parent: DOT-COM-1)	-	Test/Analysis: perform physical tests with the antenna and simulations to verify.	✓
DOT-COM-AN-4	The antenna shall withstand radiation levels of up to <TBD>krad.	-	Analysis: perform simulation.	n

Table 12.2: Requirements for communications - continued.

Requirement ID	Requirement	Rationale	Verification Method	Compliance
DOT-COM-4	The antenna shall be able to receive commands from Earth for all mission phases.	This would allow for changes in the schedule, e.g. for when the flyby time is more precisely known.	Analysis: perform simulation.	✓
DOT-COM-4.1	During sleep mode the antenna shall be able to receive signals with at least Eb/N0 of TBD dB. (Parent: DOT-COM-4)	This would allow to receive commands without excessive use of power	Test: perform a subsystem test in the specified mode.	n
DOT-COM-4.2	The communication subsystem shall be able to determine the direction of Earth by the received signal from Earth with an accuracy of at least TBD degrees. (Parent: DOT-COM-4).	To ensure optimal use of energy	Analysis: perform simulation.	n
DOT-COM-MS-1	The communication subsystem shall be able to transmit health and status data from the PQs to the Mothership. (Parent: DOT-LAN-MS-6)	The health and status data are then transmitted to Earth by the Mothership	Analysis: perform simulation.	✓
DOT-COM-DAT-1	The communication subsystem shall be able to down link 5.449 Gbit of data to the ground station.	-	Analysis: perform simulation.	✓
DOT-C0M-DAT-2	The Communications subsystem shall be able to communicate with Earth over the distance of minimum 1.4 million km.	-	Analysis: perform simulation.	✓

12.2. Assumptions

It is assumed the that the PQs will be able to receive signals from the ground stations, recognise the signal and pass the commands on to the C&DH. Furthermore, the Communication PQs (CPQ) are able to direct their signal by detecting a signal from Earth. At TBD time before the closest approach the CPQs will be switched on and ready for receiving a signal from Earth. The CPQs then note the time they start receiving the signal until the signal disappears. This means they are out of sight of the Earth due to the rotation of the Asteroid. Once they are back in sight they will notify the time they started receiving. This is done for a duration of TBD hours. A Master PPQ will then assign a number of CPQs to transmit a part of the data to Earth (not the same data to ensure no duplicate data will be send) as this will result in effectively increasing the data volume. The CPQs are selected based on the duration of the signal they received from Earth. Assuming the duration is approximately 40% of the asteroids rotation period, this will result in reducing the time window by 60%, if one CPQ has to transfer all of the data, since this CPQ will be facing the wrong direction for 60% of the time. Therefore, at least three CPQs are selected, regardless of their position. They will send a unique part of data which will decrease the total amount of data to be send by one CPQ to a 1/3 of the total data, effectively increasing the data rate by 3. The selected CPQs will then start receiving the compressed data from the MCU and start transmitting when they are in sight of Earth. The CPQs which are not selected will be switched off to reduce unnecessary power consumption.
Furthermore, after landing and attachment phase is over, the CPQs will communicate the health and status data of all the PQ subsystems to the Mothership. Since no performance data has been provided of the Mothership, it is assumed communicating with the Mothership will be feasible, considering the short distance to the Mothership just after landing.

12.3. Antenna Design

The antenna consists of a microstrip antenna with a RT/duroid® 6010LM substrate with a 3dB gain and a beam width of 150 degrees as can be seen in figure Figure 12.1. The dimensions of the antenna are 39.60 × 32.13 × 2.00 mm, which fits the +Z of the PQs surface. The microstrip antenna is attached with an adhesive, which is capable of working in space.

At first two antenna designs were considered, namely a deployable rod antenna and a microstrip antenna. The rod and microstrip antenna have a relatively simple design with low cost and low mass. However, for the rod antenna to radiate a clean isotropic signal the length of the antenna has to be close to the wavelength of the signal or half of it for resonance purposes. In this case, with a signal of 2200 MHz the length of the antenna has to be 6.5 cm. This antenna requires a deploying mechanism in contrast to a microstrip antenna. Furthermore, the highest achievable gain for a rod antenna is 1 dB compared to the 3dB beam width of 150 degrees of the microstrip antenna, figure Figure 12.1. For the scope of this project it can be assumed the ground station at Earth will receive the signal with at least 3dB gain. This value is also used for the antenna gain in the link budget calculation which will is explained in section 12.6.

Figure 12.1 shows the radiation pattern of a microstrip antenna with similar dimensions to the antenna de-

signed for this mission. The microstrip antenna used for Figure 12.1 has a resonance frequency at 2.95 GHz. It was assumed a similar performance can be achieved while operating at 2.200 GHz with the designed antenna. First the microstrip antenna, the width W, in meters, is calculated using $W = \frac{\lambda}{2} \cdot \left[\sqrt{\frac{\epsilon_r+1}{2}}\right]^{-1}$, $\lambda = \frac{3 \cdot 10^8 m/s}{f}$. with a wavelength λ of 0.131 meters, a dielectric constant ϵ_r of 10.2 (of the RT/duroid 6010LM substrate) and a frequency f of 2200 MHz. This gives a width of 27.60 mm for the microstrip antenna patch. With the width known, the effective dielectric constant ϵ_{eff} can then be calculated using $\epsilon_{eff} = \frac{\epsilon_r+1}{2} + \frac{\epsilon_r-1}{2}(1+12h/W)^{-0.5}$ while assuming a height h of the substrate of 2 mm. This gives an effective dielectric constant of 8.96. The length L, in meters, is calculated using $L = \frac{\lambda}{2 \cdot \sqrt{\epsilon_{eff}}} - 0.824h \left[\frac{(\epsilon_{eff}+3)(\frac{W}{h}+0.264)}{(\epsilon_{eff}-0.258)(\frac{W}{h}+0.8)}\right]$. This gives a length of 20.13 mm for the microstrip antenna patch. Now, the length L_s and the width W_s of the substrate can be calculated with $L_s = 6h + L, \quad W_s = 6h + W$.

The antenna feed strip is connected at the corner of the antenna to give it a circular polarisation. This reduces the polarisation loss. Furthermore, the available configurations of the DSN 34-m BWG antenna allow for either a right or left circular polarised (RCP or LCP) signal to be received. The substrate is attached with an adhesive on the +Z surface of the CPQs.

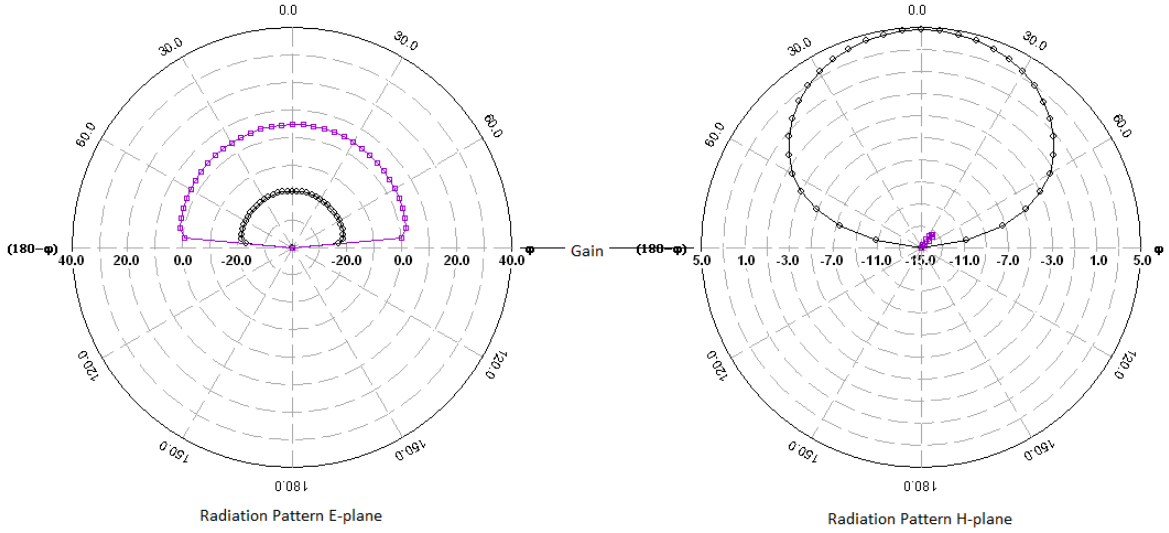

Figure 12.1: Radiation pattern at 2.95 GHz [22]

12.4. Modulation, Power Amplifier & Transceiver

The modulation method used is Gaussian filtered Minimum Shift Keying (GMSK). GMSK has constant signal envelope, which makes it possible to use non-linear amplifiers. Furthermore, GMSK has an efficient bandwidth modulation with a bit error rate (BER) of 10^{-4}, similar to the performance of Binary Phase Shift Keying (BPSK)[23] with a code rate of 0.5. The minimum energy per bit over noise ratio required to ensure a proper link with the ground station is 3.93 dB included a 3 dB margin [24]. The power amplifier used as a reference for this design is the TGA2237 made by TriQuint (Qorvo) [1]. The power amplifiers dimensions are 2.4 × 1.8 × 0.1 mm, it operates at a current of 360 mA and is capable of delivering an output power of 10 W. The power-added efficiency (PAE) is higher than 60% at a frequency of

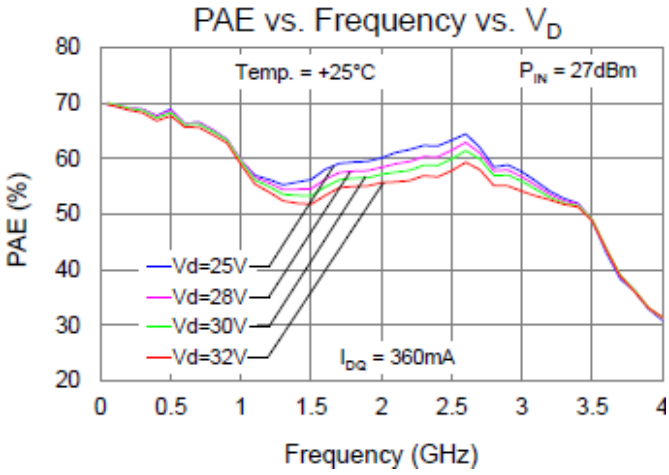

Figure 12.2: Amplifier efficiency, see footnote 1

[1] https://www.qorvo.com/products/p/TGA2237 [accessed on 01/07/2019]

2.200 GHz and for a Voltage of 25V_D as can be seen in
Figure 12.2. Since the amplifier considered in this design has 6V_D, the expected efficiency can be much higher in reality. Hence, it is safe to assume an efficiency of 70% for further calculations.
The transceiver has to be custom made, since no COTS transceivers with the desired dimensions and modulation methods could be found. The transceiver is assumed to fit in the CPQs with: a GMSK modulator, a demodulator, a diplexer (to switch between transmitting and receiving) and low-pass filter, low noise amplifier (to amplify the received ground station signals). The block diagram for the transceiver with the power amplifier can be seen in Figure 12.3. The total system loss for the transceiver is assumed to be 2dB with margins included [25].

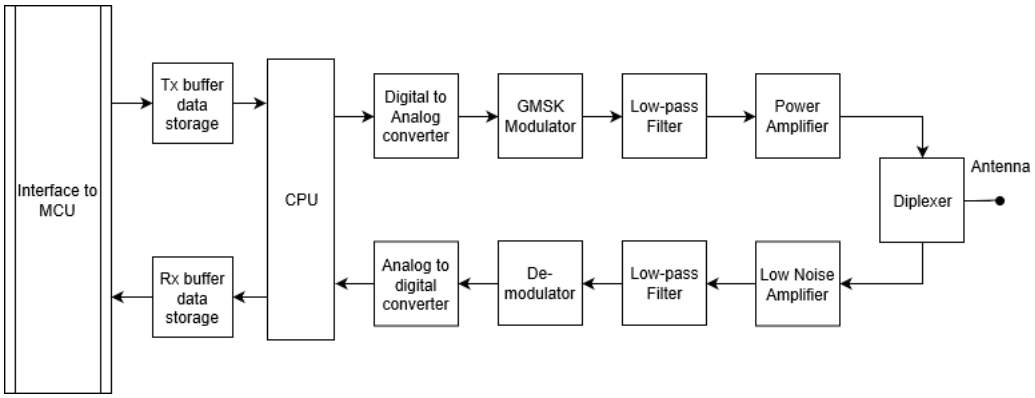

Figure 12.3: Transceiver block diagram

12.5. Ground Station & Signal Analysis

With the S-band frequency the NASA DSN 34-m beam wave guided (BWG) antennas are considered. The ground station antennas are located in the United States (California), Spain (Madrid), and Australia (Canberra). These three ground stations makes it possible to transmit data at all times during the close approach as can be seen in picture Figure 12.4. The gain over system noise temperature (G/T) is 40.8 dB for all the DSN 34-m BWG ground station antennas. The reason for choosing the S-band and considering these ground stations is explained in this section.

Before one chooses a frequency band to operate in, a check has to be made with the International Telecommunication Union (ITU) and it has to be confirmed there are ground station antennas which are capable of receiving the frequency available. The considered frequency bands with the available ground stations are shown in Table 12.3. These frequency bands comply with the ITU regulations.

Table 12.3: Ground stations with frequency bands

Frequency band	**Ground Stations**	**G/T [dB]**	**Free Space Path Loss [dB]**	**Global coverage**
UHF-band	GMRT, India FAST, China	32 -	207.4	No
S-band	NASA DSN Estrack	40.8 -	222.6	Yes
X-band	NASA DSN Estrack	54.2 -	233.9	Yes

The free space path loss L_{FSP}, in dB, is calculated by $L_{FSP} = 20Log_{10}(4\pi \cdot R/\lambda)$ with a distance R of 1.4E9 meters and a wavelength λ of 0.136 meters. From this table it can be seen that the X-band would be the preferable choice. However, the non-linear power amplifiers found for the X-band have an efficiency of at best 0.3 while the power amplifiers for the S-band and UHF-band were 0.6 or higher. This low efficiency increases the amount of power required and the generated heat by the power amplifier significantly. Furthermore, due to the uncertainty of the asteroids trajectory, having a global coverage ground station significantly increases the success rate of the mission. Therefore, the best option would be the S-band with either the NASA DSN ground stations or the Estrack ground stations. Since no publicly available information was found on the performances of the

Estrack antennas, further calculations have been based on the values found in the "DSN Telecommunications Link Design Handbook[26]".

With a frequency of 2200 MHz, the ionospheric losses are assumed to be 0.2 dB and the losses due to atmospheric attenuation for an elevation angle of 20 are assumed to be 0.1 dB [27].

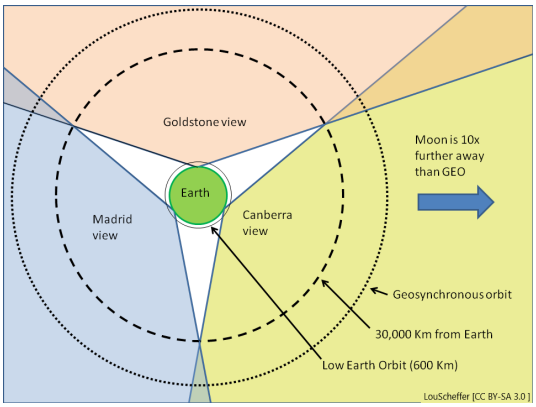

Figure 12.4: Field of view of the DSN ground station network. Viewed from the north pole of the Earth

12.6. Link Budget

A link budget has been created to ensure a communication link can be established with Earth. For this a python program was made. The link budget program uses the output of a Monte Carlo simulation which consists of the communication distances and communication time windows for 5000 possible closest approaches. The free space loss is calculated by the program for a range of distances provided by the Monte Carlo simulation. The program optimises for the required power, whilst fulfilling the one way 2σ reliability (97.5%) and the given constraints, to ensure all the data will be received. The two main limiting constraints are the total required energy needed to transmit all the data shall not exceed 125 Wh (chapter 13), and the heat generated shall not exceed 2.1 W (chapter 14). The results are plotted in Figure 12.5. As can be seen from the plots, a successful link can be achieved for 97.5% of the possible 5000 trajectories, if the CPQs are designed for a distance of 1,459,000 km with a time window of 17.85 hours. The complete link budget is shown in Table 12.4.

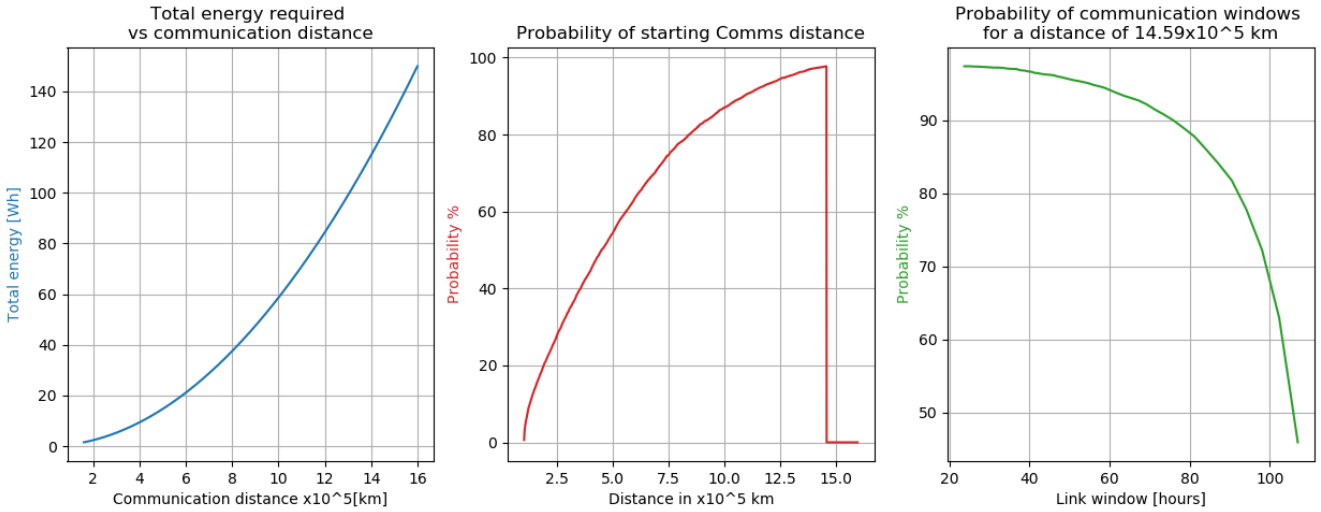

Figure 12.5: Link budget results with given constraints

Table 12.4: Link budget with a reliability of 97.5%

CPQ parameters			**Data & Modulation**		
Downlink frequency	2200	MHz	Data volume	5.449	Gbits
Power available	7	W	Data rate	88.92	kb/s
Tx power	4.9	W	GMSK (1/2 code rate)	Eb/N0 req 1.93 dB	
S/C losses	2	dB	Occupied bandwidth	200	kHz
Antenna Tx Gain	3		**Ground station DSN 34-m BWG parameters**		
Propagation parameters			G/T	40.8	dB
Distance	1,458,000	km	Pointing loss	0.1	dB
Path loss	222.57	dB	**Eb/N0**		
Atmospheric Attenuation	0.1	dB	margins	3	dB
Ionospheric Attenuation	0.2	dB	**Link margin**	3.93	dB

12.6.1. Link Budget Computations

The link budget python program is written as such to minimise for the power required. With the given values in Table 12.4, the Effective Isotropic Radiated Power $EIRP$ in dBm is calculated as $EIRP = E_b/N_0 - L_T - (G/T) - 228.6 + R_{data}$. With E_b/N_0 of 3.93 dB, total losses L_T (including L_{FSP}, iono- and atmospheric losses), the Boltzmann constant 228.6 in dB, and the data rate R_{data} in dB (bits/s) for the range of distances with corresponding time windows. With the $EIRP$, the required power is calculated given an efficiency of the system of 70% and antenna gain of 3 dB and system loss of 2 dB. Additionally, the check is done for the power required constraint. The probability for the trajectories which meet the constraints is calculated as well as the probability for the distances given. Also, the probability for different communication windows is plotted for the most probable closest approach. These results are plotted and shown in Figure 12.5.

12.7. Communication Flow Diagram

The Communication Flow Diagram (CFD), shown in Figure A.1, shows the flow of data between the subsystems and between the PPQs, the CPQs, the Mothership and the Ground Station. Since the spacecraft is fully autonomous it does not require an operator. However, in some cases the Ground Station may want to send commands to switch mode o the spacecraft. The Ground Station commands are shown as red lines.[5]

13

Electrical Power System

Since the main purpose of the mission is to obtain scientific measurements from the payload sensors and send this to Earth, it requires power. The power needs to be generated by a power generating source such as solar cells and in most cases, the power needs to be stored such as in batteries. Furthermore, power management is critical with every mission. Power management which is controlled primarily by the battery board will allow all the subsystems to operate with different power demands. In this section the aforementioned components of the Electrical Power System (EPS) will be discussed thoroughly and a detailed process of the design of these components will be presented.

13.1. Requirements

The overview of the requirements set on the Electrical Power System is presented in Table 13.1 below. A connection of some requirements to a parent requirement is indicated in the **Requirement** column. If the compliance is not yet investigated or cannot be proven at this time, the compliance box contains a "n".

Table 13.1: Requirements for EPS.

Requirement ID	Requirement	Rationale	Verification Method	Compliance
DOT-EPS-M	The mass of the Electric Power System shall not exceed the value specified in the mass budget including the current contingency level.	-	Inspection: measurements on the assembly	✓
DOT-EPS-V	The stack height of the Electric Power System shall not exceed the value specified in the volume budget.	-	Inspection: measurements on the assembly	✓
DOT-EPS-BAT-1	The batteries of the Electric Power System energy storage shall be operational for no more than <TBD>cycles. (Parent: DOT-DUR-1-EPS)	To maximise the Depth of Discharge and to ensure that the battery life is greater than the time on the asteroid's surface	Demonstration: operating batteries for the specified time	✓
DOT-EPS-BAT-2	The batteries of the Electric Power System energy storage shall have capacity loss of no more than <TBD>Ah. (Parent: DOT-DUR-1-EPS)	Losses in battery are minimised, such that the battery can perform for the entire month	Test: operating batteries and analysing performance	✓
DOT-DUR-1-EPS-2	The EPS shall provide the power during all the operational modes as specified in the power budget.	-	Analysis: perform simulation based on EPS performance specifications	✓
DOT-EPS-MISC	The EPS shall consist of solar panels, batteries, battery board and EPS board.	-	Inspection: design review	✓
DOT-EPS-REG-1	The battery board shall regulate the charging and discharging voltage.	Voltages for charging and discharging will be solely regulated by the battery board	Demonstration: perform a demonstration with the battery board with batteries to show the capabilities of the battery board.	✓
DOT-EPS-REG-2	The battery board shall regulate the power generated by the solar cells.	Battery board will also regulate the power generated by the solar cells to maximise power output	Demonstration: perform a demonstration with the battery board and solar panels to show the capabilities of the battery board.	✓
DOT-EPS-CABLE	The power transferred in the cable shall suffer losses of no more than 3% of its input value.	Losses in cable will occur due to Ohmic heating, this requirement will prevent thermal issues	Test: operate the cables with the power levels that would be encountered in the mission and measure the losses.	✓

13.2. Power Generating Source: Solar Cells

This section will present the steps that were taken to choosing and designing the solar cells used on the PQs for power generation.

13.2.1. Identifying Power Generating Sources

The required power can be generated on-board the spacecraft by several power generating sources. There are many different power generating sources that have their advantages and disadvantages, thus a selection must be made. In Figure 13.1, several primary energy sources are listed.

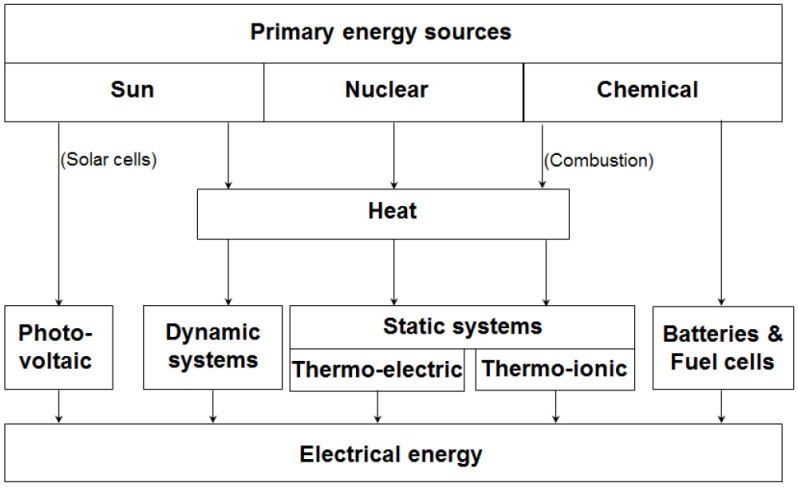

Figure 13.1: Available electrical power generation options [28]

Firstly, nuclear power is discarded primarily due to the fact it has a low specific power and energy density which would require a large volume and mass to produce a significant amount of power. Furthermore, nuclear power also is not chosen because of the **DOT-SAF-1** requirement described in chapter 2, as nuclear material is deemed as hazardous.

Dynamic systems involve using a concentrator to focus the sunlight onto a heat receiver which heats a gas that drives a turbine to generate electricity. This system is too complex to implement, as these systems are much bigger than the PQ form factor, have a low TRL and a low efficiency [28].

Static systems such as thermo-electric and thermo-ionic systems both use heat to generate electricity. Both systems have operating temperatures in the range of 27 K and 727 K, and 1400-1800 K respectively; they also have low efficiencies [28]. This would be too complex to integrate, since PocketQubes have a low thermal capacitance compared to CubeSats which would cause an issue for thermal control [17].

Fuel cells are another power generating system by converting chemical energy to electrical energy by a pair of redox reactions. This requires reactants to be taken on the PQs which would have to be stored and would consume a volume greater than the form factor of the PQ to produce the power required.

Finally, photovoltaic cells convert solar radiation directly to electrical energy by means of a semi-conductor diode. This power generating system is the most advanced and widely used of all aforementioned power generating systems. This is due to their high efficiency, high power and energy densities, as well as TRL. Therefore, the power generating source for the ANTREA system was chosen to be made of solar cells.

13.2.2. Design of Solar Panels

Since solar cells were chosen as the power generating source, the solar cell had to be chosen and had to be sized. Based on many CubeSats and several PocketQubes that have been developed, Triangular Advanced Solar Cells (TASC) were used[1][2]. TASC [29] are state of the art solar cells that have been used on many Cubesats; they are triple junction Gallium Arsenide cells with a high efficiency. These solar cells have a low mass (0.234 g) and low area (2.277 cm^2) per cell allowing multiple cells to be added to small surfaces[3]. Furthermore, these solar cells are cheaper than most other solar cells making it ideal for the use in this project. The solar cell has an efficiency of 27% at AM0 which is defined as the spectrum outside the atmosphere so it represents the space environment [29].

Many different configurations were proposed and analysed, such as using flexible solar cells between every PQ on the net. This was deemed unfeasible as there would be a high probability that the flexible solar cells would become damaged due to the landing loads. Another issue would be that the highest performing flexible solar cell is Alta's devices solar cell which has a high efficiency of 29%, however, it has a high bending radius of 5 cm. This would make the net complex to bend and fit inside the Deployer and would possibly have to be much shorter to fit with this flexible solar cell. Secondly, deployable solar cells were analysed to maximise the

[1] http://www.50dollarsat.info/ [Accessed 23 June 2019]
[2] http://gnd.bme.hu/smog1/index.php [Accessed 23 June 2019]
[3] http://www.spectrolab.com/DataSheets/PV/PV_NM_TASC_ITJ.pdf [Accessed 24 June 2019]

surface area of the cells and thus to maximise the power generation. However, having a deployable mechanism for a 1p PQ is too complex and volume consuming and therefore was also discarded for this mission. Finally, it was decided that solar cells would be on the PQ itself. There is only one solar panel on the +Z side of the PPQs, the -Z side will be facing the asteroid's surface. For PPQ-1, one of the sides is used for the temperature sensors, this would allow the other sides, namely -X, +Y and -Y to be used for the solar panels. However, since solar cells are designed to absorb the sunlight, a portion of this absorbed sunlight is transformed into heat. This presents an issue when controlling the temperature inside the PQ, it was calculated that adding any more cells on the PPQ would increase the temperature above the operating temperature range of the batteries. For PPQ-2, there are image sensors on two sides of the PQ, allowing the other sides namely, -X and -Y to be used for the solar panels. However, this would present the same issue as for PPQ-1 since the batteries are the limiting case. Furthermore, the CPQs do not have a solar panel on any sides for the same reason and because there is an antenna on the +Z side which also generates heat; this is elaborated in chapter 14. Therefore, for the PPQs there are solar panels only on the +Z side and for the CPQs there are no solar panels, the power generated for the CPQs is by the transfer of power using a power cable which will be clarified in section 13.4[4].

The solar cells are a triangular shape with an approximate rectangular area of 1.55×3.18 cm with a cell gap of 0.46 mm as seen in Figure 13.2.

They are placed equidistant from each other on the 5×5 cm side, this allows six cells to be placed on the PPQ. A distance of 0.875 mm is between each pair of solar cells and between the top/bottom pair of solar cell and the X side. A distance of 9.1 mm is between each solar cell and the Y side. Each pair of solar cells consists of two cells connected in series and every pair is connected in parallel which defines the solar panel. The solar cell has a maximum power point voltage and current of V_{mp} = 2.19 V and I_{mp} = 28 mA. By connecting them in this way, results in a maximum power point voltage and current of V_{mp} = 4.38 V and I_{mp} = 84 mA respectively. Regarding the physical characteristics, the mass per cell is 0.234 g resulting in a solar cell mass of 1.404 g per PPQ. The thickness of the solar cell is 0.19 mm resulting in a total volume of 0.04326 cm^3 per PPQ.

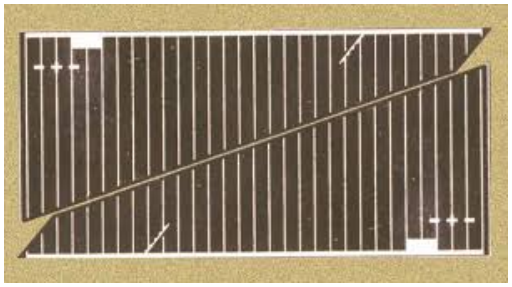

Figure 13.2: Picture of two Triangular Advanced Solar Cells.

With the solar cells known and the position where the panel will be, the power generated can be calculated. The power generated by the solar cells can be calculated using: $I_{EOL} = \frac{I_s \cdot I_d \cdot \eta_l \cdot \eta_c \cdot L_d cos(\theta_a)}{D_w^2}$ where I_{EOL} is the end-of-life irradiance received by the solar cells in W/m^2, I_s is the average solar intensity received on Earth of 1367 W/m^2, I_d [-]is the inherent degradation meaning the losses due to design constraints and shadowing of the cells, η_l [-] and η_c [-] are the efficiencies of the line loss due to wires and the solar cell respectively, L_d [-] is the time dependent degradation loss, θ_a [°] is the incident angle between the Sun and the solar cell and finally, D_w is the worst case distance between the asteroid and the Sun measured in Astronomical Units (AU). The time dependent degradation loss can be calculated by $L_d = (1-D)^L$ where D is the percentage degradation per year of the chosen solar cell and L is the lifetime of the Lander in years. Based on the astrodynamic analysis, the worst case distance between the Lander on the asteroid and the Sun is 1.16 AU, when the Lander lands on the asteroid a month before close-approach[5]. The degradation per year is assumed to be 2.75% per year for Gallium Arsenide solar cells, this is an overestimation since this assumption is based on a spacecraft in LEO. Since a detailed radiation analysis has not been performed, this value for the degradation per year is assumed to be the worst case. The worst case lifetime of the Lander is 1 month and 5 days, this is the total amount of time to perform the scientific measurements and send the data to Earth. After this point, the lander begins its end-of-life phase where the payload is off and the PQs will attempt to communicate with Earth until the PQs are unable to due to degradation. Therefore, the solar cells are sized only for the scientific measurement and communication phases. This results in a time dependent degradation loss of L_d = 0.9973. The inherent degra-

[4] http://www.spectrolab.com/DataSheets/PV/PV_NM_TASC_ITJ.pdf [Accessed 29 June 2019]
[5] https://ssd.jpl.nasa.gov/sbdb.cgi?sstr=2017FU102;old=0;orb=1;cov=0;log=0;cad=0#orb [Accessed 24 June 2019]

dation loss is assumed to be a nominal value of 0.72, this value takes into account the losses due to design and assembly, temperature of array and the shadowing of cells [25]. The line loss is the power loss in the wires due to Ohmic heating of the wire and is assumed to be 0.92 [25]. Finally, the cosine angle loss $cos(\theta_a)$ is averaged by assuming that the asteroid rotates uniformly along its axis and that its axis rotation coincides with the axis of the body. This assumes that the asteroid spends the same time in eclipse and in sunlight. This is a very crude assumption, however, since the properties of the asteroid are not known, the axis of rotation of the asteroid cannot be calculated. By considering the assumed rotation time of the asteroid 90-3600 s, the cosine angle loss is 0.63651 and 0.63659 respectively. This value was rounded to 0.6365 and was simply calculated by assuming the incident angle varies uniformly with time and becomes a maximum at one quarter of the total rotational period which then after decreases to 0.

With all constant values stated, the End of Life power generated is 116.59 W/m^2. Finally, since the crude assumption of the rotation axis of the asteroid was implemented, the power generated was scaled down by a factor of 0.75 since it is unlikely that the rotational axis coincides with the body axis. The reasoning for 0.75 is explained briefly as this would mean that there could be a percentage of PQs that never see the sunlight, however, this would also mean that there would be a percentage of PQs that always sees the Sun. This is a rare case, where the asteroid does not rotate or if a sufficient amount of the PQs fail upon landing such that there is little to no distribution of PQs on the asteroid's surface. Therefore, the eclipse time will be different than the day time and the rotational axis could be changing. For this reason, the factor 0.75 was used as a margin. This scales down the power generated to 87.44 W/m^2. Furthermore, it must be noted that during eclipse, the solar cells will not be able to generate power. However, the PQs on the opposite side where it is in contact with sunlight will transfer part of their power through the power cables to the PQs that are in eclipse. This fact is also taken into account by the factor of 0.75. The power generated by the solar cell in Watts was calculated by $P_{EOL} = I_{EOL} \cdot A_{SA}$ where P_{EOL} is the End of Life power in W and A_{SA} is the solar panel area. The solar panel area is simply $A_{SA} = N \cdot A_{SC}$ where N is the number of solar cells on the solar panel and A_{SC} is the area per solar cell. Since six solar cells are used, the solar panel area is 13.662 cm^2, which results in a power generation of 0.11946 W per PPQ.

To summarise, the solar cells generate the power required for the PPQs and transfer power to the PPQs when these are in eclipse and transfer power to CPQs when the communication phase has started. The power generated by the solar cells is relatively low, the highest total average power is 19.52275 W from chapter 5, this means the battery will discharge its energy to the load and then the solar cells will slow charge the batteries.

13.3. Power Storage Source: Batteries

For every space mission which spends some of its time in eclipse, an energy source is required to store the power that is needed during eclipse. There are two types of power storage sources namely: batteries and capacitors. The latter uses two conductors separated by an insulated dielectric and stores charge without the use of chemicals. The former, consists of two electrodes immersed in a conductor, where a chemical reaction takes place which generates a potential difference between the electrodes. Capacitors have a much lower charging/discharging time, lower specific energy and a much higher cost compared to batteries. For these reasons, batteries were chosen as the power storage source for this mission. Lithium-ion batteries were chosen as they have among the highest specific energy (Wh/kg) and energy density (Wh/L). As described in chapter 8, each bullet contains three Sony/Murata US18650VTC5A batteries of 2600 mAh and a nominal voltage of 3.6 V as seen in Figure 13.3. These batteries produce most of the power required during the energy most intensive phase which is the communication phase. In chapter 12, it was mentioned that the total energy required to transmit the data shall not exceed 192 Wh. The required

Figure 13.3: Sony/Murata US18650VTC5A battery.[6]

[6] https://www.nkon.nl/sony-us18650vtc5a-flat-top.html?gclid=CjwKCAjwmNzoBRBOEiwAr2V27ZycOCEkvVvbHYfJm5KFXTx9t3qNI9k62nFbO4ngPkPH
BwE [Accessed 29 June 2019]

capacity is calculated using $C_{req} = \frac{\frac{E_{req}}{DoD_{bat}\cdot\eta_{tot}\cdot V_{cell}} - \frac{E_{bullets}\cdot DoD_{bullets}}{V_{bullet}} - \frac{P_{EOL}\cdot(T_t - T_e)}{T_t}\cdot N_{PPQ}\cdot F_c}{N_{tot}}$ where C_{req} is the total battery required capacity, DoD_{bat} and $DoD_{bullets}$ is the depth of discharge of the batteries and bullets respectively, which is defined as the amount of extracted energy from the battery at each discharge cycle, η_{tot} is the total efficiency of the battery, V_{cell} is the voltage across each battery, $E_{bullets}$ is the energy produced by the batteries in the bullets, V_{bullet} is the voltage across the batteries in the bullets, T_t is the total rotational period of the asteroid, T_e is the time spent in eclipse, N_{PPQ} is the number of PPQs being used, F_c is a factor taking into account the percentage of PQs in eclipse and N_{tot} is the total amount of PQs being used. Since the solar cells will be slow charging the batteries, the batteries will have few cycles in the order of 100 and therefore, the DoD is approximated to be 90% for the batteries in the PQs and 95% for the batteries in the bullets. The reasoning behind these values is because the PQ batteries will be discharged for less than 100 cycles and the batteries in the bullets are only being used primarily during the communication phase. The batteries in the bullets will lose part of its capacity over time and therefore, instead of using 100% DoD, a DoD of 95% is chosen. These values are reasonable when comparing the DoD curve for a typical Lithium-ion battery in Figure 13.4. This DoD curve shows that when considering a Lithium-ion battery at 90% DoD, the battery will have approximately 3000 cycles. This is more than enough for the scientific measurement and communication phases and therefore this DoD was chosen. The total efficiency η_{tot} is assumed to be 80% [25]. The voltage across each cell V_{cell} is 3.7 V based on batteries that fit the form factor of the PQ. E_{bullet} is 112.32 Wh since there are three batteries in four weights. The fraction $\frac{T_t - T_e}{T_t}$ is simply 0.5 since the aforementioned assumption stated that the asteroid spends the same amount of time in eclipse and in sunlight. N_{PPQ} and N_{tot} are 59 and 69 respectively. Finally F_C is assumed to be 0.5. These result in a required capacity of C_{req} = 0.5766 Wh.

The batteries that fit in the form factor of the PQ are called prismatic batteries in the shape of a rectangle. Most of these batteries have a nominal voltage of 3.7 V and a discharge rate of 0.2 C. This means it takes 5 h to discharge the battery. However, if the cell is discharged at a faster rate than its rated discharge rate, then its capacity will actually be lower than its rated capacity; this is known as Peukert's law. This is defined by $C_{req} = C\cdot\left[\frac{C}{I_{actual}\cdot t_D}\right]^{k-1}$ and $t_{D-actual} = \frac{C_{actual}}{I_{actual}}$ where C_{req} is the actual required battery capacity, C is the required rated battery capacity, I_{actual} is the actual discharge current, t_D is the rated discharge time and k is Peukert's constant which is between 1.03 and 1.06 for Lithium-ion batteries [25]. The equation can be rearranged to calculate what the required rated battery capacity is, based on the actual battery capacity by $C = C_{req}\cdot\left[\frac{t_D}{t_{D-actual}}\right]^{\frac{k-1}{k}}$. The rated discharge is 0.2 C so t_D is 5 h and by the rotation period of the asteroid the actual discharge time is $t_{D-actual}$ is 1800 s so 0.5 h. This results in a required rated battery capacity of 0.6569 Ah.

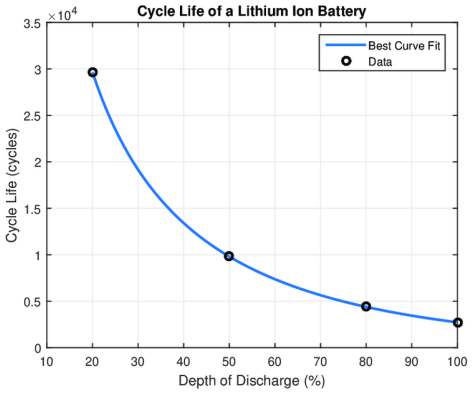

Figure 13.4: Depth of discharge versus cycle life of the lithium-ion battery [30].

There were no prismatic batteries that fit in the form factor of the PQ whilst also having a rated battery capacity of 0.6569 Ah. Therefore, two batteries were used each of 0.33 Ah each connected in parallel adding the battery capacity to 0.66 Ah. The battery has dimensions 30 × 20 × 6 mm and a mass of 23 g per cell resulting in a total mass of 46 g[7]. The batteries are placed in the middle of the stack with one placed on top of the other. It must be clarified that these prismatic batteries are not space regulated and therefore, additional testing needs to be done to ensure these batteries are functional in the harsh space environment. To summarise, there are two prismatic 0.33 Ah batteries placed on every PQ, that store the power required for the entire mission and there are the batteries in the bullets which store the power required solely for the communication phase.

[7] https://www.alibaba.com/product-detail/GEB-3-7V-Rechargeable-Lithium-Polymer_1802135109.html?spm=a2700.7724857.normalList.55.5663156ffPVKDR [Accessed 29 June 2019]

13.4. Power Management and Distribution

A spacecraft has to be able to manage and distribute its power to the OBC, payload, thermal control and the communications subsystems. Each of these requires a different voltage and therefore, it is crucial to distribute the power in such a way that all the subsystems can function. Furthermore, the battery is being charged by the solar cells whose voltage must be regulated to prevent overcharging of the batteries leading to degradation of the batteries.

Firstly, the charging regulator is considered, there are several charging regulators used for solar cells, the two most common ones are Sequential Switching Shunt Regulator (S3R) and Maximum Power Point Tracking (MPPT). S3R controls the power by switching power at different sections of the solar panel to the bus. This, however, can only be done if the voltage from the solar panel is matched to the voltage of the bus whilst also being stable throughout the mission. MPPTs adapts the solar panel voltage to the required bus voltage whilst maximising the power yielded by the solar cells. Therefore, considering these differences and the fact that MPPT regulators do not require a regulated bus they were chosen. Each pair of solar cells contains its own MPPT and thus three MPPTs are used that are placed on the EPS stack. For the MPPT, bq25505 was chosen made by Texas Instruments, it is defined as a boost charger with battery management which maximises the power generated by the solar cells, whilst also regulating the voltage to 3.7 V to charge the batteries. The bq25505 has dimensions of 3.5 × 3.5 × 1 mm and is used as the MPPT and charge regulator on each PPQ and CPQ to aid in regulating the power[8].

Furthermore, the bus has an unregulated voltage of 3.7 V and therefore, regulators are required since not all the loads require 3.7 V and thus LM8850 regulator made by Texas Instruments is used which is simply a DC-DC converter which converts the 3.7 V to 3.6-5.7 V allowing the different subsystems to function[9].

As mentioned in the previous sections, a power cable is used to distribute the power required to the PPQs when these specific PPQs are in eclipse, and to distribute the power to the CPQs required during communications. There is a DC-DC boost converter used to increase the voltage to limit Ohmic heating and thus limit the loss in power. The chosen DC-DC boost converter is LT8335 made by Linear Technology that converts 3.7 V of the bus voltage to 28 V and has a maximum output current of 2 A[10]. The cable is sized to limit the power loss to 3%, a cable length of maximum 13.75 m is considered between the bullets and the PQs until the next PQ distributes its power. This loss in power is calculated by $P_{loss} = I_{cable}^2 \cdot R_{cable}$ where P_{loss} is the power loss in the cable, I_{cable} is the current carried by the cable and R_{cable} is the resistance of the cable. The resistance of the cable is calculated by $R_{cable} = \frac{\rho_{cable} \cdot L}{A}$ where ρ_{cable} is the resistivity which is a material property in $\Omega \cdot m$. The resistivity at the asteroid's temperature is corrected to a value of 1.037568×10^{-8} by using $\rho_{cable} = \alpha \cdot \Delta T \cdot \rho_0$ with an α as the resistivity temperature coefficient of 0.0039 K^{-1}, ρ_0 as the resistivity of the material at 20°C of 1.68×10^{-8} $\Omega \cdot m$ for copper and using the maximum temperature on the asteroid as 160°C. Due to the sizing of the cable on the net, the diameter for the power cable was chosen to be 0.41 mm and a mass of 0.1 kg for a roll of 69 m and a current capacity of 0.45 A. This results in a resistance of 1.1357 Ω[11]. The power loss is then 0.24 W and thus calculating the percentage power loss by $\%Powerloss = \frac{P_{loss}}{V_{cable} \cdot I_{cable}}$ where V_{cable} and I_{cable} is 28 V and 0.46 A respectively: the percentage power loss 1.86% and thus meets the requirement of having a power loss of less than 3%.

Finally, the electrical block diagram for the EPS can be seen for PPQs and CPQs in Figure 13.5 and Figure 13.6 respectively. This diagram shows the overview of how the EPS manages and distributes the power from the solar cells to the required load.

[8] http://www.ti.com/lit/ds/symlink/bq25505.pdf [Accessed 24 June 2019]
[9] http://www.ti.com/lit/ds/symlink/lm8850.pdf [Accessed 24 June 2019]
[10] https://www.analog.com/media/en/technical-documentation/data-sheets/8335f.pdf [Accessed 24 June 2019]
[11] https://docs-emea.rs-online.com/webdocs/1292/0900766b8129257d.pdf [Accessed 24 June 2016]

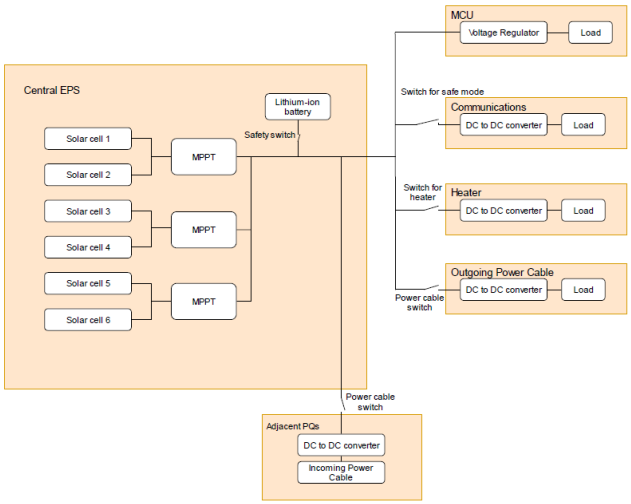

Figure 13.5: Electrical Block Diagram for PPQs.

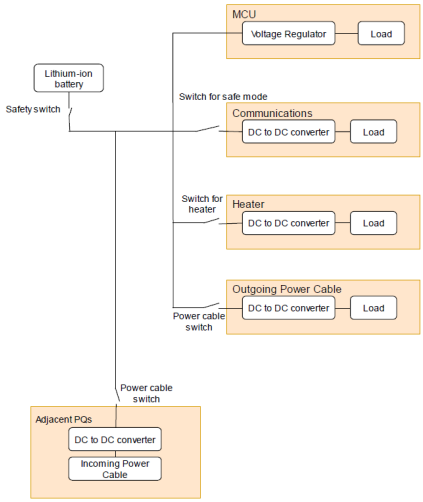

Figure 13.6: Electrical Block Diagram for CPQs.

14
THERMAL CONTROL

In this chapter, the thermal control for the PQs will be presented. Both passive control and active control were investigated. The thermal control depends on the thermal environment and the power distribution during the mission. First the thermal requirements are determined, then the thermal environment is investigated, including associated heat fluxes. Thereafter, the thermal control model is explained in detail.

14.1. REQUIREMENTS

Before the thermal control can be designed, the requirements it has to meet are established. Thermal control is a highly dependent subsystem that has to be designed to match the needs of all other subsystems. The overview of the requirements set on the Thermal Control subsystem is presented in Table 14.1 below. A connection of some requirements to a parent requirement is indicated in the **Requirement** column. If the compliance is not yet investigated or cannot be proven at this time, the compliance box contains a "n".

Table 14.1: Requirements for thermal control.

Requirement ID	Requirement	Rationale	Verification Method	Compliance
DOT-TH-M	The mass of the Thermal Control subsystem shall not exceed the value specified in the mass budget including the current contingency level.	This is based on the user requirement regarding the maximum mass of the entire system.	Inspection: measurements on the assembly.	✓
DOT-TH-V	The volume of the Thermal Control subsystem shall not exceed the value specified in the volume budget including the current contingency level.	This is based on the user requirement regarding the maximum volume of the entire system.	Inspection: measurements on the assembly.	✓
DOT-TH-P	The average power of the Thermal Control subsystem shall not exceed the value specified in the power budget.	This is based on the limiting power that could be provided during this mission		✓
DOT-TH-1	The thermal control shall provide a continuous temperature range between the most limiting storage temperatures as long as the desired lifetime of the payload and systems is desired. (Parent: DOT-SAF-3.1)	This is based on the user requirements regarding the scientific data that has to be collected to determine the asteroids characteristics. The measurement sensors require a certain temperature to perform measurement accurately.	Analysis: perform simulation/ Test: physical test on a full scale model.	✓

Table 14.2: Requirements for thermal control (continued).

Requirement ID	Requirement	Rationale	Verification Method	Compliance
DOT-TH-2	During measurements, the thermal control shall provide the operating temperature of the specific instrument that performs the measurements. (Parent: DOT-SAF-3.1, DOT-PAY-MON-1-4, DOT-PAY-IMG-NIR-6, DOT-PAY-MON-6, DOT-PAY-IMG-COL-6, DOT-PAY-IMU-4))	The measurement sensors do not need to operate continuously, therefore, it is only required to provide the operating temperature during measurement time.	Analysis: perform simulation/ Test: physical test on a full scale model.	✓
DOT-TH-3	During communication, the thermal control shall provide the operating temperature of the communication system. (Parent: DOT-SAF-3.1)	The communication subsystems do not need to operate continuously, therefore it is only required to provide the operating temperature during the communication window.	Analysis: perform simulation/ Test: physical test on a full scale model.	✓
DOT-TH-4	The thermal control shall provide the operating temperature of the battery during recharging for <TBD>time. (Parent: DOT-SAF-3.1)	To allow energy storage, the batteries need to be at the operating temperature to be able to storage power most efficiently	Analysis: perform simulation/ Test: physical test on a full scale model.	✓
DOT-TH-5	The thermal control shall provide the operating temperature of the battery during discharging for <TBD>time. (Parent: DOT-SAF-3.1)	To allow power distribution, the batteries need to be at the operating temperature to be able to power other instruments	Analysis: perform simulation/ Test: physical test on a full scale model.	✓

To determine the required temperature range, the operating temperatures of all subsystems and instruments are needed. An overview of the different requirements are given in table Table 14.3 and Table 14.4.

Table 14.3: Thermal limits of all components

	Minimal temperature		Maximal temperature	
	Storage	Operating	Operating	Storage
Communication				
- Transceiver	-50	-40	85	150
- Antenna	-120	-100	100	120
EPS				
- Batteries (discharging)	-20	-20	60	60
- Batteries (recharging)	-20	0	45	60
- Solar panels	-200	-150	110	130
General electronics	-40	-20	60	75
Structure				
- Damping material	-29	-29	71	400
- Structure FR4			142	142
- Rod	-195	-195	121	121
C&DH				
- MCU	-55	-55	105	125
- Memory	-65	-55	125	150
Net				
- Power cable	-200	-200	260	260
-Communication wire	-200	-200	260	260
- Structural cable	-150	-150	100	100
Limitation	-20	0	45	60

Table 14.4: Thermal limits of payload

	Minimal temperature		Maximal temperature	
	Storage	Operating	Operating	Storage
IMU	-50	-40	85	150
Temperature sensor	-65	-40	85	150
Image sensor	-40	-40	85	150
Mass spectrometer	-40	-20	55	55
Radio experiment	-50	-40	85	120
Limitation	-40	-20	55	55

The payload only has to be stored for a certain amount of time, then perform measurements after which they are no longer needed. This means that there is not a fixed temperature range that has to be met at all times, but rather different ranges during the mission. As can be seen, the most driving requirements results in a temperature range between -20 and 60 degrees Celsius as surviving temperature (both from the batteries). The batteries have two different modes; discharging and charging. Their specific temperatures for each of them, only have to be met when being in that mode.

14.2. Thermal Environment

The thermal environment provides a heat flux input for the PQ. There are multiple sources of heat, this includes:

- Direct solar flux
- Asteroid solar reflection due to albedo
- Infrared radiation of the asteroid
- Other nearby solar reflecting and infrared radiation from the moon or Earth
- Heat flux input from space components
- Solar panel reflection and infrared radiation
- Nearby spacecraft (PocketQubes) solar reflection and infrared radiation
- Free molecule heating
- Charged particle heating

When investigating all these sources, some are so small that they can be neglected. Firstly, the effects of other spacecraft (the other PQs) will be minimal, unless they are extremely close to each other. Since the PQs are quite far (1.25 m) from each other and especially when the size of the PQ is considered, it can be assumed that this flux input received from other PQs can be neglected. The Moon and Earth will only be relatively close by during the last days of this mission, when sending the data back to Earth during the Close Approach. However, even then, the influences from the Moon and Earth are small. Beyond a GEO orbit there is close to no Infrared radiation observed from the Earth. Since the Close Approach distance is further than that, this is neglected as well. Furthermore, the solar panels are on the PQ and do not reflect more radiation towards the PQ and they can therefore be assumed negligible. The last two sources of the list are also neglected, since free molecule heating is mainly encountered during launch ascent after fairing jettison. However, the Mothership takes care of the thermal control during this phase. The charged particle heating is only significant at cryogenic temperatures and very weak for room temperatures. There are no cryogenic temperatures present on the PQ.

After establishing which bodies and characteristics determine the thermal environment, these heat flux inputs can be investigated more closely.

Direct Solar Flux

The flux density (S) in W/m^2 depends on the distance from the sun. The luminosity of the sun can be calculated using Equation 14.2 [left]. Then using Equation 14.1 [right] the flux density of the sun can be calculated.

$$P_{sun} = 4\pi R_{sun} \sigma T_{sun}^4 \quad \text{and} \quad S_{sun} = \frac{P_{sun}}{4\pi d^2} \tag{14.1}$$

For the left equation the radius R_{sun} equals 6.995*10^8 and T_{sun} equals 5778 K. The luminosity of the Sun is $3.886x10^26W$. And for the right equation, where d is the distance from the sun to the asteroid in m. During deployment (at the end of February 2036) this distance is roughly 1.16 AU. During communication, this distance will be around 1.0 AU. During the simulation, this distance will be updated every day based on the distance data provided by JPL Horizons[1].

Indirect Solar Flux

The flux density of visual light of the asteroid depends on the amount of incoming solar flux that is reflected by the asteroid. This depends on the Albedo (a) of the asteroid. The Albedo of an asteroid can range between 0.05 to more than 0.50. For now, an Albedo of 0.14 is assumed, this is based on the fact that the absolute magnitude also uses this Albedo. The indirect solar flux can be calculated using Equation 14.2.

$$S_{asteroid} = aS_{sun} \tag{14.2}$$

Infrared Radiation

The flux density of infrared radiation of the asteroid depends on the temperature of the asteroid. The mean temperature of the asteroid can be calculated using Equation 14.3.

$$T_{asteroid_{mean}} = \left(\frac{P_{sun}(1-a)}{16\pi\sigma\epsilon d^2} \right)^{\frac{1}{4}} \tag{14.3}$$

[1] https://cneos.jpl.nasa.gov/ca/ [Accessed 12 June 2019]

Where σ is the Stefan-Boltzmann constant ($5.670374419 \times 10^{-8} Wm^{-2}K^{-4}$) and ϵ is the emissivity of the asteroid; which is assumed to be 0.9. Also for this calculation the distance of the asteroid is updated every day based on the distance data provided by JPL Horizons[2]. From this mean temperature, the maximum temperature (the temperature at the sun side of the asteroid or hot side) can be calculated as well as the minimum temperature (in the shadow side of the asteroid or cold side). As nothing is known about the thermal inertia of the asteroid, the worst case is assumed. This assumes that the asteroid indeed obtains these extreme temperatures and it also assumes that these conditions are met instantly when going at sunset and sunrise. The maximum temperature and the minimum temperature can be calculated using Equation 14.4

$$T_{asteroid_{hot}} = \sqrt{2} T_{asteroid_{mean}} \quad \text{and} \quad T_{asteroid_{cold}} = 2T_{asteroid_{mean}} - T_{asteroid_{hot}} \tag{14.4}$$

With these temperatures, the amount of heat flux by the Infrared Radiation can be calculated for both cases, the hot case in the sun side and the cold case in the shadow side. See Equation 14.5.

$$S_{IR_{hot}} = \epsilon \sigma T_{asteroid_{hot}} \quad \text{and} \quad S_{IR_{cold}} = \epsilon \sigma T_{asteroid_{cold}} \tag{14.5}$$

As a side note, it is assumed that the PQ itself does not influence the temperature. This is not entirely true, since shadow will decrease the temperature. However, as stated before, the most extreme temperatures are taken.

Heat flux input from space components

The heat flux input from space components are assumed as follows. Eventually, all power input of the subsystems such as the payload instruments, batteries and general electronics will become heat. The only energy that does not stay in the PQ as heat is the communication waves that are sent to Earth or that are used for doing measurements. For the battery it is assumed (see chapter 13) that they store electrical energy perfectly and that no energy is transformed into heat.

14.3. Thermal Control Model

Once the environment is known, a model can be made to simulate the PQ behaviour regarding its temperature. First, one should find when the thermal control has to be operational, how many types of PQs are used and what all these different types of PQ contain. Furthermore, the position of the other subsystems (such as batteries, payload and communication) and the power distribution have to be known.

14.3.1. Thermal Control Phases for Entire Mission

Typically, the thermal control can be split over different phases or modes for the entire mission. In every phase, different sources of heat are present. This mission can also be divided into different phases. 1) the launch and orbit around Earth, 2) the journey from Earth to the asteroid, 3) the landing on the asteroid, 4) the active phase to perform measurements and 5) the active phase to communicate to Earth.

For this mission, the Mothership takes care of the thermal control. Phase 3 is very short, only 1 minute. Due to the similarities in environment with phase 4 (same distance from the sun and only 132 m from the Asteroid), and that the PQs have thermal inertia, this phase is not modelled. It is assumed that when phase 4 provides the correct temperatures, phase 3 will be acceptable temperature-wise. For phases 4 and 5 a python program was made to simulate the temperature as accurately as possible.

14.3.2. Types of PQs

The PQs connected to the net are not all the same. There are three types of PQs present that have a different function and there are bullets which all have thermal control. The most driving requirements result in a temperature range between -20 and 60 degrees Celsius as surviving temperature, are the the batteries. Since batteries are present in all the PQ types, this range is the same for all of them. Their layout, however, is different.

The PPQ has a size of 50x50x50 mm and a mass of 126.2 g for PPQ-1 and a mass of 135.7 g for PPQ-2. The positive z side of the PPQ will be covered with solar panels. These solar panels have an emissivity of 0.85 and a absorption of 0.92. From the light energy that is absorbed 30% will be stored as electrical energy, the remaining

[2] https://cneos.jpl.nasa.gov/ca/ [Accessed 12 June 2019]

70% will become heat (chapter 13). Furthermore, they all have an antenna. The PPQs contain all the payload. The sensors that are on the outside (and therefore influencing passive thermal control) are as follows: The PPQ-1 has three temperature sensors on the outside (positive X side) and PPQ-2 has four cameras connected to the outside of the PQ. There is one camera connected to the negative Z side, two cameras on the positive X side and one camera on the positive Y side. The size of every camera is 14.22x14.22 mm (thus consuming 16.2% and 8.1% of the +X and +Y side respectively. It is assumed that the emissivity of the camera is 0.95 and the absorption is 0.27[3]. The PPQ-1, has three slits in positive X side of the PPQ-1 for the temperature sensors. These slits are 2 mm by 6.8 mm (so 1.6 % of the surface). The absorption here is 1 and the emissivity is 1.

The CPQ has a size of 50x50x50 mm and a mass of 146 g. The positive Z side is partly covered by the antenna (51%). The antenna plate (which is mainly made of copper) has a emissivity of 0.15 and an absorption of 0.63.[4]

The bullets are 190 mm long and have a diameter of 48 mm. It will be made out of an exterior structure of 1 kg of steel and the rest will mainly be batteries.

14.3.3. Heat Transfer

Some general assumptions were made for the heat transfer. Firstly, the rotation time had to be assumed. It is estimated that the rotational time is between 90 s and 3600 s. For the thermal control a rotational time of 3600 s is used as this would be the worst case scenario. Secondly, it is assumed that there will be no conduction between the PQ and the asteroid, nor between the PQ and the net. As there is no pushing force that pushes the PQ on the asteroid and the net is also connect to the negative Z side, there will be only a very small surface that touches the asteroid. Therefore, this conduction is neglected. The net itself is connected to the negative Z side of the PQ, however, the structure is cylindrical, so only a small surface of the net is in contact with the PQ. Therefore, this is neglected. However, when conduction is included, it depends on the type of PQ if the consequences will be positive or negative. First of all, it will depend on the asteroid temperature. Currently it is unknown if the extreme temperatures that are mentioned are obtained or that the temperature of the asteroid will stay more closely to the average temperature value. When the extreme temperature are obtained, this will have negative consequences. Especially for the CPQs during the communication phase of the mission. When the temperatures are close to the average temperature, it will be positive, as heat of the CPQ can then be more easily transferred to the asteroid leading to a less high maximum temperature of the CPQ.

Absorbed Environmental Heat

The absorbed environmental heat (Q_{env}) can be calculated using the Equation 14.6. There is a hot and a cold environment, that will switch instantly at half the period (thus every 1800 s).

$$Q_{env_{cold}} = S_{IR_{cold}} \sum \epsilon A_{IR} \quad \text{and} \quad Q_{env_{hot}} = S_{sun} \sum \alpha A_{sum} + S_{asteroid} \sum \alpha A_{asteroid} + S_{IR_{hot}} \sum \epsilon A_{IR}. \tag{14.6}$$

For the hot case, the worst case scenario is that the sun hits the maximum amount of surface area. This maximum occurs when the sunlight is aligned with the body diagonal of the cube and therefore the projected area has the shape of a hexagon. The area of a hexagon is $A = (3\sqrt{3}(s^2))/2$. The side (s) can be calculated by projecting the length of the side of a PQ onto the body diagonal. This will scale its side (s) to $50 * \sqrt{2}/\sqrt{3}$ or an A_{sun} of 0.004330 m^2. However, this is split over two different surfaces and thus two different absorption properties. For both the PPQs and the CPQs, the full positive z side and part of the sides are in the sun. The bullets have a maximum A_{sun} of diameter (48 mm) times height (190 mm). The $A_{asteroid}$ is related to the indirect solar flux. Only the sides of the PQ (both PPQ and CPQ) will receive this heat input. It is assumed that half of every side will receive this reflected light. For the bullets, this area is half the total outside surface of the cylindrical shaped weight. ($A_{cylinder} = 2\pi r^2 + 2\pi rh$) divided by two. The S_{IR} is observed by the bottom and the sides of the PPQ and CPQ. Again, it is assumed that half of the sides will receive this infrared radiation. Again, there is differences in emissivity per side. For the weights, it is the same area as the $A_{asteroid}$.

[3] http://www-eng.lbl.gov/~dw/projects/DW4229_LHC_detector_analysis/calculations/emissivity2.pdf [Accessed 19 June 2019]
[4] http://matweb.com/search/DataSheetaspx?MatGUID=9aebe83845c04c1db5126fada6f76f7e [Accessed 20 June 2019]

All sides (so six in total) are assumed to have one average value for ϵ and one average value for α. This average is the Weighted arithmetic mean value of all the different materials present on that side.

Internal heat (power) due to components

The heat flux input from components differ immensely per PPQ. The PPQs and CPQ all have a command and data handling subsystem (with a duty cycle of 100%) of 2.4 mW and a internal temperature sensor (with a duty cycle of 100%) of $3.77 * 10^{-3}$ mW. So the total constant Q_{in} = 2.4 mW for all PQs. The power input (thus heat input) during the mission is divided over different modes, as can be seen in chapter 5. The bullets will have a retracting mechanism to roll in the net, this will generate 7 W of heat for 10 minutes.

Infrared dissipation of spacecraft

It is assumed that there is no heat transfer between the net and the PQ, therefore, only the total surface of the PQ is taken into account. The following formula is used $Q_{out} = \sum \epsilon A_{out}$.

14.3.4. Temperature of PQ

The temperature of the PQ can now be calculated to according to Equation 14.7.

$$T = \left(\frac{Q_{env} + Q_{in}}{\sigma Q_{in}}\right)^{\frac{1}{4}} \tag{14.7}$$

Initially, a python program was made to optimise the material properties (alpha and epsilon) of the positive z-side, the sides (both x and y sides) and negative z-side of the PQ. As explained before, the weighted arithmetic mean value is used. However, there was no combination of α and ϵ that could make the PQ stay within the required temperature limits.

Insulation

To reduce the large amplitude in temperature change between day and night cycle, insulation could be added. This insulation would mainly reduce the heat loss. In the spacecraft industry multi-layer insulation is commonly used. To calculate the heat flow rate, the Equation 14.8 can be used

$$Q_{insulation} = UA\Delta T \quad \text{with} \quad U = 4\sigma T^3 \frac{1}{N(\frac{2}{\epsilon} - 1) + 1} \tag{14.8}$$

Where N is the amount of layers and T the mean of the temperatures (in K) of the two layers ΔT chances continuously. $Q_{insulation}$ is defined positive when going from the inside to the outside. Therefore, this value needs to be subtracted from the Q_{in}.

For the insulation material, Kapton is chosen. The available thicknesses between 7.5 μm to 125 μm. This can be coated with silver or aluminium. This, however, are theoretical equations. In reality there will always be small holes in the insulation as air that is trapped inside it before launch has to escape when arrived in space. There will also be holes in the insulation layer due to the need for deployment of payload (the temperature sensors). To account for this, the $Q_{insulation}$ is scaled down based on the reduced surface. It is assumed that this is valid.

Typically, the layers are spaced as close to each other as possible (0.25 mm). As this mission aims to land on the asteroid, the impact on the PQ will be big and might damage the insulation layer (or outer surface layer). When layers touch, their insulation function is lost. Therefore, a slightly bigger spacing is preferred.

14.4. Thermal Control Design

The are a few general inputs that are the same for all types of PQs. Firstly, the temperature inside the Mothership is 20°C. Also, it is assumed that 90% of the mass is inside the insulation and that the remaining mass is outside. The thermal inertia is taken to be 920 J/kg K[5], however, it is already checked that the PQs are not sensitive to this. When for example a value of 450 J/(KG-K), the temperature of the PQ is also within the acceptable range.

[5] https://www.engineersedge.com/materials/specific_heat_capacity_of_metals_13259.htm [Accessed 17 June 2019]

14.4.1. PPQ

The different types of PPQ have different characteristics and are therefore treated separately. The PPQs payload have to be active for one month, therefore it the simulation is done from the 1st of March until the 31st of March.

PPQ-1

The outside surface of the PPQ-1 will be entirely made out of aluminium. The positive X side has the temperature sensors that required a slit. Therefore the Weighted arithmetic mean value of $\alpha = 0.11$ and $\epsilon = 0.31$. As stated before, the positive z side has the solar panels, which have a $\alpha = 0.64$ and a $\epsilon = 0.85$. All other sides have a $\alpha = 0.10$ and a $\epsilon = 0.30$[6].

The power input varies over time (as can be found in chapter 5). The exact time (datum) when the modes are active is not yet defined, but for now, it is assumed that they are turned on once a week. Thus, the first 96 second the landing mode is on, directly followed by science mode A, then one week later science mode B is turned on for 3600 s, then in week 2 science mode C is turned on for 3600 s and lastly in week three science mode D is turned on. However, as can be seen in Figure 14.1 it does not matter when the science modes are turned on.

Regarding the design, there are two insulation layers present, they are made of Kapton with a thin aluminium film ($\epsilon = 0.3$). The maximum thickness of this material is taken, thus 13 μm as it would be more stiff this way. The space between the sheets is 0.5 mm.

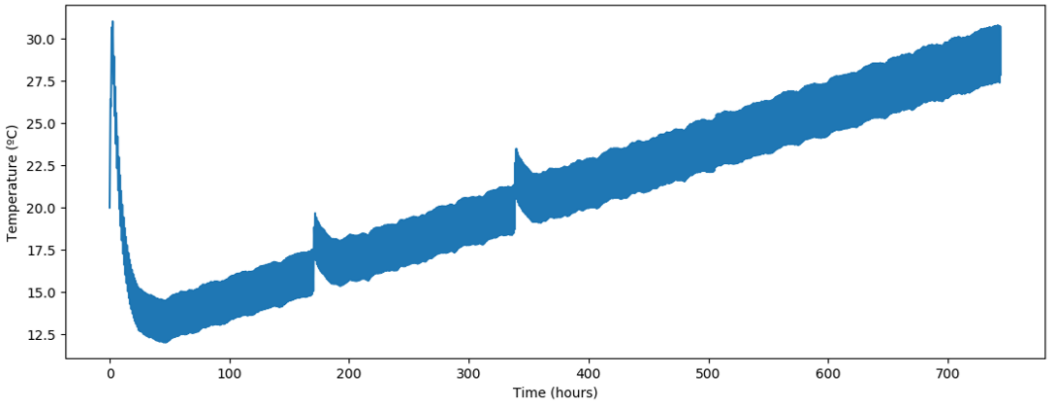

Figure 14.1: Temperature over mission time for PPQ-1

PPQ-2

The outside surface of the PPQ-2 will also be entirely made out of aluminium. The PPQ-2 has two cameras on the positive X side, this side has therefore the weighted arithmetic mean value of $\alpha = 0.13$ and $\epsilon = 0.40$, the positive Y side has one camera resulting in the $\alpha = 0.11$ and a $\epsilon = 0.35$, the negative X, and both y sides have a $\alpha = 0.10$ and a $\epsilon = 0.30$. As stated before, the positive z side has the solar panels, which have a $\alpha = 0.64$ and a $\epsilon = 0.85$. The negative Z side also has an $\epsilon = 0.30$.

The power input varied over time (as can be found in chapter 5). The exact timing of the modes is not yet defined, but for now, it is assumed that they are turned on once a week. Thus, the same as described previously for the PPQ-1. It has to be noted that science modes A and C have different powers for PPQ-1 and PPQ-2 as they carry different payload. Also for the PPQ-2, it as can be seen in Figure 14.2 that it does not matter when the science modes are turned on.

Regarding the design, there are two insulation layers present, they are made of Kapton with an aluminium layer ($\epsilon = 0.3$). The maximum thickness of this material is taken, thus 13 μm as it would be more stiff this way. The space between the sheets is 0.5 mm.

[6] http://matweb.com/search/DataSheet.aspx?MatGUID=0cd1edf33ac145ee93a0aa6fc666c0e0 [Accessed 19 June 2019]

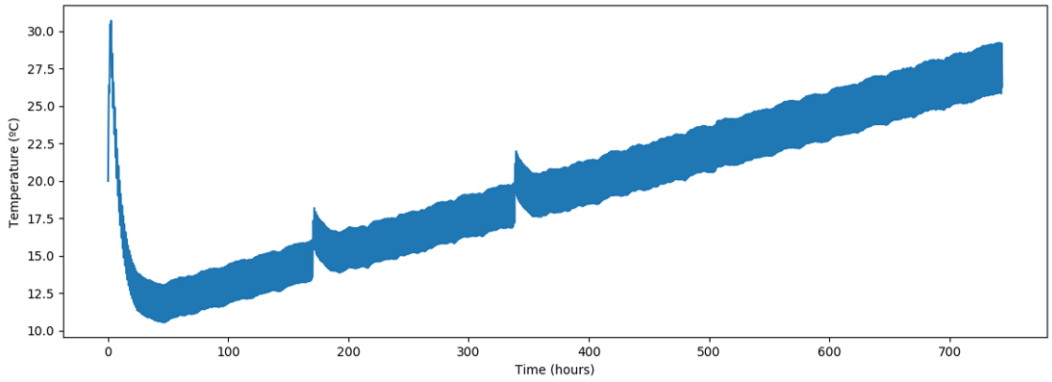

Figure 14.2: Temperature over mission time for PPQ-2

As a comparison, the PPQ-2 is slightly warmer than PPQ-1. This makes sense as the camera's are made of a dark material and are therefore absorb more heat. When the rotation period of the asteroid is increase, the temperature will be more constant and that would be acceptable as well.

14.4.2. CPQ

Also the CPQ will be made out of aluminium outside, however, this will be painted grey. The emissivity of grey paint is $\epsilon = 0.95$[7] and the absorption is $\alpha = 0.25$[8] . The positive Z side is a Weighted arithmetic mean value of $\alpha = 0.20$ and $\epsilon = 0.54$.

The power only chances twice. The communication subsystem is active just after landing to let the Mothership (Earth) know which PQs are healthy. Part of this power will be send away as waves and part of this power will be transferred into heat. It is assumed that 40% of the power transformed into heat. Then, the CPQ will only use 0.024 W until it starts sending data back to Earth. For now, it is assumed that the communication with Earth will take 18.85 hours and that the communication will be switched off and on every half a period (so every 1800 s) as it will only be in Earth's view for half the period.

Regarding the design, only one insulation layer made out of kapton is present, that will have a $\epsilon = 0.95$. Therefore the kapton will be covered by a black layer. The maximum thickness of this material is taken, thus 13 μm as it would be more stiff this way. The space between the sheets is 0.5 mm.

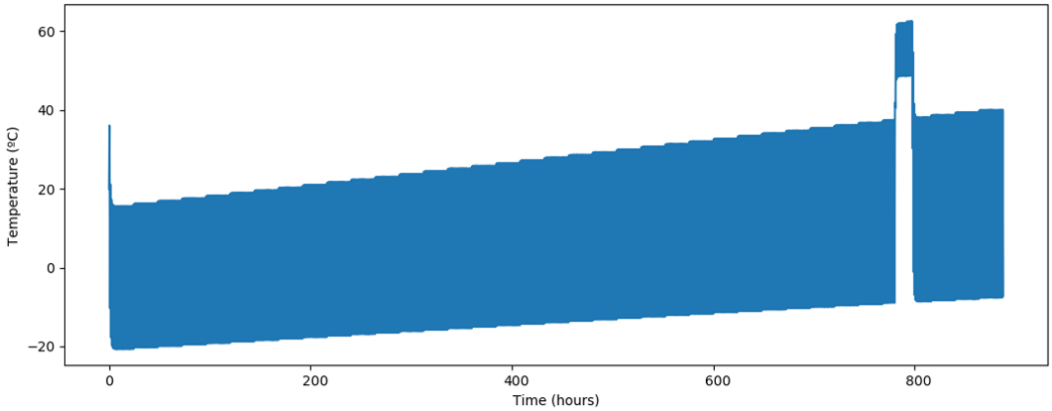

Figure 14.3: Temperature over mission time for CPQ

Due to the fact that there is less insulation, the temperatures fluctuate more. It is not possible to add more layers of insulation be able to keep the CPQ warmer in the first month as it then would overheat during the communication window. However, discharging is possible as the temperature always stays above -20 °C. Recharging can only be done when the PQ is warm enough, this is not a problem.

Since in this case the rotation speed of 3600 s is beneficial since the CPQ will become warmer. Therefore, also for the CPQ the worst case is simulated and then indeed the temperature for the first five days will be be-

[7] http://www-eng.lbl.gov/~dw/projects/DW4229_LHC_detector_analysis/calculations/emissivity2.pdf [Accessed 22 June 2019]
[8] https://www.engineeringtoolbox.com/light-material-reflecting-factor-d_1842.html [Accessed 22 June 2019]

low 0 °C and recharging will not be possible. However, the EPS is designed in such a way that it will be not be a problem.

14.4.3. BULLETS

For the bullets, the inputs, the heat capacity of lead (490 J/kg K[9]), the emisivity of lead (0.63) and the absorption of lead (0.62)[10]. It is found that no insulation layer is needed and that the Bullet has the right thermal conditions without the need of thermal control. Figure 14.4 shows the temperature of the bullets over the time interval from 1st of March until the 6th of April.

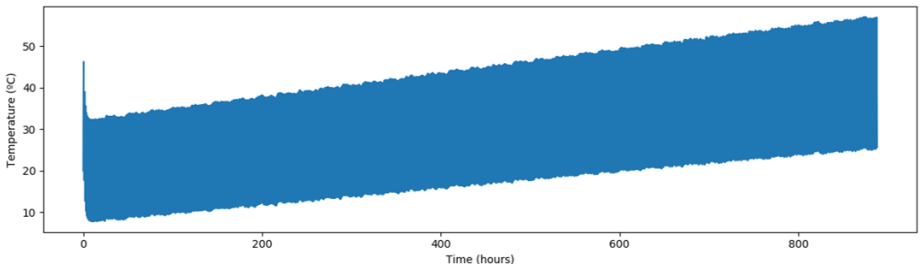

Figure 14.4: Temperature over mission time for Bullets

As stated before, during the first 10 minutes the Bullets have the reeling mechanism active that generates 7 W. This is clearly visible in the graph. As the assumption made in chapter 13 that the batteries have no heat loss, a simulation was performed that included only a 90% efficiency. Thus that 10% of the energy would become heat during the communication phase this is the highest. Still, the bullets would stay under a temperature of 60 degrees Celsius.

15
COMMAND AND DATA HANDLING

The following chapter presents the design of the Command and Data Handling (C&DH) subsystem, often referred to as the 'brain and nervous system' of the spacecraft. It is extremely important for the correct functioning of the whole system, as it is responsible for sending commands, handling the data flow within the system and performing health checks of all the other subsystems.

The first section (section 15.1) outlines the system requirements that are applicable to the subsystem. Then, the functions of C&DH will be stated, explained and visualised by means of diagrams in section 15.2. This is followed by the summary of the subsystem design, which is broken down into the data flow design, section 15.3, the software design, section 15.4, and the hardware design, section 15.5.

15.1. SUBSYSTEM REQUIREMENTS

The overview of the requirements set on the Command and Data Handling subsystem is presented in Table 15.1 below. A connection of some requirements to a parent requirement is indicated in the **Requirement** column. If the compliance is not yet investigated or cannot be proven at this time, the compliance box contains a "n".

[9] https://www.engineeringtoolbox.com/specific-heat-capacity-d_391.html [Accessed 14 June 2019]
[10] http://matweb.com/search/DataSheet.aspx?MatGUID=ebd6d2cdfdca4fc285885cc4749c36b1 [Accessed 14 June 2019]

Table 15.1: Requirements for the Command and Data Handling subsystem of the PQ.

Requirement ID	Requirement	Rationale	Verification Method	Compliance
DOT-LAN-PQ-2	The PQs shall be able to perform a self-test.	This is to verify if all subsystems are functioning and to allow failures to be mitigated.	Analysis: perform simulations.	✓
DOT-LAN-PQ-2.1	The self-test shall verify the functioning of the PQ subsystems, log the results and send it to the Mothership.	After the Mothership receives the results, it will send it to Earth.	Analysis: perform simulations.	n
DOT-CDH-V	The stack height of the Command and Data Handling Subsystem shall not exceed the value specified in the volume budget.	The subsystem shall fit within the PQ.	Inspection: measurements on the assembly.	✓
DOT-CDH-M	The mass of the Command and Data Handling Subsystem> shall not exceed the value specified in the mass budget including the current contingency level.	-	Inspection: measurements on the assembly.	✓
DOT-CDH-1	The Command and Data Handling subsystem components shall withstand radiation levels of up to <TBD>krad.	Due to long exposure and high radiation levels, it has to be assured the C&DH can operate without failure in those conditions.	Analysis: perform simulations.	n
DOT-CDH-2	The average power of Command and Data Handling subsystem shall not exceed the value specified in the power budget.	-		✓
DOT-CDH-3	The Command and Data Handling subsystem shall be able to store 6 Gbit of scientific data in each PQ. (Parent: DOT-DUR-1-DAT-2)	All PQs have to have the capability to store all of the compressed scientific data (volume < 6 Gbit)	Test: component (data storage) tests.	✓
DOT-CDH-4	The Command and Data Handling shall be able to store <TBD>Mbit of telemetry data in each PQ. (Parent: DOT-DUR-1-DAT-2)	-	Test: component (data storage) tests.	n
DOT-CDH-5	The Command and Data Handling subsystem shall be able to acquire and store telemetry autonomously. (Parent: DOT-DUR-1-DAT-2)	During large part of the mission the system has to perform autonomously.	Demonstration: check whether the C&DH is capable to perform this operation autonomously	✓
DOT-CDH-6	The Command and Data Handling subsystem shall be able to activate the scientific instruments autonomously. (Parent: DOT-DUR-1-DAT-2)	See: DOT-CDH-5	Demonstration: check whether the C&DH is capable to perform this operation autonomously	✓
DOT-CDH-7	The Command and Data Handling subsystem shall be able to switch between the operational modes autonomously. (Parent: DOT-DUR-1-DAT-2)	See: DOT-CDH-5	Demonstration: check whether the C&DH is capable to perform this operation autonomously	✓
DOT-CDH-8	The Command and Data Handling subsystem shall be able to initialise within <TBD>s.	For precise planning of all mission phases exact timing of C&DH has to be known.	Inspection: measure the time of the subsystem initialising.	n
DOT-CDH-9	The Command and Data Handling subsystem shall be able to perform a valid transition into safe mode if the telemetry data from all subsystems is not received after <TBD>s. \	-	Test: verify whether the subsystem will go to safe mode in specific condition imposed on the telemetry reception.	n
DOT-CDH-10	The Command and Data Handling subsystem shall be able to perform a valid transition from the safe mode to an operational mode after telemetry issue has been resolved, within <TBD>s.	The system needs to recover as fast as possible so that the nominal mission operations can be continued.	Test: verify whether the subsystem will go to a nominal operational mode in specific condition imposed on the telemetry reception.	n
DOT-CDH-11	The Command and Data Handling subsystem shall be able to perform a valid transition to the EoL mode after receiving a command from the ground segment.	-	Test: verify whether the subsystem will transition to the EoL mode after it is commanded to do so by the ground segment.	n
DOT-PAY-SOL-1	The Command and Data Handling shall register the voltage output of the solar arrays with an accuracy of <TBD>V. (Parent DOT-LAN-PQ-SC-1.5)	Required for acquiring scientific data.	Test: conduct a test with a solar array receiving radiation and compare with theoretical results.	n

15.2. Subsystem Functions

Before considering the design of the data flow, the major functions to be performed by the subsystem shall be reviewed. They are:

- Data processing
- Sending commands to subsystems and receiving data from subsystems (internal communications)
- Sending commands, receiving commands, sending compressed data and receiving compressed data from other PQs (external communications)
- Storing data
- Compressing data
- Handling commands received from ground/Mothership
- Fault detection
- Selecting and performing transition to different modes
- Time keeping
- Performing telemetry

15.3. Data Flow Design

In the following section, the design of the data flow is detailed. This is a crucial part of the design with implications both on the software and hardware of C&DH.

Data Bus Choice

In order to construct the data flow architecture, the data bus choice has to be made first. Initially, the I^2C bus was considered, as it is very commonly used in both CubeSats and PocketQubes and results in a relatively simple architecture [31]. However, it was found that it is incapable of accommodating the expected data rates (above the theoretical limit of 400 kbit/s [32]). Upon a consultation with an expert (ir. Jasper Bouwmeester, personal communication, 17 June, 2019), SPI, RS422, RS485 data buses were chosen for further evaluation.

The previously mentioned options had to comply with all the payload instruments (the choice of the CPU unit can be dependent on the chosen data bus) in order to be evaluated further. It was found that this condition was satisfied solely by the SPI data bus. Additionally, SPI offers simple hardware interfacing, offers full duplex communication and simple software implementation[1]. This is desirable in terms of minimising the development and integration costs, and in general decreasing the complexity of the system.

The required components would to support this bus include the CPU, a memory storage, a real time clock and, potentially, pull up resistors. However, some microcontrollers have embedded CPU, RTC and pull up resistors. This strongly influenced the hardware choice (elaborated on in section 15.5).

Data Flow Architecture

Regarding the physical design of the data flow, 3 different architectures need to be considered. This is due to the fact that the data transfer will be performed in basically three different setups in the system. Internal communications, hence data flow inside of the PQ, will have a different architecture for the PPQ and the CPQ. They will be, however, comparable for the PPQ-1 and PPQ-2. The third architecture that shall be designed is the data flow in between the PQs (external communications).

All the previously described data transfers will make use of the SPI data bus. What differs is the configuration for the external and internal communications. The internal communications will function based on the **independent slave** configuration, whereas the external communications will be handled with a **daisy chain** configuration.[2] The independent slave configuartion has all the slave devices connected to the master, whereas for the daisy chain configuration they are connected in series: the first slave's output is connected to the proceeding slave's input.

The reasoning behind using the independent slave configuration inside of the PQ that the slave devices are operating simultaneously in different configurations and in some modes solely one device is active. For the external communications on the other hand, a daisy chain connection allow for an optimised data flow network topology.

The baseline data flow network topology assumes that selected PPQs would serve as masters for the system and the remaining PPQs would act as slaves. A master PPQ would be gather the compressed data from its slave PPQs, so that it could be redistributed to selected CPQs and readied for the phase in which the data is down-

[1] https://en.wikipedia.org/wiki/Serial_Peripheral_Interface [Accessed 16 June 2019]
[2] https://www.maximintegrated.com/en/app-notes/index.mvp/id/3947[Accessed23June2016]

linked to Earth (COMMS mode; see section 5.5). The handing of this operation is detailed in section 15.4. For the distribution of the master PPQs, consult section 5.7.

Figure 15.3 and Figure 15.2 graphically represent the SPI data bus for the internal communications. The representation of the external communications data flow architecture is shown in Figure 15.1. There is 4 data interfaces: SCLK (Serial Clock), MOSI (Master Out Slave In), MISO (Master In Slave Out), SS (Slave Select).

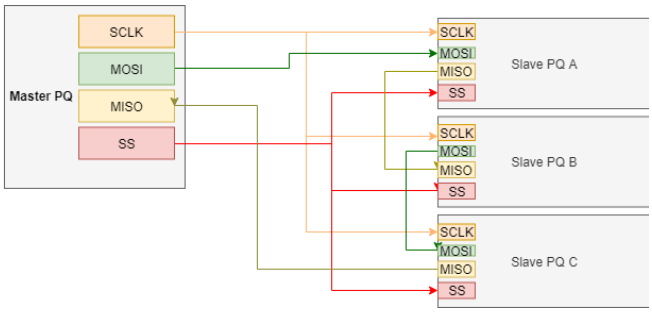

Figure 15.1: The SPI architecture baseline showcasing the data flow in between PQs.

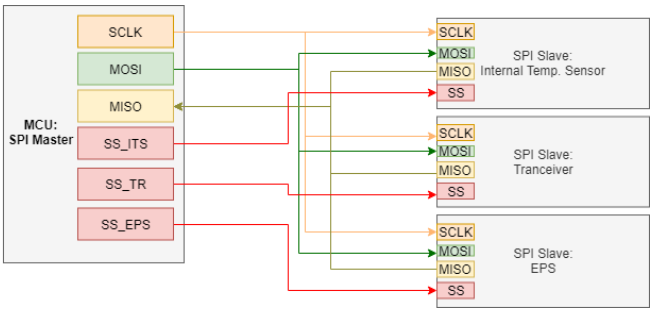

Figure 15.2: The SPI architecture baseline showcasing the data flow inside the CPQ.

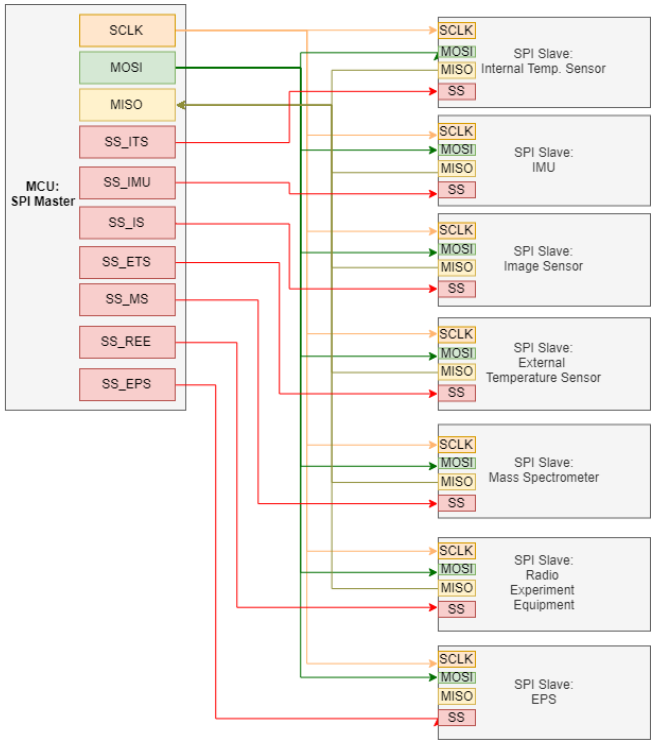

Figure 15.3: The SPI architecture baseline showcasing the data flow inside the PPQ.

15.4. Software Design

Looking at the subsystems requirements, the ones that relate to the software performance are DOT-LAN-PQ-2, DOT-LAN-PQ-2.1, DOT-CDH-5, DOT-CDH-6, DOT-CDH-7, DOT-CDH-9, DOT-CDH-10, DOT-CDH-11. The following section aims to show that the design of the software is **valid**, in terms of compliance with the requirements.

It has to be noted that the software design is at a very preliminary stage and the following is intended to act as a baseline for further stages of the design.

The main software functions are outlined in Figure 15.4. The functions are translated into steps that the software would need to take in order to achieve a certain action. In the further design stages, the blocks of the diagram would be translated into units of code.

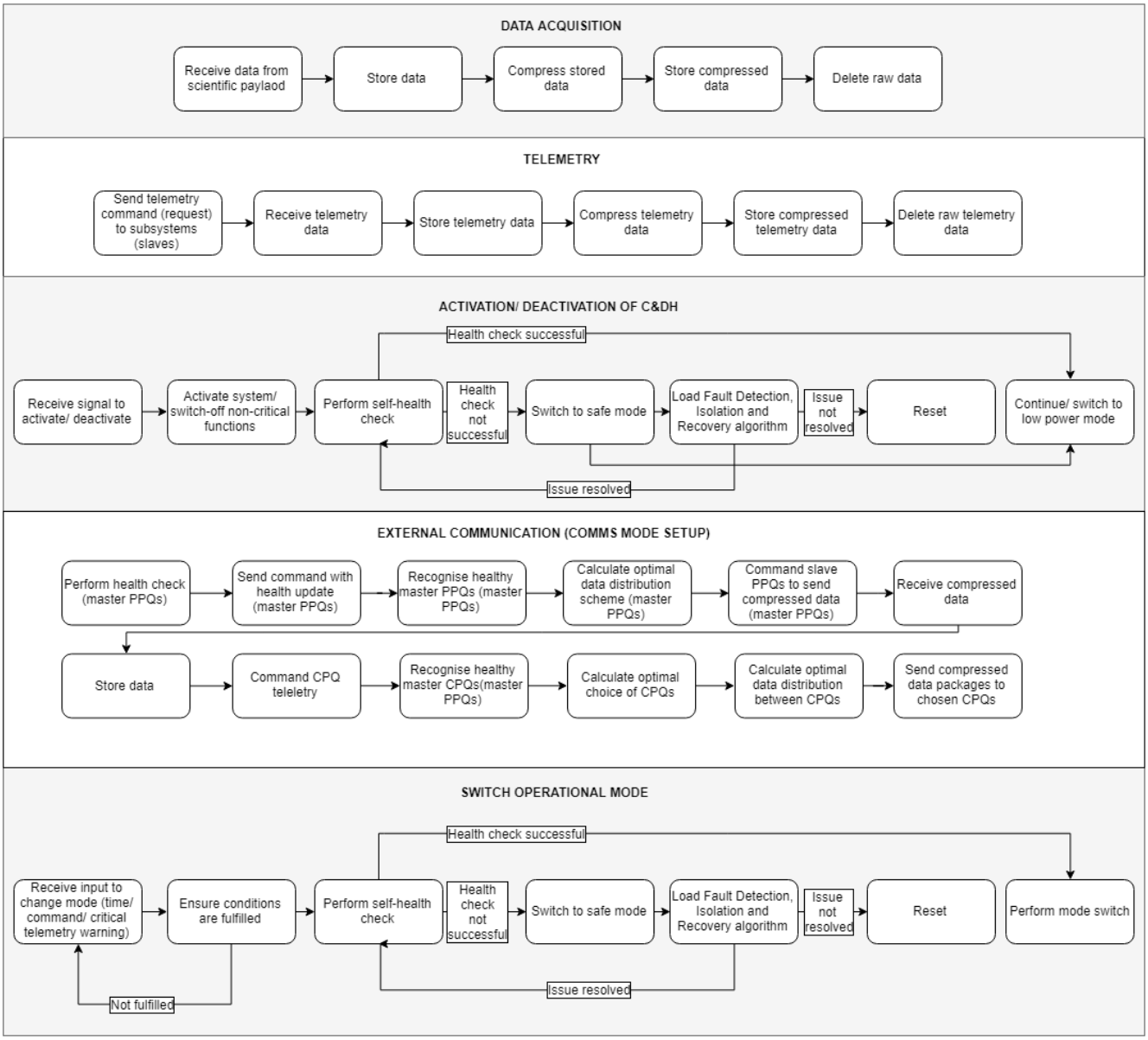

Figure 15.4: The software block diagram outlining the execution in steps of the most important functions to be done by the C&DH software

With the software designed to match the implementation of all functions shown in Figure 15.4, most of the software requirements (DOT-LAN-PQ-2, DOT-CDH-5, DOT-CDH-6, DOT-CDH-7, DOT-CDH-11) set on the software can be met and hence it is indicated that they are complied with. The requirements for which the compliance cannot be yet determined are: DOT-LAN-PQ-2.1, DOT-CDH-9, DOT-CDH-10. Those requirements are focusing purely on the software execution performance and thus without a detailed performance analysis of the software, it cannot be ruled whether the software design can meet them. What is more, the exact values required from software performance have not been specified at this stage of the project (they remain marked as TBD).

15.5. Hardware Design

Having presented the preliminary design of both the data flow and software, the hardware choice can proceed. The main requirements that connect to the C&DH hardware are DOT-CDH-V, DOT-CDH-M, DOT-CDH-1, DOT-CDH-2, DOT-CDH-3, DOT-CDH-4, DOT-PAY-SOL-1. What follows is the main outline of the hardware design, including sizing and selection of COTS components for the system.

Hardware Architecture

Figure 15.5 presents the layout of the C&DH hardware. It was suggested after consultations with an expert (ir. Jasper Bouwmeester, personal communication, 17 June, 2019), that for the specific software needs for this mission, a 32 bit CPU with a clock frequency of at least 1MHz should be chosen for optimised performance. The available options included an MCU (Microcontroller unit) and a microprocessor. An MCU was chosen, despite the fact they usually offer much worse computing performance compared to microprocessors. However, it is more suitable for this application and can meet the hardware requirements. MCUs often offer an RTC, non-volatile memory unit and a better variety of interfaces.

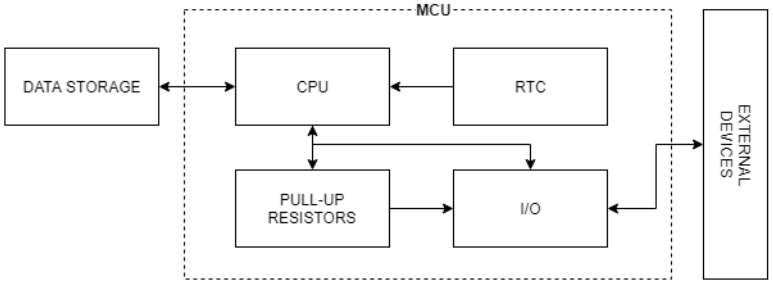

Figure 15.5: The C&DH hardware architecture diagram

Regarding the components, the subsystem has a simple setup. With the current definition of the C&DH, the elements include a MCU, Data storage, a PCB board and harness inside the PQ. The outside harness is included in the NET budgets. Both however, are sized in this section, for minimisation of power losses.

Component choice

As mentioned in section 15.3, the chosen components have to be compliant with the SPI data bus. The selected components (Table 15.3) fulfil this condition. The chosen MCU is a 32 bit with a 16 MHz clock frequency.[3] The data storage unit can store up to 8 Gbit of data.[4] Both components are radiation hardened (up to 60 krad) to prevent a risk of errors caused by cosmic radiation, such as latch-ups.[5] The hardware complies with DOT-CDH-V, DOT-CDH-M, DOT-CDH-2, DOT-CDH-3 and deliver the desired performance. DOT-PAY-SOL-1 is not specified and hence it cannot be stated that it is complied with. Regarding DOT-CDH-1 and DOT-CDH-4, it also cannot be specified, however, taking into account the fact that components are rad-hard and provide 33% more data storage than required, it is likely that they can be complied with. In order to state this with absolute confidence, the requirements need to be refined. In order to accomplish that, an accurate radiation simulation and telemetry data estimation need to be conducted.

Cable Sizing

The cables for harness of C&DH subsystem were sized for an assumed power loss level. Using the relation: $Power[P] = Voltage[V] \times Current[I]$ and maximum current and voltage in a cable, the power in a cable can be calculated. Then, making use of Puillet's law[6]: $A = \rho \frac{l}{R}$ (where l is the cable length and A is the cross-sectional area) and assuming a maximum power loss (as a fraction of the power in the cable) it is possible to arrive at the minimum diameter of a power cable. The results are presented in Table 15.2. A voltage of 3.0 V and a current of 6 mW were used.[7] The length of the external cable was taken as the distance in between PQs. For the internal cable, it is the required cable length required to reach from one extreme on the top stack of the PQ to another extreme on the bottom stack of the PQ (PQ has a maximum stack height of 0.039 m and a maximum stack dimension of 0.037 m; roughly it gives $3 \times 0.04 = 0.12$ m).

The mass of the external cable is described in chapter 8. The mass of the internal cabling, assuming 28 cables of maximum length (Figure 15.3) is calculated to be 1.1 g. The value from the previous estimation was

[3] http://www.ti.com/lit/ds/symlink/msp430fr5969-sp.pdf [Accessed 15 June 2019]
[4] http://www.3d-plus.com/data/doc/products/references/3dfp_0706_2.pdf [Accessed 15 June 2019]
[5] https://en.wikipedia.org/wiki/Radiation_hardening [Accessed 15 June 2019]
[6] https://en.wikipedia.org/wiki/Electrical_resistivity_and_conductivity [Accessed 20 June 2019]
[7] http://www.ti.com/lit/ds/symlink/msp430fr5969-sp.pdf [Accessed 15 June 2019]

4.1 g. This value is taken in order to account for harness mounting and insulation. Should a more detailed cable sizing be performed, the value shall be updated to a more accurate estimate.

Table 15.2: Resulting data cables diameters

Type	Power [W]	Maximum loss [%]	Length [m]	Material	Min. diameter [mm]
Internal harness	0.018	0.01	0.12	Copper	0.2
External harness	0.018	0.10	1.25	Copper	0.2

Table 15.3: The list of hardware components of the C&DH subsystem including functions, dimensions, mass, and required power.

Name	Function	Dimensions [mm]	Mass [g]	Peak power [W]
Texas Instruments MSP430FR5969-SP Radiation Hardened Mixed-Signal Microcontroller	*Processing, Command, Time keeping, Telemetry, Data compression, Fault detection, Pull-up/Pull-down*	7.15 × 7.15 × 1.00	1.3	5×10^{-6}
3D Plus 3DFN8G08VS1706 8 Gbit NAND FLASH Memory module	*Data Storage*	3.48 × 20.40 × 4.10	1.7	-
PCB	*Accomodating physical and electrical connections*	37.00 × 37.00 × 1.00	2.5	-
Harness/cabling	*Electrical connection, data transfer*	-	4.1	-

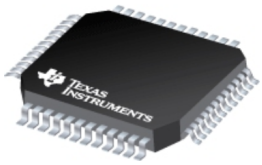

Figure 15.6: The MSP430FR5969-SP MCU selected for the C&DH [8]

16
SPACECRAFT OPERATIONS

The operations and logistics are an integral part of the ANTREA mission. The operations described here focus on the ground segment and spacecraft interaction and the team responsible to operate the spacecraft. The description starts about a year before launch, for a more general project organisational overview, consult chapter 26.

16.1. REQUIREMENTS

The overview of the requirements related to Astrodynamics is presented in Table 16.1 below. A connection of some requirements to a parent requirement is indicated in the **Requirement** column. If the compliance is not yet investigated or cannot be proven at this time, the compliance box contains a "n".

[8] http://www.ti.com/product/MSP430FR5969-SP [Accessed 29 June 2019]

Table 16.1: Requirements for ground segment.

Requirement ID	Requirement	Rationale	Verification Method	Satisfied (Y/N)
DOT-GS-1	The mission shall use and be compatible with the standards of the ESA ESTRACK network as well as the NASA deep space network.	This offers flexibility.	Inspection	✓
DOT-GS-2	The ANTREA mission shall be operated by ESA/ESOC.	ESA missions are usually operated by ESOC.	Inspection	✓
DOT-GS-3	The ground segment shall provide for coverage during the 28 hour downlink window. (Parent: DOT-COM-DAT-1)	A 28 hour downlink window is required.	Inspection	✓
DOT-GS-4	The ground segment shall cope with the data volume defined in DOT-COM-DAT-1.	Required to achieve scientific output	Analysis	✓
DOT-GS-5	The ground segment shall be able to send commands to the PQs every 24 hours during data acquisition mode.	Emergency capability in case the system is not able to recover to nominal operations autonomously.	Analysis: RF simulation	✓
DOT-GS-6	The ground segment shall be able to receive health updates every 24 hours during the data acquisition mode.	Considered possible at this stage of the design. Maybe not used in final design.	Analysis	✓
DOT-GS-7	The ground segment shall send a signal to enable determining Earths position by the communications subsystem as defined in DOT-COM-4.2.	The communication subsystem requires this signal to determine Earths position.	Analysis: RF simulations	✓
DOT-GS-8	The ground segment shall receive data at a minimum elevation angle of 20 degrees. (Parent: DOT-GS-3)	Makes sure a ground station is in view at all times.	Analysis: RF simulations	✓
DOT-GS-9	The science data shall be made available to the scientific community via the ESA Planetary Science Archive.	Ensures transparency and maximum scientific yield	Inspection	✓

16.2. Organisation

Top level organisation

The ground segment will be headed by a chief spacecraft operations managers (SOM) at ESA ESOC in Darmstadt. He/she will have full responsibility on the day to day spacecraft operations as well as planning activities. It is in the spacecraft operations managers (SOM) responsibility to minimise risk and maximise scientific output, in addition to altering the mission planning if necessary. The chief SOM reports to the project manager, who is in charge of updating the ESA management on mission progress. The engineering ground segment consists of experts in all vital spacecraft subsystems. They are in charge of monitoring the spacecraft health and executing commands agreed upon in mission planning. This engineering team is in contact with a science team, consisting of the Principal Investigators (PI's) of all scientific instruments and their teams. They are being updated on the spacecraft performance and possible limitations. In cooperation with the engineering team, they reschedule the scientific planning in case a problem occurs and optimise the output to circumvent the problem as much as possible.

Ground station

The NASA Deep-space network (DSN) is used for downlink of scientific data [26]. It is operated by JPL and owned by NASA. As a result, a contract between NASA and ESA has to be set up detailing the time each of the three ground stations is required, what modulation and amplifying methods are used, etc. This should be done approximately 5 years before the expected downlink window, since ANTREA only possess one opportunity to downlink. In addition, rather than setting a specific date and time it has to be kept slightly undefined as the exact close approach time will only be known a few months prior. The consequence in case this window is not available to the mission would be catastrophic as no data could be downlinked. In addition to the 28.5 hours for primary downlink, more preceding time slots are required to track the asteroid accurately by use of ranging. However, this may not require the DSN and smaller antennas could be used. In addition, in case it is decided that an emergency up- and downlink shall be established every 24 hours, another smaller antenna network is required. A diagram presenting the ground segment organisation and the interaction with the space segment can be found in Figure 16.1.

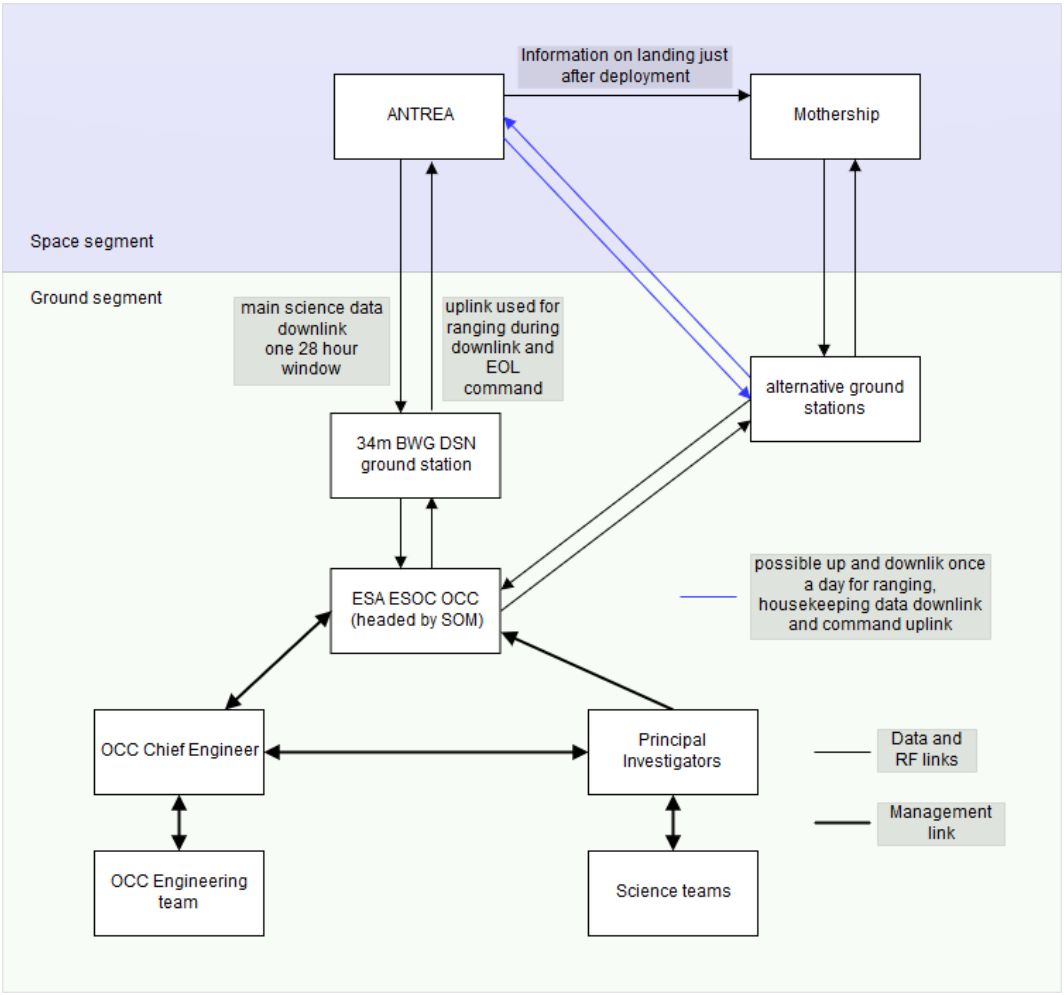

Figure 16.1: Mission design and communication diagram

PAYLOAD DATA HANDLING

The raw science data will be downlinked to the respective ground stations and then sent to ESA ESOC OCC (Operations control center). ESOC provides data corrected for eventual errors induced in the transmission path to the scientific investigators. In practice, this is done via the ESOC DDS (Data distribution system). Along with the data, ANTREA anomalies, ancillary data and instrument calibration information will be provided to the science teams. Once the data have been sorted in a scientifically useful format by the PIs and their teams, the ANTREA science operations center will calibrate and correct the output to make it scientifically useful [33]. Lastly, the data will be uploaded to the ESA Planetary Science Archive (PSA) that enables access to scientists worldwide. An illustration of the data flow can be found in figure Figure 16.2.

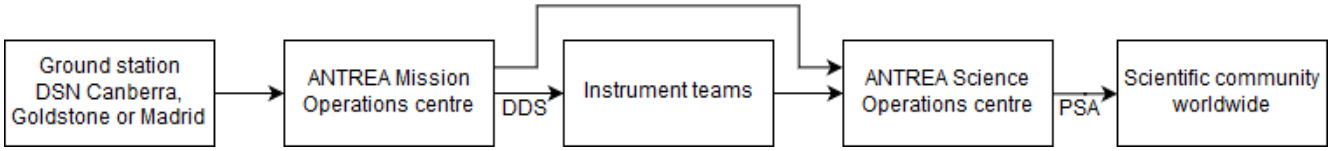

Figure 16.2: Payload data flow block diagram

17

VERIFICATION OF CALCULATIONS

During the design of ANTREA all calculations needed to be verified. Any errors in calculations can threaten the success of the mission. Therefore, verification of the calculations is of utmost importance. This chapter will discuss the verification procedures and results for all the subsystems.

Astrodynamics

The validity of the Monte-Carlo simulation of the asteroids trajectory was verified by comparing the periapsis distance obtained using GMAT for the nominal trajectory to the one listed in the JPL Small Body Database. The difference between the two was found to be around 30000 km which while significant is much smaller than the differences produced by the uncertainties in the asteroids orbit and is therefore acceptable. The differences can be explained by the fact that the two models used to propagate the trajectories are slightly different. Furthermore the approach for obtaining the random initial values was verified by sampling a large amount of theses vectors and then calculating the covariance matrix from those to see if it matched the original one which was indeed the case. Finally as an overall system test the standard deviations for the positions of the potential trajectories just before close approach was calculated and found to be close to the ones given by JPL Horizons.

The Mothership trajectory was more difficult to verify, as no precise external simulation exists. Therefore, it had to be verified by comparing ΔV results obtained from GMAT for the trajectory with two impulsive burns with the ones obtained from the pork-chop plot, which is an analytical method. There is a difference of 10% between these two for the TOI. One factor that contributes to this error is that the analytical method assumes that the Mothership starts with its excess velocity at the centre of the Earth, while in reality it will only achieve this velocity at roughly 1M km from the Earth. On the other hand the arrival ΔV only has an error of 0.25%, due to the asteroid having such a weak gravity. Furthermore, the propagators used for the Mothership trajectory were the same as the ones used for the asteroid trajectory modelling, which already proved to be very accurate. Finally GMAT itself has already been extensively verified and validated by NASA [34] including interplanetary trajectories.

Net

Most calculations for the net preliminary sizing were performed in Excel and Python. All calculations were verified by unit tests. To provide an example, the verification of the sizing calculations of the motor, battery, gears and ESC in the bullets is presented. The equations and the logical flows were explained in item 8.3. The following parameters were set to the following variables: $r_{spindle} = 1$ m, $T_m = 1$ Nm, $\omega = 1$ rad/s, $r = 1$ [-], $\eta_m = 1$ [-], $\eta_r = 1$ [-], $\eta_e = 1$ [-] and $d_{reel} = 3600$ m. The results were as expected 1 m/s reel-in velocity, 1 Nm spindle torque T_s, 1 N cable force F, 1 W mechanical power P_{mech}, 1 W electrical power P_{elec}, 0 W dissipated power (heat) P_{diss}, 3600 s reel-in time t, 1 Wh electrical energy required E and finally 108.32 Wh (to 100% Depth-of-discharge) would left in the batteries after reel-in. This adds up as 1 Wh is used per bullet and 112.32 Wh are available at a state-of-charge of 100%. Additionally, individual parameters were altered and it was checked if the overall outcome still made sense. For example, one efficiency parameter changes from 1 to 0.5, which results in the mechanical power being conserved, the electrical power input doubled (also energy required doubled) and the amount of dissipated power being equal to the mechanical power.

The software *ADRiNET - The Toolchain for Dynamic Simulation of Elastic and Deformable Net-like Structure* along with a discrete model of the net was provided by SKA-Polska. The simulation has been developed under an ESA contract and was verified and validated for space applications. [16] Consequently, no further verification activities on the simulation algorithm itself were executed. Python programs were written to adapt xml and $hdf5$ input files. These were verified by visual and programmatic inspection, i.e. checking if values equal certain set values or if the sum of a number of data equals the expected sum.

Deployer

Most of the calculations were performed with Python to allow to find results for the equation with many variables. Most of the parameters were unknown when designing, therefore the program allowed to calculate for multiple combinations of variables which could show the possible iterations to choose. The programs were verified by performing unit tests. The theory used behind the calculations and the assumptions made were discussed and agreed upon with different experts in the field, namely Dr. S.R. Turteltaub and Dr. C.D. Rans. This encouraged the team in using a correct approach to the problem.

All calculations were checked whether the output was of the expected type and unit. This was done by replacing the unknowns by simple units, or by solving already developed exercises to confirm that the output was leading to the correct answer.

Structure of PQ

The calculations made for the design of the PQ's structure were done multiple times, both analytically and using a calculation tool. Some very simple unit tests and an overall system test was performed and resulted in the following:

- Considering the landing design load F_{load}, values of 1 g and 1 m/s were entered for the mass and velocity of the PQ respectively, for the calculation of the impulse, and a shock absorption time of 1 s was entered, which indeed resulted in the applied safety factor of 1.5.
- Those same input values also resulted in a kinetic energy of 0.5 J, which makes sense as it corresponds to the 1/2 fraction at the beginning of the kinetic energy formula, which then resulted in a 1 mm thickness of FR-4. This makes sense as the tool was designed to yield a thickness that would be higher than FR-4's Izod impact, which is of 0.37 J/mm.
- For the launch loads and vibrations calculation, the same verification procedures as in chapter 17 were performed.

Payload

The calculations done for the payload considered the calculation of the power by multiplying the current and voltage which was done by hand and checked multiple times. A current of 20 mA with a voltage of 10 V thus equals a power of 200 mW. The program showed this as well and the calculation is thus verified. The mass of the PPQs was calculated by multiplying the mass of an instrument with the amount of that instrument in the PQ and then adding all the masses of all the different instruments together. The amount of instruments was set to zero for all payload instruments to see if the output is the expected zero. This was the case thus the calculation was verified. The mass and power of the mass spectrometer were extrapolated from a bigger one. Its volume is 29716000 mm^3 and its mass is 13000 g. This thus equals 0,000437475 g per cubic mm. If this is multiplied by the volume of the smaller mass spectrometer its mass is given. It's volume was set to 1 mm^3 to check if this indeed results in 0,000437475 g. This was the case and the calculation was thus verified.

Finally, the calculations for the data volumes were the most extensive. The calculations were done in Excel and all cells were checked for its correctness. The number of PPQs was changed to see if with this indeed all data volumes changed, which was the case for all. For each instrument the calculation was also checked by changing one item at the time. For example, the temperature sensors generate 90.73 Mb. When the amount of bits of the sampling frequency is halved the data volume should become 47.53 Mb which was indeed the case. Furthermore, switching from 3 to only 1 temperature sensors should reduce the data volume to 30.24 Mb which was the case as well. Finally, doubling the operating time also doubled the data volume to 181.45 Mb. Performing these tests showed that the data volume calculation for all instruments were correct and are thus verified.

Mechanisms

The mechanism of the temperature sensor was build from scratch around the torsional spring. All calculations were checked in different ways. The calculation of the maximum shear force in the second arm due to it being kept stowed was verified by setting the deflection angle to zero. This makes the applied force zero and thus also the maximum shear force. Doing this made the shear force indeed zero so the calculation was verified. The design of the temperature deployment mechanism was verified by changing one dimension to see if it adapts all other dimensions with it. The width of the rings was changed from 1.5 mm to 2 mm which should increase the width of the mechanism from 12.048 mm to 14.048 mm as there are 4 rings. The program showed the same result. The size of the hole was then increased by 1mm. This should decrease the length of the vertical part of the second arm from 32.318 mm to 31.318 mm. The program showed that this was indeed the case. More of these checks were performed and it has been concluded that the calculations are verified. Creating the CAD drawings of the parts added another test. This showed that the hole of for the temperature sensor was actually made too big to have a 1 mm clearance between the hole and where the mechanism starts.

For the sizing of the heating wire, a Microsoft Excel spreadsheet was used. In order to verify the correctness of the calculations, a simple unit test was performed. The sheet takes required heat, specific heat, temperature difference, mass of the heated object, heating wire resistivity, wire diameter and heating time as inputs. It

outputs the wire length. All inputs were set to 1, which should output a wire length equal to $\pi/4$. The output length was equal to 0.785, which is exactly the expected value. The tool can be hence considered verified.

Cable Sizing

The tool used for sizing the power and data cables was a Microsoft Excel spreadsheet. The inputs included material properties, maximum voltages and maximum currents, assumed maximum losses (as a fraction), and cable lengths. The output was the minimum diameter for a given cable. The verification procedure was done by doing a unit test. The inputs for the test were: loss of 1 W, length of 1 m, maximum current of 1 A. Analytical calculation leads to simplifications in formulas and a minimum cross-sectional area with the same magnitude as the resistivity of the used material.
Inputting the unit values, the result was 1.68×10^{-8} m^2, which is equal to the magnitude of the resistivity of copper. This test is assumed to be a sufficient proof for the verification of the tool.

Thermal Control

The Python program used to simulate the Thermal Control was verified by changing certain values to prove that the result behaves as expected. When decreasing the rotational period, the temperature changes became close to no fluctuations as was expected. Therefore, when having a rotational speed of 3600 s at a time of 102 hours, the fluctuation is between 21.4 °C and -0.5 °C, when decreasing the rotation to 90 seconds this goes to 9.3 °C and 8.4 °C for PPQ-1.

When increasing the (temporary) power inputs of the science modes the temperature increases (temporary) as well, as expected. For example, when the science mode C of PPQ-2 is increased by a factor 10, the heat will go from a peak of 22.0 °C to a peak of 44.8 °C. When the heat capacity of the PQ is reduced, the temperature changes become bigger. This was expected. When the insulation layer is removed, the inside temperature of the PQ becomes close to equal to the outside of the temperature, this was also expected.

Communications

The computations performed by the link budget python program were verified with several methods. The program was written in such a way that every part of the link budget is written as a function. This method of coding gave a straightforward option to verify chunks of codes. For example, a function was made to compute the total propagation losses. This function used as inputs; the distance from the asteroid to the ground station and the frequency used, and had as output the total propagation losses in dB (FSPL + ionospheric loss + atmospheric losses) and the wavelength in meters. This could be easily verified by executing the program in console, recalling the function, trying different inputs and comparing them with the values obtained using analytical methods. Furthermore, the complete link budget is compared with the link budget excel sheet obtained from communication expert and Space Systems Engineer Dr. S. Speretta for the verification of the complete link budget calculations. Furthermore, most of the assumed values are obtained in accordance with Dr. S. Speretta with additional margins added as was advised.

Regarding the Monte Carlo simulation and the probability calculations, the verification is done by changing the value for the constraint, e.g. from 2.1 W to 1000 W, and getting a result of 100% probability of data transfer for all the possible trajectories with the varying time windows. Similarly lowering the value for the constraint of 2.1 lowers the probability of a successful data transfer for the given close approaches and time windows.

III
DESIGN EVALUATION

18
SENSITIVITY ANALYSIS

In order to establish the degree of feasibility a sensitivity analysis was performed. For this analysis the effect of changed mission and system parameters on the different sub-systems was evaluated. The main parameters that were investigated were the ones who are still unknown and for which assumptions were made, such as the asteroids rotation speed and axis and its surface properties. For each of these parameters the primary effects were found and then the N^2 chart, which can be found in Figure 5.5, was used to find the sub-systems that would be affected.

18.1. SUBSYSTEMS

The sensitivity analysis will be performed for each sub-system as well as for the cost budget.

MOTHERSHIP

Since the only part of the Mothership that is designed in this project is its trajectory, only that part will be analysed here. The trajectory is most sensitive to changes in the target asteroid, as that would require a whole redesign. This could happen if during some later design stage another asteroid is found which better satisfies the requirements. This would however not have a large impact, as the design of the Lander would be completely unaffected and the Mothership hasn't been designed yet.

Furthermore, the trajectory and in particular the number of burns will depend on the accuracy of the Mothership's thrusters, as less precise thrusters mean that correction manoeuvres will have to be performed. The effect of small errors in the burn length can be seen in Table 18.1, where for each burn some key parameters are given at the time of the next burn if the burn length is 0.1% shorter or longer and no correction burns are performed. As can be seen in the table, almost all burns are quite sensitive. Errors in the TOI and RVB1 would result in large changes in the phase angle, whereas errors in the RVB3 would result in the Mothership being too far from the asteroid for deployment to safely occur. This means that for all three of these burns a correction manoeuvre would have to be performed at some point which is less sensitive to errors.

Table 18.1: Sensitivity to burn precision.

		lower(-0.1%)	nominal	higher(+0.1%)
TOI	RVB1 distance [km]	1014872	1031414	1086630
	RVB1 phase angle [°]	34.86	15.814	44.88
	RVB1 ΔV [m/s]	0.549	0.513	0.474
RVB1	RVB2 distance [km]	10853	10012	10485
	RVB2 phase angle [°]	19.866	0.0249	20.576
	RVB2 ΔV [m/s]	0.078	0.106	0.078
RVB2	RVB3 distance [km]	10826	11075	11325
	RVB3 ΔV [m/s]	0.0056	0.0057	0.006
RVB3	RVB4 distance [km]	13.981	0.775[1]	14.662

Finally, the performance of the instruments used for finding the asteroid will have a large impact on the sequence of rendezvous manoeuvres. For example, on the 1st of October if the Mothership is 1M km away from the asteroid and has a phase angle of 0 ∘, then the asteroids apparent magnitude as seen from the Mothership will be 18.84 . If the instruments on the Mothership are not able to detect objects of that magnitude, then the trajectory will need to be adapted to establish a search pattern through the asteroid probability region.

DEPLOYER

For the deployment system the main parameters that can influence it are the mass of the bullets and their ejection speeds. These would affect the energy that would have to be delivered by the springs and consequently have an influence on the springs stiffness's. The effect of increasing mass would have a linear effect on the spring energy and therefore the stiffness, whereas the deployment speed would have a quadratic effect. Changes in the spring stiffness would also result in a linear change in the spring force which would affect the

[1] The nominal value is higher than the deployment distance due to round-off errors in the nominal ΔV.

pin-puller.
The stiffer spring will lead to an increase in mass and possibly a slight increase in volume, and the increased spring force might require a larger pin-puller with increased volume and mass. The effect of larger ejection velocity on required spring force and consequently pin-puller mass can be seen in Figure 18.1, where the red dot indicates the current design and the red and green lines indicate the maximum achievable ejection velocity and spring force respectively using pin-pullers.

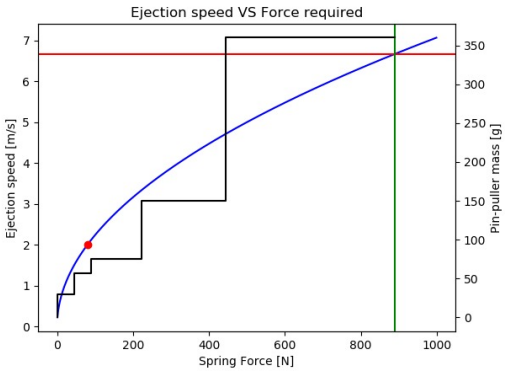

Figure 18.1: Sizing of the spring and pin-puller as a function of ejection velocity.

Net

The successful deployment of the net and its subsequent entangling around the asteroid depends on many factors. The most important ones are the bullet mass to net mass ratio, the deployment angle, the ejection speed, and the asteroid's size. For the net to properly deploy and expand to its full size, it needs to have a high bullet mass to net mass ratio. In this ratio the PQ mass is included in the net mass. This means that an increase in PQ mass would necessitate an increase of the bullet mass for the net to deploy properly at the same angle. Increasing the deployment angle would also help with deploying the net with lower mass ratios, however, this would lead to a lower volume in the Deployer being available for the net and PQs. The influence of the mentioned design parameters on net performance under nominal conditions were discussed extensively in subsection 8.4.1. Entangling around the asteroid for a secure attachment and a proper distribution of the PQs around its surface requires a fully deployed net with a sufficient size with respect to the asteroids diameter and a sufficient forward velocity of the bullets at the moment of impact. The size of the asteroid has a relatively large uncertainty and could therefore have a large impact on the performance of the net, as a larger asteroid would mean that the PQs would be distributed over the entire surface and that the net would be less securely attached. Furthermore, if the asteroid has a high rotation speed then a high bullet velocity might be required to make the net entangle. On the other hand the cables should be able to sustain very large increases in deployment and impact speed without breaking as they are currently designed with a very large safety factor. The performance of the net under non-nominal conditions was analysed for two cases for the net design recommended in section 28.2. At first, it was assumed one of the bullets is ejected at a slower velocity than nominal due to some failure in the deployment system. It was found that for a nominal ejection velocity of 4 m/s, the system can tolerate one bullet ejected at 2 m/s and still open the net and entangle the asteroid. The deployment and the net hitting the asteroid is depicted in 18.2a and 18.2b. The second non-nominal case was a misalignment of the deployment axis with the line Mothership - Asteroid, which could occur due to a partial failure or lacking precision of the ADCS on the Mothership. It was found that the system can tolerate a misalignment of 4.6 degrees along the diagonal of the net (presented in 18.2c) and 3.15 degrees along the sides of the net and still entangle successfully. To conclude, the net is relatively robust to the two most likely non-nominal conditions that might occur during deployment.

PQ Structure

The current design of the internal and external structure of the PQs is very dependent on the surface composition of the asteroid. Especially the hardness of the surface will have a very large impact on the magnitude of the impact shocks experienced during landing. Furthermore, the effects of radiation on the structure have not been studied in great detail and therefore all the thicknesses include a safety factor of two. Finally, the structure is also linearly sensitive to changes in PQ mass and landing speed, as those could both lead to higher impact forces.

Concerning changes in the landing speed, a change in 1 m/s would not change the required thickness of the structure (both FR-4 and Sorbothane) for the worst case of landing on one of the cube's corners, as the minimum thickness of 1.32 mm required to sustain FR-4's lowest strength of 131 MPa remains below the designed 2 mm structure, as the PQ's velocity is increased from 2 m/s to 3 m/s. However, when considering the

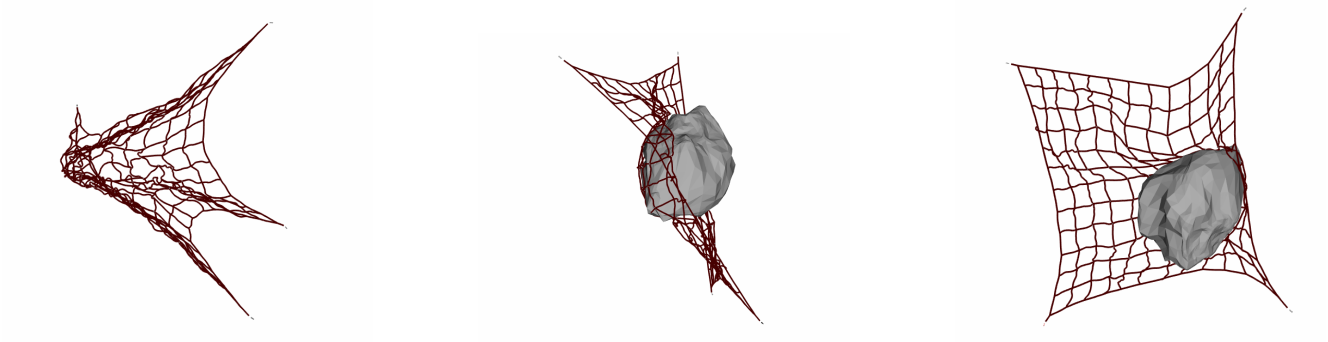

(a) (b) (c)

Figure 18.2: Sensitivity of recommended net to non-nominal conditions. v_{eject} = 4 m/s, m_{bullet} = 4 kg, θ = 20°, m_{PQ} = 0.15 kg, $V_{initial}$ = 2 m/s applied 2 s after bullet ejection, $d_{asteroid}$ = 35.2 m, $P_{asteroid}$ = 90 s. (a) 8.08s after bullet ejection, one bullet (top left) 2 m/s slower; (b) 14.71s after bullet ejection, one bullet (top left) 2 m/s slower; (c) 14.43s after bullet ejection, asteroid misalignment along the net diagonal of 4.6°.

second worst case scenario of having a spike from the asteroid's surface pierce through the structure, for the same change in velocity, the kinetic energy increases from 0.4 J to 0.9 J, which results in a needed thickness of 3 mm concerning the FR-4 walls, as a 2 mm thickness would only sustain an impact of 0.74 J.

In terms of changes in the PQ's mass, it was proven that an increase up to a mass of 365 g has no effect on the structure's design, for both worst case scenarios. Above that, FR-4's Izod impact becomes the restricting factor again, and the walls' thickness would have to be raised from 2 mm to 3 mm.

Considering the maximum landing load that could be sustained by the structure as it is designed right now, the result is 410 N. To conclude, the structure is thus quite sensitive to changes in the PQs' mass, landing velocity, but also the absorption time of the shock, which means that care has to be taken during an eventual re-design.

Scientific Payload

The main uncertainties that still remains for the scientific payload is the duration of the measurements and the precision at which they have to be taken. Both can have a large effect on the data volume, with in particular changes in measurements taken by the image sensor having the largest effect as that instrument currently contributes the vast majority of the data volume, as can be seen in Table 18.2 which lists the effect of doubling the measurement periods on the data volume. A higher data volume leads to a higher data-rate which would require a higher power communication system and more energy to be delivered by the EPS. Furthermore, the image sensors are also the heaviest instruments, 6.8 g, and they consume the most power, 620 mW. This means that adding more image sensors would have a very large effect on the rest of of the system. Finally the amount temperature sensors that can be taken depends heavily on the depth of the mechanism, so making it more flat would allow more of them to be used therefore improving their performance.

Table 18.2: Increase in data volume when measurement period is doubled. Ordered from lowest to highest change.

Name measurement	Increase data volume
Gyroscopes	0.12%
Temperature sensor	0.16%
Magnetometer	0.31%
Solar panels	0.32%
Radio experiment	0.76%
Mass spectrometer	0.94%
Landing images 1	1.03%
Landing images 2	2.15%
Landing images 3	24.09%
Accelerometers	26.18%
Surface images	43.36%

C&DH

The current design of the C&DH sub-system is relatively insensitive to changes in most system parameters. Its use of radiation hardened components means that it could safely sustain much higher levels of radiation than it is currently expected to receive. Furthermore, the current memory capacity is at least an order of magnitude larger than what is required to store all of the scientific data. Finally, since it uses so little power, it would be quite insensitive to changes in the available power. The only change that could have a significant effect would be a higher data-rate as that could require changes in the data-bus.

Thermal Control

One of main assumptions that was made for the design of the thermal control sub-system was that the rotation axis of the asteroid would be perpendicular to incoming sunlight and that therefore every PQ would spend an equal amount of time in the sunlight as in darkness. If the rotation axis were to be tilted, then this would lead to some drastic changes in the internal temperatures, with the worst case being that the PQ would be either in the dark or in the sun-light for the entire mission. This would lead to some PQs either not being able to perform all of their measurements. Other uncertain parameters that would influence the temperature are the albedo and emissivity of the asteroid, which could make all of the PQs hotter or colder. Furthermore, the exact thermal capacity of the PQs hasn't been calculated properly, so that could have an influence on the PQs ability to survive large rotation periods. The CPQs are currently much more sensitive to design changes or changes in the asteroid parameters than the PPQs. This as the CPQs can't survive any increases in communication sub-systems output, or changes in asteroid surface characteristics, or changes in PQ surface properties, because both the minimum and maximum temperatures are at their limit .The PPQs on the other hand can survive large changes in asteroid's albedo(0.05-0.55), thermal capacity (two times smaller) power consumption(3 times larger), and illumination time fraction(35-65%).

EPS

The EPS is sensitive to the orientation of the asteroids rotation axis in a similar way as the thermal control, as the total amount of sunlight wouldn't be distributed equally across all the PQs. This EPS is however better able to cope with this as it could use the power cables connecting every PPQ to the nearest CPQ to equally redistribute the generated energy. Furthermore, the EPS heavily relies on the batteries in the bullets for providing the energy required by communication sub-system. On the other hand, it isn't very sensitive to changes in the rotation period of the asteroid, as it will be able to redistribute power using power cables.

Communications

The communication subsystem has to close the link for a certain distance and be able to transfer all the data given the time window. As explained before, the Monte Carlo simulation is used for the possible distances and communication time windows. Hence, for a sensitivity analysis, some parameters were changed and the probability of closing a link for the possible trajectories was recalculated and checked if it meets the one sided 2σ requirement whilst respecting the constraints. If not, the changes required to meet the reliability requirements were assessed and the impact on the design was given with low, medium, high. In Table 18.3 the changed parameters and the impact on the final design are shown. Overall, by increasing some of these parameters an increase in the required energy is to be expected. However, choosing a ground station which has no similar performance as the DSN ground station, will result in altering the communication subsystem as a whole. For example, to be able to communicate the data to the GMRT, an UHF-band frequency has to be chosen. This will result in a completely different antenna design.

Table 18.3: Sensitivity analysis for different parameters

Amplifier efficiency reduction	optimal	0.1	0.2
efficiency	0.7	0.6	0.5
Reliability %	97.5	95.4	92.2
impact	-	low	high
Energy required for 2σ [Wh]	125	155	205 Wh

Compressed data volume increased in %	optimal	25%	50%
Data volume [Gbits]	5.449	6.811	7.449
Reliability %	97.5	94.8	92.1
impact	-	medium	high
Energy required for 2σ [Wh]		160	200

Frequency increased by:	optimal	50 MHz	100 MHz
Frequency	2200	2250	2300
Reliability %	97.5	97.1	96.5
impact	-	low	low
Energy required for 2σ [Wh]		133	140

G/T similar to GMRT, operating at S-band	40.9 dB	32.5 dB	25 dB
Ground station	DSN 34m BWG	GMRT	other
Reliability %	97.5	55.0	0
impact		high	high
Energy required for 2σ [Wh]		N/A	N/A

Cost

The main contributor to the cost of this project will be the testing costs. However, in this stage of the design the amount of testing costs is still relatively unknown, which is increased by the fact that in case a component or sub-systems fails testing, it might have to be redesigned and re-tested. These two factors might still lead to

increases in the total cost of ANTREA.

18.2. Conclusion

To conclude, most sub-systems are relatively insensitive to changes in system parameters, but some like the thermal control for the CPQs are very sensitive to even small changes. Furthermore, the cost of testing has not been analysed in sufficient detail to analyse its sensitivity. Therefore, from a technical point of view, the only design change that could have a drastic impact under nominal conditions would be an increase in the data-volume that needs to be sent, which would increase communication power, and therefore make the CPQs exceed their temperature limits.

19

Performance Analysis

This chapter aims to analyse the technical capabilities of the lander. Aspects taken into account are the performance of net deployment, scientific payload, communications, electric power system and thermal control, data handling and the PQ platform. The chapter concludes with an overall performance assessment.

Deployment performance and Deployer assessment

The net deployment sequence is fixed by the design and cannot be altered in flight. This results in a fixed deployment distance from the asteroid that is required for successful deployment. The design therefore requires absolute accuracy and reliability by the Mothership GNC and propulsion subsystem. The bullets are ejected by springs that store 4.13 Joules of energy, which results in a bullet ejection velocity of 2.03 m/s under an angle of 10 degrees to asteroid nadir. The simulations showed these numbers are insufficient for successful net deployment, a new design is proposed in chapter 28. The lander takes up a volume of 16.6 d/m^3 in the Deployer, while the net itself requires 5 d/m^3. This corresponds to a net packing factor of 0.143. The Deployer was designed to sustain launch loads up to 10.5 g and the lowest natural frequencies are of 2315.27 Hz in the longitudinal and 1642.61 Hz in the lateral direction, which are more than 20 higher than the base excitation frequency.

Scientific Payload Performance

The performance of the scientific payload is dependent on multiple factors, namely the environmental conditions in space and more specifically the ones present on the asteroid's surface, the survival of the PQs to the launch, mission, deployment, and landing loads, the successful deployment of structural mechanisms, as well as the successful switching in the correct operational mode. With the payload design that was elaborated, if all previously mentioned factors are optimal, then the ANTREA system will be able to measure the shape and size, surface composition and roughness, material properties, temperature distribution, hardness, and dynamic motion of the asteroid. On a subsystem level, the performance of the payload part of the mission shall thus not be a problem. However, on a system level, there is a chance that the scientific measurements can not even be done if for example the deployment of the net fails, or the correct wrapping of the net on the asteroid's surface, which is supposed to ensure overall distribution of the PQs around the asteroid.

When the net wraps around the asteroid properly the PPQs will be distributed. The mesh distance between the PPQ-1s is 1.77 m and 2.80 m differing per PPQ-1. The mesh distance between the PPQ-2s is 1.25 m and 2.50 m differing per PPQ-2. In this distribution the shape is directly derived from pictures taken during landing with a resolution of 256 × 256 pixels. The size can be derived from this as well. The temperature of the asteroid is directly measured with a temperature gradient of -11.79 mV/°C. The surface roughness is directly derived from pictures with a resolution of 1280 × 1024 pixels from which the surface composition can be derived. The elements and molecules in the surface are derived with a mass spectrometer. The internal material composition is determined with a radio experiment conducted at 8.5 GHz, and possibly other frequencies, which gives a resolution of approximately 3.5 cm. The decay in amplitude and phase shift is directly measured from which the material properties permeability and permittivity are derived. The accelerometers in the IMU have an acceleration range of ±2 g to ±16 g. The gyroscopes have switchable ranges from ±125 °/s to ±2000°/s. Finally the magnetometers have a magnetic field range of 1300 μT (x-, y-axis); ± μT (z-axis). In terms of data volume, a total of 54.490 Gb of scientific data can be generated by the instruments which would have to be sent to Earth. This is in the capabilities of the communication subsystem, by applying a compression rate of 10, without

losses.

Communications Performance

The downlink communications are performed on a frequency of 2200 MHz on a bandwidth of 125 kHz. A total data volume of 5.449 Gbits can be transmitted in a time of 17.85 hours, resulting in a data rate of 88.94 kb/s. Link budget calculations in combination with Monte Carlo trajectory simulations showed the probability of successfully downlinking this amount of data is 97.5% within a maximum energy usage of 125 Wh. The nominal communications distance is 1.458 million km, but the 97.5 % probability includes closer asteroid approaches. 3 CPQs can be active at the same time consuming 7 W each. In this case, the total communication time decreases while the data rate increases. Most importantly however, the overall energy used remains unchanged. This flexibility renders the communications subsystem redundant to single point failures as 10 CPQs are present. The used GMSK (Gaussian Minimum Shift Keying) requires a E_b/N_0 of 1.93 dB which enhances performance.

Electric Power System Performance

The EPS is capable of compensating for single points of failure as the system is connected to all PQs in the net. This means if one PQ would malfunction, the other PQs would be able to function. This would reduce the total amount of power generated, consequently it would also reduce the amount of data and hence reduce the power required for the communications. The EPS generates 0.12 W per PPQ on average, which results in a total of 7.05 W on 59 PPQs. The energy storage capacity is split up between batteries in the PQs providing 2.442 Wh (if discharged to 100% DoD) each, totalling 168.5 Wh. The four bullets on the net offer an additional 112 Wh, culminating in the total energy storage capacity of 281 Wh. Less than 100 cycles are expected and thus a high Depth-of-discharge of 90% is applied. The on-board voltage within the PQs is 3.7 V, while for power transfer from PQ to PQ DC-DC converters are used to increase the voltage to 12.6 V, thereby limiting the Ohmic losses in the cables.

Autonomous Operations and Data Handling Capabilities

Upon landing on the target asteroid, ANTREA is capable of autonomously performing scientific measurements for a duration of one month. The software design ensures safe operations, by detecting faults and being able to perform recovery on its own. The highly redundant network of Command & Data Handling units can also autonomously switching in between operational modes, which allows it to downlink the gathered data without receiving ground commands. The data handling network can store up to 552 Gbit of data in total, with every unit capable of storing the entirety of the generated data if its compressed. Internal data bus allows for commanding and handling data from multiple scientific payloads simultaneously. The processing is done by an 32 bit, ultra low power (0.005 mW) MCU with a clock frequency of 16 MHz.

Assessment of PQs as a Lander

Assessing the performance of the design as an asteroid lander is essential to reflect on the technical choices made by the team. Choosing a net was, from the team's point of view and from the conclusions made from multiple trade-offs, the best way to successfully attach the system to an asteroid and spread the PQs on its surface in a distributed way. The performance of the Lander in those terms was thus concluded to be high. On the other hand, when considering the net and its system pf PQs in terms of its landing capabilities, it must be noted that there is a chance for some of the PQs not to survive the landing loads, if the worst case scenarios are considered (them landing on one of their edges or corners that are not protected by the damping material, or them landing on a spike of the asteroid's surface which could pierce through the structure).

In terms of thermal control, and the system's general capabilities to surviving the harsh asteroid environment for the whole duration of the mission, it was found that the designed Kapton internal layer, the four heaters placed next to the image sensors, and the external paint colour would be enough to keep the PQ's internal elements within their operational temperature ranges. It should be noted however, that the subsystem is quite sensitive to changes in other subsystems, especially for their performance on the CPQs, as the calculations showed performance that lies on both their cold and hot extremes.

20
Risk Analysis

Risk management involves identifying risk for all of the mission elements and subsystems. Identifying risk consists of the probability that the hazardous event occurs and the severity of the effect of the hazard on the mission. A risk map has then been created in section 20.4 to give a better overview of all the risks with the probability and severity of the hazardous events. Thereafter, a risk mitigation plan is proposed to decrease the probability of the hazardous event to occur, or its severity, or both. Finally, an iterated risk map is shown to clearly identify the improvements as a result of the mitigation plan.

The probability of the risk is qualified as very low, low, medium, high and very high. These probability levels refer to the risk map respectively as proven flight design, extrapolated from existing flight design, based on existing non-flight, working laboratory model, feasible in theory.

20.1. General Risks (G)

This section focuses on the general risks which apply to all components of the mission and the spacecraft. The general risk focuses mainly on the manufacturing tolerance, launch loads and vibrations.

G1 The PCB boards will break. The probability is very low, as these are well tested for use in space and landing missions. The severity is marginal, due to redundancy. Depending on the component this can potentially result in losing the PQ.
G2 The PQ will flip over. The probability is low, as the net will hold the PQs in the desired attitude. The severity is marginal, due to redundancy. If the flipped PQ is a PPQ, some of the instruments will not be able to perform their measurements and, as a result, reduce the mission performance of that specific PPQ.
G3 The PQ structure will fail during launch due to launch loads and vibrations. The probability is very low as the materials used for the PQ structure are frequently used for all kinds of space missions, thus well tested. The severity is marginal, if couple PQs structure get damaged or destroyed completely since this is already taken in to account by having 69 PQs. However, it is important to check for that the broken parts will not damage the whole system from inside.
G4 The PQs structure will get destroyed by the impact force of the landing, due to the ejection velocity of the bullets and the fast rotation of the asteroid. The probability is high, as these are based on working laboratory models. The severity is marginal, due to redundancy.
G5 The PQs manufacturing tolerances are not met, which results in less volume inside and components not fitting. The probability is very low. The severity is negligible, as this problem is detected during assembly and fixed easily, due to the fact that manufacturers provide guarantee.
G6 The microstrip antenna will get damaged. The probability is low, as this has been tested before in space missions. The severity is marginal, due to redundancy.
G7 Instruments attached to the outer surface of the PQs will be inoperable, caused by collision with other PQs inside the deployer during launch and deployment phase. Probability is high, as this has not been done or tested before and thus based on laboratory model. The severity is critical, as this will result in significant reduction in the performance of the scientific payload and less operable CPQs due to damaged antennas.

20.2. Risk Analysis of the Mission Phases

First the risk of the different mission phases are identified. The mission phases consist of the rendezvous, deployment, approach of the lander and attachment (landing). The risk of launch and transfer are not considered since they are beyond the scope of this design. After that, the risk of the subsystems not performing properly are identified.

Rendezvous (R)

In this section the risks for the rendezvous are identified and the probability and severity are determined. The focus lies on the risks concerning the the Mothership detecting the asteroid and performing manoeuvres.

R1 The Mothership fails to detect the asteroid. The probability is low, as other missions to asteroids have been successfully completed. The severity would be catastrophic and result in a complete mission failure.
R2 Failure of one of the Motherships thrusters. This has a very low probability, as it is very well tested with flight proven component. The event would have critical consequences, perhaps the mission could still continue with remaining thrusters but technical performance would be reduced (less accuracy in manoeuvres).
R3 A non-nominal burn would affect the approach of the Mothership and result in a undesired rendezvous. The probability is assessed as low: the design would be extrapolated from existing flight designs. The severity would be marginal due to the fact that this can be corrected for.
R4 The final rendezvous distance is misjudged, the manoeuvre and landing will not be performed successfully. The probability is low, as extensive simulations and calculations can be performed to ensure a desired approach path of the S/C. The severity is critical, as this event results in a questionable mission success.
R5 Missing the burn time window will result in a sub-optimal trajectory of the Mothership, and result in unsuccessful landing. The probability is very low due to the maturity of the technology used and the components reliability are proven in flight. The severity is marginal, since the approach can still be corrected for.
R6 A failure of ADCS will result in an unknown orientation of the Mothership relative to the asteroid and the control will therefore be impossible. The probability is very low due to the maturity of the technology used and the applied redundancy. The severity will be catastrophic, since this will result in a total mission failure.

DEPLOYMENT (D)

In this section the identified risks of the net deployment are listed with the corresponding probability and severity of the risk event. The deployment risk is divided in the following parts; deployment (**D**), net (**DN**), springs deploying bullets (**DS**) and the deployment door (**DD**).

D1 Missing the asteroid. The probability of this event is low, since it is extrapolated from existing flight design. The severity will be catastrophic if the deployer shoots the net and it completely misses the asteroid.

DN1 The net with the PQs gets entangled in the deployer during launch, transfer and rendezvous. The probability is low as a similar manoeuvre was performed successfully by the RemoveDEBRIS mission. This event can be prevented with a good design. The severity is critical as an entangled net will not fully deploy, this would result in not wrapping around the asteroid and reduce the probability of successful attachment.

DS1 The springs fail to uniformly launch the bullets connected to the net will result in a undesired approach angle towards the asteroid. The probability is very low due to the maturity of spring systems technology. The severity will be critical as there is still the probability of attachment if at least 2 bullets manage to wrap around the asteroid.
DS2 One of the springs fails to launch the bullets. The probability is very low due to the fact that, although these springs are custom made, they can be tested extensively without the need of extraordinary equipments. The severity is catastrophic, since this event will result in the net not deploying successfully, and potentially damaging the Mothership as well.
DS3 All of the springs fail to launch the bullets results in no deployment. The probability is very low due to the maturity of the technology. The severity is catastrophic, since if there is no deployment the mission will result in a complete failure.
DS4 The springs will deploy the bullets while the deployment door is still closed. The probability is very low due to extensive testing with a smart locking mechanism which will prevent this event from occurring at all. The severity will be catastrophic, as this will result in a total mission failure due to the failed deployment and damage done to the net, PQs and the Mothership.

DD1 The door of the deployer does not open. The probability is very low due to the maturity of the spring system opening the door. The severity is catastrophic, due to the fact the deployment will not happen and the mission will result in total failure.
DD2 The door open partially due to degraded springs. Since the door's weight is very small relative to the weight

of the bullets, this will result in a failed uniform launch of the bullets. Furthermore, it would add rotation to the bullets which were blocked by the door and change the path angle of the bullets slightly. The probability is very low due to maturity of the spring technology and the degradation of the springs can be taken in to account during the design. The severity will be critical to catastrophic, since the additional rotation of the bullets might entangle the net during approach.

Approach (A)

After deployment the net needs to be fully stretched before hitting the asteroid. The risks concerning this part of the mission are identified and listed below.

A1 The net retracts due to the elasticity of the net and the masses of the PQs. The probability is medium, as this was clearly shown in simulation test of the nets approach to the asteroid. The severity is critical as this will reduce the probability of successful attachment.
A2 The net gets entangled due to the oscillation in the system (bullets, net and PQs) induced by the constantly occurring linear momentum exchange between the bullets and the net. The probability is medium due to the possibility of extensive simulation and testing. The severity is catastrophic as the net would not be able to wrap around the asteroid.
A3 The net does not deploy to its full span before hitting the asteroid. This can cause problems for the landing and permanent asteroid entanglement. The probability is medium since the net is extrapolated from existing design and the severity catastrophic as the mission success may be compromised.
A4 The net fully deploys but the asteroid is too far away. This would result in the bullets retracting and closing the net before it gets a chance to wrap the asteroid. The probability is medium due to extensive ground testing possibilities and extrapolation from existing designs. The impact would be catastrophic as the PQs cannot land on the asteroid.

Landing and Attachment (L)

In this section the identified risks concerning the landing phase and wrapping of the rotating asteroid are listed.

L1 The reeling mechanism will not function. The probability is low, as it is extrapolated from existing design. The severity is marginal, since this mechanism is there to increase the probability of a successful entanglement after the wrapping to ensure the net will not detach.
L2 The bullet threads will not entangle after wrapping. The probability depends on the size of the asteroid. If the asteroid's largest diameter is smaller than 8 meters the probability of not entangling is very low, as was shown in the simulations. However, if the diameter is larger than 8 meters, the probability will be very high. The severity is critical, since the hooks on the bullets might still be able to attach on the asteroid.
L3 The asteroid is rotating faster than expected. Depending on the orientation of the deployment axis with respect to the rotation axis, that could lead to the bullets unwrapping itself. The probability is high considering the uncertainties of the selected asteroid. The consequences will be catastrophic as a failed attachment result in mission failure.

20.3. Risk Analysis of the Subsystems

In this section the risk unique to the subsystems are identified. The probability and severity of the risks are analysed.

Payload (PL)

The risks concerning payload mainly focuses on not being able to perform measurement or generating useless data due to some component failing.

PL1 The Payload will get damaged by cause of the launch vibrations, landing forces and the harsh environment of space. The probability is high, due to the fact that the chosen Payload consist of commercially of the shelf components, which are not space ready neither designed to survive these loads. The severity is marginal, as there many PQs dedicated to Payload (PPQ) and there are several of these sensors on one PPQ.

PL2 The wire which keeps the antenna for the radio experiment and the temperature sensor mechanism retracted, will not be cut. The probability is medium, as this method is a downsized version of the mechanism that cuts parachute. However, this is not tested in a smaller size. The severity will be marginal, as there are three temperature sensors mechanisms on the same PPQ.
PL3 The signal transmitted for radio experiment is distorted by factors other than the asteroid. The probability is medium, as this has not been done before in similar way on asteroid and can only be tested on earth. The risk is critical, as there are no other instruments which can determine the internal structure and composition of the asteroid.
PL4 The deployed temperature sensor is not able to touch the ground. The probability is high due to the uncertainty of the irregularities of the asteroid's surface. The severity is critical, as there are three temperature sensors on the same side of the PPQ, which means if one fails to touch the surface due to a cavity the other will have the same issue. This results in a sub-optimal distribution of temperature measurements over the asteroid.
PL5 The heater element of the image sensor fails. The probability is low, due to the maturity of the technology and it is well tested in many space missions. The severity is critical, since if the heater element fails the sensor will not function.
PL6 No dust particles will insert in the gap or land on the mass spectrometer. The probability is high due to uncertainties of dust particles being present on the asteroid at all. The severity is marginal, as there are more instruments to determine the material properties of the asteroid, albeit with less quality.

Communications (COM)

The risk concerning the communications subsystem is mainly focused receiving and transmitting of data.

COM1 The signal transmitted from Earth is to weak to be detected. The probability is very low, since this can be simulated and tested well. Additionally, applying the proper margins during design phase will lower the probability of this event. The severity is catastrophic, as the CPQs which do not receive a signal are switched off by the C&DH.
COM2 The signal is transmitted in the wrong direction. The probability is low, as the technique explained in section 12.3 is simple, compared to phase-locking and phased array antennas, which are well tested and performed in space. However, there is no existing mission that tried communicating directly with Earth without ADCS from the surface of a rotating asteroid. The severity is catastrophic, as the signal will not be received at the ground station and thus the mission will result in complete failure.
COM3 The signals transmitted from the CPQs have a Signal-to-Noise ratio too small to be detected. The probability is very low, due to the maturity of the technology and the safety margins used. The severity is catastrophic, if the scientific data cannot be received at the ground station, this will result in complete mission failure.
COM4 The communication subsystem does not recognise the commands sent from the ground station. The probability is very low as this has been done by most of the space missions. The severity is catastrophic, if for the worst case, the command is to start the comms mode at an earlier date than what was planned for, due to asteroid trajectory uncertainties before launch.
COM5 The asteroid's trajectory deviates more than what has been accounted for and results in a different close approach and communication time window. As a consequence the communication with Earth is not possible anymore. Probability low, as the S/C is designed for the worst case prediction of the 2017 FU102 asteroid's trajectory. The severity is catastrophic, as this will result in complete mission failure.

EPS (E)

The risks involving the Electrical Power Subsystem (EPS) and their probability and severity.

E1 Batteries will become damaged and their characteristics will be worse due to impact or being punctured. The probability is very low, as batteries are used for all space missions and due to maturity of the technology. The severity is critical, as this will result in damaging the PQ it resides in and result in loss of the scientific payload.
E2 Short circuit in the PQs due to the vibrations during launch or due to the impact forces of the landing,

some power cables might detach and get in contact with other electronic components. The probability is, very low as this can easily be prevented by designing properly and taking these forces and vibration into account. Depending on the component, the severity is assessed to be critical, as this will result in damaging the affected component and results in putting the PQ out of service.
E3 Maximum power point trackers (MPPT) malfunction. The probability is very low considering the maturity of the technology. The severity is marginal, due to redundancy as there are 6 of these MPPTs per solar cell.
E4 Overcharging the batteries will make them burn aggressively, results in damaging the PQ it resides in. The probability is very low considering the maturity of the technology and the use of MPPT combined with voltage regulators. The severity is critical, as this will result in losing the PQ and the scientific payload.

Command & Data Handling (CD)

Risks involving Command & Data Handling (C&DH) are listed below. The probability and severity are described.

CD1 Errors in the software due to bad programming (e.g. bugs). Probability is low, as bugs and errors are common and well known with software programming, and debugging is a standard procedure. Furthermore, software simulation can be performed to check if the system is performing as it should be. Severity ranges from marginal to critical depending on the type of error.
CD2 There could be not enough data storage, as a result of damaged data storage and/or the payload generating too much data. The probability is very low, as the total available data storage is a factor of 10 larger than the uncompressed data volume that is to be transmitted to the ground station. The severity will be critical, as this will greatly reduce the performance of the mission.
CD3 The PQ could unexpectedly switch to safety mode, by cause of unknown reasons. The probability is very low considering the maturity of the technology. Furthermore, if this this event did not occur during simulation test the probability is very low it will happen during the mission. The severity is marginal, as this can potentially interrupt the scientific Payload duty cycle. However, it can still recover from safety mode and the Payload instruments will have to redo the last measurement. But the severity will be critical if this event would occurs during the communication phase with Earth. As a consequence, only part of the data will be received.
CD4 The PQ could unexpectedly switch to end of life mode, by cause of unknown reasons. Probability is very low, as this mode requires a command from ground station. The severity will be catastrophic, as the system is not designed to get out of the end of life mode autonomously.

20.4. Risk Map

After analysing all risk events, a risk map was made to give a clear overview of all the risk events, shown in Table 20.1. From the risk map it can be seen which risk events have the priority for risk mitigation. For all the risk events located in the red and orange boxes, a risk mitigation plan was made in section 20.5. The results are shown in the reiterated risk map in Table 20.2. The risk events changed location on the risk map are shown in bold.

Table 20.1: Risk map

Probability					
	Feasible in theory			L2	
	Working laboratory model		G4, PL1, PL6	PL4, G7	L3
	Based on existing non-flight		PL2	PL3, A1	A2, A3, A4
	Extrapolated from existing flight design		G2, G6, R3, L1	R4, DN1, PL5	R1, D1, COM1, COM2, COM5
	Proven flight design	G5	G1, G3, R5, E3	R2, DS1, E1, E2, E4, CD1, CD2, CD3	R6, DS2, DS3, DS4, DD1, DD2, COM3, COM4, CD4
		Negligible	Marginal	Critical	Catastrophic
		Severity			

Table 20.2: Posterior mitigation risk map

Probability	Negligible	Marginal	Critical	Catastrophic
Feasible in theory / Working laboratory model				
Based on existing non-flight / Extrapolated from existing flight design		PL2, **L2**, **PL6**		**L3**
		G2, G6, R3, L1, **G4**, **PL3**	R4, DN1, PL5, **G7**, **A1**, **A3**, **COM1**	
Proven flight design	G5	G1, G3, R5, E3, **PL1**, **PL4**	R2, DS1, E1, E2, E4, CD1, CD2, CD3, **A4**, **COM2**	**R1**, R6, DS2, DS3, DS4, **D1**, CD4, **A2**, DD1, DD2, COM3, COM4, **COM5**
	Severity			

20.5. Risk Mitigation Plan

In this section the risk mitigation plan is described. The strategy is to decrease the missions total risk by looking at all the risks in the orange and red boxes, and considering a mitigation plan to decrease the probability of the hazardous event happening or reducing the severity of the risk or preferably both.

General risks

G4 The PQs structure can be designed for the fastest asteroid rotation possible and perform extensive load testing. This will result in reducing the probability to low.

G7 An extensive analysis and research into packing of the net, with integrated PQ, has to be performed in order to ensure that the instruments attached to the outer surfaces of the PQs will not become inoperable as a result of the launch, deployment and landing loads and vibrations. It is likely that more spacing between the PQs and potential also between the PQ and net can be achieved. There is also volume available for this extra spacing. This will decrease the probability from high to low.

Rendezvous

R1 Analysis on the expected asteroid footprint in the visual and other electromagnetic spectra can be performed to model the detection phase and draw conclusions in order to improve the design. To further improve searching methods, better telescopes or other exploratory instruments can be included in the Mothership. This will decrease the probability to very low.

Deployment

D1 By thoroughly planning and testing this manoeuvre, creating accurate simulations, the probability of this risk can be decreased to very low.

Approach

A1 The probability of this event can be reduced by testing and comparing different net materials to minimise this effect. Additionally, further analysis can be performed on redistributing the PQs on the net, changing the mass of the bullets or trying different ejection velocity of the bullets. This reduces the probability to low.

A2 To prevent this event from happening, beside extensive testing, is considering the shape of the PQs and equipping the PQs with e.g. a protective film to ensure other parts of the net will not get stuck on the PQs. The combination of selecting different shapes with a layer and extensive testing, will reduce the probability to very low.

A3 By simulating the approach with range of ejection velocities and distances the probability of this event can be reduced to low. Furthermore, by choosing a more preferable capture angle which as lower facing area, the severity of this event will drop to critical. This means despite the net is not fully deployed, it is still able to wrap around it.

A4 To prevent this event from happening, the Mothership can perform extra checks before deploying to ensure the Mothership is at the desired distance for deployment. Additionally, similar mitigation plan as **A1** can be applied to reduce the severity of this event to critical and further reduce the probability to very low.

Landing

L2 To compensate for the asteroid being larger than 8 meters, the net can be made bigger at the expense of available volume for the PQs. Another way of decreasing the probability of this event is by selecting a smaller asteroid. Further investigation on the selected asteroid might increase the certainty of the asteroid's size. Additionally equipping the net it self with methods to hold on to asteroid will decrease the severity. By reducing the uncertainties, the probability can be reduced to medium and severity to marginal, as there are more options to attach the PQs on the asteroid's surface.
L3 By making sure the Mothership selects the desired landing attitude with respect to the rotation of the asteroid the probability of successful landing and attachment will increase. Performing thoroughly simulation test for the worst case of the asteroid's rotation, will result in a better design of the net. This results in decreasing the probability of this event to medium.

Subsystems

PL1 By making the scientific payload space ready or selecting scientific instruments which are designed for deep space and tested in similar missions, will reduce the probability to very low.
PL3 Testing intensively with assembled PQs integrated on the net, these distortions can be accounted for and trying different possible configuration of the antenna or transceiver the distortions can be minimised, as a result lowering the risk probability to low. Additionally, by analysing these distortions before hand and taking them into account when analysing the data, reduces the consequence to marginal.
PL4 The probability of this event can be lowered by distributing the sensors on multiple sides of the PPQs, however this will result in reduced performance since the same measurement cannot be taken at the same location over time. This is assuming the temperature sensor can accurately measure one time after deployment. Another option is designing the temperature sensor to survive for a longer period of time after deployment, this will eliminate the performance reduction. As a result of redistributing, the probability will be very low and the consequence of one sensor not being able to touch the surface will be negligible.
PL6 Attaching some sharp devices near the opening of the mass spectrometer might scrap some material from the surface of the asteroid into the opening. This method is independent on whether the asteroid has dust particles or not. This reduces the probability to medium.

COM1 To reduce the consequences, the C&DH can be designed as such that it will not turn off the CPQs, instead it will command all the CPQs to start transmitting the data in all directions. Furthermore, as a last resort, the Mothership's trajectory can be designed to minimise the drift and stay in a relative near vicinity to redirect the transmitted signal from the CPQs towards Earth. However, this method will reduce the mission performance since not all of data will be transmitted to earth. As a result the consequence is assessed to be critical.
COM2 The severity can be reduced in a similar manner as described in **COM1**. Moreover, further testing of the method will increase the reliability. Hence, the severity is critical and the probability of this event can be reduced to very low.
COM5 The prediction models of the trajectory of the asteroid is assumed be more accurate before the launch date and the S/C can still be adapted to prevent this event. Therefore, reducing the probability to very low.

21
Reliability, Availability, Maintainability, and Safety

In this chapter, the Reliability, Availability, Maintainability and Safety (RAMS) characteristics will be reflected in terms of the ANTREA design. Reliability is the ability to perform a function under certain conditions for a certain period of time. The user requirement states that the PPQs shall be able to withstand all launch, mission, deployment and asteroid landing loads with a reliability rate of 80% or higher. Availability is the ability of the system to operate effectively during the required period of time. It therefore implies that the operational time of the spacecraft shall be maximised. To achieve this, it has to be assured that the spacecraft will not remain in a failure loop. Maintainability is the ability to maintain the system in time. Safety is the ability of a system to not cause danger in case of fault, failure or malfunction.

21.1. Redundancy Philosophy

The redundancy philosophy is applied for the DOT mission. This is applied in the design of the ANTREA at system level, but also at subsystem level. Obviously, there is redundancy in the amount of PQs. The is a form of redundancy, as measurements can still be preformed when some PPQ are lost, however, the distribution of the measurements are compromised. It thus reduces the impact of a failure. It is desired that all PPQs work as then the distribution is optimised. However, when some scientific instruments do not work, still scientific data can be gathered although it is less distributed over the asteroid. This is the same for the CPQs, there are 10 present. They are spread over the net to improve reliability. If one of them fails, the other one can still perform the task of sending data. This reduces the impact of failure, even though it is still possible that due to the failure of a CPQ not all data will be sent to Earth (this will depend on the orbit and rotation of the asteroid). The C&DH unit only has redundancy in the amount of PQs present. Every PQ has one C&DH unit and when it fails, the entire PQ will fail as it can no longer perform any tasks. However, 69 PQs are taken onto this mission and as stated before, still scientific data can be gathered on PQs that do have a working C&DH unit and only the distribution of the scientific data is compromised. Furthermore, as stated in the reliability section, the C&DH has a high reliability as it is already tested for space and it is know that it can withstand the thermal environment and radiation. The batteries have redundancy as it is assumed that only the batteries of 3 out of 4 bullets will work. No contingency is required in terms of energy storage as it is assumed that if a PPQ is damaged upon impact, the energy storage capacity is reduced by the same factor as the energy usage. For the solar panels, redundancy is also present, as it is also possible to recharge the batteries with less solar panels. It will take more time, but this time is also available. Lastly, the deployer also contains redundant elements. There are two springs to open the door, however if one spring fails the other spring would still be sufficient to open the door although it will then open more slowly. This will not unbalance the door, the hinge of the door is large enough to not let it move in an other direction than the opening direction.
All of these redundancies are passive redundancies, there is no redundancy present in the sense that there are two components of which one is inactive and can be turned on in case its associated component fails.

21.2. Reliability

The User Requirement regarding reliably is only for the sensors, thus the PPQs. To obtain a reliability of 80%, testing will need to be done to make sure that the sequential actions have a high enough reliability. The requirements of the other parts such are the Net, Deployer and communication system are as follows;

DOT-LAN-PQ-1 : The PQs shall sustain the loads at every phase of the mission with a reliability rate of 80 % or higher. *User requirement.*

DOT-LAND-MD-15: The Deployers shall sustain the loads at launch and trajectory with a reliability rate of TBD % or higher. *The deployer is only required to sustain the launch en trajectory loads as it will not land itself..*

DOT-LAND-COM-2: The Communication phase shall be successful with a reliability rate of TBD % or higher. *communicating data back to Earth is a crucial phase of this mission, and it will mainly depend on power available and the flight path of the asteroid*

DOT-LAND-1: The overall mission shall be successful with a reliability rate of TBD % or higher. *To make it worth spending all this money, the mission shall have sufficient reliability*

DOT-LAN-MS The Mothership phase shall be able to find the targeted asteroid with a reliability rate of TBD % or higher. *It is important that the Mothership is able to detect the asteroid*

DOT-LAN-NET-1 The Net shall be able to wrap around the targeted asteroid with a reliability rate of TBD % or higher. *Based on the requirements relating to preforming measurements on the asteroid.*

DOT-LAN-NET-1.1 The Net shall be able to wrap correctly around the targeted asteroid with a reliability rate of TBD % or higher. *With correctly, it is meant that all PQ will be able to touch the asteroid with that reliability rate*

All this reliability will be obtained by extensive testing of all parts of ANTREA. It is therefore planned to be achieved in the testing phase of the mission. As the design is currently only in phase A, this is therefore some-

thing that has to be checked in the future.

The reliability that the mission will become a success can also be estimated, although this is still a rough estimation, as not many reliability aspects are known from the mission. The launch always has a risk of failure, which is estimated to be 100% [2]. The flight path of asteroid 2017 FU102 is now quite inaccurate as the mission is still almost 15 years in the future. However, this path can likely be estimated more accurately by the time the DOT mission launches. Also, the approach of the asteroid will be from the sun side, making it more likely that the asteroid is visible. In chapter 11 the requirements regarding the accuracy of the performance are mentioned. As it is currently unknown what the accuracy is, it can not be estimated how high the chance is that these requirements are met. It has to be mentioned that a lot of redundancy is present, increasing the reliability of success.

21.3. AVAILABILITY

The Failure Detection, Isolation and Recovery (FDIR) algorithm shall be able to ensure that the autonomy and failure tolerance requirements are fulfilled at system level. The main purpose of this is to protect the mission and to prevent a lose of the mission in case only a component fails. To be able to assure this, first the possible failures should be considered. Listed below is a partial list of possible failures.

- The structure of the PQ is compromised
- The solar panel breaks or does not work
- The payload is damaged upon impact or does not work for some reason
- The CPQs do not detect the signal from Earth
- The C&DH does not work
- Mechanisms do not deploy

Some of those failure modes can be monitored by the FDIR, however, some of them can not be monitored. For the ones that can be monitored, symptoms related to that failure should be described in detail. During monitoring, the current output values should be compared with the nominal range to see if the system performs as expected. A failure that can be monitored is for example the payload that is not working. The symptom of that would be out of range of the data rate or that the signal of the health check is not obtained. Another failure can be that the voltage regulator is not working correctly, the symptoms of this are that the measured voltage would be out of range. Those two failures can be recovered by preforming an action. For example, to send another command, to reset the system or to permanently turn off the payload to allow the survival of other components of the PQ. It is possible that the payload is not recovered after the reset of the system, it can be possible that the mechanism that deploys it failed (this can happen for the temperature sensors and antenna). There is no action possible to make the mechanisms work in case of failure. The same is for a fracture of the structure, this can be monitored (detected) by a temperature out of range. However, nothing can be done to recover from this. It has to be noted that there are symptoms that are ambiguous. A temperature out of range can be a symptom of many failures. The sensor itself can be the cause of it, the location of the PQ (for example in a crater, resulting in constant coldness), the structure being broken, etc.

To make sure the PQ does not remain in failure the following will be done. The PQ goes into Safe mode, then the Failure, Detection, Isolation and Recovery algorithm will detect the problem. When possible, the problem will be fixed by either giving another command or after a certain time the system will be reset. Then, a health check will be preformed and when this results in being healthy, the PQ goes out of the Safe mode.

If for some reason the PQ's health check will only result in 'not healthy', the component that causes that will be turned off. In case this is still not enough to recover, the PQ will be turned off completely. This has an affect on the distributions of the measurements, however, it will not result in a complete failure of the mission. Lastly, there is redundancy in the power cables and data cables. When for some reason, it is no longer possible to transfer data over a specific cable between two PQs, the power can also be transferred between those over other cables.

21.4. MAINTAINABILITY

For the DOT mission, maintenance after launch is not possible. It is simply impossible to perform repairs once ANTREA is launched as it is such a complex mission. However, this is already accounted for during the design

phase.
The net is made in such a way that it can compensate for single points of failure, except for the single point failure between the square net and bullets. The structure of the net is over-designed with a high factor to be sure it will not fail. The bullets of the net contain a reeling mechanism. This mechanism is to increase the chance of success and to improve the attachment of the PQs to the asteroid. However, the net should also be able to function without this reeling mechanism. Additionally, there is redundancy in the structure of the PQ, as the structure is designed to survive 1.5 times the expected landing loads. Also, the damping material is there solely for damping and does not carry structural loads.
Furthermore, there is a communication window to reprogram software in the time interval when measurements are preformed on the asteroid (thus in March 2036). During the communication window, there can also be reprogramming of software. However, this does compromise the communication time to send data to Earth.

As written before, there is no redundancy in the sense that one component can be switched off and a redundant (back up) component can take over the task. However, the C&DH for example makes back-up of the scientific data obtained. Data collected by a PPQ, will also be saved on another PQ to ensure that the data is stored. Thus, in case a PQ collects data for a bit less then a month and is then lost, all data obtained by that PQ is not lost as it is also saved on another PQ. For all payload, there is redundancy present in amounts; there are 49 PPQ-1s and 10 PPQ-2s and 10 CPQs. Therefore, the mission objective will still be fulfilled even though some PQs are lost during the mission.

Finally, there should also be verification of the effectiveness of the recovery methods. As the design is currently in phase A, this can not yet be verified. However, in a later design phase, this will be done.

21.5. Safety

After the ANTREA starts on its transfer orbit, it is no longer harmful for the Earth or for people. The only harm that can be caused is during the production or storage of the ANTREA system. As mentioned in the production plan, the lithium batteries and solar panels should be handled according to safety regulations.

Safety and reliability are achieved through: fault avoidance, fault removal, fault tolerance, fault detection and diagnosis and automatic supervision. A FMEA or FMECA has to be performed to achieve this. These analyses are performed on the functional and physical design with the purpose of identifying the potential failure modes and classify them accordingly based on the severity (within FMEA) and/or criticality (FMECA) of their consequences. Mitigation plans are proposed within the analysis and with the purpose of integrating them within the final design. Practical means of failure detection and recovery actions shall be identified for each potential event. The aim of the FMEA/FMECA shall be used in order to support the verification of the reliability, maintainability, logistics, test and the Failure Detection, Isolation and Recovery policy. Within these analyses, failure propagation is assessed including the identification of potential chain failures.

22

Sustainability

As technology grows, sustainability becomes an increasingly more important aspect of design. Sustainability is defined in the context of this project as the philosophy of designing a product such that a negative environmental impact is limited as much as possible. Moreover, a sustainable design is a lot more favourable on the market and is a leading factor to what customers buy in the aerospace industry. From chapter 3, sustainability was a criterion with multiple sub-criteria and had a weight of 4.7%.

In this chapter, the approach to sustainability is discussed to brief the reader how sustainability was tackled in this project. Furthermore, a sustainable development strategy is defined where the project will be categorised in several phases and the requirements for a sustainable design will be clearly defined. Finally, the contribution to sustainability will be discussed to show how the mission helps by being sustainable.

22.1. Approach to Sustainability

There are several factors that contribute to sustainability, to ensure a sustainable design all of these factors must be taken into account. Firstly, the design should be reusable since reusing the entire or parts of the de-

sign would lead to lower consumption of resources. If the technology used can be reused for missions landing on asteroids and possibly other missions, this would significantly reduce the required resources. One way of ensuring a reusable design is by the use of Commercially Off-The-Shelf (COTS) components. Since COTS components are designed to be able to be used in a wide variety of missions, they are preferred compared to components that are designed only for a specific case. Furthermore, the processes regarding production and manufacturing are more resource efficient in terms of energy and cost, as opposed to custom made components. COTS components are however, not specifically designed to operate in the harsh environments of space mainly being the radiation and high variations in temperature.

Another factor that contributes to sustainability is the use of hazardous materials which is defined as harmful to the environment and to humans. It is necessary to reduce the use of these harmful substances as they contribute to pollution, dangerous work environment and a produce a higher ecological footprint. Therefore, the use of hazardous materials should be limited.

Scalability is another factor that contributes to sustainability, if the design is scalable then few modifications are required to be applicable to a similar mission. This in turn, decreases the development and manufacturing costs making the overall procedure more efficient and sustainable.

As stated in chapter 2, there are two user requirements that concern sustainability.

DOT-SAF-1 : The materials used for the production of the spacecraft shall not be hazardous to its environment. *User requirement.*

DOT-MOD-1 : The Lander System shall be usable with minor modifications for other asteroids with sizes up to 1 km. *User requirement.*

Therefore, the use of hazardous materials and designing a scalable design took the highest priority when considering sustainability for the design. All materials that have been used in this mission are non-hazardous with the exception of the solar cells as they are made out of Gallium Arsenide, and the bullets which contain lead. However, there is not enough studies conducted to show if Gallium Arsenide is hazardous to humans. There is only evidence that it can be toxic to animals [35]. Furthermore, lead is known to be toxic and causes lead poisoning if lead found in the body. Hence, handling lead during manufacturing must be taken with utmost care, to ensure lead poisoning is limited as much as possible. Lead was chosen primarily due to its high density and its ability to shield from radiation. The lead used could be replaced with other materials with high density to eliminate the issue of toxicity. In spite of this, most other dense materials are either also toxic or extremely rare and therefore expensive. The design is scalable by increasing the size of the net and increasing the amount of PQs. Since the form factor of the PQ is small and relatively new, little to no COTS components could be used for the design and thus custom made components were primarily chosen.

22.2. Sustainable Development Strategy

The project consists of six phase with each phase a sustainable strategy is determined.

Phase 0 focuses on the user requirements and defining what the mission must accomplish. The sustainable strategy is to define the missions contribution to sustainability which will be discussed in detail in the proceeding section.

Phase A defines the functions of the system, different types of useful technologies and a design trade-off is conducted. The sustainability strategy is identifying the sustainability requirements based on the user requirements: scalable, reusable and non-hazardous materials. Sustainability technologies are identified such as choosing the trajectory such that ΔV is minimised which will require less fuel, choosing solar cells that are the left-overs of cut solar cells (TASC). Finally, the weight factor of sustainability (4.7%) is taken account during the trade-off.

Phase B consolidates the system specifications, preliminary subsystem specifications are developed based on the user requirements and a risk analysis is performed on the entire system. The sustainable strategy is to integrate the sustainable technology found in phase A to the mission needs. TASC were used mainly due to their high power density and cost but also because it is sustainable by using the left-overs of cut solar cells. Using COTS components was also imposed, however, it was limited due to the form factor of the PQ. Moreover, the risk to sustainability on the environment is analysed to see the overall affect the project has on the environment

and to limit this effect. For this, certain scenarios must be considered for example, if the launch fails and debris from the mission enters the atmosphere, the effect it has on the environment is reduced as much as possible. For this reason, the use of non-hazardous material to the environment is crucial.

Phase C focuses on the final design concept in which the subsystems are designed in detailed and verification of the models and requirements are performed. The sustainable strategy is to verify if each subsystem complies with the sustainability requirements. Since, Gallium Arsenide is a potential carcinogenic and shows evidence of being hazardous to animals, the requirement is not met. However, the performance of the mission takes priority and is adequate if a small percentage of the system contains Gallium Arsenide.

Phase D focuses on the physical design aspect of the project where fabrication, assembly, integration and testing occur. The sustainable strategy is to identify and use sustainable fabrication methods. Several sustainable fabrication methods are 3D machining which reduces time and cost, the structure of the PQ would be able to made by the use of a 3D machine. The manufacture of components has for centuries mostly relied on the removal of material to create a certain shape. This produces a large amount of waste both in material and in energy required. Casting components creates the shape whilst decreasing the waste compared to removal of material, but even this process requires a high amount of energy to produce molten material and then shape it. However, one can reuse the removed material during shaping. A more detailed description of the different manufacturing methods are described in chapter 23.

Phase E focuses on a review on the operational readiness of the project and an end-of-life procedure is thoroughly described. The sustainable strategy is to clearly define and end-of-life plan for the mission to ensure that disposal of the entire system is done in a efficient mannered way. Since the lander will be on the asteroid, the landers will remain on the asteroid after its end-of-life period. The Mothership however, must be either put into a graveyard orbit or is allowed to drift away depending on its position relative to the Earth and other satellites at end-of-life. This will then conclude the mission by validating if the mission did what it was intended to do.

The aforementioned project phases and respective sustainable strategies are summarised in Table 22.1. The project is currently in Phase C as of the writing of this report.

Table 22.1: Project phases with strategies to sustainable development.

Phase	Project phase contains:	Sustainable strategy
0	Top level specifications and mission definition	Defining mission's contribution to sustainability
A	- Preliminary system functional analysis, specifications and function tree - Technology identification - Design trade-off	Identifying: - Sustainability requirements - Sustainability technology Applying: - Sustainability weight factor during trade-off
B	- Consolidation of system specifications - Preliminary subsystem specifications - Risk analysis	- Integrating sustainable technology - Prioritising COTS components - Analysing risk to sustainability of the environment
C	- Final design concept - Detailed subsystem design - Test of models - Verification of the requirements	- Verifying sustainability requirements are met - Test effects on sustainability of the target environment
D	- Fabrication, assembly and integration - Detailed integration and test procedure	- Using sustainable fabrication methods
E	- Operation readiness review - End-of-life / disposal plan	- End-of-life / disposal poses no harm to the sustainability of the target environment

22.3. Contribution to Sustainability

As mentioned in the previous section, Phase 0 describes the mission's contribution to sustainability which is elaborated in this section. The contribution to sustainability is correlated with the Market Analysis performed in chapter 4. Customers want to buy a sustainable design and therefore, the system must contribute positively to the environment. The mission's purpose is to take measurements of the asteroid for 1 month to measure

the properties of the asteroid and to improve the models used on Earth. This would allow humans to better detect asteroids and come up with a strategy to mitigate should the asteroid be headed on a collision course with Earth. The asteroid's properties would also allow humans to better understand asteroids so that asteroid mining can be exploited and therefore, reduce the consumption of Earth's natural resources.

There are four important characteristics when it comes to the design philosophy with regards to sustainability. These are the 4 **R**'s: **R**eduction, **R**euse, **R**ecycle and **R**ecovery. Reduction of waste is ensured by choosing the appropriate manufacturing method and materials used which is done after the detailed design phase. Furthermore, parts of the mission can be reused, for example the design of the deployer can be used for a mission involving a net to remove debris, this would significantly reduce development costs. Reusing and adapting the PQs such that radio experiments can be performed. Recycling waste material from machining the components is possible by melting the scraps and forming them into usable materials.

The data measured can be sold to companies to create sustainable life in space. This could be for instance, using the more efficient landing technique to create a base on the moon with resources such that missions can be performed from the moon, as opposed to the Earth which would significantly reduce the resources required.

23
Production Plan

The production plan presents the activities required to construct the ANTREA system. The Manufacturing, Assembly, Integration and Test processes will be discussed in this chapter. The manufacturing begins after the detailed design is finished. Note that in this report, the preliminary design is presented and not the final detailed design of the system.

23.1. Manufacturing, Assembly, Integration and Test process

Figure 23.1 shows the Manufacturing, Assembly, Integration and Test process. First the components have to be verified, after which the assembly process can start. During assembly the components are connected together into elements and those elements are combined into subsystems for verification and validation purposes. The subsystems are built and verified either by demonstration, testing, analysis or inspection. From this, the subsystems can be assembled into one complete system. The complete system has to be validated to assure the User Requirements of the system are met[1].

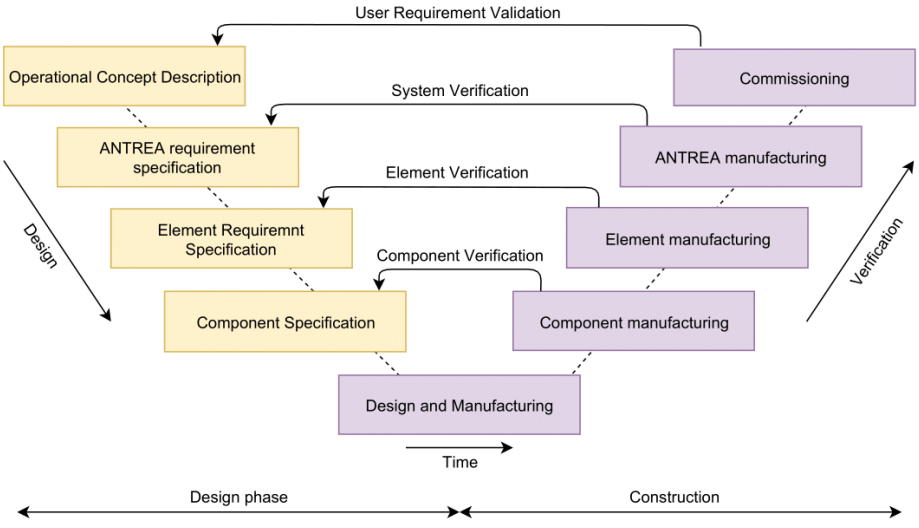

Figure 23.1: Process organisation of Manufacturing, Assembly, Integration and Test process.

23.2. Design and Manufacturing

Before the actual manufacturing, the production phase will have to be prepared. Firstly, the production constraints need to be identified. There are no real production constrains for ANTREA. The only parts that should

[1] http://www.esa.int/Our_Activities/Space_Science/Building_and_testing_spacecraft [Accessed 19 June 2019]

be handled according to higher safety regulations are the lithium batteries as they can explode when not handled with care. Furthermore, the Gallium Arsenide used for the solar panels can cause health problems and need special handling. Hereafter, manufacturers of the components of hardware and software have to be contracted. This includes scheduling of the work and determination of the manufacturing procedures. The production preparation and planning will be done by a production manager, who has to be guided by system engineers and other technical engineers. When the procedures and schedules are known, the required equipment has to be gained. At last, also personnel needs to be hired and trained to perform the procedures.

23.3. Component Manufacturing

The small parts will be manufactured first. This phase can be done in different locations for different components at the same time. As a start, the raw materials have to be obtained and stored at some location. After that, the components can be manufactured. Some components such as the outside layer of the PQ will require a surface treatment. All those actions need to be done efficiently to reduce the amount of waste, since this will increase the sustainability of the ANTREA design. When the component is put together, it can be verified. After verification a review has to be made, to decide if the component is within the acceptance range, and does not contain errors. Furthermore, the component has to be authorised for use. Lastly, the component needs to be prepared for transport. To reduce the production time, different components can be manufactured in parallel.

23.4. Element Manufacturing

All manufactured components have to be transferred to one location to be assembled into one part. After this, multiple parts can be linked and connected to each other to create a subsystem. Since different parts are connected, a reconcilability test has to be performed to see if they can be connected without any problems. Then the subsystem needs to be verified. Quality control is performed after which the subsystems are prepared for transport. It is highly likely that transport will not be done instantly, therefore the subsystem might need to be stored for a while. During this storage, it is important that the lithium batteries and solar panels (which contain Gallium Arsenide) are stored in a facility that provides care.

23.5. ANTREA Manufacturing

The different subsystems have to be obtained and integrated into one system. First the different PQ types themselves have to be assembled. The stacks can be built, layer by layer. After the PQs are assembled, the PQs can be connected to the net, to yield the ANTREA system. The system then has to be verified by testing. Components that are tested consist of, for example, the electrical systems to ensure that electrical signals generated by one component will be received and understood by another component. Furthermore, the software is tested, to ensure it covers all operating modes and procedures.

23.6. Commissioning

Although the spacecraft is already in commission from the moment the previous manufacturing phase is finished, to be able to perform what it is designed for, more actions have to be taken. The launcher has to be contracted. The launch date has to be determined. The spacecraft needs to be prepared for transport. Eventually, the spacecraft is transported and assembled on the launcher. Then, pre-launch procedures have to be performed and finally, ANTREA is launched into a Highly Elliptical Orbit (HEO) after which health checks have to be done. Subsequently, the ANTREA will begin its journey along the transfer orbit. Upon arrival to the asteroid using a rendezvous manoeuvre ANTREA will land on the asteroid, and will start the science measurements which will be communicated back to Earth later on.

24
Cost Analysis

The aim of miniaturising spacecraft is to make space a more affordable option. It is therefore important to keep the cost of this mission as low as possible. However, as this miniaturisation of spacecraft is still a new development, high development and testing cost will be present. Still, the aim is to at least make the PQs and the net as cheap as possible.

24.1. HARDWARE COST

The cost for the ANTREA is estimated based on the cost of all the subsystems it contains. The budget is split over the cost for the PQ and its subsystems and the cost for the Net and Deployer. The (material) cost of all subsystems is determined as can be seen in the tables below. To convert euros to USD a currency rate of 1.138945 is used. Additionally, all presented cost are for the fiscal year of 2019. As ANTREA will be manufactured quite far in the future, inflation will influence the price.

In Table 24.1 an overview of the payload cost is given. There is one IMU per PPQ, additionally there are four temperature sensors in PPQ-1 and one in PPQ-2. Furthermore, there is one image sensor in PPQ-1 and four in PPQ-2. Moreover, there is one antenna per PPQ, as well as one transceiver per PPQ. Lastly, there is also one mass spectrometer per PPQ.

Table 24.1: Cost for payload

	Price per instrument (euro)	**total price PPQ-1**	**total price PPQ-2**
- IMU	3.72 [1]	37.20	182.28
- temperature sensor	0.35 [2]	17.40	17.05
- image sensor	99.29 [3]	992.90	19460.84
- antenna	0.40 [4]	4.01	19.66
- transciever	90.54 [5]	905.40	4436.46
- mass spectrometer	100 [assumed]	1000	4900
	total (euro)	2957	29016
	total (USD)	3368	33048

In Table 24.2 the cost of the structure and mechanisms can be found. There are four wire cutters on PPQ-1 and one wire cutter on PPQ-2. The cost for the wire cutter is based on the "technical Data Information Sheet". Futhermore, there are four temperature mechanisms per PPQ-1. To clarify, the total price PPQ-1, PPQ-2 and CPQ, refers to the total price for mechanisms and structure, not the absolute total price of PPQ-1, PPQ-2 and CPQ.

Table 24.2: Cost for structure and mechanisms

	Price per mechanism	**Total price PPQ-1**	**Total price PPQ-2**	**Total price CPQ**
Mechanisms				
- wire cutter	122	488	122	0
- temperature mechanism	7.42 [6] [7]	74.20	0	0
	Price per PQ	**Total price PPQ-1**	**Total price PPQ-2**	**Total price CPQ**
Structure				
- damping	10.95 [8]	109.50	536.55	109.50
- rod	0.03 [9]	0.30	1.47	0.30
- walls	2.03	20.30	99.49	20.30
	Total price (euro)	692.30	759.51	130.10
	Total price (USD)	788	865	149

In Table 24.3 the cost estimation of the C&DH unit can be seen. The C&DH unit is a COTS component that is

[1] https://www.rutronik24.com/product/bosch+se/0273.141.179-1nv/5242196.html [Accessed 29 June 2019]
[2] https://nl.mouser.com/ProductDetail/STMicroelectronics/STLM20DD9F?qs=sGAEpiMZZMuXfccvO5Dzaut3CC8WwBcw [Accessed 29 June 2019]
[3] https://nl.farnell.com/on-semiconductor/noip1sn1300a-qdi/image-sensor-monochrome-lcc-48/dp/2630258 [Accessed 29 June 2019]
[4] https://www.amazon.com/Lufkin-W606PM-Executive-Diameter-Millimeters/dp/B000ZU92PE [Accessed 29 June 2019]
[5] https://store.qorvo.com/products/detail/QPM1002-Qorvo/615014/ [Accessed 29 June 2019]
[6] https://www.indiamart.com/proddetail/aluminum-alloy-7075-t6-12603836155.html [Accessed 29 June 2019]
[7] https://www.thespringstore.com/pt016-188-5875-mw-rh-0750-n-in.html?unit_measure=me [Accessed 29 June 2019]
[8] https://www.sorbothane.com/ [Accessed 29 June 2019]
[9] https://www.weerg.com/en/materials-cnc-machining/aluminum-7075-t651-ergal-2.html [Accessed 29 June 2019]

space ready. It has a high price, but the testing cost will be less. In Table 24.4 the cost of all components of the communication system can be found. All cost of the transiever come frome [10]

Table 24.3: Cost for C&DH unit

	Price per C& DH unit
Texas Instruments MSP430FR5969-SP Radiation Hard-ened Mixed-Signal Microcontroller	2803.69[11]
PCB	50.00 [12]
Total per PQ (USD)	2853.69
Total (USD)	196905

Table 24.4: Cost of communication

	Component name	Price per CPQ
Communication		
- Antenna		
– Substrate	RT/duroid 6010LM	85 [13]
– Microstrip	Custom made	300 [14]
- Transceiver		
– RF Filter	880148	277.12
– RF Switch	TGS2303	91.50
– RF power limiter	TGL2205	39.60
– Duplexer	890085	59.68
– Amplifier	QPA9119	8.05
– Voltage variable attenuator	TGL2767	30
Total per CPQ (USD)		890.95
Total (USD)		8910

In Table 24.5 the cost of the EPS can be found. The price for the solar cells are extrapolated from "Solar Panel Design Decision and General Information Sheet" 2012 Alexander L Carrere. Only the PPQs have solar panels, the CPQs have no solar panels.

Table 24.5: Cost of EPS

	Component name	Price per PPQ	Price per CPQ
EPS			
- Battery	GEB602030C[15]	10	10
- Solar cells	Spectrolab TASC	15	0
- MPPT	BQ25505[16]	12	12
- Payload voltage regulator	LM8850 [17]	1	1
- Power cable voltage regulator	LTC3105[18]	3.28	3.28
Total per PQ (USD)		41.28	26.28
Total (USD)		2436	263

In Table 24.6 the cost of the net and bullets can be seen. The net is assumed to cost 10,000 USD due to the high complexity and integration of the power and data cables inclusive interfaces with the PQs. Furthermore, there are three batteries present in every bullet.

[10] Qorv.com [Accessed 29 June 2019]
[11] https://www.digikey.com/products/en?mpart=M4FR5969SPHPT-MLS&v=296 [Accessed 29 June 2019]
[12] https://www.pcbcart.com/quote [Accessed 29 June 2019]
[13] ZAUBA.com [Accessed 29 June 2019]
[14] pasternack.com [Accessed 29 June 2019 (extrapolated from this source]
[15] https://www.alibaba.com/product-detail/GEB-3-7V-Rechargeable-Lithium-Polymer_1802135109.html?spm=a2700.7724857.normalList.55.5663156ffPVKDR [Accessed 29 June 2019]
[16] https://eu.mouser.com/Search/Refine?N=4294759686&Keyword=BQ25505RGRR [Accessed 29 June 2019]
[17] https://eu.mouser.com/Search/Refine?N=4294759686&Keyword=LM8850URE/NOPB [Accessed 29 June 2019]
[18] https://www.analog.com/en/products/ltc3105.html#product-discussions [Accessed 29 June 2019]

Table 24.6: Cost of Net and Bullets

	Price per Bullet
Bullet	
- BL motor	173 [19]
- Electrical speed control	150 [20]
- Planetary gearbox	204 [21]
- Batteries (x3)	14 [22]
- Gel	100 [assumption]
- Lead	150 [assumption]
- Stainless Steel casing	300 [assumption]
- Cable, drum and other	100 [assumption]
Total per per bullet	1191
Net itself (including power and data cables)	10000 {assumption]
Total (USD)	14764

Table 24.7: Cost of Deployer

	Price (USD)
Deployer	
- Pinpuller (4x)	40000 [23]
- Material	5000 [24]
Total (USD)	45000

The cost of the deployer can be found in Table 24.7. It can also be seen that the pin pullers take up most of the Deployer's budget. However, they were deemed necessary as can be read in chapter 9.
In Table 24.8 the overview of all hardware cost can be seen. As the design is still in an early phase, the cost estimation is rough and changes are likely. It can be seen that the hardware cost are taking less then 10% of the budget. This shows that miniaturisation in the future (when testing cost will reduce as it is then an established technology) indeed will become a cheaper option. One PQ will cost around 3,575 USD.

Table 24.8: Overview of all hardware cost

	Total cost (USD)
Components of PQs	
- Payload	36416
- Mechanics & Structure	1802
- C&DH unit	196905
- EPS	2699
- Communication	8910
Total PQ	**246732**

PQ	246732
Net & Bullets	14764
Deployer	45000
Total hardware cost	**306496**

The labour is estimated as follows. In the chapter 26, the phases A until D will take eight years. A group of 10 employees will work on this project during that time. However, it is not needed that they work full time. For example the system engineer or manager are only needed for a very limited amount of time every week. It is assumed that on average those 10 people work for 40% of the time. The average cost for a full time employee will be 110,000 USD. This will result in a total labour cost of 3,520,000 USD.

24.2. TESTING

Before the testing costs can be presented, the tests that have to be performed have to be known. To gain an overview, a Testing Flow diagram has been made, see Figure 24.1.

[19] https://www.maxongroup.com/maxon/view/product/283838 [Accessed 29 June 2019]
[20] https://www.faulhaber.com/en/products/series/sc-1801-p/ [Accessed 29 June 2019]
[21] https://www.maxongroup.com/maxon/view/product/gear/planetary/GPX/GPX22/GPX22-4-Stufig-HP/GPX22HPKLSL0590CPLW [Accessed 29 June 2019]
[22] https://www.nkon.nl/sony-us18650vtc5a-flat-top.html?gclid=Cj0KCQjwi43oBRDBARIsAExSRQF0jprnoUkSivOfDaER-JT_crZJIOrtZEJe3XYwJzGLUUN7KCl5hZEaArRqEALw_wcB [Accessed 29 June 2019]
[23] Tiniaerospace.com [Accessed 29 June 2019]
[24] https://www.weerg.com/en/materials-cnc-machining/aluminum-7075-t651-ergal-2.htmll [Accessed 29 June 2019]

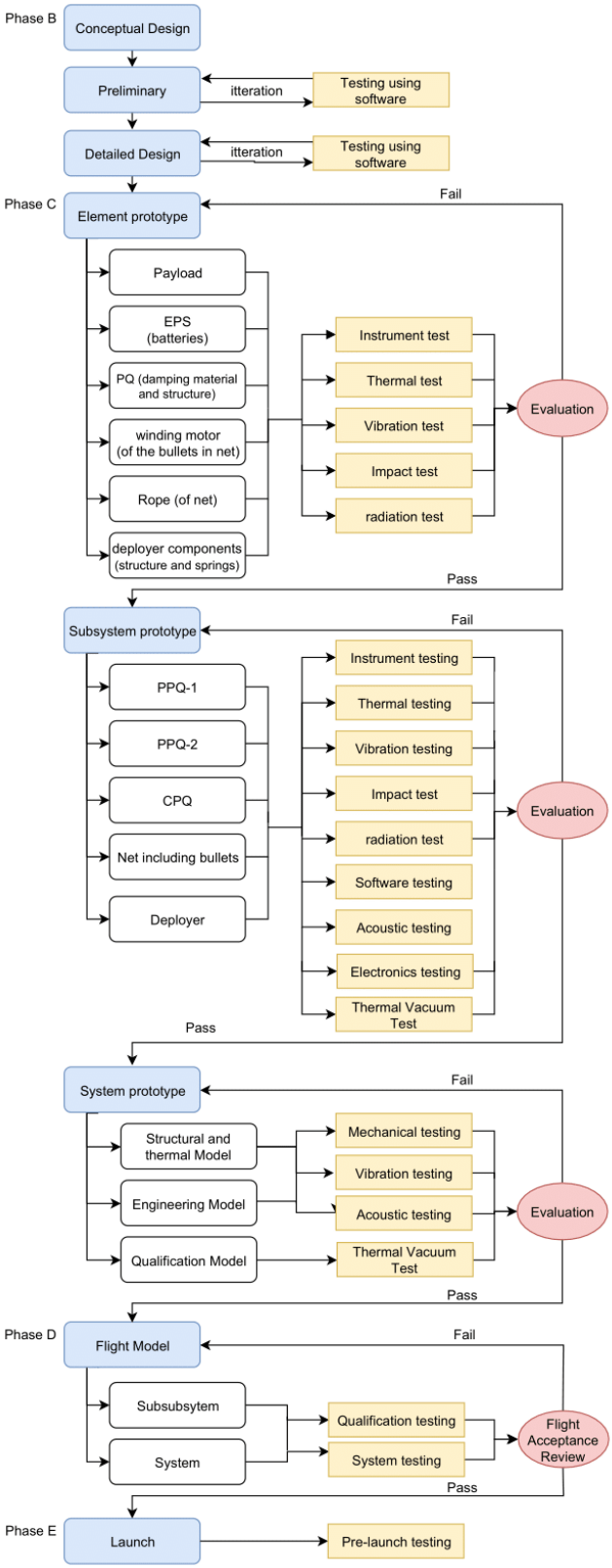

Figure 24.1: Testing Flow Diagram

It is assumed that all the components are already tested and do not need further testing. Subsystems, however, do need to be tested. In the case of the payload, all instruments (the IMU, temperature sensor, image sensors and mass spectrometer) have to be tested as they are not space ready. The temperature range is already known, thus the thermal test is not needed. For the EPS, the batteries have to be tested, the solar panels are space

ready and do not need to be tested. For the PQ, the damping material and the deploying mechanisms need to be tested extensively, as they are crucial for this mission. Furthermore, the structure (rods with the side plates) need to be able to withstand the impact loads. Inside the bullets is a winding motor which needs to be tested. The rope of the net is tested component wise, however, in this design the rope consist of multiple materials (the power wire, structural cable and data cable). As one combination it still needs to be tested for bending, tension, torsion and damping. Lastly, the deployer structure and springs require testing. Regarding the spring, vibration and resistance testing is important as well as to test at which speed it will eject for different compression forces. The communication subsystem is space ready and does not need component testing.

- Instrument testing: To test if the instrument works, in case of the payload it is testing if it indeed performs the measurements. In case of the net, it tests if it opens and closes correctly. This can be tested in a drop tower.
- Thermal Test: To test or check what the temperature ranges are within which the prototype still functions correctly. And, to determine what the potential deviations will be present for example when the payload sensors are outside the operating range.
- Vibration test: To replicate the conditions expected during launch. During vibration tests the spacecraft is progressively shaken at different strengths on a vibrating table. The conditions created here are typically 25% higher then during the actual launch.
- Impact test: Also called Shock Test, is performed to replicate the shock as expected during landing.
- Radiation test: To replicate the radiation experienced during the mission and to test if the prototype can survive this.
- Software testing: This includes multiple tests, it starts wit a unit test, followed by a module test after which a stand-alone Functional test will be performed. Then, it has to be integrated in the system to allow for system testing [25]. The OBC will undergo a software test.
- Acoustic testing: During acoustic tests, the spacecraft is placed in a reverberating chamber and subjected to very intense noise similar to that is encounter during launch.
- Electronic testing: To test if all electronics work. This includes testing of the subsystem prototype to test if the PQs internal electronics work correctly. Furthermore, the system prototype is tested to test if the electronics between PQ and net or between PQ and PQ work correctly.
- Thermal Vacuum Test: The satellite is placed inside a vacuum chamber with a sun simulator to reproduce the extreme variations in temperature experienced in space.
- Qualification testing: This testing includes all aforementioned tests.

To clarify, in Figure 24.1 the element prototypes already refer to multiple subsystems being linked together. Secondly, by subsystem prototype testing the different PQ configurations are tested. In this case this means the different types of PQs, the Deployer and the Net including the bullets. Here, the interfaces between the subsystems will be tested. For example, to test if the payload sensors communicate correctly with the On-Board Computer or to test if the power is distributed correctly through the PQ. Furthermore, the electronics and software of the subsystem are tested. Note that the communication is now also tested.
In phase D, the actual spacecraft that will perform the mission will be tested. All elements have to be tested for the "system testing" to check if they work, this includes testing of the payload, EPS, electronics, OBC, communication, the software, mechanics (pointing), etc.

24.3. Testing cost

As explained in the chapter 4 there are multiple other parties that can use technology tested for this mission. Especially the subsystem prototype testing can be easily used by others, as it mainly consists of basic subsystems that could be used for any spacecraft or any mission. Therefore, not all testing cost will be regarded as cost for the DOT mission. Part of the testing cost can be seen as an investment for future missions. Especially making subsystems space ready is very useful, as they will the become COTS components for future space missions. It is assumed that of all testing cost 20% of the testing cost is investment in the future and is therefore not part of the ANTREA cost budget.

As ANTREA contains almost no COST components that are space ready, as almost no COST components where small enough to fit inside the PQ, the testing cost will be relatively high. Furthermore, as it is a new technology this will increase the amount of testing and will probably lead to altering the design after a test has failed. According to Dr. A. Cervone the testing cost can be expected between the 1.5 and 2 million USD. As it is still early in the design, the highest estimated will be taken, thus 2 million USD. This can be roughly divided over the different prototype testing. Element prototype testing and subsystem testing will cost around $\frac{3}{10}$ of a million. Around 1.5 million is used for the system prototype and $\frac{1}{5}$ million is used for the Flight Model testing. This can be seen in Table 24.9
The prototype testing and subsystem testings are just rough estimations. However, the system prototype testing is based on individual tests.

The testing of the deployer including vibrations will cost 100,000 USD. This test will be performed three times. The hardware testing of ANTREA will cost 50,000 USD and will be done four times. The testing of the net (in the drop tower) is likely to cost 200,000 USD and will be done three times. The system test will cost around 25,000 USD, this will be done four times as well. The radiation testing is expensive and will come down to a total cost of 800 USD per hour[25]. It is estimated that radiation is needed for one working week. An overview can be seen in Table 24.10.

Table 24.9: Overview overall testing cost

	Testing cost (USD)
Element prototype testing	300 000
Subsystem Prototype testing	
System Prototype testing	1496000
Flight model testing	200 000
Total	**±2 M**

Table 24.10: System Prototype testing cost

Test	**Price per test**	**Number of testings**	**Total cost**
Deployer testing	100 000	5	500 000
Hardware PQ testing	50 000	4	200 000
Net Testing	200 000	3	600 000
System Test	25 000	4	100 000
Radiation Test	800 USD/hour	120 hours	96 000
Total cost of system prototype testing (USD)			1 496 000

As stated before, 20% of this testing cost will be seen as investment in the future. This results in 1.6 million USD as testing cost that is part of the DOT mission.

24.4. Total Cost ANTREA mission

In previous sections all cost were explained in great detail. This can be summarised into the overall cost of the ANTREA mission. The cost of ANTREA will be ±5.5 million USD as can be seen in Table 24.11. It has to be stressed that this is an preliminary estimation, and that the budgets have to be re-evaluated as the design progresses to obtain more accurate cost numbers.

Table 24.11: Total Cost ANTREA

	ANTREA cost (USD)
Hardware	306 496
Software	60 000
Labour	3 520 000
Testing	1 600 000
Total	**±5.5 Million**

25 Verification and Validation of the Design

This chapter describes the verification and validation of the ANTREA design. In order to prove that the design is verified, all of the requirements imposed by the customer need to be complied with. This translates to a design that satisfies the needs of the customer. This chapter also concludes the closure of the requirements at this stage of the project. What is more, the preliminary efforts to validate the design are elaborated on.

The verification and validations procedures are visualised by means of a V-diagram (Figure 25.1). An analogy to the flow of the ANTREA design can be made. The mission need helped to define the design. This was then translated into system requirements. A functional analysis of the subsystems was then conducted. This was

[25] https://ntrs.nasa.gov/archive/nasa/casi.ntrs.nasa.gov/20170002727.pdf [Accessed 15 June 2019]

used to shape subsystem requirements. After the last iteration, every technical department completed the verification of the subsystem requirements. This is concluded in chapter 7 - chapter 15, where traceability matrices with the requirements and explanations can be found. After the system design was reviewed (see chapter 19), the compliance of the system to its requirements (and the customer requirements) was investigated.

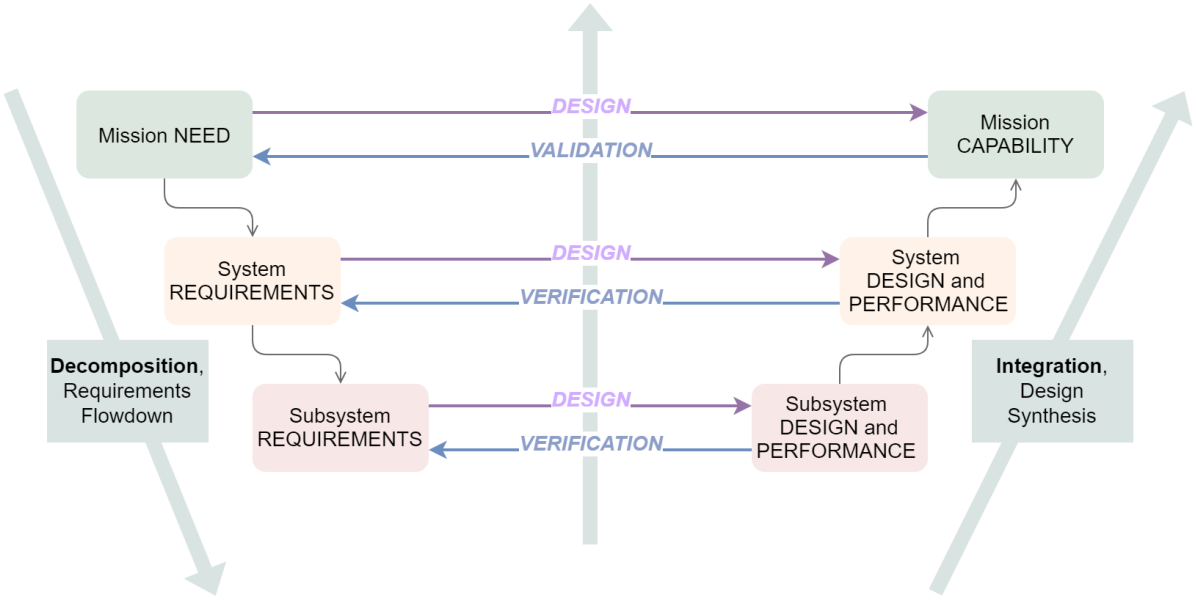

Figure 25.1: V diagram.

25.1. User Requirements Compliance Matrix

Table 25.1 is the full set of customer requirements that were given to the team. A "✓" is put where the requirement is met, a "x" is put where the requirement is not met. If the compliance is not yet investigated or cannot be proven at this time, the compliance box contains a "n".

Table 25.1: The traceability matrix with the customer requirements.

User Requirement ID	Compliance	Explanation
DOT-AST-1	✓	The estimate of the probability of that event >99.8% (chapter 7)
DOT-AST-2	✓	The estimated size of the target asteroid is between 4-11 m
DOT-COST-1	x	Estimated cost: 5,500,000 USD
DOT-SCH-1	✓	Arrival in 2036 (chapter 7)
DOT-DUR-1	✓	Measurements will span over the entire month (chapter 11)
DOT-SAF-1	✓	No substances posing major hazard to the environment present.
DOT-LAN	✓	-
DOT-LAN-MS	✓	-
DOT-LAN-MS-3	✓	
DOT-LAN-MS-4	n	-
DOT-LAN-MS-5	n	-
DOT-LAN-MS-6	✓	-
DOT-LAN-MD	✓	-
DOT-LAN-MD-1	✓	Calculations show the Deployer can withstand the loads at all mission phases
DOT-LAN-MD-3	✓	The total system mass according to most recent estimate is 23.6 kg
DOT-LAN-MD-4	✓	The Deployer carrying the rest of the system fits in a 30 × 30 × 30 cm
DOT-LAN-PQ-1	n	Has to be proven by testing
DOT-LAN-PQ-SC-1.1	n	-
DOT-LAN-PQ-SC-1.2	n	-
DOT-LAN-PQ-SC-1.3	n	-
DOT-LAN-PQ-SC-1.4	n	-
DOT-LAN-PQ-SC-1.5	n	-
DOT-LAN-PQ-SC-1.6	n	-
DOT-LAN-PQ-SC-2	✓	The PQs are capable of performing measurements distributed around the asteroid
DOT-MOD-1	✓	With minor modifications (adding attachments) the design could be able to land on larger asteroids.

25.2. Feasibility Analysis

The team was tasked with designing a technology solution using PocketQubes for in-situ characterisation of a very small Near-Earth object.

The worked out solution is a network of PQs, connected by a net that would provide not only structural, but also electrical power and data connection. The net would be deployed by means of a spring based ejection system, located in a Deployer. The Deployer design meets all the requirements set by the customer (DOT-LAN-MD-1, DOT-LAN-MD-4).

The scientific payload on the PQs is capable of measuring the shape and size, surface composition, material properties, temperature distribution, hardness, and dynamic motion of the asteroid. Despite the small scale of the platform, an advanced miniaturised system was developed that can to the user requirements on the asteroid study.

The resulting design also consists of a fully autonomous command unit and a communication system capable of downlinking scientific data gathered over one month on the asteroid. An EPS satisfying the power needs of the system was implemented.

The volume requirements were considerably more constraining than the mass budgets. This resulted overall mass not to only be within the customer specified constraint (50 kg, DOT-LAN-MD-3), but it actually remained 53% below it at 23.6 kg. In reality, this could translate to a much lower overall mission cost (including the mothership), since every extra kilogram sent to deep space can cost up to millions of euros.

It was concluded that if small modifications were done to the design (mainly the addition of attachment mechanisms), the net could be used to land on larger asteroids (up to 1 km in size).

On the other hand, the directly mission related estimated costs exceed the customer requirements. Despite this, preliminary validation efforts were carried out to test the feasibility of the design.

The preliminary validation efforts were focused on performing a simulation of the net deployment and entangling around the asteroid. This method was assumed to be sufficient for the validation at this stage. The simulation itself was verified and validated during a parabolic flight campaign and was approved by ESA[16]. The simulation revealed that certain changes to the design need to be met, which is elaborated on in section 28.2.

On a concluding remark, the overall product of the project, the ANTREA design, cannot be deemed to be a ready valid product, yet offers a baseline with great potential in the future. Miniaturisation has been and will continue to be a driving force in space exploration. The ability to connect an intensely researched new technology (nets for active debris removal) that may even have commercial application with an efficiently set up deep space science mission remains unique to ANTREA. In the next phases of the design, the constraints imposed on the design, would likely need to be renegotiated with the customer, so that the changes required for improving the performance of the net could be implemented.

IV
FUTURE OF THE PROJECT

26
PROJECT DESIGN AND DEVELOPMENT LOGIC

26.1. PROJECT DESIGN AND LOGISTICS

This section relates to the logical order of activities to be executed in the post-DSE phases of the project. It was decided to follow the planning corresponding to the project phases of a typical project life cycle described by ESA[1]. The following phases are relevant to this type of planning, that have already been conducted by the team:

PHASE 0: MISSION ANALYSIS, NEEDS IDENTIFICATION, DESIGN

This phase was used to focus on familiarising the team with the user requirements, identifying the science performance goals, operations constraints, and Mission Need Statement. Project logic diagrams were developed, as well as an organisational risk assessment. Seven design concepts were then developed to comply with the mission statement, taking into account the technical and programmatic constraints identified by the project initiator Dr. Angelo Cervone, and top level customer Silvana Radu. A first trade-off was conducted with three winners at the end. Initial technical designs of those three concepts were then produced, as well as a management plan, and a system engineering plan. The feasibility of every design was assessed in terms of deployment, approach, landing and attachment of the system on the asteroid's surface, as well as in terms of production, programmation, and operations. A more in-depth risk assessment and sustainability plan were developed, as well as a final technical requirements specification for each concept, by comparing them against the identified needs. A second trade-off was performed and the ANTREA design was chosen.

This phase ends with a Mission Design Review (MDR), which was assumed to correspond to the team's Midterm Review, where the three concepts, and the winner of their trade-off were presented, and the readiness of the project to move into the next phase was assessed. A total of 6 weeks were assigned to this phase, within the DSE time constraints. Regarding the fact that this mission displays highly complex payload due to its miniaturisation, and combines elements that make it a new technology (using PQs on a net) would most probably result this phase to last around 2 years. However, the team had to adapt to DSE regulations and time constraints.

PHASE A: FEASIBILITY

A schedule was defined for the coming weeks. The winner concept of the final trade-off was then started to be designed in detail. All activities needed in order to develop the system were analysed, i.e.: all needed subsystems, other aspects such as astrodynamics, operations, verification and validation of requirements, sensitivity analysis, performance analysis, a final risk and sustainability plan were conducted, and a production plan was layed out. All space and ground segments were thus developed. A total of 5 weeks was allocated to the phase where the team would do a preliminary complete design of the whole system. However, for this phase to properly end, more work would have to be put into the design of each of these subsystems, answering un-answered questions, fixing the design's flaws that limit it from theoretically being fully operational, as well as the organisation of a Preliminary Requirement Review (PRR). During this review, a definition of the mission baseline is usually done, and the feasibility of the User Requirements is assessed in more detail. A total of 1 year is allocated to this phase.

[1] https://www.skatelescope.org/public/2011-11-18_WBS-SOW_Development_Reference_Documents/ECSS-M-ST-10C_Rev.1(6March2009).pdf [Accessed 15 June 2019]

Phase B: Preliminary Definition

Before this phase can begin, a System Requirements Review (SRR) must occur, where a freeze of the highest level requirements is done. After that, the completion of the preliminary design of ANTREA must be conducted. Moreover, other crucial phases have to be conducted in order to reach a final design that can be launched and successfully operated to meet the user requirements. A total of 4 months are dedicated to the review process of the Preliminary Design Review, such that time is available for the team to assess Review Item Discrepancies, and have meetings to discuss resulting actions. A total of 2 years is allocated to this phase as a whole, such that enough time is available for a more detailed analysis of the system, a re-iteration of the requirements if needed, and an eventual re-definition of the design, according to potential newly-introduced requirements. The following list displays the phases of the project that are yet to come, what they correspond to, and relevant reviews that occur during them.

Phase C: Detailed definition

During this phase the design of components and assemblies of the ANTREA design have to be finalised and done in more detail. A detailed definition of all interfaces should be worked upon and engineering models should be build. Moreover, the team should also start planning for assembly, integration, verification and testing (AIV/T). This means that production, development testing and pre-qualification of selected critical elements and components should be done. In the case of the ANTREA design, it is essential to test and qualify the Deployer and deployment of the net itself, in similar environmental conditions as the ones it will be operated in in space. Indeed, deploying a net in space with PQs present at its nodes has never been done in the past and would require extensive preliminary testing and qualification to ensure that the mission can successfully be conducted. Furthermore, all chosen payload instruments were not found to be space ready, and would thus also require extensive testing to prove that they can be operational in the conditions of the mission. During Phase C, the team should also start writing the User Manual of the system, and issue a preliminary one. The system's risk assessment, and sustainable development strategy should also be updated and evaluated in more detail, as the design would grow in more detail as well. All space and ground segment elements should be designed and developed during this phase, which ends with a Critical Design Review (CDR). This can take form of multiple reviews: the instruments critical design review, the Lander's critical design review, and the ground segment design review. This reviews serve as a confirmation of the detailed design at unit level, the qualification and validation status of the critical processes and their readiness for deployment for phase D, and confirm the system's compatibility with external interfaces. If passed, it authorises for completion of qualification, manufacturing and assembly of flight units, for release of the final design, assembly, integration and test planning, and of the user manual. A total of 2 years have been allocated to this phase. This is because this phase of the project life cycle is the one that will require the most manpower utilisation, communications between them which takes time, testing, hardware production and programmatic risk assessments which should not be rushed for a successful system to be yielded. Besides, the subject of this project is new and very pioneering in certain aspects, namely: the deployment of a PQ loaded net in space, and the application of miniaturised scientific instruments for instance. Finally, this phase is the one where the majority of costs, expenditures and cost overruns might occur. It is thus necessary to allocate this phase enough time, for such budget overruns to be avoided or at least minimised.

Phase D: Qualification and Production

In this phase, verification of all segments shall be conducted through test, analysis, demonstration or inspection, such that they are qualified, through a Qualification Review (QR) that is held during the course of the phase. This review shall confirm that the verification process has demonstrated that the design, including margins, meets the previously defined requirements. During this phase, two versions of the design shall be built: a Structural and Thermal Model (STM) and an Engineering Model (EM). These models are subjected to test conditions to replicate the conditions present namely during launch. It can then be verified, that the design's subsystems all sustain the given loads and can work properly together in a launcher and with ground systems that should be compatible. A Qualification Model (QM) can also be built during this phase, to test for system performance under environmental testings including thermal vacuum tests for example.

Reproducibility of the design is also assessed. During this phase, manufacturing, assembly and testing of flight hardware and software shall be completed, as well as the operations plan between the space and the ground segments. An Acceptance Review (AR) can then take place at the end of the phase. The primary objective of this review is to confirm that the conducted verifications have proven that the system is free of workmanship errors and is ready for further operational use. Another review must be conducted at the end of this phase, namely the Operational Readiness Review (ORR). Its main objectives are to verify readiness of the operational procedures and their compatibility with the flight system, to verify readiness of the operations team, and to accept and release the ground segment for operations. A Flight Model (FM) is also build during this phase, which is the one that will be launched into space. A total of 2 years are allocated to this phase, which begins with qualifications of the designs and ends with the shipment of the system to the launch site.

Phase E: Utilisation

During this phase, the launch operations are prepared in terms of the space and ground segment, followed by a Flight Readiness Review (FRR) and a Launch Readiness Review (LRR), and all launch and early orbital operations are performed. In the case of the team's mission, this would consist in finalising arrangements at ESA ESOC and the nomination of the responsible Spacecraft operations manager in addition to setting up the launch operations in the chosen launch site of CSG (Kourou, French Guyana). Other major tasks of this phase consist in performing all necessary on-orbit verification and operations including commissioning activities after launch, as well as all other ground support activities in order to support the mission. For commissioning activities, a series of on-orbit tests should be conducted, to verify that all elements of the system are performing within the specified performance parameters. A Commissioning Result Review (CRR) must be held after completion of the on-orbit commissioning activities. After completion of this review, the system operations can be handed over to the project initiator. The mission can then perform its intended functions, i.e.: the launcher shall bring the Mothership in a highly elliptic orbit, the Mothership shall bring ANTREA to the target asteroid, ANTREA shall be be deployed from the Deployer, it shall then approach, land and secure itself around the asteroid, to prepare the system for scientific measurements from the on-board payload instruments. The scientific data shall then be communicated back to the Mothership and to Earth, to then be able to scientifically analyse it. The disposal plan shall also be finalised during this phase, after which an End of Life Readiness Review (LRR) can be conducted which consists in verifying that the mission has completed its service, and ensuring that all on-orbit elements are ready to allow for safe disposal of the system.

Phase F: End of Life

The disposal plan is implemented. In the case of this mission, the plan is for the net to stay wrapped around the asteroid and to serve as a communication and/or tracking element of the asteroid in the future. A total of 6.49 W would for example guarantee the following situation to work: the system could be communicated with and tracked from Earth up to a distance of 1 AU, considering a maximum data package of 20 bit, a typical ranging frequency of 100 MHz, and a ground station of G/t of 20 dB.
A Mission Close-out Review (MCR) is held at the end of this phase, to ensure that all mission disposal activities have adequately been completed.

A summary of these phases is displayed in Figure 26.1. A timed version can be found in Figure A.4 in appendix A.

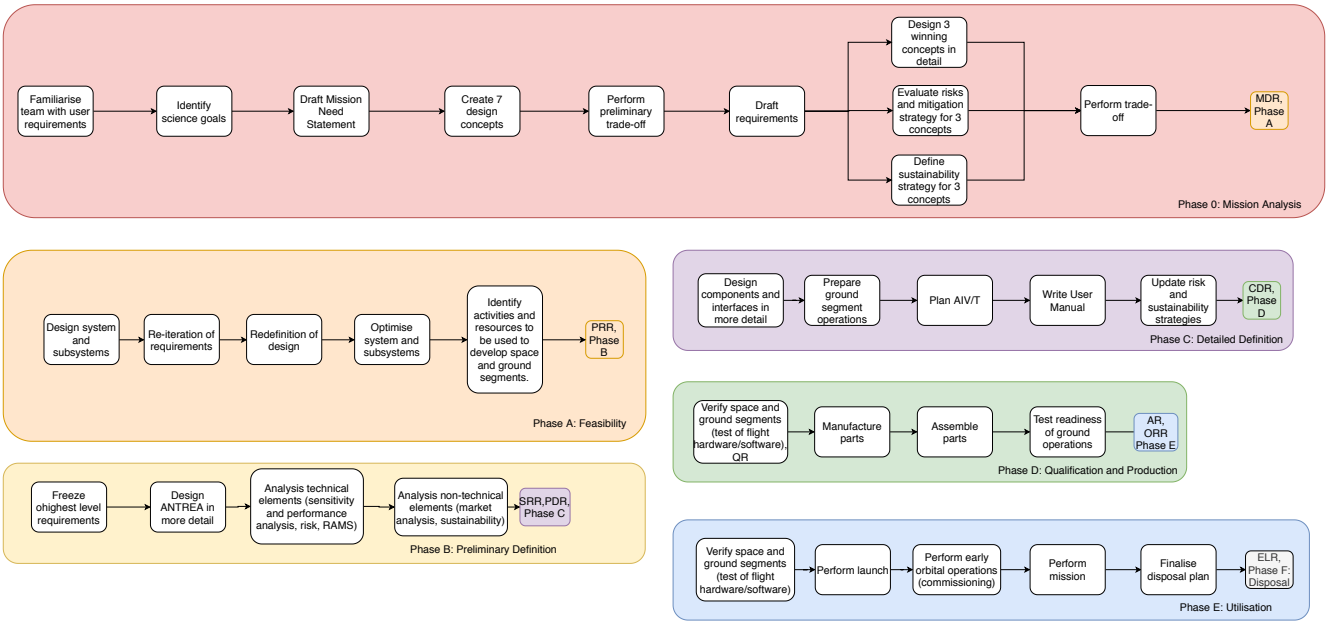

Figure 26.1: Project Design and Development Logic of the mission.

27
Conclusion

The purpose of this project and of the Defend Our Territory (DOT) mission as a whole was to design an asteroid sensing network of PocketQubes, to characterise a very small near Earth asteroid. By performing trade-offs and extensive simulations, the ANTREA design (Advanced Net To Rescue Earth from Asteroids) was found to be the best one to perform this task. This design scored best on performance, risk and feasibility criteria, which where the main criteria upon which the designs were assessed during the trade-offs. This design consists of a 15 × 15 m net, which possesses PocketQubes (PQs) attached at its nodes. These PQs will contain scientific payload that will measure the eight asteroid characteristics as required by the project's customer, namely: size, shape, surface composition, materials, roughness, hardness, temperature distribution, and dynamics of the asteroid. The very small near Earth asteroid that will be investigated is asteroid 2017 FU102, which has a close approach with Earth in April of 2036.

The main reason for choosing a net as the team's final design is directly linked to the higher chances that the design possesses in terms of landing and attaching the system on the asteroid's surfaces, as well as to evenly distribute the PQs around it. 69 PQs will be present on this net, weighing between 150 and 180 g. There are three types of PocketQubes present in the net; one for communication purposes (CPQ) and two for payload purposes (PPQ-1 and PPQ-2). During the design phase, the team's efforts were focused on designing the net itself, its deployer, as well as the PQs' subsystems such as their structure, electrical power system, communications, thermal control, command and data handling, and payload instruments.

The net is partly made out of technora fibre, and partly made out of technora hull fibre, with two power and four data cables going through it. The Deployer is a cube of 30 × 30 × 30 cm, from which the +Z face will open as a door. The ejection tubes present in the Deployer consist of 4 cylinders put at an angle of 10 degrees with respect to the vertical axis. Springs will eject the bullets present at the net's four ends, at an ejection speed of 2 m/s. The Deployer and tubes are made out of aluminium AL-7075 T6. The internal structure of all PQs consist of four aluminium rods that will sustain the other subsystems' instruments by the method of stacks. A damping layer of Sorbothane material was added to the side of the PQs that will most probably be in contact with the asteroid's surface during landing of the net, to increase the chances of a successful landing. The payload instruments taken on this mission are: temperature sensors, monochrome image sensors, colour image sensors, near infrared image sensors, Inertial Measurement Units, mass spectrometers, transceivers and antennas to perform radio science. All together, they will collect a total of 54.490 Gb of data. This data will be communicated to Earth by the CPQs. The electrical power system consists of small batteries in all PocketQubes, while the

main batteries are located in the bullets. The PPQs have solar panels on the +Z side (top side). Thermal control is satisfied passively, except for a small heater that is located next to the cameras and mass spectrometer which are turned on during part of the landing and the science phase. For data handling, a Serial Peripheral Interface (SPI) data bus was chosen, for which internal communication (between subsystems within the PocketQubes) will have an independent slave configuration, with the Micro Controller Unit (MCU) acting as the master. The external communications (between the PocketQubes) will have a daisy chain configuration, with MCU units on selected PQs acting as a master and the MCUs in their proximity acting as slaves. The PocketQubes and net are connect to each other with brackets, positioned on their -Z face. i.e.: the face of contact between the PQs and the asteroid's surface.

The further development of the DOT mission was also established at the end of this report. Currently a preliminary detailed design, consisting of five iterations, was made. Next, a final detailed design has to be made, exploring the subsystems in more detail and applying all recommendations that will be stated later in this report. When the design is finished, testing will be performed on the susbystems' components, subsystems themselves and system as a whole. A cost analysis was performed for these testing operations and the ANTREA overall cost was estimated to be of 5.5 million euros. The outline of the production plan was also established.

Having invested intensive work to select the design and to design its subsystems during the preliminary design phase, the team is confident that ANTREA will be a promising platform to complete the mission to the target asteroid, as well as to conduct the necessary measurements for a better understanding of small near Earth asteroids . This way, the team's mission will have potential to improve asteroid models made from Earth observations, and to thus better protect planet Earth from a future potential asteroid crash, thus defending our territory to a greater extent.

28
Recommendations

28.1. Organisational Recommendations

Team Organisation

In terms of recommendations that concern the team's organisation, some points are relevant to be raised:

The team's structure was divided in such a way that every team member had a managerial and technical role. This was useful as specific technical departments were getting expertise in their area as the project went on. However, some general overview of every subsystem was lost during the project by some members of the group, which could have helped in saving effort and time in mis-communications, or absent communication of technical elements. Moreover, as the project went on, some of the technical roles previously assigned had to be altered and the result was that team members with more management-demanding tasks such as the Project Manager or Systems Engineers ended up also in charge of their technical departments (Structure of the PQ, and Command and Data Handling respectively), which hindered their managerial capabilities and efficiency. In the future, care should be taken as not to assign these two team members with technical chief positions.

Concerning the project's schedule and time constraints, some more effort should have been put into respecting the clearly defined deadlines. In the case of this project, the non-technical elements were sometimes not started until the technical design iterations were over, which was against what had been planned in the project Gantt chart. The team was thus very time constrained towards the end of the project, which resulted in stress and rush, which could have been avoided. To increase efficiency of the team, the deadlines should have been made more strict upon the team members, and a mitigation plan against the risk of not respecting the elaborated schedule should have been defined.

The morning and evening team meetings were deemed very useful, however, they were sometimes too rushed, or on the other hand regarded as a waste of time. More care should be put into assessing if today's meeting should take longer or shorter than the defined 45 min length, before the meeting actually starts, to ensure optimisation of the team members' time.

System Engineering

Reflecting upon the technical progress that was made during the detailed design phase, technical management and systems engineering implementation could be further improved. Below, some recommendations on how to improve the overall integration of the system and make the technical design more efficient are listed.

It is suggested that after the major design iterations, a meeting outlining the most recent design developments are presented by every department. This would allow for a better overview of the design for all departments. Implementing this could encourage a more detailed investigation into the interfaces between all subsystems. Those meetings could also serve as an update for every department that would ensure the entire team uses the same values for elements that have influence on more than one subsystem.

To even further improve the efficiency of the design integration, a tool could be made that links all subsystems in terms of mass, volume, power and data rates so that any iteration would automatically change all values. This would certainly require investing a good amount of time. However, it would maximise the efficiency of the designing and likely speed up the process as a long term effect.

In terms of the clarity of the design, a table should be made to summarise all elements of the four defined segments (PPQs, CPQs, Deployer and Lander), in terms of mass, volume, cost, data rates but also in terms of all instruments present in their system, their dimensions, performance, and specific characteristics relevant to each systems.

28.2. Technical Recommendations

The following recommendations are specific to each department.

Astrodynamics

The astrodynamics analysis could still be improved in several ways, mainly in the Mothership trajectory part. This is because that part heavily depends on the design of the Mothership, for which mainly the propulsion system will need to be to be designed for the astrodynamic analysis to progress. For example the manoeuvres are currently all simulated as impulsive burns, whereas once the thrust is known, they can be simulated as finite burns. Furthermore the sensitivity analysis could be expanded by taking into account spacecraft pointing errors and thruster misalignments. The rendezvous manoeuvres can also be more detailed by incorporating the performance of the Motherships sensors into its design and increasing the number of burns to gradually decrease the relative velocity as the Mothership approaches the asteroid. The fact that the asteroid could be found in a significantly different location than the nominal position can be simulated by applying a random offset to the asteroids position halfway through the approach. Then the ΔV needed to adjust the trajectory for this changed position can be calculated and accounted for in the ΔV budget. It might also be useful to investigate a low-thrust transfer orbit, as this could reduce the total mass of the propulsion system. Another way of reducing the propellant mass required for the Mothership would be having the launcher put the Mothership into a higher energy orbit. The current apogee limit is only based on the apogee of another mission launched using Vega. A more detailed investigation into the exact maximum performance could prove that higher apogees are possible, especially if the Vega C or Vega E are used. Finally the Monte-Carlo analysis could be slightly improved by including an analysis of the probability density of the ground-track to find which ground-stations would most likely be in view.

Design of the Net

Several flaws in the current net design were found that can removed as the design development continues. These issues were addressed in chapter 8. First of all, the classical deployment sequence as used in active debris removal nets was deemed unfeasible for the *ANTREA* net. As the simulations proved, the $\frac{\text{bullet mass}}{\text{net mass}}$ ratio is too low to deploy the net and guarantee entanglement. The bullets simply do not possess enough inertia to open a net filled with 69 0.15 kg PQs in an orderly manner with a high success rate. A functioning design was found but comes along with a reduction in PQs and possibly a reduction in scientific performance. The bullet mass can be increased to 4 kg, thereby enabling the bullets to keep their current dimensions or just increasing in size very slightly. At the same time, to offset for the still low $\frac{\text{Bullet mass}}{\text{Net mass}}$ ratio, the center part of the net can be ejected at 2 m/s approximately 2 s after bullet ejection. The acceleration of the net would then not solely be taken care of the bullets and the momentum exchange between net and bullets could be reduced, which

improves deployment stability. A possible implementation is presented in Figure 28.2. The 2 kg extra mass on each of the bullets would still leave 16.5 kg available for the extra net ejection and more powerful bullet ejection system (they are twice as heavy now and ejected at 4 m/s, requiring 8 times more ejection energy). This extra ejection system and the bullet ejection angle of 20 degrees would certainly reduce the volume available in the Deployer and therefore the amount of PQs (this would require some more iterations as if the mass in the net decreases, other parameters such as the bullet mass would be affected and could possibly be lowered). In case the volume requirement can be renegotiated with the customer, the current PQ configuration could be kept without surpassing the 50 kg mass requirement. An illustration of the deployment sequence of the suggested final design can be found in 28.1a, 28.1b and 28.1c.

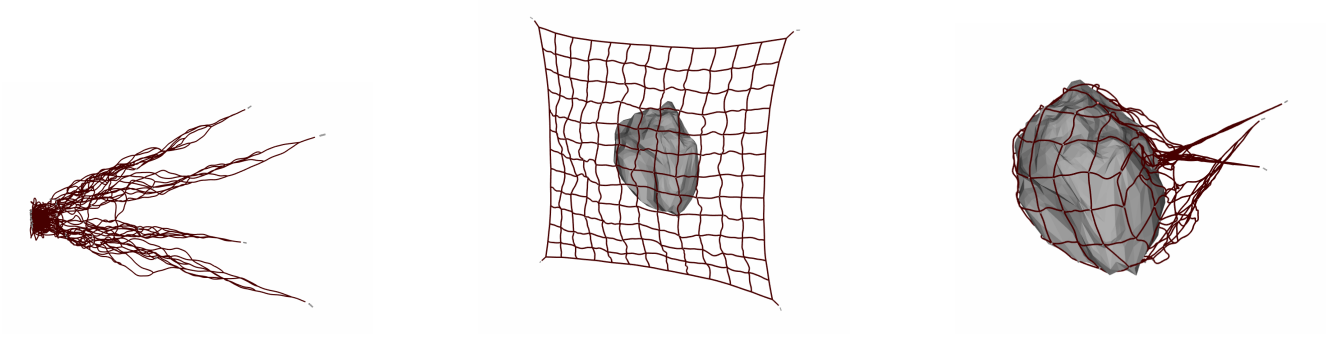

(a) (b) (c)

Figure 28.1: Recommended net design deployment. v_{eject} = 4 m/s, m_{bullet} = 4 kg, θ = 20°, m_{PQ} = 0.15 kg, $V_{initial}$ = 2 m/s applied 2 s after bullet ejection, $d_{asteroid}$ = 35.2 m, $P_{asteroid}$ = 90 s. (a) 3.25s after bullet ejection; (b) 12.86s after bullet ejection; (c) 20.88s after bullet ejection.

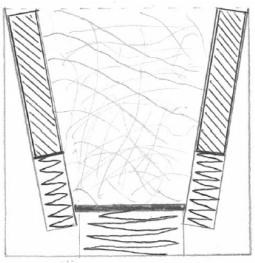

Figure 28.2: Concept with extra spring in deployer to eject net

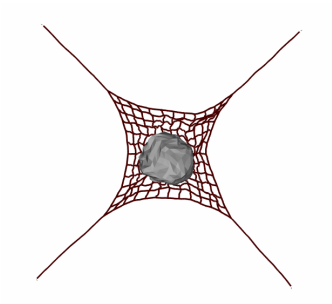

Figure 28.3: Concept of net with longer links

It is recommended to apply different materials to the rope consisting of the structural Technora segment, 4 data and 2 power cables (all copper). As explained in section 8.2, the copper takes up most of the loads due to the stiffness ratios. A switch to Dyneema, (E-modulus 110 GPa[1]), for the structural fiber and silver, (E-modulus 76 GPa[2]), as a the electrically conducting material can improve this situation. On top of that, the lower electrical resistivity of silver would decrease the cable diameter slightly, while the mass would be conserved due to a similar increase in density. Concerning the structure of the net in general, more simulations and scaled testing have to be performed to determine the actual forces in the cables, thereby allowing the ropes to be resized. Testing shall include environmental testing in thermal-vacuum chambers.

The shape of the net could be reconsidered as well. Longer links from the net edges to the bullets, see Figure 28.3, could increase the asteroid size the net is capable of wrapping around. In general a 4 bullet square net is the state-of-the-art, however possibly only due to limited experience. For a square layout, and any symmetrical layout thus including the hexagonal 6 bullet *RemoveDEBRIS* net, a minor chance persists that the bullets collide with each other on the backside of the target and prevent entanglement. This risk cannot be eliminated but significantly reduced by ejecting an asymmetric net. A possible shape are three differently sized triangles clustered together and ejected by three bullets. For all net shapes, the bullets could be ejected with a slight bias to the velocity vector in order to let the net rotate while deployment, which could increase stability.

Designing to a higher detail is required in the upcoming stage, including designing and deciding on the types

[1] http://matweb.com/search/DataSheet.aspx?MatGUID=4481722d60e54cc3b3c112eb3d4b9d02 [Accessed 15 June 2019]

[2] http://matweb.com/search/DataSheet.aspx?MatGUID=63cbd043a31f4f739ddb7632c1443d33 [Accessed 15 June 2019]

of knot in the cables. Furthermore, the mechanical properties of all final rope segments have to be measured to enable more realistic calculations. The bullets shall be fitted with hooks to entangle with the net once parts of it are already on the asteroid surface. Together with exploring this option, the use of the reel-in mechanism in combination with the hooks on the bullets has to be evaluated quantitatively. Furthermore, the final net design shall be analysed and tested for a possibly high electrical impedance interfering with RF signals. This could have a severe impact on the communications subsystem and the planned radio science experiments.
In general a significant amount of challenging obstacles can be expected as the design presents a first in multiple ways. The risks of increased testing and a resulting cost budget overrun has to be respected and mitigated as much as possible.

Deployer

For the Deployer, future iterations would require more precise calculations. The current calculations are preliminary due to the assumptions made. The main recommendations would be the use of FEM analysis software to validate the loads and vibrations analysis. Further iterations could use different materials to make the structure lighter such as composite materials. With respect to the ejection system, one should look into the spring relaxation that will decrease the performances of the springs as they will be compressed for a long time, which would require more stiff springs. The net would require a higher ejection velocity and a higher mass of the weights, therefore the required force in the springs will increase very fast as their length is constrained. It will maybe not be possible to use of the shelve pin-pullers and the system should eventually be changed towards a gas deployment system.

Structure of the PQ

In terms of the PQs' structure, some elements of the calculations could have been done in a more accurate way. First of all, the materials and their thicknesses could have been chosen with aim to optimise the structure, in terms of weight and performance, instead designing a system that is feasible, sustains the loads, but is not lightweight. By following this philosophy, all loads (including mission and deployment ones, which were disregarded in these calculations) should have been computed first, and then the materials, thicknesses, and overall structural design should have been chosen and performed next, to match the loads. The stress concentrations induced by the compression and tension of the holes in both the FR 4 structure and the Sorbothane layer should be looked into. Moreover, the machining of the structure should be looked into, to determine in more detail how the loads would be transferred through the walls. A final recommendation would be to investigate the principle of superposition between the FR-4 and the Sorbothane layers, in order to have a more accurate view on the stresses experienced by the different materials, and on the distance they would displace during critical mission phases such as launch and landing.

In terms of the mechanisms some recommendations could be done. More research can be done into the temperature sensor mechanism to see if it can be made even smaller. The torsional spring was now limiting the size. If a smaller torsional spring with the same performance can be made or found at a different company it would already decrease the size of the mechanism. A smaller mechanism would allow more PPQs to have temperature sensors and would thereby increase the distribution of the measurement which is favourable. Also the size of the hole which was found to be incorrect should be iterated. Secondly, some more structural analysis could be performed on the mechanisms to make sure they survive all the loads from launch till landing. Thirdly, the wires to keep the mechanisms stowed are cut with a wire cutter which will be down-scaled from an existing one. More research in the feasibility of making this wire cutter could be done. Also the option of designing a burn wire could be explored. With that also the wire itself could be refined.

Payload

In terms of the payload some more research could have been done. First of all, more research into the appropriate frequencies for the radio experiment could be done. The radio experiment will be conducted for five different frequencies. Which five different frequencies are the best to use can be further researched. Secondly, the highest bandwidth is now chosen for the accelerometers and magnetometers in the IMU. More research

could have been done into what bandwidth is the optimal to select for the purpose of the DOT mission. Thirdly, the amount of bits per readout for the magnetometer, solar panels, radio experiment and mass spectrometer could be refined as they are now merely assumptions. Fourthly, all the data concerning the mass spectrometer except for its dimensions were based on assumptions as it was taken from an article which did only specify the dimensions. More accurate information about this instrument is desirable. Finally, more research and further consultations with the customer are required to determine the accuracy levels and required resolutions for the payload measurements.

Communication

A considerable amount of assumptions, and therefore contingency, have been included during the design of the communication subsystem as a result of the uncertainties of the asteroids size, rotation and trajectory of the close approach. The assumed values are in accordance with Space Systems Engineer Dr. S. Speretta. No similar missions were launched before that could be used as a reference or for statistical data. As of now the communications subsystem is over-designed. If, at a later stage, more accurate data could be obtained regarding the asteroids characteristics, the amount of contingencies could be reduced significantly. Furthermore, extra effort could be put into finding possible ground stations, since, as for now, only NASA DSN ground stations are considered. In case it is possible to find more ground stations operating at the UHF-band, the design would have drastically changed. The power required would have drastically dropped, a more efficient amplifier can be obtained. Operating at UHF-band would drastically change the antenna design as well, since the size of the patch antenna needed to would not be able to fit on the Z+ surface of the CPQ, assuming the ground stations have similar performances as the Giant Metrewave Radio Telescope.

Electrical Power System

For the EPS, many assumptions were used. Many of them were taken from The New SMAD [25]. The New SMAD does not have much information on pico-satellites and thus many of the assumptions are based on much larger spacecraft. A recommendation for this would be to look at previous missions involving PocketQubes and CubeSats to use a value that is more suitable to pico-satellites.

Furthermore, a crude assumption was assuming that the rotational axis coincides with the axis of the body. This could be improved by performing an in-depth literature study on the mechanics of asteroids and then performing an analysis using a program such as GMAT to visualise the rotation of the asteroid. This would improve the assumption based on the cosine angle loss and would change the time the PQs are in sunlight and eclipse and thus changing the power generated by the solar cells.

The batteries in the PQs are not space ready, it was mentioned that additional testing was required but no margins were used or methods to ensure that would allow the batteries to function in space. To improve on this, more time should have been spent to see how prismatic batteries react in space environment and to research how any adverse effects can be mitigated.

Thermal Control

Multiple assumptions where made for the thermal control. The assumption that the rotation of the asteroid is such that the PQs are half of the time in the sun and half of the time in the shadow, might need to be looked into more. Currently, the PPQs stay in the correct temperature range when they are in the sun or shadow for 65% of the time. It would be preferable to increase this a bit more, to at least 75% of the time.

Secondly, the CPQs are now sensitive to changes as the range is close to the minimal and maximal acceptable values. The ratio between generating heat inside and radiating heat has a maximum for small satellites. However, with different budgets this can be improved to make the maximum temperature decrease slightly. By putting a material with a different α and ϵ, this allows the CPQs radiate even more heat than they currently do. However, as written previously, this has a maximum. The consequence of this is that a heater is needed before the communication phase begins (this requires a change in the budgets). Another option that would make the thermal control of the CPQs even less sensitive to changes, is to investigate if more than three CPQs can send data, as the power (and thus heat) per CPQ during the communication phase will be lower in this way. Yet, another possibility that should be investigated is to not have batteries in the CPQs, as those batteries do not

even provide that much energy (as most comes from the batteries located in the bullets). This would stretch the acceptable temperature range to -40 degrees Celsius to 60 degrees Celsius. Lastly, stage three should be simulated more accurately.

Command and Data Handling

The current design of the C&DH has mostly included high level estimations and was lacking more detailed design.

In terms of the data flow design, optimising the network topology (external communications, in between PQs) to increase the redundancy of the system and minimise power losses could improve the design significantly. This mainly implies changing the locations of the master PPQs in the system, but also optimising the distribution of physical connections in between them. In order to do that, a numerical tool could be made, which would trail a large number of possible topologies and select the most optimal ones. A step further would be to employ a numerical tool that would use machine learning algorithms to enable a more efficient way of determining the most optimal topology.

Performing a more detailed radiation simulation to investigate accurate radiation levels is suggested for the next phase of the design. This would influence the components choice, consequently components cost and testing cost. At this stage, radiation hardened components were chosen, however if the radiation levels are below 10 krad, simpler, more efficient and cheaper components could be chosen.

More research should be done into the choice of cabling. The sizing of the harness was done based on some very high level estimations, but a more detailed analysis could yield more cost and weight efficient options.
Lastly, increasing the redundancy of C&DH subsystem would be highly recommended. Installing more CPU units per PQ could make the lander more reliable. This was difficult to implement with expensive radiation hardened components.

Cost

The cost budgets made so far only provide a rough estimation. It is advised that for the next phase of the project those budgets should be reevaluated: a more detailed breakdown would be recommendable. Once the detailed design phase is completed, it will become apparent which test every component, subsystem and segment needs to undergo, which will be a valuable insight for cost planning.

REFERENCES

[1] Miettinen, A., Sarmaja-Korjonen, K., Sonninen, E., Jungner, H., Lempiäinen, T., Ylikoski, K., Carpelan, C., and Mäkiaho, J. "The palaeoenvironment of the 'Antrea net find'." *Iskos*.

[2] Arianespace. "Vega User's Manual." 2014.

[3] Group 01. "DSE Defend Our Territory: Final Baseline Report."

[4] "Margin philosophy for science assessment studies." Standard, European Space Agency 2012.

[5] Group 01. "DSE Defend Our Territory: Final Midterm Report."

[6] Forshaw, J. L., Aglietti, G. S., Navarathinam, N., Kadhem, H., Salmon, T., Pisseloup, A., Joffre, E., Chabot, T., Retat, I., Axthelm, R., Barraclough, S., Ratcliffe, A., Bernal, C., Chaumette, F., Pollini, A., and Steyn, W. H. "RemoveDEBRIS: An in-orbit active debris removal demonstration mission." *Acta Astronautica*, vol. 127, (2016), pp. 448 – 463. doi:https://doi.org/10.1016/j.actaastro.2016.06.018. URL http://www.sciencedirect.com/science/article/pii/S009457651530117X.

[7] EADS Space Transportation. "ROGER - Phase A final report." 2003.

[8] ESA European Space Research and Technology Centre. "e.deorbit Implementation Plan." 2015.

[9] Battista, U., Landini, A., Gołębiowski, W., Michalczyk, R., Czerwiński, A., Duda, K., and Sochaczewska, A. "Design of net ejector for space debris capturing." 7th European Conference on Space Debris, ESA/ESOC Darmstadt.

[10] Retat, I., Axthelm, R., Schlossstein, U., Klotz, B., Tritsch, W., and Vahsen, S. "Net Capture Mechanism for Debris Removal Demonstration Mission." *7th European Conference on Space Debris*, edited by T. Flohrer and F. Schmitz.

[11] Medina, A., Cercós, L., Stefanescu, R., Benvenuto, R., Lavagna, M., González, I., Rodríguez, N., and Wormnes, K. "Capturing nets for active debris removal: a follow-up on microgravity experiment design to validate flexible dynamic models." *ESA*.

[12] Merriam, E. G., Berg, A. B., Willig, A., Parness, A., Frey, T., and Howell, L. L. "Microspine Gripping Mechanism for Asteroid Capture." Tech. rep., NASA may 2016.

[13] Parness, A., Evans, T., Raff, W., King, J., Carpenter, K., Willig, A., Grimes-York, J., Berg, A., Fouad, E., and Wiltsie, N. *Maturing Microspine Grippers for Space Applications through Test Campaigns*. doi:10.2514/6.2017-5311. URL https://arc.aiaa.org/doi/abs/10.2514/6.2017-5311.

[14] Desbiens, A. L., and Cutkosky, M. R. "Landing and Perching on Vertical Surfaces with Microspines for Small Unmanned Air Vehicles." *Journal of Intelligent and Robotic Systems*, vol. 57, (2009), pp. 313–327.

[15] Mehanovic, D., Bass, J., Courteau, T., Rancourt, D., and Lussier Desbiens, A. "Autonomous Thrust-Assisted Perching of a Fixed-Wing UAV on Vertical Surfaces." *Biomimetic and Biohybrid Systems*, edited by M. Mangan, M. Cutkosky, A. Mura, P. F. Verschure, T. Prescott, and N. Lepora. Springer International Publishing, Cham, pp. 302–314.

[16] Gołębiowski, W., Michalczyk, R., Dyrek, M., Battista, U., and Wormnes, K. "Validated simulator for space debris removal with nets and other flexible tethers applications." *Acta Astronautica*, vol. 129, (2016), pp. 229 – 240. doi:https://doi.org/10.1016/j.actaastro.2016.08.037. URL http://www.sciencedirect.com/science/article/pii/S009457651630008X.

[17] Speretta, S., Pérez Soriano, T., Bouwmeester, J., Carvajal Godínez, J., Menicucci, A., Watts, T., Sundaramoorthy, P., Guo, J., and Gill, E. "Cubesats to Pocketqubes: Opportunities and Challenges." *Proceedings of the 67th International Astronautical Congress (IAC)*.

[18] Radu, S., Uludag, M., Speretta, S., Bouwmeester, J., Dunn, A., Walkinshaw, T., Kaled Da Cas, P., and Cappelletti, C. "The PocketQube Standard."

[19] Ubbels, W. J., Bonnema, A. R., van Breukelen, E. D., Doorn, J. H., van den Eikhoff, R., Van der Linden, E., Aalbers, G. T., Rotteveel, J., Hamann, R. J., and Verhoeven, C. J. M. "Delfi-C3: a student nanosatellite as a test-bed for thin film solar cells and wireless onboard communication." *Proceedings of 2nd International Conference on Recent Advances in Space Technologies, 2005. RAST 2005.* pp. 167–172. doi:10.1109/RAST.2005.1512556.

[20] Meng, X., Zhang, X., Zhai, Y., and Xu, W. "Mini 2000: A Robust Miniature Mass Spectrometer with Continuous Atmospheric Pressure Interface." *Instruments*, vol. 2, (2018), p. 2. doi:10.3390/instruments2010002.

[21] Leugoud, R. J. "Seismic detection utilizing a mini sensor." *2011 Monitoring Research Review: Ground-Based Nuclear Explosion Monitoring Technologies*. pp. 322–325. Sponsored by the U.S. Department of Energy, Award No. DE-FG02-08ER85090.

[22] S. Chatterjee, D. C., S. Kumar. "Design of Compact Microstrip Antenna for S-Band Microwave Communication." 2012.

[23] Shambayati, S., and Lee, D. K. "GMSK modulation for deep space applications." 2012.

[24] Hamkins, J. "Lower Error Floors for NASA LDPC Codes." 2011.

[25] Wertz, J. R., Everett, D. F., and Puschell, J. J. *Space Mission Engineering: The New SMAD*. 1^{st} ed. Microcosm Press, Hawthorne, California, United States 2011.

[26] Chang, C. "DSN Telecommunications Link Design Handbook." may 2017.

[27] Peter, E. G. "The Development of Solar Power Satellites." 1979.

[28] Cervone, Dr.. A., and Zandbergen, Ir.. B. T. C. "Electrical Power Systems for Aerospace Vehicles."

[29] I. Vertat, A. V. "Efficient and Reliable Solar Panels for Small CubeSat Picosatellites." *International Journal of Photoenergy*, vol. 2014.

[30] K. Mallon, B. F., F. Assadian. "Analysis of On-Board Photovoltaics for a Battery Electric Bus and Their Impact on Battery Lifespan." *Energies*.

[31] Speretta, S., Perez Soriano, T., Bouwmeester, J., Carvajal Godinez, J., Menicucci, A., Watts, T., Sundaramoorthy, P., Guo, J., and Gill, E. "Cubesats to pocketqubes. Opportunities and challenges." *67th International Astronautical Congress*.

[32] Bouwmeester, J. "Spacecraft Technology. Command and Data Handling lecture notes."

[33] Delhaise, F., Ercolani, A., Zender, J., Barthelemy, M., Trautner2, R., and Arviset, C. "Spacecraft and Payload Data Handling." *ESA Special Publication*.

[34] Hughes, S. P., Qureshi, R. H., Cooley, S. D., and Parker, J. "Verification and Validation of the General Mission Analysis Tool (GMAT)." *AIAA/AAS Astrodynamics Specialist Conference*. doi:10.2514/6.2014-4151.

[35] Tanaka, A. "Toxicity of indium arsenide, gallium arsenide, and aluminium gallium arsenide." *Elsevier*.

A

TABLES AND DIAGRAMS

Table A.1: Final Trade-off

	AHP Weights	SINGLE	FLEX	NET
Performance	**33.9**			
Payload mass	11.0	10.50% of total available mass G	6.48% of total available mass Y	18.56% of total available mass B
Available power	11.1	Stage 1: partly active (Stage 2: sequentially active) G	Stage1: partly active (Stage 2: fully active) G	Both stages fully active (Stage 2: sequentially active) B
Measurement types	25.6	6 out of 8 G	All B	All B
Approach & facing	17.0	Partial distribution, partial facing Y	Full distribution (ADCS), partial facing G	Full distribution, full facing B
Data rate	23.9	52.00 kBit/s R	1018 kBit/s G	1218 kBit/s G
Payload volume	11.4	Unknown	Unknown	Unknown
Feasibility	**35.0**			
Deployment	16.0	Few subsystems G	Complex, voluminous Y	Few subsystems G
Approach	10.1	No control but accurate deployment G	Accurate controlled approach (ADCS) but complex system Y	Deployment assures accurate and controlled approach B
Landing	17.4	Not present	Harpoon is unpredictable Y	Behaviour net predictable B
Attachment	32.5	Complex, nothing to prevent failure Y	No pushing force G	Pushing force, redundancy B
Measurements	23.9	Best attachment B	Some PQs can float Y	Some PQs can float Y
Risk	**19.8**	Highest risk is medium/high Y	Highest risk is medium/high Y	Highest risk is medium/high Y
Severity	64.1			
Probability	35.9			
Innovation	**6.6**	Similar to Hayabusa mission Y	Never done before B	Technique used in debris capture mission G
Sustainability	**4.7**			
COTS components	15.2	COTS components can be used G	Poor use of COTS components Y	Medium use of COTS components G
Scalability	38.8	Can land anywhere B	Scalable up to 100m but no more Y	Send bigger and/or multiple nets with adaptation of attachment G
Toxicity	28.8	Unknown	Unknown	Unknown
Ecological footprint	17.2	Unknown	Unknown	Unknown
Scores		**2.132**	**2.308**	**3.565**
Ranking		**3**	**2**	**1**

Weights

Excellent	B	6
Acceptable	G	4
Not satisfactory	Y	1
Unacceptable	R	0

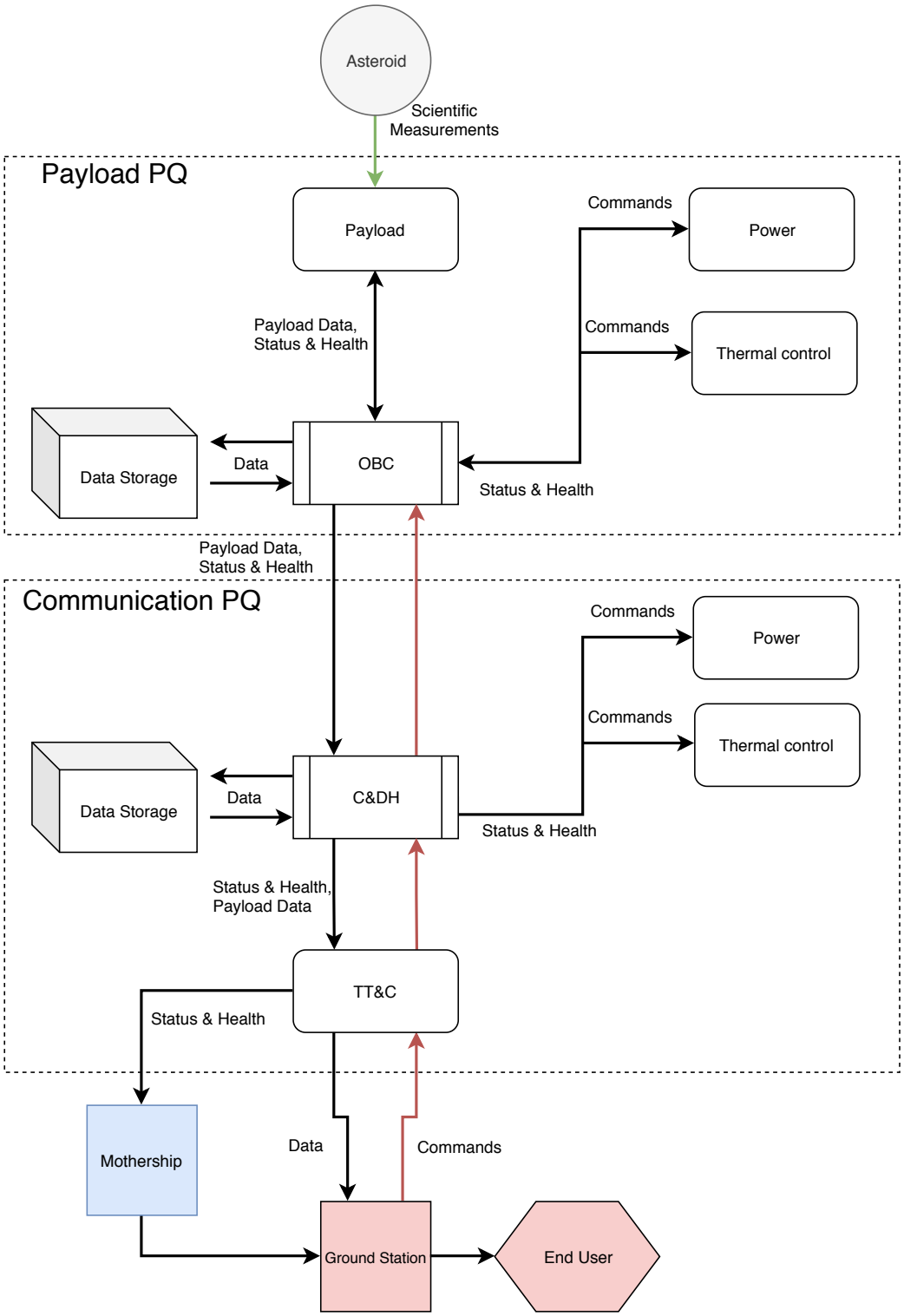

Figure A.1: Communication Data Flow

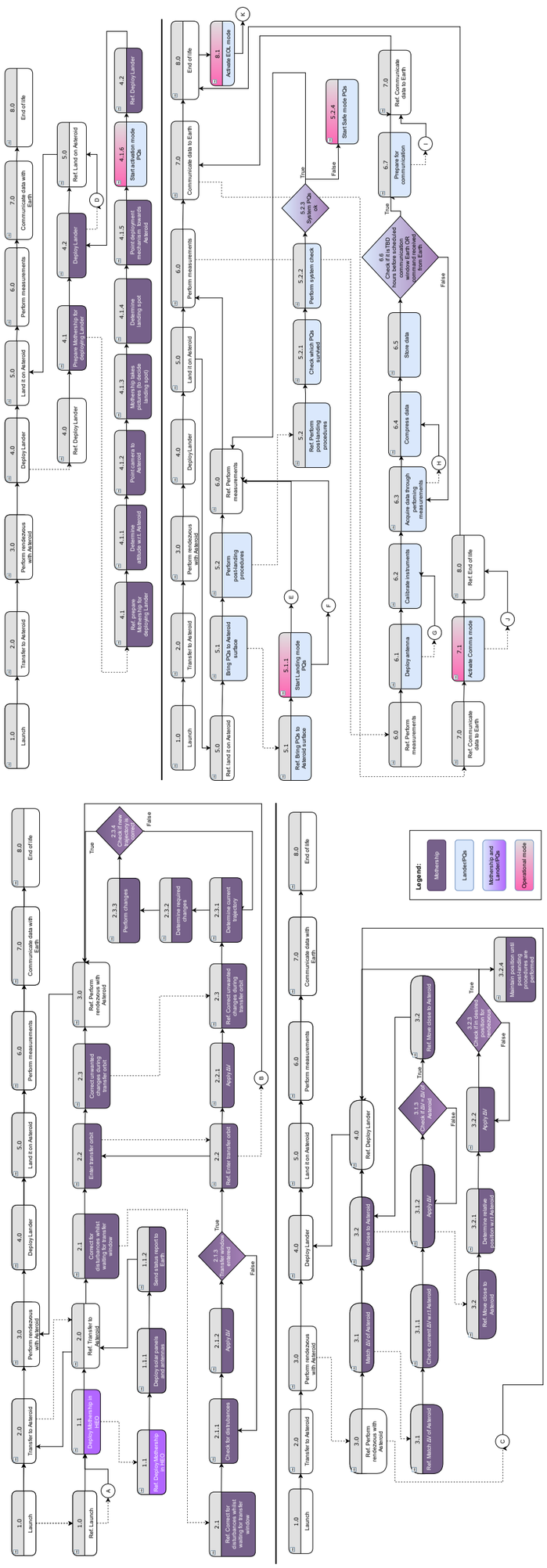

Figure A.1: Functional Flow Diagram of ANTREA design (page 1).

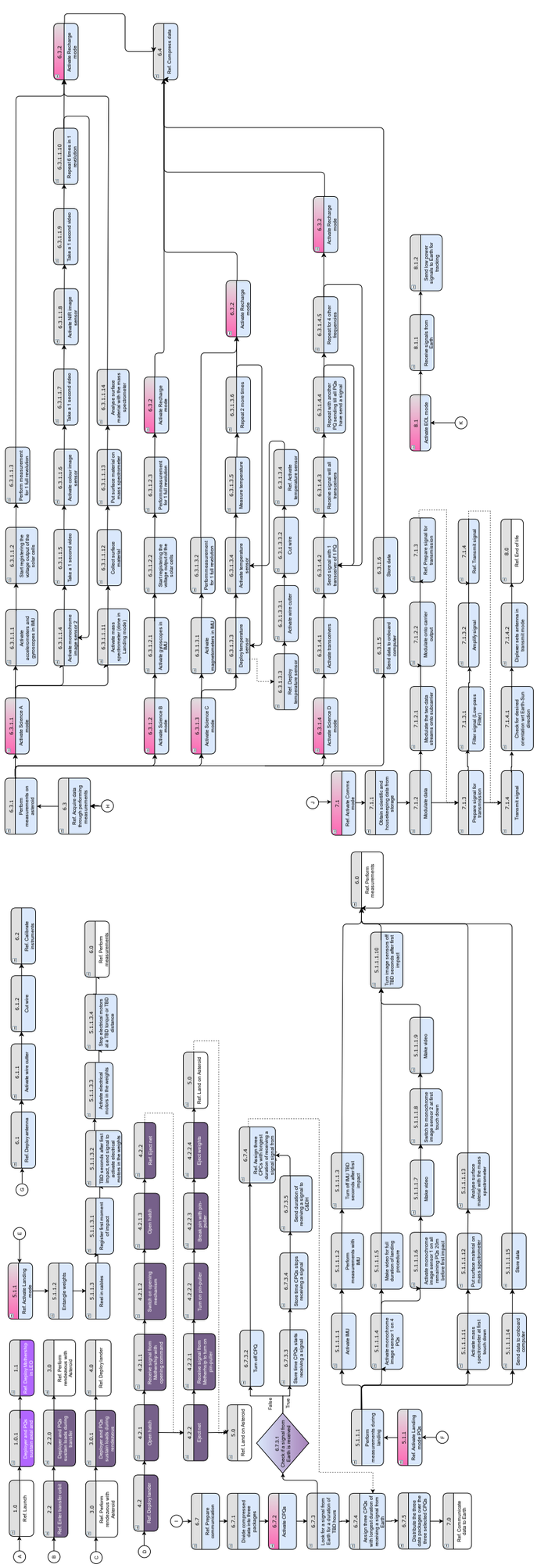

Figure A.2: Functional Flow Diagram of the ANTREA design (page 2).

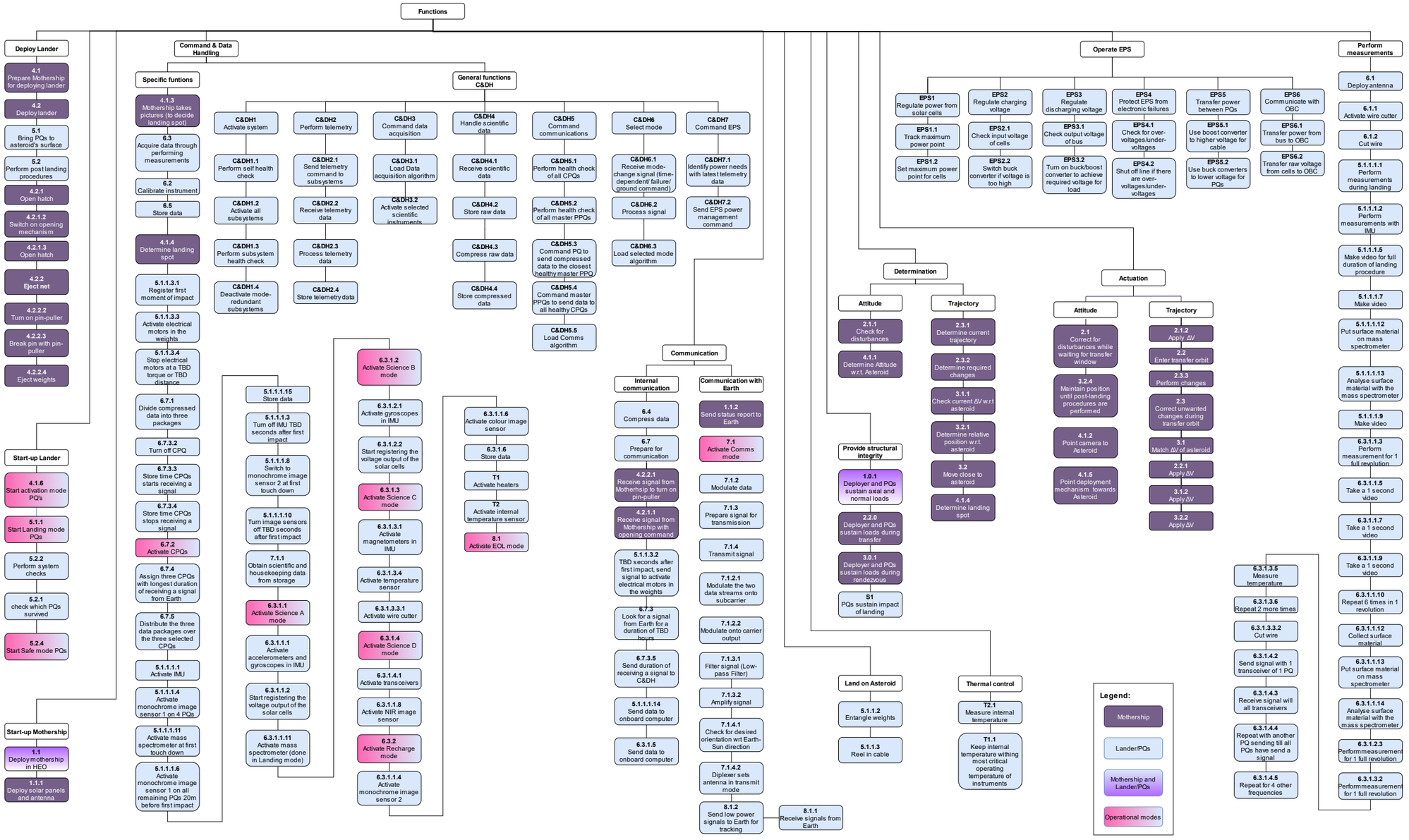

Figure A.3: Functional Breakdown Structure of the ANTREA design.

ID	Task Mode	Task Name	Duration	Start	Finish	Predecessors
1		DSE Office Work	54 days	Tue 23-4-19	Fri 5-7-19	
2		Final Review	1 day	Mon 8-7-19	Mon 8-7-19	1
3		Team Holiday	43 days	Tue 9-7-19	Thu 5-9-19	2
4		**Review of where the team stands at**	**50 days**	**Fri 6-9-19**	**Thu 14-11-19**	**3**
5		Review of the team's objectives	20 days	Fri 6-9-19	Thu 3-10-19	
6		Review of organisational structure	15 days	Fri 6-9-19	Thu 26-9-19	
7		Identification of resources	20 days	Fri 6-9-19	Thu 3-10-19	
8		Market Analysis	50 days	Fri 6-9-19	Thu 14-11-19	
9		Preparation of Proposal for investors	150 days	Fri 15-11-19	Thu 11-6-20	8
10		Preparation of proposal for contractors	150 days	Fri 12-6-20	Thu 7-1-21	9
11		**Phase C: Detailed definition**	**740 days**	**Fri 8-1-21**	**Thu 9-11-23**	**10**
12		Communication	110 days	Fri 8-1-21	Thu 10-6-21	
26		Astrodynamics	110 days	Fri 8-1-21	Thu 10-6-21	
13		Communication iteration	50 days	Fri 11-6-21	Thu 19-8-21	12
27		Astrodynamics iteration	50 days	Fri 11-6-21	Thu 19-8-21	26
14		Command and Data Handling	110 days	Fri 20-8-21	Thu 20-1-22	13
16		Thermal Control	110 days	Fri 20-8-21	Thu 20-1-22	27
18		Electrical Power System	110 days	Fri 20-8-21	Thu 20-1-22	13
15		Command and Data Handling iteration	50 days	Fri 21-1-22	Thu 31-3-22	14
17		Thermal Control iteration	50 days	Fri 21-1-22	Thu 31-3-22	16
19		Electrical Power System iteration	50 days	Fri 21-1-22	Thu 31-3-22	18
20		Payload	110 days	Fri 1-4-22	Thu 1-9-22	17
22		PQ Structure	110 days	Fri 1-4-22	Thu 1-9-22	19
21		Payload iteration	50 days	Fri 2-9-22	Thu 10-11-22	20
23		PQ Structure iteration	50 days	Fri 2-9-22	Thu 10-11-22	22
24		Deployer	110 days	Fri 11-11-22	Thu 13-4-23	21
25		Deployer iteration	50 days	Fri 14-4-23	Thu 22-6-23	24
28		Preliminary testing and qualification	50 days	Fri 23-6-23	Thu 31-8-23	25
29		Writing User's Manual	50 days	Fri 1-9-23	Thu 9-11-23	28
30		**Phase D: Qualification and Production**	**735 days**	**Fri 10-11-23**	**Thu 3-9-26**	**11**
31		Testing	245 days	Fri 10-11-23	Thu 17-10-24	
32		Qualification	245 days	Fri 18-10-24	Thu 25-9-25	31
33		Production	245 days	Fri 26-9-25	Thu 3-9-26	32
34		**Phase E: Utilisation**	**1128 days**	**Tue 15-3-33**	**Thu 9-7-37**	
35		Launch from CSG (Kourou, French Guiana)	1 day	Tue 15-3-33	Tue 15-3-33	
39		Trajectory to asteroid	730 days	Wed 16-3-33	Tue 1-1-36	35
36		Deployment from Mothership	1 day	Wed 2-1-36	Wed 2-1-36	39
37		Scientific measurements on asteroid	30 days	Thu 3-1-36	Wed 13-2-36	36
38		Communication with Earth window	1 day	Thu 14-2-36	Thu 14-2-36	37
40		Phase F: End of Life	5 days	Fri 15-2-36	Thu 21-2-36	38

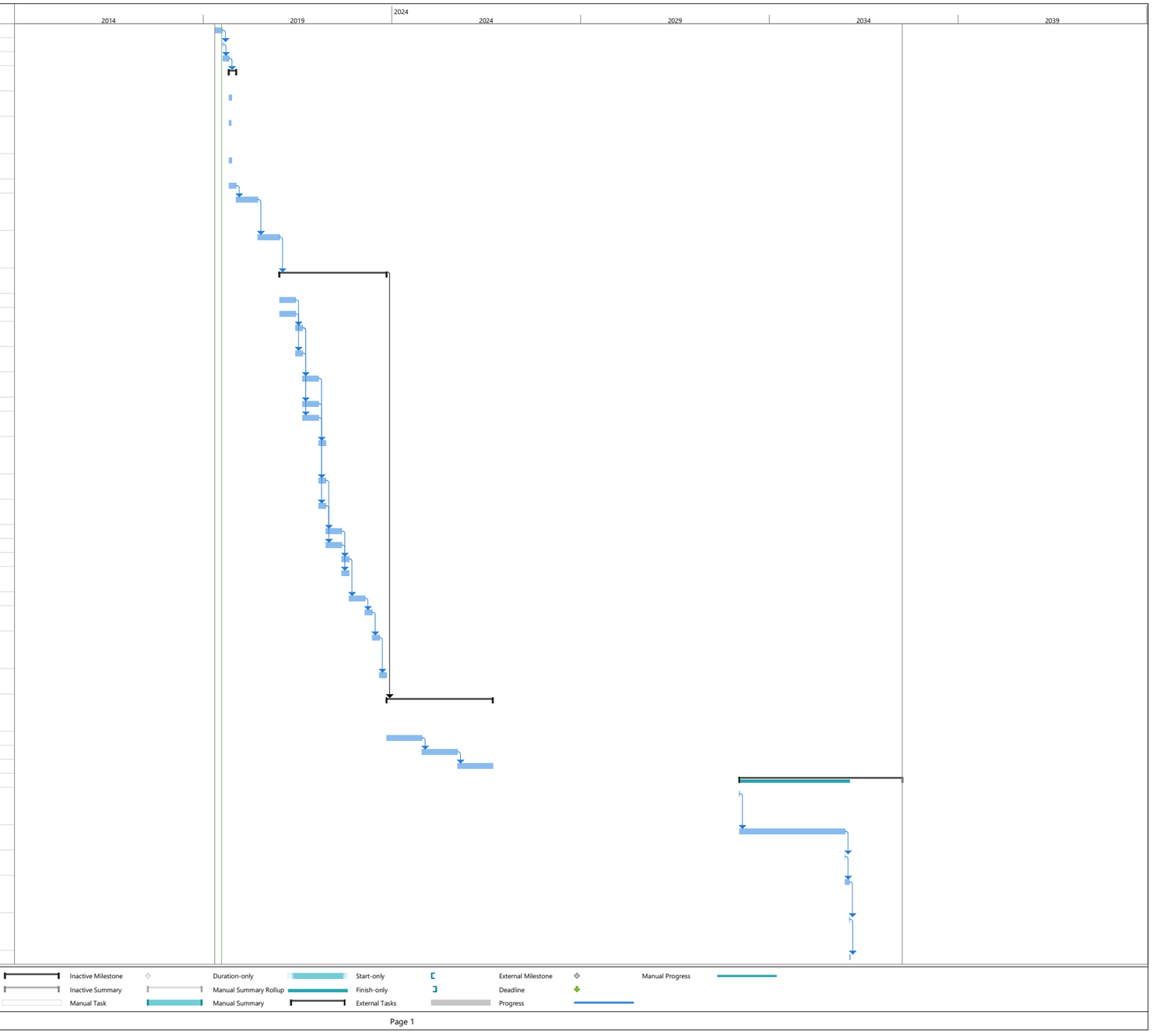

Figure A.4: Gantt chart displaying potential next phases of the project.

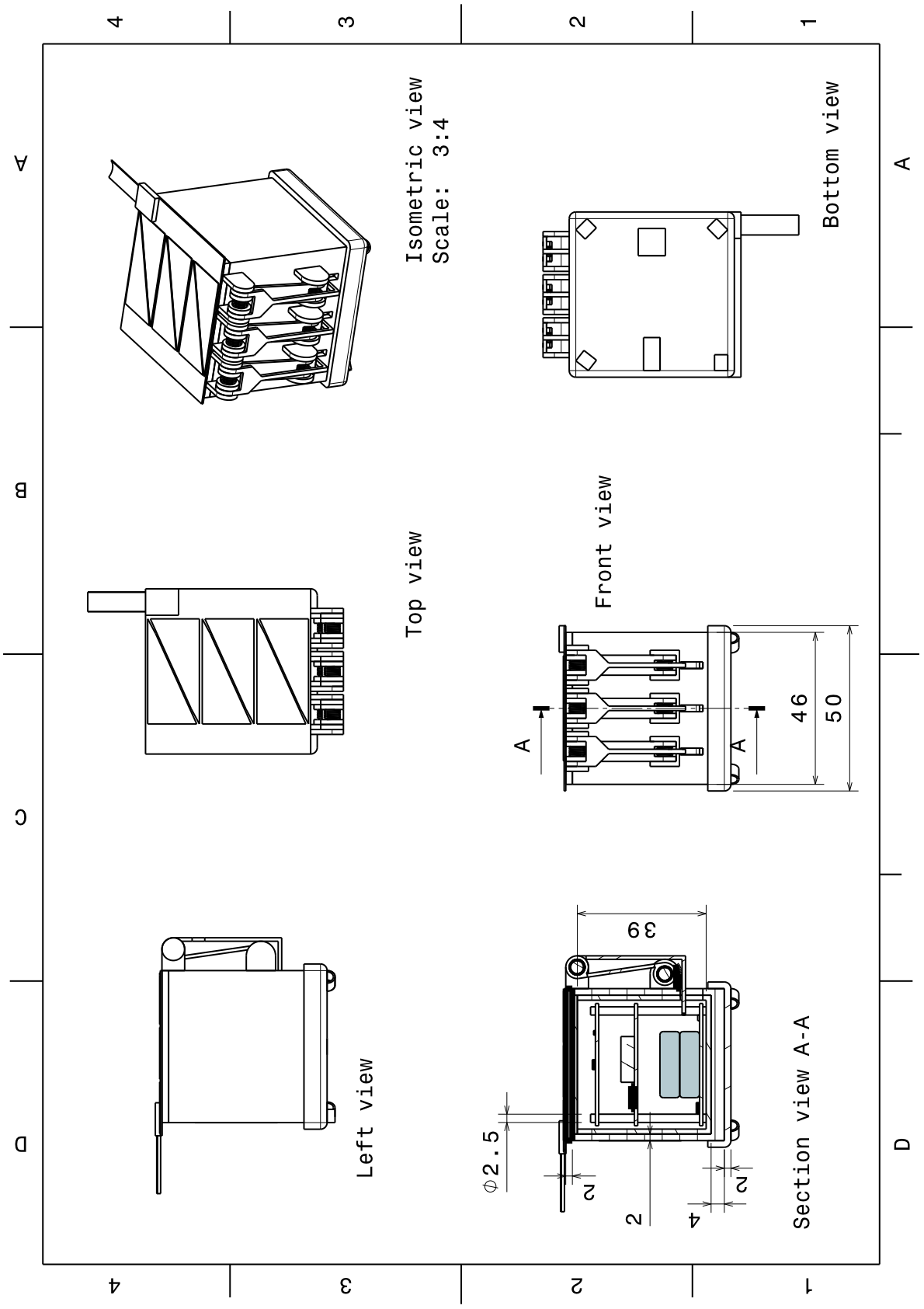

Figure A.5: CATIA technical drawing of a PPQ-1

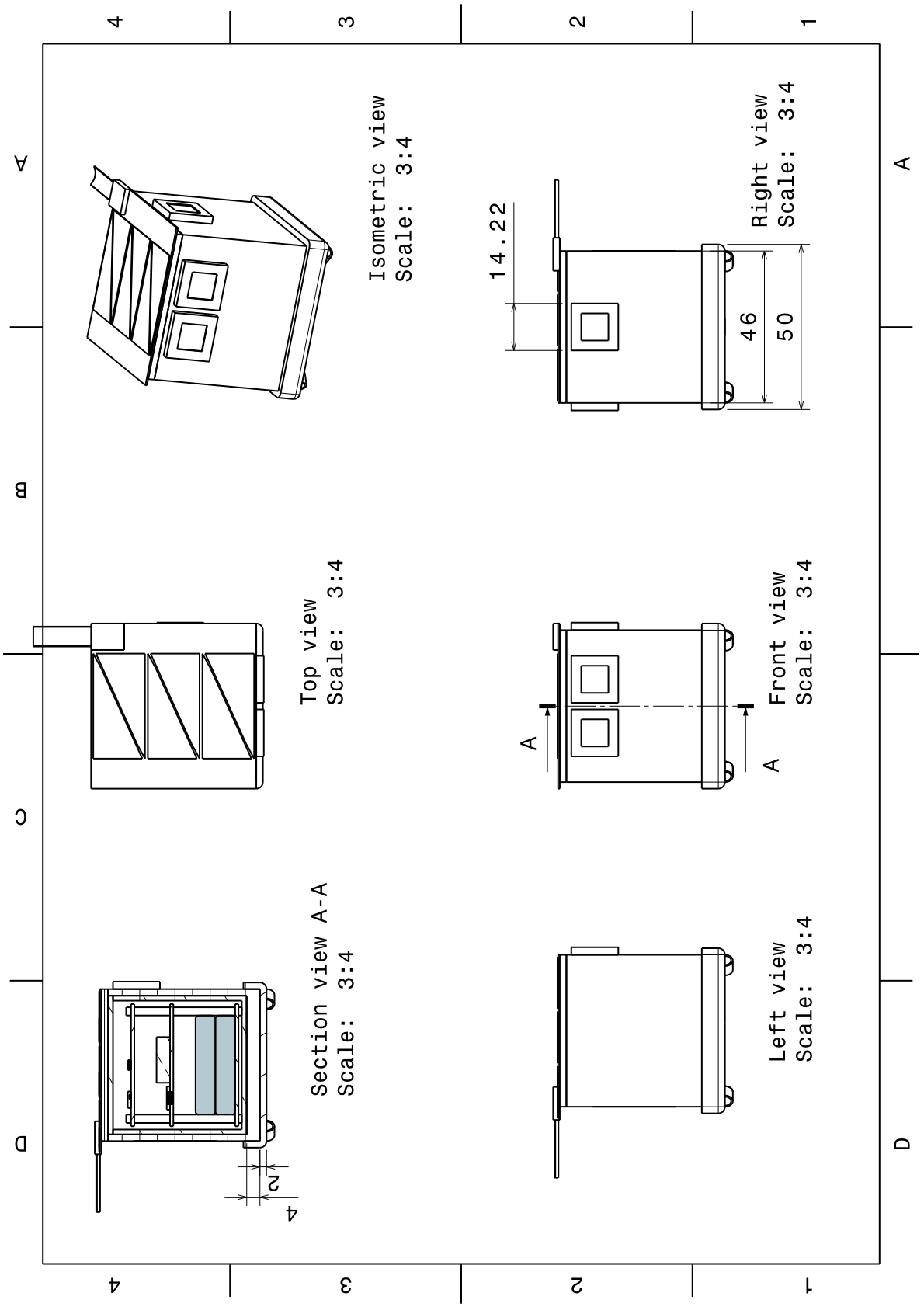

Figure A.6: CATIA technical drawing of a PPQ-2

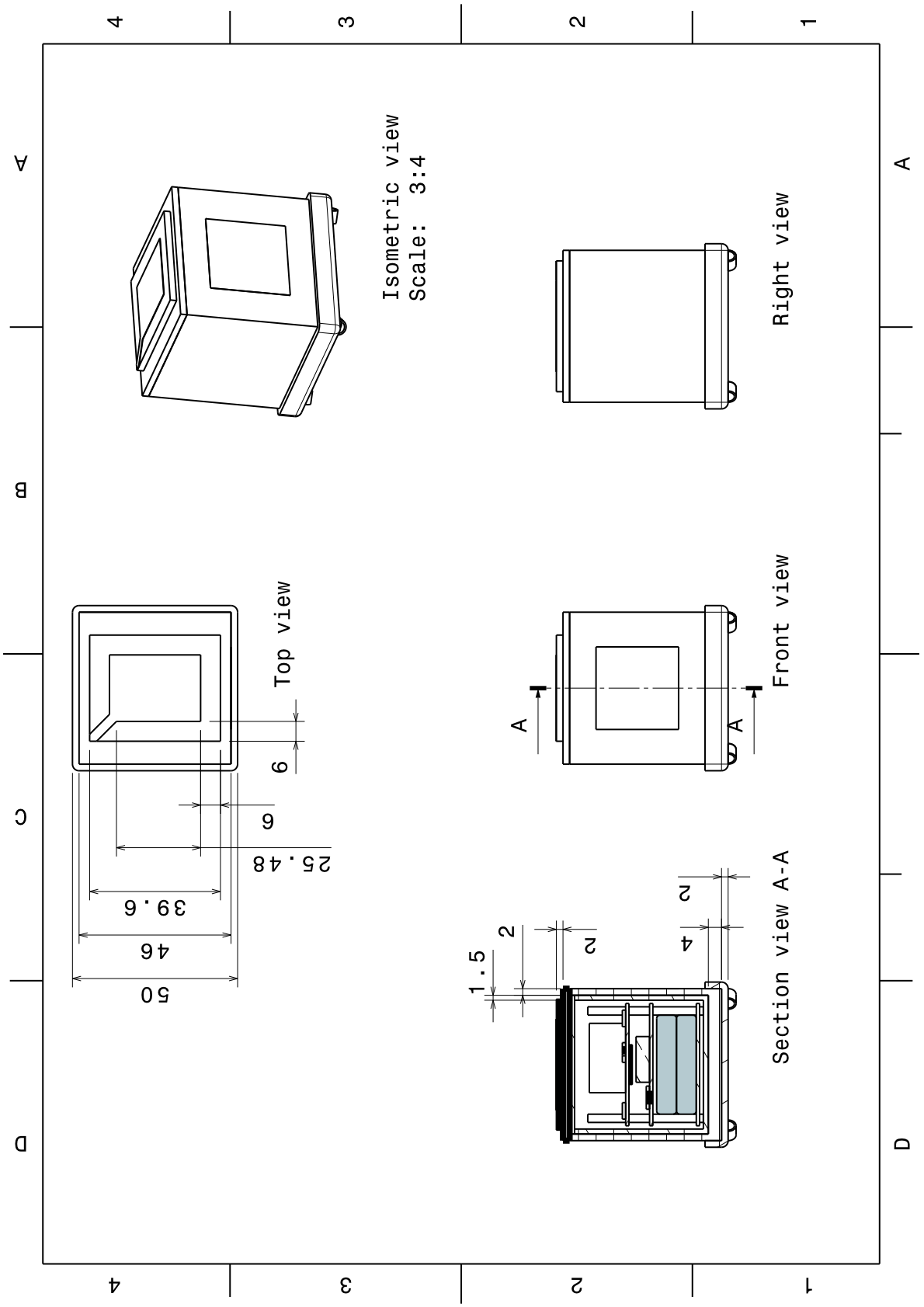

Figure A.7: CATIA technical drawing of a CPQ

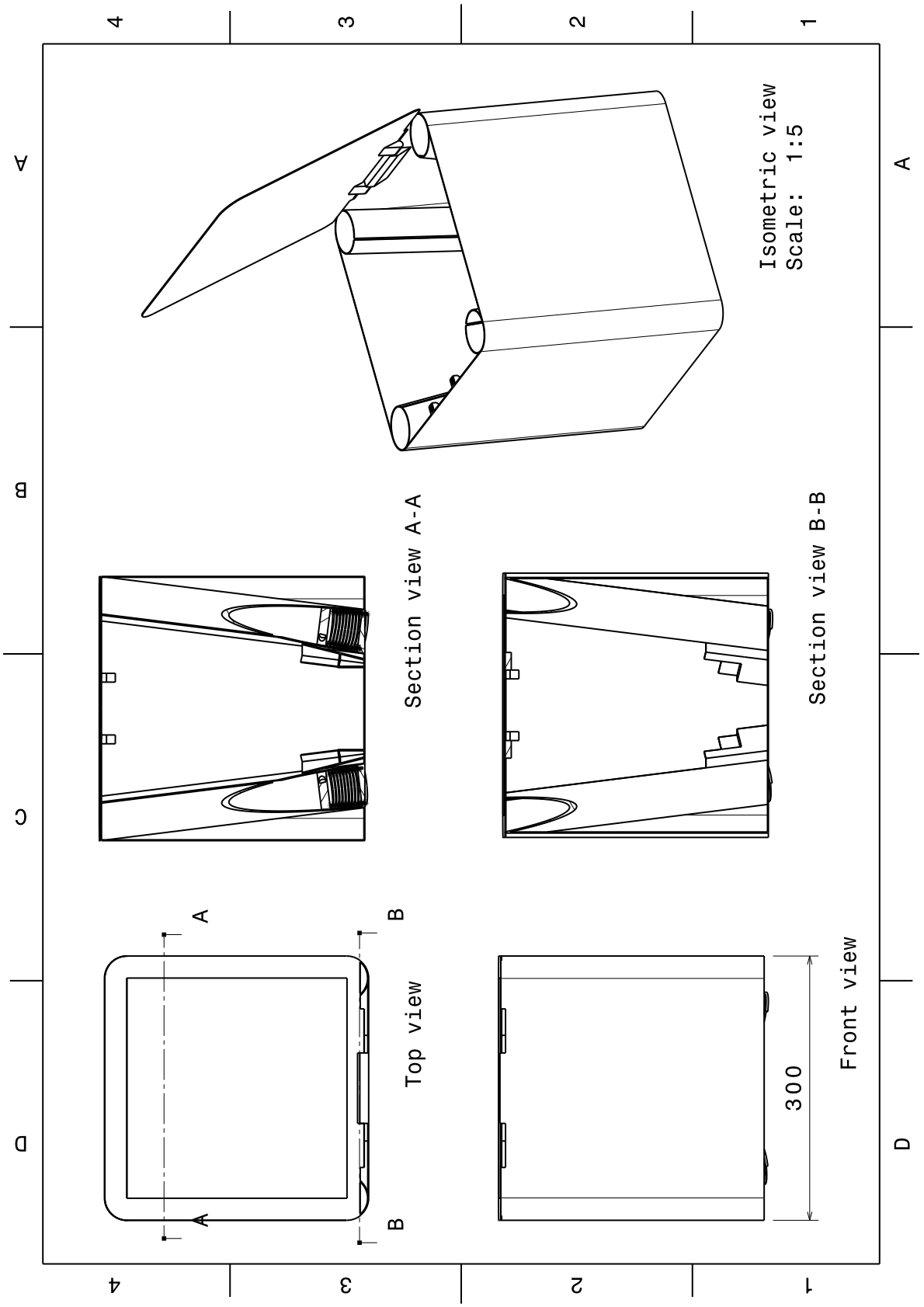

Figure A.8: CATIA technical drawing of the Deployer